GENETIC AND EPIGENETIC MECHANISMS REGULATING SMOOTH MUSCLE CELL DIFFERENTIATION

Kevin Dale Mangum

A dissertation submitted to the faculty at the University of North Carolina at Chapel Hill in partial fulfillment of the requirements for the degree of Doctor of Philosophy in Pathology in the School of Medicine.

Chapel Hill
2017

Approved by:

Christopher P. Mack

Victoria L. Bautch

Jiandong Liu

Praveen Sethupathy

Joan M. Taylor

ABSTRACT

Kevin Dale Mangum: Genetic and Epigenetic Mechanisms Regulating Smooth Muscle
Cell Differentiation
(Under the direction of Christopher P. Mack)

Smooth muscle differentiation is a complex process, involving numerous

molecular, genetic, and epigenetic mechanisms. Notably, smooth muscle cells (SMCs)

retain marked plasticity in their ability to convert between synthetic and more

differentiated contractile gene programs. In vascular diseases, including hypertension,

atherosclerosis, and restenosis, SMCs dedifferentiate from their healthy, mature state to

a more immature "phenotypically modulated" cell type capable of migrating,

proliferating, and producing extracellular matrix, all of which contribute to disease.

Additionally, genetic alterations in various components of the smooth muscle

transcriptional machinery result in cardiovascular disease and even death. Thus, a more

complete understanding of the exact mechanisms regulating SMC differentiation is

crucial for the development of novel targets in the diagnosis and treatment of vascular

disease.

The work herein interrogates several points along the RhoA axis and defines

their roles in SMC differentiation. First, the genetic and epigenetic mechanisms

regulating expression of a smooth muscle-specific gene, GRAF3, are uncovered.

GRAF3, also referred to as ARHGAP42, was first described by my collaborators in Joan

Taylor's Lab as a smooth muscle selective Rho-GAP essential for blood pressure

control in mice. Single nucleotide polymorphisms in the GRAF3 gene were associated

with changes in blood pressure, and the rs604723 T-allele variant located in a highly conserved DHS increased GRAF3 expression by promoting SRF binding to this region. In addition to SRF, we show that the transcription activity of this region as well as GRAF3 expression are controlled by the transcription factors, RBPJ and TEAD1.

In subsequent chapters, we describe novel mechanisms regulating function of MRTF-A. Given that MRTF-A is essential for full activation of smooth muscle-specific gene expression, we hypothesize that these newly identified mechanisms regulate SMC differentiation. We describe our approach for identifying post-translational modifications and binding partners that regulate MRTF-A function. In our search for novel MRTF-A binding partners, we identified the putative histone lysine methyltransferase, PRDM6, and demonstrated that it was required for SMC differentiation. In overexpression experiments in COS-7 cells, we detected significant methylation on MRTF-A. Surprisingly, SMYD2 and SET7/9 strongly methylated MRTF-A, but PRDM6 did not. We found that SMDY2 methylated K27 within MRTF-A's highly conserved basic nuclear localization signal. SMYD2-mediated methylation at K27 inhibited MRTF localization as well as MRTF-dependent activation of SMC transcription.

ACKNOWLEDGMENTS

helped my transition into the Program are Alison Regan, Carol Herion, and Mohanish Deshmuk. Thank you all for taking a chance on me. I can't tell begin to explain how much saying yes in that moment impacted me.

It's hard to imagine four years without good company. I really hit the jackpot in the Mack-Taylor Lab by being surrounded be so many kind, dedicated, and intelligent individuals. Laura-Weise Cross, even though you've already graduated, I was so lucky to work with you for the majority of my grad school experience. Kaitlin Lenhart, a previous graduate student in the Taylor Lab, always provided me with encouragement and helpful advice at the start of my graduate school career. Thank you, Rachel Dee for always smiling and being so wonderful to work with. I'm also fortunate to have worked with my other lab members: Xue Bai, Qiang Zhu, and Zack Opheim.

To my family, thank you for supporting me during my endeavors, especially my Mom and Dad. I know it's been a long road and you've been there every step of the way. To Tanner Mangum, you made it so easy for me to take a step back from science and laugh a little, which has been so invaluable. Thank you Trish for being there as well. Your support means everything to me. I have to acknowledge my grandparents, and roots in general, for helping me stay humble. Meme, especially, thank you for teaching me that "there's more than one way to skin a cat." I truly believe that this contributed to my scientific creativity from a very early age.

To my friend Negeen Hamedani, thank you for your encouragement over the last five years. I'm so grateful to have you as a friend.

TABLE OF CONTENTS

LIST OF FIGURES

LIST OF TABLES

LIST OF ABBREVIATIONS

ACE: Angiotensin Converting Enzyme

AII: Angiotensin II

AJ: Adherens Junction

ATP: Adenosine Triphosphate

BP: Blood Pressure

BSA: Bovine Serum Albumin

CAD: Coronary Artery Disease

CADASIL: Cerebral Autosomal-Dominant Arteriopathy with Subcortical   Infarcts and Leukoencephalopathy

CNN: Calponin

COS: CV-1 in Origin with SV40 genes

CRISPR: Clustered Regularly Interspaced Short Palindromic Repeats

CRM-1:   Chromosomal Mainenance-1

CT: Threshold Cycle

DAPI: 4',6-Diamidino-2-Phenylindole, Dihydrochloride

DAPT: *N*-[(3,5-Difluorophenyl)acetyl]-L-alanyl-2-phenyl]glycine-1,1-dimethylethyl ester

DHS: Dnase-I Hypersensitive Site

DMEM: Dulbecco's Modified Eagle Medium

DNA: Deoxyribonucleic Acid

DOCA: Deoxycorticosterone acetate

DTT: Dithiothreitol

EC: Endothelial Cell

EDTA: Ethylenediaminetetraacetic Acid

EEL: External Elastic Lamina

EMSA: Electrophoretic Mobility Shift Assay

ENCODE: Encyclopedia of DNA Elements

ERK: Extracellular signal-related kinase

ES: Embryonic Stem

EV: Empty Vector

FAK: Focal Adhesion Kinase

FBS: Fetal Bovine Serum

FCS: Fetal Calf Serum

GAP: GTPase Activating Protein

GAPDH: Glyceraldehyde 3-phosphate dehydrogenase

GDP: Guanosine-5'-diphosphate

GEF: Guanine nucleotide exchange factor

GFP: Green Fluorescent Protein

GO: Gene Ontology

GPCR: G Protein Coupled Receptor

GRAF: GTPase Regulator Associated with Focal Adhesion Kinase

GST: Glutathione-S-transferase

GTP: Guanosine-5'-triphosphate

GWAS: Genome Wide Association Study

HEPES: 4-(2-hydroxyethyl)-1-piperazineethanesulfonic acid

HTN: Hypertension

IACUC: Institutional Animal Care and Use Committee

ID:	Identify/Identification
IEL:	Internal Elastic Lamina
IP:	Immunoprecipitation
IRB:	Institutional Review Board
IV:	Intravenous
KCL:	Potassium Chloride
LARG:	Leukemia-associated Rho **GEF**
LD:	Linkage Disequilibrium
LNC:	Long Non-coding
LZ:	Leucine Zipper
MADS:	MCM1, Agamous, Deficiencs, SRF
MAF:	Mean Allele Frequency
MAML:	Mastermind-like
MCAT:	Muscle-CAT
MEK:	MAP/ERK kinase
MHC:	Myosin Heavy Chain
MLC:	Myosin Light Chain
MLCK:	Myosin Light Chain Kinase
MRTF:	Myocardin-Related Transcription Factor
MYOSLID:	MYOcardin-induced Smooth muscle LncRNA, Inducer of Differentiation
MYPT:	Myosin Phosphatase Targeting Protein
NEB:	New England Biolabs
NICD:	Notch Intracellular Domain
NIH:	National Institutes of Health

NLS:	Nuclear Localization Sequence/Signal
NTC:	Non-Targeting Control
PAGE:	Polyacrylamide Gel Electrophoresis
PBS:	Phosphate Buffered Saline
PCR:	Polymerase Chain Reaction
PDGF:	Platelet Derived Growth Factor
PDZ:	Psd-95 (Post Synaptic Density Protein), DlgA (Drosophila Disc Large Tumor Suppressor) and ZO1 (Zonula Occludens-1 Protein)
PH:	Plekstrin Homology
PKA:	Protein Kinase A
PKC:	Protein Kinase C
PKMT:	Protein Lysine Methyltransferase
PMSF:	Phenylmethylsulfonyl Fluoride
PTM:	Post Translational Modification
RBPJ:	Recombination Signal Binding **Protein** For Immunoglobulin Kappa J Region
RIPA:	Radioimmunoprecipitation assay buffer
RNA:	Ribonucleic acid
ROCK:	Rho-associatd protein kinase
RT:	Real Time
SAM:	S-adenosylmethione
SAP:	SAF-A/B, Acinus and PIAS
SDS:	Sodium Dodecyl Sulfate
SEM:	Standard Error of the Mean
SET:	Su(var)3-9, Enhancer-of-zeste and Trithorax

SFM: Serum Free Media

SM: Smooth Muscle

SMA: Smooth Muscle Alpha-Actin

SMC: Smoth Muscle Cell

SMMHC: Smooth Muscle Myosin Heavy Chain

SMYD: SET And MYND Domain Containing

SNF: SWItch/Sucrose Non-Fermentable

SNP: Single Nucleotide Polymoerphism

SRF: Serum Response Factor

STAT: Signal transducer and activator of transcription

SUMO: Small Ubiquitin-like Modifier

SWI: SWItch/Sucrose Non-Fermentable

TAD: Transcriptional Activation Domain

TAGLN: Transgelin

TEAD: TEA domain family member 1

TEF: Transcriptional Enhancer Factor

TET: Ten-eleven Translocation

TGF: Transforming Growth Factor

TK: Tyrosine Kinase

TSS: Transcription Start Site

UCSC: University of California, Santa Cruz

UNC: University of North Carolina

UTR: Untranslated Region

VEGF: Vascular endothelial growth factor

VSMC: Vascular Smooth Muscle Cell

CHAPTER 1: BACKGROUND AND SIGNIFICANCE

Blood vessel development, structure, and function

Blood vessels supply the developing embryo and adult with sufficient oxygen and nutrients required to support organ growth, function, and life. The mature artery is comprised of three main layers: the tunica intima, tunica media, and tunica adventitia (Figure 1). The tunica intima, which is the innermost layer, consists of a single lining of endothelial cells and is separated from the tunica media by the internal elastic lamina. The tunica media is composed of multiple sheets of vascular smooth muscle cells (SMCs), which contract to regulate vessel diameter, tone, and, consequently, downstream tissue perfusion. The external elastic lamina separates the tunica media and the tunica adventitia, which is formed from connective tissue. The connective tissue of the adventitia houses peripheral nerves, immune cells, fibroblasts, and resident vascular progenitor cells that are thought to play a role in vascular disease and repair (1, 2).

The embryonic vascular system begins as an endothelial network, which arises from undifferentiated precursors, called angioblasts. Extensive remodeling of the endothelial network is driven by vascular endothelial growth vector (VEGF), which stimulates vascular sprouting from tip cells (3). S1P signaling limits endothelial sprouting, thereby stabilizing the developing network (4, 5). As such, mice lacking endothelial-specific S1PR1 have deformed vasculature due to excessive sprouting (6). Although endothelial cells are required for initiation of blood vessel development, they

alone are unable to maintain and stabilize the developing vascular system (7, 8).

Maturation and stabilization of the developing vasculature by SMCs is essential for a

functional vascular network. After extensive remodeling of the endothelial plexus, the

first step in vascular maturation is investment of the plexus by mural cells (smooth

muscle cells and pericytes), which relies heavily on PDGF, TGFβ, and Notch signaling

(8-10). Intact PDGF-B/PDGF-Rβ signaling is required for SMC investment during blood

vessel development, as global homozygous deletion of the PDGF-B ligand or its

receptor results in hemorrhage and embryonic lethality from diminished SMC coverage

in capillary beds (12). Another important regulator of SMC migration during vessel

development is Notch signaling, loss of which leads to significantly reduced SMC

coverage in developing vessels (13). This will be discussed in greater detail below.

During vessel maturation, SMCs begin to express essential proteins that are

required for their function. Several of these proteins are routinely used to specify the

smooth muscle lineage, and hence termed "smooth muscle-specific" genes. Smooth

muscle alpha actin (*ACTA2/SMA*) and transgelin (*TAGLN/SM22*) and are the earliest

genes expressed by the SMC, while calponin (*CNN*) and smooth muscle-myosin heavy

chain (*MYH11/SM-MHC*) are considered more mature markers of SMC differentiation

since they are expressed later along the differentiation timeline. SMA is the first marker

to be expressed and can be seen in mouse as early as E8.5. Transgene expression

using the smooth muscle alpha actin promoter to drive LacZ reporter activity was

detected at E10.5 (14). SM22 is expressed at ~E9.5 in mouse and persists into

adulthood in all smooth muscle tissues. However, in the heart, SM22 is transiently

expressed between E8.0 and E12.5, and between E9.5 and E12.5 in skeletal muscle

cells (15). SM-MHC transcripts are detected first in the aorta and its arches at E10.5, in

other locations beginning at E12.5, and then in all smooth muscle tissues by E17.5 (16).

Finally, calponin is expressed in the heart as early as E8.5 but persists until E13.5, at

which time calponin transcripts are detected in smooth muscle-containing tissues (17).

Developmental diversity of SMCs

SMCs have a profound developmental diversity, since they are not derived from

a single embryonic origin (18). Rather, various primordial embryonic tissues give rise to

the different SMC lineages that are found in the adult, and each lineage is regionally

specified according to which tissue it arose from. Consequently, SMCs throughout the

adult arterial tree form a patchwork of the different embryonic origins from which they

derive. Genetic fate mapping approaches have been particularly helpful in delineating

these different sources of SMCs, which include the neural crest, second heart field,

proepicardium, somites, splanchnic mesoderm, mesothelium, and various

mesangioblasts and stem cells. Neural crest cells migrate then differentiate into SMCs

within the ascending and arch portions of the aorta as well as the carotid arteries.

Second heart field cells migrate to the cardiac outflow track where they form SMCs at

the base of the aortic root and pulmonary trunk. SMCs of the coronary arteries are

derived from the proepicardium, while those in the descending aorta arise from somites.

Role of SMC phenotypic switching in cardiovascular disease

Unlike cardiac and skeletal muscle, smooth muscle cells do not terminally

differentiate, but, instead, retain marked plasticity in their ability to switch between

synthetic and contractile phenotypes (19, 20). Such phenotypic switching is a hallmark

of SMCs and can be directly correlated with their differentiation (i.e. more differentiated

SMCs express a more contractile gene program) (Figure 1.1). Downregulation of these

contractile genes and upregulation of growth-related, proliferate, and synthetic genes is
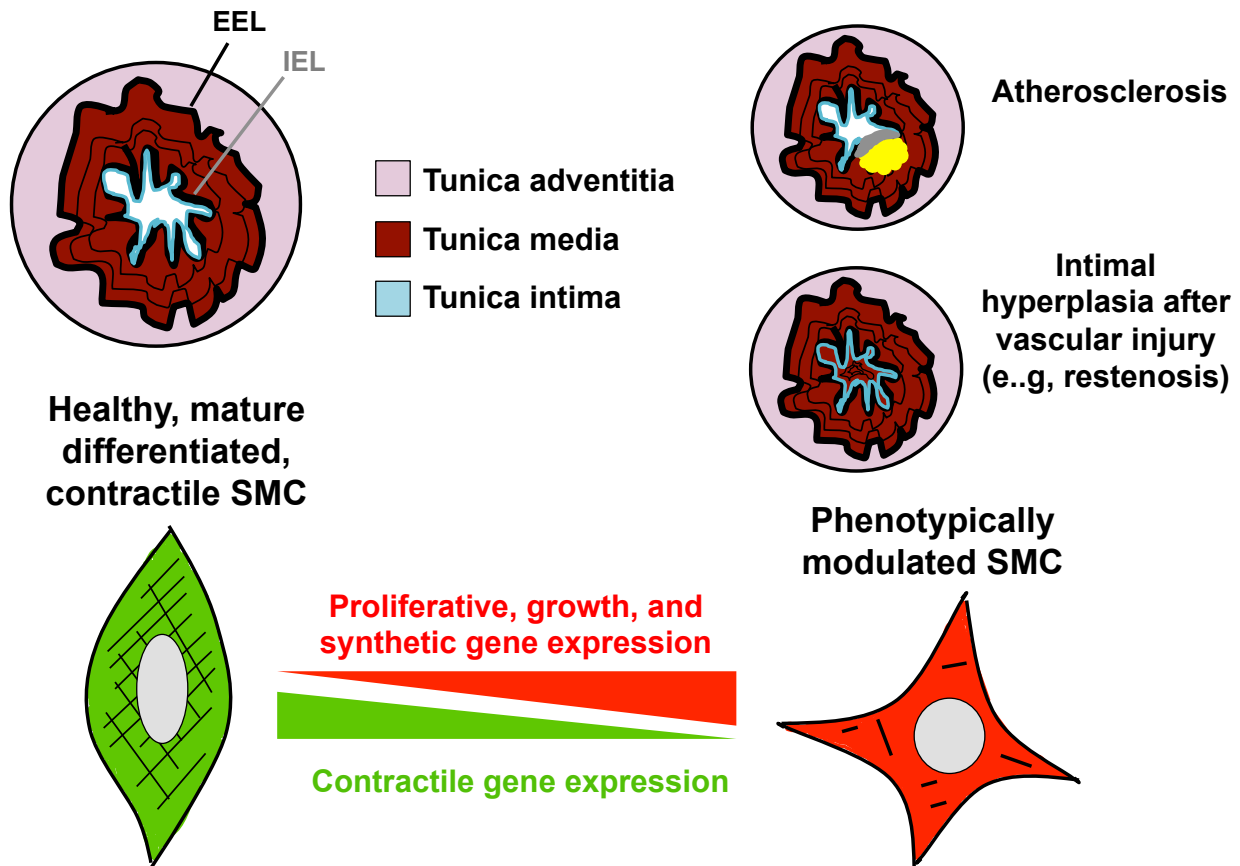
Figure 1.1. SMC vessel structure and phenotypic switching. Blood vessels are comprised of three layers: The Tunica intima (composed of endothelial cells), Tunica media (composed of SMCs), and the Tunica adventitia (composed of connective tissue and nerves). The internal elastic lamina (IEL) separates the tunica intima from the tunica media, while the external elastic lamina (EEL) separates the tunica media and the adventitia. In the healthy blood vessel, SMCs are quiescent and express high levels of contractile genes (SMA, SM22, CNN, and SM-MHC). However, during atherosclerosis or after vascular injury (e.g., restenosis), SMCs undergo extensive phenotypic switching characterized by loss of contractile markers and upregulation of proliferate genes. In the case of vascular injury, SMCs undergo intimal hyperplasia.

not only a hallmark of vascular disease, but contributes significantly to disease pathogenesis (21-23). Thus, SMCs play a fundamental role in the development of several vascular diseases, including atherosclerosis, restenosis post-angioplasty, aortic aneurysm, and hypertension. The contribution of the SMC within the context of each specific disease will be discussed, and the discussion on hypertension is saved for a subsequent section.

Atherosclerosis

Atherosclerosis is the leading cause of morbidity and mortality in the United States (24). The disease begins as a fatty streak on the luminal surface of blood vessels. With age, the fatty plaque enlarges and endothelial cells retain lipoprotein particles that evoke an inflammatory response by macrophages (25-27). The low-grade inflammation leads to endothelial and SMC activation. In response to this, SMCs undergo extensive phenotypic switching characterized by a downregulation in contractile gene expression, increase in proliferation and early growth response genes, as well as production and deposition of extracellular matrix (22, 23). Eary in disease, phenotypic modulation of the SMC is adaptive and allows for vessel repair by walling off the underlying thrombogenic material with a fibrous cap, thereby preventing clot formation. With chronic inflammation, however, macrophages secrete proteases that degrade the extracellular matrix of the stable fibrous cap, resulting in an unstable plaque with a thin cap (28). Continued inflammation leads to unstable plaque rupture, clot formation, and myocardial infarction/stroke.

Several transcription mechanisms mediating phenotypic modulation in SMCs have been identified (29). *First*, it is well established that PDGF-BB is a strong repressor of smooth muscle differentiation in cultured SMC (30). PDGF-BB binds to its tyrosine

kinase receptor and activates the Ras/Raf/MEK/ERK kinase pathway to stimulate Elk-1 phosphorylation and subsequent SRF-dependent early growth response genes (31). In response to PDGF-BB, phosphorylated Elk-1 (pElk-1) outcompetes myocardin, MRTF-A, and MRTF-B for SRF, ultimately leading to inhibition of mature SMC genes. pElk-1 recruits HDACs, thereby leading to decreased H4 acetylation and reduced SMC gene expression (32-35). To what degree PDGF-BB ligand contributes to SMC phenotypic modulation during atherosclerosis in vivo, however, is less understood. Although PDGF receptor blockade reduced atherosclerotic fibrous cap formation in athero-prone ApoE -/- mice, it is unclear how much of this is due to an SMC-specific effect since PDGFRβ was inhibited in several cell types in these studies (36). The Olson Lab inhibited the PDGFRβ-activated transcription factor, STAT1, in SMCs and found that plaque size was reduced in a mouse model of atherosclerosis. This study suggests that aberrant PDGF signaling activates STAT-mediated pathways specifically in vascular SMC to contribute to atherosclerotic lesion formation (37). Despite these data, however, SMC-specific PDGF receptor deletion mouse models will be required to directly assess the role of PDGFRβ activation in SMC. *Second*, dynamic binding of repressive complexes at GC repressors within SMC-specific promoters drastically reduces smooth muscle gene expression during disease. Proximal promoter regions within several smooth muscle genes that drive SMC-specific expression in vivo have been identified (14, 38, 39). Interestingly, a GC repressor in the SM22 promoter was required for downregulation of SM22 expression during atherosclerosis in vivo. Mutation of this GC repressor inhibited reduction of SM22-LacZ transgene expression in an ApoE -/- atherosclerosis mouse model (40). Although SRF is required for SMC differentiation, it can bind activating or repressing co-factors, as seen above for pElk-1 in response to PDGF-BB stimulation,

6

and can thus toggle between active or repressive transcriptional modules, respectively (41). During phenotypic switching, SRF binds KLF4, which inhibits SMC differentiation by binding to GC repressors in smooth muscle promoters (42, 43). Several studies have demonstrated that KLF4 is required for SMC phenotypic switching during atherosclerosis. In ApoE -/- mice a repressive complex consisting of KFL4, pELk-1, and HDAC2 is recruited to GC repressors in the SM22 promoter (44). Furthermore, in cultured SMC at least, KLF4 overexpression significantly reduces myocardin expression as well as that of smooth muscle-specific markers, suggesting that KLF4 is an important repressor of SMC differentiation during phenotypic switching (45).

Restenosis

Angioplasty uses balloon dilatation or metal stents to open a coronary artery that has been occluded from atherosclerotic narrowing. While these treatments improve mortality, they are associated with eventual restenosis, which usually occurs within 6 months after the procedure (46, 47). While bare metal stents reduce the likelihood of restenosis to 25% compared to the 60% chance associated with balloon angioplasty alone, there still remains considerable risk of restenosis from stenting (48, 49). Restenosis is caused by injury to the intimal surface of the artery, which stimulates SMC proliferation and migration around the stented region, a process referred to as intimal hyperplasia. Intimal hyperplasia can result in vessel occlusion and myocardial infarction. Several studies using wire injury models of restenosis have shown that PDGF-BB is required for the excess SMC proliferation and migration seen intimal hyperplasia (50-52). Similar to the changes that occur in atherosclerosis, SMCs undergo phenotypic modulation and lose their contractile protein repertoire. In fact, many of the same mechanisms that mediate transcriptional repression of SMC genes in atherosclerosis

7

also lead to phenotypic switching after vascular injury and restenosis, such as KLF4 binding to GC repressors in smooth muscle-specific gene promoters (40). Additionally, GATA-6, a transcription factor expressed in healthy, quiescent SMCs, is significantly downregulated with balloon injury to carotid arteries in mice (53, 54). As a result, SMC differentiation is inhibited and neointimas subsequently form. In this same model, smooth muscle gene expression is restored with GATA-6 rescue but not with a GATA-6 construct lacking the DNA binding domain. This study indicates that downregulation of GATA-6 after balloon angioplasty drives repression of smooth muscle gene expression.

Transcriptional regulation of SMC differentiation

The processes controlling SMC gene transcription are exceedingly complex, since multiple factors and different combinations thereof contribute to SMC differentiation and phenotype (29). In its vascular niche, the SMC responds to a myriad of growth factors, injury stimuli, extracellular matrix, components, cell-cell contacts, diffusible factors, and mechanical cell stretch, all of which converge to regulate smooth muscle gene expression. How all of these cues are integrated within the SMC to control differentiation is a major focus of vascular research and a key question in understanding how the SMC converts between contractile and synthetic gene programs so readily during development and different disease states. The transcription mechanisms underlying phenotypic switching of the SMC during disease have been presented above. In the sections that follow, the transcription factors and signaling molecules that regulate SMC differentiation under normal conditions will be presented.

Regulation of SMC differentiation by SRF, myocardin, and the MRTFs

In contrast to cardiac and skeletal muscle, a single transcriptional "master regulator" of smooth muscle-specific differentiation has yet to be identified. SRF,

although critical for SMC differentiation, also regulates cardiac and skeletal muscle gene expression and thus cannot be considered a master regulator of SMC-specific transcription (55-57). In fact, cardiac, skeletal, and smooth muscle express many of the same transcription factors, suggesting that additional transcription mechanisms and/or factors distinguish a SMC from a cardiomyocyte and skeletal muscle cell. As indicated above, unique combinations of transcription factors with isoform-specific distribution contribute to SMC-specific gene expression. Additionally, as will be discussed below, transcription factor binding is intricately tied to the epigenetic signature of the SMC.

SMC differentiation is controlled by serum response factor (SRF), which was first identified as a MADS box-containing protein that binds a serum element in the c-fos gene (58) The MADS box family of transcription factors are highly conserved and play critical roles in transcriptional regulation (59). The MADS box mediates DNA binding, homodimerization, as well as interaction with other transcription factors (60, 61). SRF is essential for differentiation of the mesoderm, as SRF null mouse embryonic stem cells fail to develop into this lineage or express muscle-specific genes (e.g., smooth muscle alpha actin) (59). SRF binds to consensus $CC(A/T)_6GG$ (CArG) sequences in the promoters and enhancer elements in virtually all smooth muscle-specific genes, and the SRF-CArG association is critical for SMC differentiation (62-67).

Several seminal studies demonstrated that CArG elements in the SMA and SM-MHC promoters were essential for SMC-specific expression in vivo (66, 38, 39). One of these studies, for example, showed that a large region including the promoter and first intron of the SM-MHC gene, which contain several CArG boxes, were sufficient to recapitulate SMC-specific expression in a variety of tissues (38). Further mutational analyses revealed that the promoter CArG regions were required for the smooth

9

muscle-selective expression pattern, but the intronic CArG was only required for

expression in large arteries (39). These data suggest that CArG elements can function

differentially depending on their genomic context. Furthermore, studies from our lab

using LacZ transgenic mouse models indicated that a CArG in the promoter of the

mDia2 promoter was required for smooth muscle-specific expression in various tissues,

including aorta, bladder, and lung (unpublished data). Recently, our group and others

have used CRISPR/Cas9 gene editing to delete CArG elements in vivo. CRISPR/Cas9

technology has become the "holy grail" for studying gene function, since it allows

researchers to edit a gene or critical gene region in its endogenous context. Such an

approach is particularly useful for identifying key regulatory regions important for gene

expression because the effects of deletions on native chromatin interactions can be

studied, which was not possible with previous transgenic reporter approaches (e.g.,

promoter-Lacz). As demonstration of this approach's utility, CRISPR/Cas9-mediated

deletion of a CArG in the endogenous calponin mouse gene drastically reduced its

expression in vivo, thereby allowing identification of an essential regulatory element (69,

70).

Although SRF is required for SMC differentiation, it is unable to fully drive smooth

muscle gene expression. Additional co-activators including myocardin and the

myocardin-related transcription factors (MRTF-A and -B) bind to SRF to fully

transactivate SMC differentiation (71-79). Also, SRF binding to either of these

transcription factors increases its association with SMC promoters (63). Although the

myocardin family members are required to stimulate SRF-dependent gene expression,

each co-factor has its own unique expression pattern and, consequently, its own

associated distinct phenotype in response to its deletion in vivo. Myocardin, although

expressed in several cell types, is preferentially expressed in SMCs and cardiomyocytes and its deletion results in fatal yolk sac and vascular defects associated with loss of smooth muscle marker gene expression (80, 81). Alternatively, MRTF-B ablation results in failed differentiation of neural crest-derived SMCs, causing late embryonic lethality (~E17.5) due to aortic arch and outflow track defects (82). Finally, MRTF-A null mice display defective myoepithelial differentiation, which causes decreased mammary gland function and eventually involution. As a result, pups of MRTF-A -/- mothers exhibit a failure to thrive syndrome from decreased feeding and malnourishment (83).

Regulation of SMC differentiation by RhoA signaling

The Rho GTPases consist of a family of proteins that translate extracellular cues into signaling cascades that regulate critical cell functions including migration, polarity, maintenance of cell-cell junctions, and contraction (84-87). The 22 different Rho GTPases fall into one of three categories: RhoA, Rac-1, or Cdc42. While each Rho GTPase has its own predominant function within the cell, coordination between all of the individual GTPases is required for successful cell motility. In general, Rac-1 and Cdc42 act at the cell's leading edge to stimulate lamellipodia and filopodia formation, respectively, while RhoA activation at the back of the cell stimulates retraction through actomyosin contraction. RhoA is also responsible for actin stress fiber formation (88). Precise spatiotemporal regulation of Rho GTPase activity is required for these coordinated cell functions to occur (89). Rho GTPases cycle through active, GTP-bound and inactive, GDP-bound states, which are catalyzed by guanine nucleotide exchange factors (GEFs) and GTPase activating proteins (GAPs), respectively (Figure 1.2A). Guanine nucleotide dissociation inhibitors (GDIs) inhibit Rho GTPases by sequestering

them in the cytosol, thereby preventing them from interacting with downstream effectors at the cell membrane (90). In total, there are approximately 80 RhoGEFs (91-93). The GEF's basic catalytic unit is a Dbl-homology (DH) domain that mediates the exchange of GDP for GTP on the Rho GTPase. A plekstrin-homology (PH) domain is located C-terminal to the DH domain and mediates the GEF's interaction with the cell membrane. Other downstream accessory regions within the GEF are variable and mediate protein-protein and protein-lipid interactions. The GEFs counterpart, RhoGAPs, catalyze the slow intrinsic hydrolytic activity of the GTPase, thereby promoting the GDP (inactive) form. RhoGAPs are comprised of about 65 different members (94). The basic catalytic unit of the RhoGAP is the GAP domain, which hydrolyzes GTP into GDP. Like GEFs, RhoGAPs often contain additional domains that mediate interactions with membrane phospholipids and other proteins.

Our lab and others have shown that MRTF-dependent SMC differentiation is activated strongly by the small GTPase, RhoA (95-97). Under basal, unstimulated conditions, MRTF-A is sequestered in the cytoplasm by G-actin. In response to G-protein coupled receptor (GPCR) stimulation by a variety of ligands (e.g., S1P), RhoA stimulates actin polymerization, a process mediated by the RhoA effectors, ROCK and mDia1/2. Conversion of G-actin to F-actin frees MRTF-A from actin, thereby unmasking a nuclear localization sequence (NLS) within the G-actin-binding RPEL domains of MRTF-A (98, 99). With the NLS exposed, MRTF-A enters the nucleus via an importin-based mechanism and then binds SRF to transactivate expression of SMC-specific genes (e.g., SM22, smooth muscle alpha-actin, calponin) required for mature SMC function (100) (Figure 1.2B). Myocardin, which cannot binding G-actin and is constitutively nuclear, is therefore different from the MRTFs in this regard.
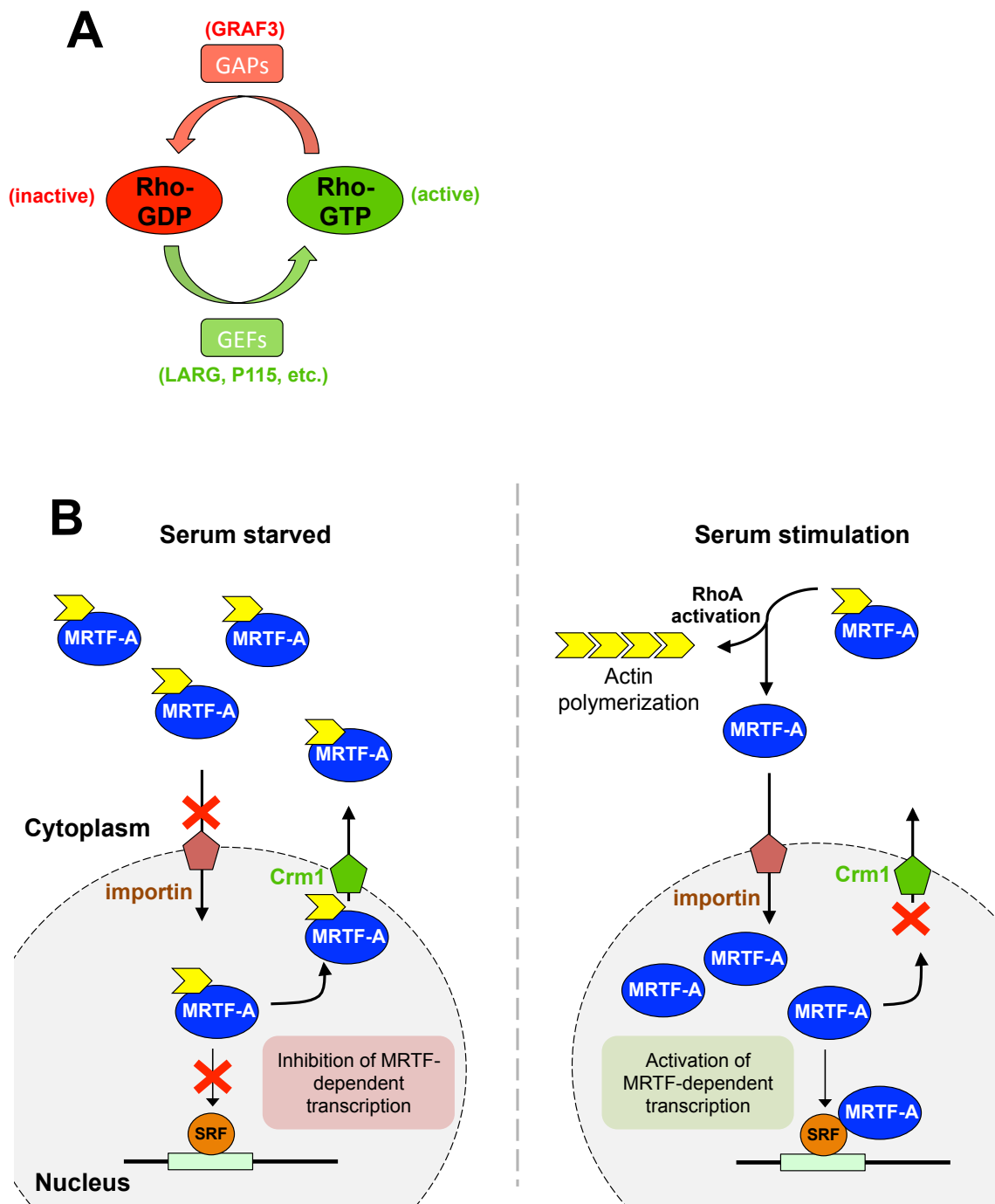
Figure 1.2. RhoA signaling regulates MRTF nuclear localization in SMC. A) RhoA GTPase cycling between active (GTP-bound) and inactive (GDP-bound) forms is catalyzed by GEFs and GAPs, respectively. **B)** Under serum starved conditions, MRTF-A is sequestered in the cytoplasm by G-actin. MRTF-A is rapidly exported out of the nucleus by Crm-1 (exportin). Serum stimulation leads to RhoA activation, which induces F-actin polymerization. MRTF-A enters the nucleus via an importin-based mechanism and activates SRF-dependent genes.

Myocardin and the MRTFs contain several conserved domains that mediate their transcriptional activity (Figure 1.3). First, myocardin, MRTF-A, and MRTF-B all possess a B1 domain located between the RPEL and glutamine-rich region near the N-terminus of the proteins. The B1 domain mediates the interaction with SRF (73). All three factors share an SAP domain, whose function is less defined. However, in other proteins, the SAP domain controls nuclear dynamics and organization (101). A leucine zipper (LZ) domain, located at the center of each transcription factor, mediates homo- and heterodimerization between myocardin and the MRTFs. Finally, at the C-terminal region, myocardin contains a transcriptional activation domain (TAD) required for complete transactivation of SRF target genes (102). Interestingly, the TAD is weakly conserved between myocardin and the MRTFs, suggesting disparate mechanisms of regulation between the two transcription factors.

Previous studies from our lab indicated that S1PR2 signals through the RhoA GEF, LARG, to drive SMC differentiation and inhibit migration (103). Other studies demonstrated that LARG knockout mice exhibit decreased sensitivity to salt-induced hypertension (104). Further, combined deletion of LARG and PDZ Rho-GEF (PRG) in mice results in vascular branching defects, indicating that combinatorial interactions between RhoA GEFs influence vascular morphogenesis and/or overlapping function between two or more GEFs exists (105). Additional experiments from the Mack Lab identified an important role for the RhoA effectors, mDia1 and mDia2, in SMC differentiation. Knockdown of mDia1/2 significantly decreased smooth muscle markers, including SM-MHC, calponin, SMA, and SM22, and further inhibition of mDia signaling prevented directional migration in SMC (106). In further support of mDia1/2's role in SMC phenotypic modulation, dominant negative mDia (DNmDia) driven by a SM22-Cre

14
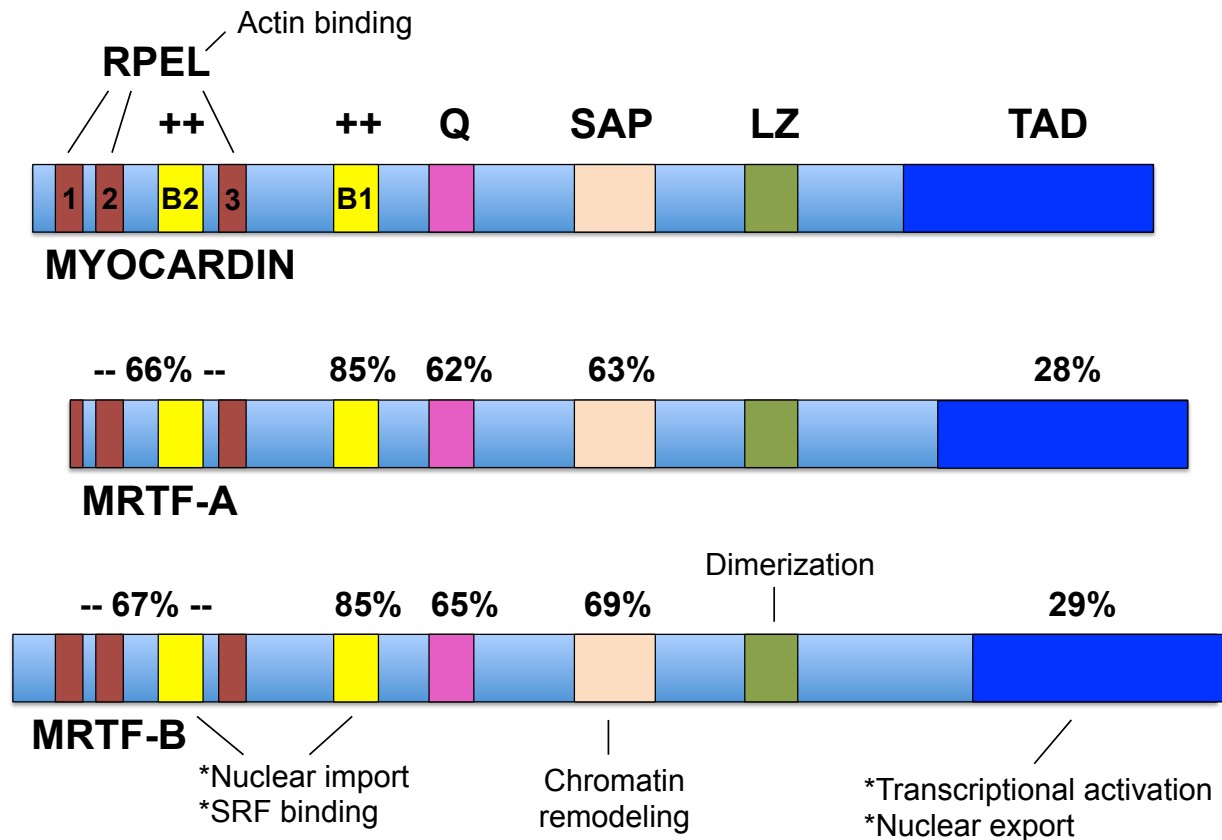
Figure 1.3. Domain structure and conservation of myocardin and the MRTFs.
Conserved domains in the mouse myocardin, MRTF-A, and MRTF-B transcription factors include RPEL domains, Basic regions (B1 and B2), a Q-rich region, SAP domain, Leucine Zipper (LZ) domain, and a transactivating domain (TAD). MRTF-A and MRTF-B share near identical sequence conservation with each other.

reporter prevented re-expression of SM-MHC and calponin 7 days after carotid artery ligation in a mice. Interestingly, ligated arteries from DNmDia mice displayed reduced neo-intimas compared to wild-type littermates, most likely due to its inhibitory effects on SMC migration and polarity. Of note, a subset of SM22-Cre+/DNmDia+ mice exhibited a runted, hairless phenotype, patent ductus arteriosus, and embryonic hemorrhagic phenotypes (107). In addition to conventional RhoA signaling, our lab and others demonstrated that nuclear RhoA signaling is a novel mechanism regulating SMC differentiation. mDia2, which shuttles between cytoplasmic and nuclear compartments, stimulates nuclear actin polymerization as well as MRTF-dependent SMC transcription. Furthermore, forced expression of NLS-tagged LARG significantly enhanced promoter activities of SMC-specific genes by upregulating RhoA signaling in the nucleus (108).

Post-translational modifications of SRF, myocardin, and MRTF-A

In addition to directly regulating chromatin dynamics, post-translational modifications (PTMs) also affect transcription factor function and downstream target gene expression (109). Some of these PTMs include phosphorylation, ubiquitylation, methylation, acetylation, and oxidation. Myocardin acetylation by p300 enhances its association with SRF, stabilizes the myocardin-SRF-CArG complex, and upregulates smooth muscle and cardiac gene expression (110, 111). Myocardin is also phosphorylated by GSK3β and ERK, which both inhibit myocardin-dependent smooth muscle transcription (112, 113). Phosphorylation of SRF at T159 by PKA inhibits its interaction with CArG boxes, thereby diminishing downstream SMC-specific promoter activity (114).

Early studies identified a critical ERK phosphorylation site within MRTFA (S454), which inhibited MRTF-A's nuclear localization by stabilizing its interaction with

16

cytoplasmic G-actin (115). More recent reports indicate that MRTF-A is phosphorylated at several other residues, each of which has varied effects on its nuclear localization (116). Interestingly, sumoylation of MRTF-A represses its ability to transactivate smooth muscle promoters, while SUMO modification activates myocardin at cardiac genes (117, 118). Clearly, tight post-translational regulation of SRF and the myocardin family of transcription factors is an important mechanism controlling smooth muscle gene expression in response to different stimuli and contexts. It will be necessary to identify additional PTMs regulating activity of smooth muscle transcription factors and their effects on SMC differentiation.

Regulation of SMC differentiation by Notch/RBPJ

Although myocardin and the MRTFs are by far the most potent drivers of SMC differentiation, additional transcription factors regulate smooth muscle gene expression. The transcription factor RBPJ is ubiquitously expressed and binds to consensus GTGGG sequences in Notch target genes (119-121). Notch/RBPJ signaling is required for arterial specification during development and maintains blood vessel integrity by inducing SMC differentiation (122, 123). Work in zebrafish revealed that Notch signaling was essential for arterial specification. Specifically, inhibition of Notch diminished expression of the arterial markers ephrinB2 and deltaC, while overexpression of Notch repressed venous specification. Further, Notch inhibition causes various vascular defects including arterio-venous shunting, cranial hemorrhage, and reduced circulation through specific vascular beds (124, 125). Deletion of the Notch3 receptor in mice leads to loss of cerebral vascular integrity due to degenerative SMCs that do not express smooth muscle markers. As a result, Notch3 deficient cerebral vessels are leaky and do not exhibit normal contractile properties (126, 127). Notch3 deficiency is phenocopied in

17

the human disease, CADASIL, in which patients suffer from transient ischemic attacks

due to subcortical infarcts. Histological examination of post-mortem tissues from

CADASIL patients revealed loss of cerebrovascular SMC, very similar to that seen in

Notch3 deficient mice (127, 128).

Notch is activated when a cell expressing jagged or delta-like ligand engages the

Notch receptor expressed on the surface of a neighboring SMC. Upon notch activation,

gamma secretase cleaves the notch intracellular domain (NICD), which translocates

into the nucleus to bind to RBPJ. Under unstimulated conditions, RBPJ binds

mastermind-like (MAML), which represses notch target genes. However, with notch

activation, NICD displaces MAML and increases RBPJ/Notch-dependent transcription.

While this model implies that RBPJ activates gene expression, independent studies

indicate that the effect of RBPJ on SMC differentiation is highly context specific (129,

130). For example, one study demonstrated that NICD overexpression and jagged-1

stimulation increased SM-MHC expression in SMC, while another study from the same

lab reported that HERP-1, a notch target gene, was induced after arterial balloon injury

and repressed myocardin-dependent smooth muscle transcription by physically

inhibiting SRF-CArG binding (131-133). Furthermore, our lab recently showed that

RBPJ binds to methylated GC repressors in the SM-MHC promoter to inhibit

transcription after vascular injury (120). All together, these studies suggest that Notch

can function as both a repressor as well as an activator of SMC differentiation

depending on its specific context.

Regulation of SMC differentiation by the TEADs

The transcriptional enhancer family (TEF)/TEA domain (TEAD) transcription

factors are downstream mediators of the Hippo signaling axis (134). In brief, activation

of Hippo leads to phosphorylation of the Mst1/2 serine/threonine kinases, which activate

another set of serine/threonine kinases, called Lats1/2. Active Lats1/2 phosphorylate

and inhibit Yap/Taz, which prevents their nuclear accumulation and subsequent

activation of the TEAD transcription factors. Thus, when the Hippo pathway is activated,

TEADs inhibit target gene expression. Only when Hippo is inactive are Yap/Taz able to

translocate to the nucleus to bind to the TEADs to relieve target gene repression. The

Hippo signaling cascade has been implicated in a variety of cellular functions, including

regulating cell size, proliferation, cell-cell communication, stem cell renewal, and

differentiation (135-137).

Members of the TEAD family, composed of TEADs 1-4, are expressed to varying

degrees in smooth, cardiac, and skeletal muscle tissues and regulate expression of

muscle-specific genes (138). TEAD1 is highly smooth muscle-specific and has been

shown to regulate SMC differentiation, although the exact direction of effect is not

understood (139, 140). All TEAD proteins contain a highly conserved N-terminal TEA

DNA-binding domain, which recognizes consensus motifs. In particular, TEAD1

recognizes the MCAT motif (CATTCCT), which is found in regulatory regions of several

smooth muscle-specific genes, including SMA (141, 142). Intriguingly, the effect of

MCAT site mutation differed significantly in SMCs versus granulation tissue fibroblasts.

While MCAT mutation abolished LacZ expression in granulation tissue, there was no

effect of the mutation in adult SMCs (143). It is possible that additional interactions

between TEAD1 and other cell-type specific transcription factors coordinate the ultimate

effect on differentiation. Indeed, interactions between TEAD1 and other transcription

factors have been identified. TEAD1 and SRF interact and cooperatively regulate

expression of the skeletal alpha-actin gene (144). TEAD1 also interacts with MEF2C to

drive expression of muscle-specific genes (145, 146). It is thought that unique

combinations between TEAD1 and other transcription factors contribute to SMC-specific

gene expression and may explain the different effects of TEAD1 on smooth muscle

differentiation at different developmental stages.

Regulation of SMC differentiation by Nkx-3.2 and GATA-6

Nkx-3.2 and GATA-6 form a tripartite complex with SRF to modulate smooth

muscle-specific differentiation. Interestingly, when either the Nkx, GATA, or CArG DNA

binding motif is mutated within the alpha1 integrin luciferase promoter construct,

transcription activity is significantly reduced, indicating cooperativity between all three of

these factors (147-149). Furthermore, Nkx-3.2, GATA-6, and SRF have overlapping

expression in the arterial SMCs, which differs from the cardiac-specific expression

patterns of Nkx-2.5 and GATA-4 (150). These studies indicate that transcription factors

other than myocardin and the MRTFs likely function in an SRF/CArG-dependent

manner to further distinguish smooth versus cardiac muscle differentiation.

Regulation of SMC differentiation by TGFβ

TGF-β upregulates SMC differentiation by activating the SMAD family of

transcription factors and is an important environmental cue for the SMC during

development and disease. In in vitro models of SMC differentiation, TGF-β converts

undifferentiated, fibroblast-like 10T1/2 cells into elongated, contractile SMCs (151).

Additionally, TGF-β plays a critical role in vascular development. Specifically, TGF-β is

required for migration and differentiation of the cardiac neural crest cells into SMCs of

the ascending aorta (152). TGF-β is also required for recruitment of SMCs to other

locations throughout the developing vascular network. Genetic deletion of both TGF-β

alleles in mice leads to embryonic lethality due to reduced SMC coverage of the yolk

sac (153). TGF-β also plays a pivotal role in development of aortic aneurysms, in which

aortic dilatation is due to degeneration of the artery's medial layer. Although aortic

aneurysms are relatively rare, they are associated with a strikingly high mortality rate.

By far, the most direct line of evidence linking SMCs and aortic aneurysms are human

mutations within the TGFβ signaling axis that lead to varying degrees of pathology. To

date, mutations have been identified in TGFBR1, TGFBR2, TGFB2, SMAD3, and

SMAD4, which are found in patients with aortic aneurysm syndromes (e.g., Loeys-Dietz

Syndrome) (154-159). Of note, smooth muscle gene expression is downregulated in

aortic aneurysm samples and is observed in a mouse model of early aortic aneurysm

formation, indicating that failed SMC differentiation may contribute to disease (160).

The SMAD family of transcription factors, specifically SMAD2, 3, and 4, are

critical for SMC differentiation and normal vascular development (152). The SMAD

transcription factors (hereon referred to as SMADs) are downstream of TGF-β signaling.

Briefly, cleaved TGF-β ligand binds to type II TGF-β receptor, which leads to

phosphorylation of the type I receptors. Subsequently, phosphorylated type I TGF-β

receptor recruits and phosphorylates SMAD2 and SMAD3, which promotes their

interaction with SMAD4. The SMAD2/3/4 complex translocates into the nucleus, where

it binds to a GTCT DNA element, but with low affinity. Given such weak binding, the

SMADs interact with other transcription factors to drive robust TGF-β-dependent gene

expression. For example, SMAD3 interacts with deltaEF1 to transactivate TGF-β-target

genes. Importantly, some of the effects of TGF-β are SRF-CArG-dependent, and

SMAD3 can interact with SRF directly to fully activate SMC-specific gene expression

(161). The SRF-SMAD3 complex recruits myocardin to potentiate this effect (162). In

further support of this, mutation of CArG elements in luciferase reporters prevents

transcriptional activation by TGF-β (163-165). In addition to these direct effects, TGF-β indirectly upregulates SMC differentiation by increasing the expression of genes that themselves enhance SMC transcription. For example, TGF-β increases expression of the RhoA GEFs, Net-1 and GEF-H1, which activate RhoA-dependent SMC-gene transcription (166, 167).

Regulation of SMC differentiation by extracellular matrix and cell stretch

Various extracellular matrix proteins signal through integrin receptors to differentially regulate SMC differentiation and phenotype (168-171). Freshly isolated SMCs grown on fibronectin are more synthetic and proliferative, while collagen IV and laminin maintain the SMC in its differentiated, contractile state (172). This response is best exemplified during the SMC's response to injury, where breakdown of extracellular matrix proteins and re-expression of fibronectin stimulates SMC dedifferentiation and proliferation (173, 174). In brief, upregulation of extracellular matrix-integrin signaling by fibronectin leads to activation of the non-receptor tyrosine kinases, focal adhesion kinase (FAK) and Src, which activate the ERK signaling pathway (175). ERK activation downregulates SMC differentiation. In contrast, collagen IV upregulates SMC differentiation by increasing expression of myocardin as well as enhancing enrichment of SRF at CArG boxes in SMC-specific gene promoters (176). The exact signaling mechanisms downstream of laminin and collagen IV that lead to increased SMC transcription, however, are less understood.

Stretch of the blood vessel, particularly in hypertension, results in increased contractile gene expression in the SMC. Additionally, prolonged stretch induces remodeling to a thicker vessel (177-179). The stretch response is largely dependent on RhoA activity, which induces actin polymerization and MRTF nuclear translocation. The

role of RhoA in the stretch response is demonstrated by inhibiton of stretch-induced

upregulation of SMC-specific gene expression in cells treated with the Rho inhibitor, C3

transferase, and to a lesser extent with the ROCK inhibitor, Y-27632 (180). Additionally,

there is some evidence that FAK, ERK, and Akt are involved in the stretch response.

Specifically, FAK and ERK phosphorylation increases in response to portal vein stretch,

and FAK activity was required for the differentiation of mesenchymal stem cells

subjected to stretch (181, 182).

Please refer to Figure 1.4 for a summary of the transcription mechanisms regulating

SMC differentiation under normal conditions as well as in the phenotypically modulated

disease-associated state.

Epigenetic mechanisms regulating SMC differentiation

Histone acetylation and methylation

Epigenetic regulation of gene expression is characterized by mechanisms that

reversibly modify DNA bases, histone tails, or transcription factors, without changes to

the DNA sequence. Thus, two cells that are genotypically identical can have completely

opposite phenotypes due to very different epigenetic mechanisms controlling their gene

expression. One of the ways epigenetic mechanisms regulate transcription is by

affecting the accessibility of critical transcription factors to DNA (183). In its native

conformation, genomic DNA is wrapped around core histones to form a nucleosome,

which is the basic unit of chromatin. Histone modifications, which alter histone charge

and thus interaction with other histone components and DNA, affect nucleosome

density and chromatin organization. Less dense, more unpacked nucleosome

configurations allow transcription factors to contact the DNA to influence gene

expression directly by recruiting other DNA binding proteins, including RNA polymerase
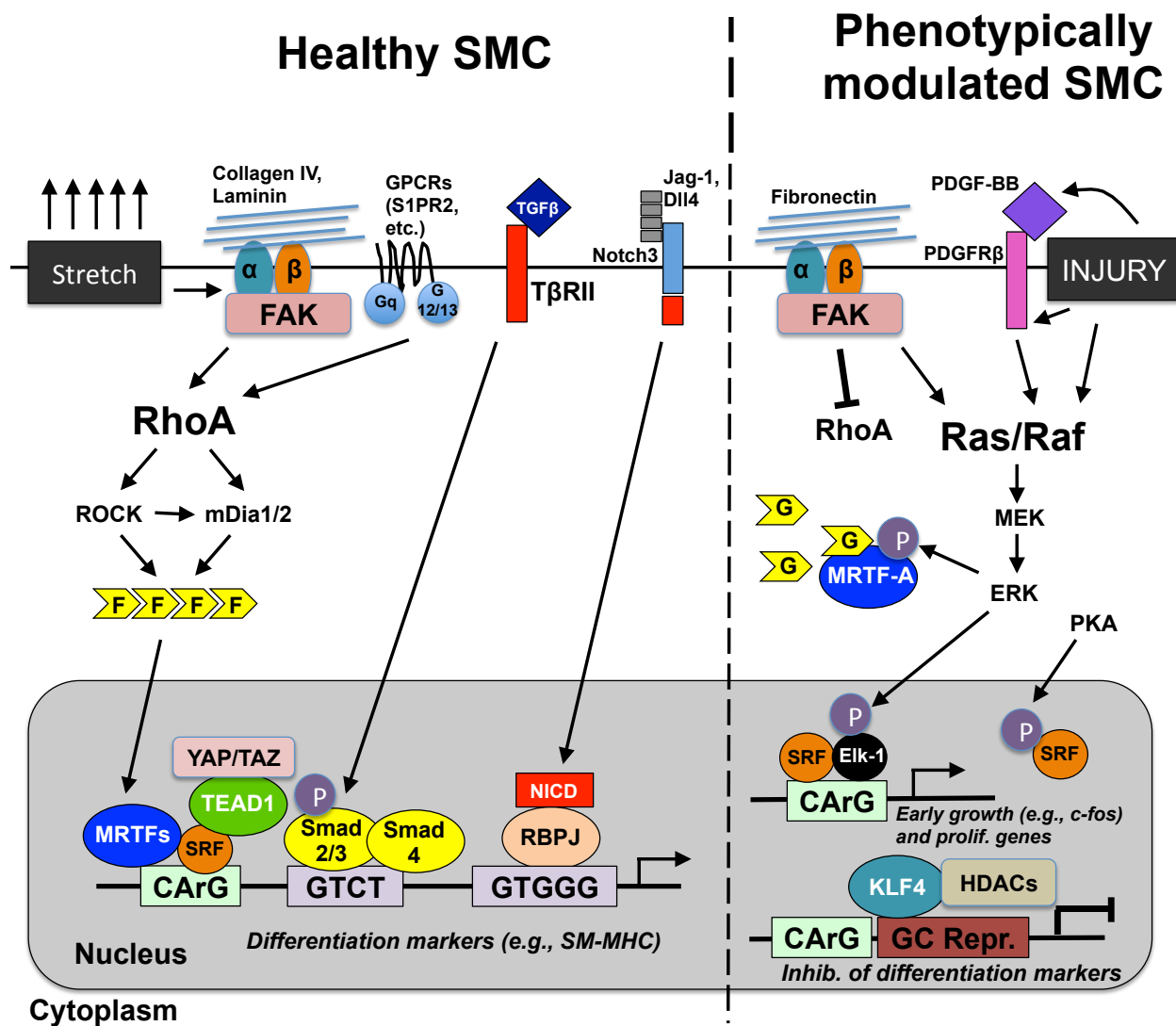
Figure 1.4. Contrasting the transcription mechanisms that regulate SMC differentiation in the healthy versus phenotypically modulated SMC. Left) Multiple environmental cues and signaling pathways converge to regulate expression of mature SMC markers (e.g., SM-MHC). These include cell stretch, extracellular matrix, and GPCR activation, which signal through RhoA. TGFβRII and Notch activation are also potent stimulators of SMC differentiation. **Right)** Signaling mechanisms regulating dedifferentiation in SMC in disease states such as atherosclerosis. Injury stimulates downstream Ras/Raf/MEK/ERK pathways directly and indirectly by activating PDGF-BB signaling. Note that FAK inhibition of RhoA is transient and later leads to RhoA activation. Expression of early response growth genes is upregulated, leading to proliferation and fibronectin production, which further propogates phenotypic switching.

24

II, to initiate transcription.

Histone acetylation and methylation occur mainly on lysines and are catalyzed by histone acetyltransferases and histone methyltransferases, respectively. These histone marks are reversed by histone deacetylases and demethylases, respectively, as their names suggest. Generally, histone acetylation leads to a more "open" chromatin configuration (referred to as euchromatin), while methylation results in both open or closed (heterochromatin) chromatin states, depending on which histone and histone tail residue is modified. H3K4 and H3K79 methylation are associated with transcriptionally active, open regions in SMC-specific genes, while H3K9, H3K27, and H4K20 methylation mark heterochromatinized gene regions (184). Several histone/chromatin modifiers that regulate SMC differentiation have been identified, and these will be discussed below.

Histone modifications are tightly connected to the SRF/CArG interaction (185). Seminal work by the Owens Lab indicated that myocardin interacted with H3K4 dimethylation and enhanced SRF binding to CArG boxes in SMC gene promoters. This same study revealed that SRF enrichment at CArGs led to H3K9 acetylation and H3K79 dimethylation, both features of active transcription, since CArG mutant promoters did not display these features of open chromatin (63). Separate studies found that myocardin induced acetylation of histones by recruiting the histone acetyltransferase, p300 (111). Thus, epigenetic mechanisms directly enhance SRF/myocardin binding to DNA, which in turn recruits histone-modifying enzymes that deposit specific marks to further promote accessibility of key transcription factors.

Chromatin and epigenetic modifiers in SMC

Additional histone modifiers in SMC have drastic effects on smooth muscle

transcription. Histone lysine methylation is catalyzed by SET (Su(var)3 to 9, Enhancer of Zeste, Trithorax) domain-containing lysine methyltransferases. Seven families of histone methylransferases exist: SUV39, SET1, SET2, RIZ, SMYD, EZ, and SUV 4-20. Some methyltransferases, including SET7/9 and SET8, do not belong to any of these families. The most studied is the SUV39 family, which includes G9a, SUV39H1, SUV39H2, SETDB1, and SETDB2 and specifically methylate H3K9. Lysine methyltransferases can mono-, di-, or tri-methylate a single lysine residue, and the degree of methylation for each methyltransferase is different (186). Additionally, each methyltransferase may methylate more than one lysine per histone. For example, SMYD2 methylates H3K4 and H3K36 (187). Adding to this complexity, methylation at one histone lysine residue may prevent or promote methylation at an adjacent lysine (183). Furthermore, there is additional crosstalk between methylation and other histone modifications, including acetylation and phosphorylation. Histone methylation is reversed by various histone demethylases, each of which recognizes different lysines on specific histones. The H3K9-specific demethylase Jmjd1a is expressed in multiple tissues, including SMCs, and decreases H3K9 methylation at CArG-containing smooth muscle promoters. Interestingly, our lab showed that Jmjd1a interacts with all three myocardin family members, and Jmjd1a overexpression resulted in significant transactivation of myocardin/MRTF-dependent transcription of SMA and SM22 promoters. Conversely, Jmjd1a knockdown in SMC inhibited MRTF-dependent gene expression, which coincided with upregulation of H3K9 dimethylation at multiple SMC-specific promoters (188).

Although SET-containing histone methyltransferases have not been examined with respect to SMC differentiation per se, there is evidence to suggest a role for them

in regulating histone methylation at smooth muscle promoter regions. Inhibiting either

SET7/9 or G9a in mice reduces renal fibrosis and expression of smooth muscle

markers, such as SMA (189, 190). Furthermore, SET7/9 induces expression of smooth

muscle genes in mouse embryonic stem cells (191). In addition to their canonical roles

in methylating histones, histone methyltransferases can also methylate non-histone

proteins. For example, YY1, a transcriptional repressor of SMC differentiation, is

methylated by SET7/9. YY1 methylation at K173 and K411 increased its binding affinity

to p53, RAD1, and ABL1 promoters (192). Whether or not SET7/9 methylation of YY1

affects binding to smooth muscle-specific promoters has yet to be determined. Also,

further studies are needed to determine if YY1 methylation affects its interaction with

SRF, since YY1 is a known SRF-interacting protein.

Brg1 and Brm, which are components of the ATP-dependent chromatin

remodeling SWI/SNF complex, are required for myocardin/MRTF-dependent gene

expression in SMC. Brg1, SRF, and MRTF-A form a transcriptional complex, and Brg1

facilitates the ability of both myocardin and MRTF-A to increase binding of SRF to CArG

boxes (193, 194).

DNA methylation and demethylation are significant epigenetic mechanisms

regulating smooth muscle gene transcription (195). The TET family of DNA

demethylases cause gene activation by oxidizing methylated-cytosine. Base excision

repair converts (i.e. demethylates) methyl-cytosine to unmethylated-cytosine. TET2

associates with CArG elements and is necessary for SMC differentiation. TET2

expression correlates with SMC phenotype and is upregulated in mature, contractile

SMCs but downsregulated after vascular injury and in atherosclerotic lesions.

Importantly, TET2 knockdown exacerbates the injury response due to further repression

of smooth muscle gene expression (195, 197).

DNase-I Hypersensitivity

DNase-I Hypersensitivity is employed to identify open chromatin regions throughout the genome. Several software programs can be used to call the DNase Hypersensitive Sites (DHS) as peaks and thus indicate regions that are accessible to transcription factors (198, 199). In this manner, DHS can be used in combination with other relevant bioinformatic datasets (ChIP-seq, 3C, conservation, etc.) to denote critical promoter and enhancer regions as well as long-range chromatin interactions that control cell type-specific gene expression (200).

Non-coding RNAs in SMC differentiation

Nearly 75% of the human genome is transcribed, but only 3% is actually translated into (i.e. "encodes") protein (201). Over the last two decades, non-coding RNAs (ncRNAs) have emerged as significant regulators of cell function, affecting processes including proliferation, apoptosis, and differentiation (201-204). Although there are several categories of ncRNAs, the two most studied are the microRNAs (miRNAs) and long non-coding RNAs (lncRNAs). miRNAs are short single-stranded RNAs about 22 nucleotides in length that generally silence gene expression by binding to the 3'UTR of mRNA to block translation (205). Importantly, a single miRNA can target multiple genes, which is once reason why miRNAs can have such drastic effects on cell phenotype. Several miRNAs that affect SMC differentiation and/or phenotype have been identified, including miR-221 and miR-222, which inhibit vascular smooth muscle differentiation and increase SMC proliferation (206, 207). Knockout of these two miRNAs in mice led to reduced SMC proliferation and neointima formation after balloon angioplasty (208). While roles have been described for additional miRNAs in regulating

SMC differentiation, the most studied miRNAs are the miR-143/145 cluster. miR-143

and miR-145, which are transcribed from the same gene locus, are highly expressed in

SMC. Numerous studies characterizing the expression pattern of the miR-143/145

cluster in vivo indicate that their expression is highly specific to vascular SMCs (209).

miR-143/145 repress proliferation by inhibiting KLF4 and Elk-1 and activate

differentiation by stabilizing myocardin (210). The miR-143/145 duo is thus a rare

example of miRNAs that selectively enhance rather than repress their target.

Interestingly, this miRNA cluster is regulated via an SRF-dependent mechanism, and

thus can increase its own expression via a feed-forward mechanism by directly targeting

and increasing myocardin levels. Furthermore, miR-145 represses several actin-

remodeling proteins, which results in substantial cytoskeletal reorganization (211, 212).

Given that actin polymerization is directly linked to MRTF nuclear translocation and

subsequent activation of SRF-dependent SMC genes, this is yet another pathway by

which mir-145 affects SMC differentiation.

Long non-coding RNAs (lncRNAs) refer to a class of ncRNAs longer than 200

nucleotides. LncRNAs are classified based on 1) where they are transcribed from

relative to a coding gene and 2) local (cis-lncRNA) or distant (trans-lncRNA) targeting.

From these two broad categories, several types of lncRNAs exist. The most studied

types include antisense transcripts (NATs), intronic, and intergenic lncRNAs. NATs are

located at the 5' or 3' ends of coding genes and contain exons that overlap those of

their gene targets. NATs can affect transcription by competing with the coding DNA

strand for RNAPol II and other transcription factors, especially if the lncRNA and coding

gene share the same promoter (213). Alternatively, the lncRNA may recruit histone

modifiers that repress transcription of the coding gene. Intronic lncRNAs originate from

the introns of the coding genes they overlap, while intergenic lncRNAs are transcribed from genomic loci between genes (214).

Several lncRNAs in SMCs have been identified. One of the first lncRNAs to be identified was ANRIL at the *CDKN2B-AS1* locus, which contains several DNA variants associated with cardiovascular disease (215) Interestingly, mutations in ANRIL lead to increased SMC proliferation and are associated with higher rates of coronary artery disease (CAD) (216). It is hypothesized that SNPs affecting ANRIL expression also control the expression of nearby cell-cycle control genes, CDKN2A and CDKN2B, and that aberrant SMC proliferation contributes to CAD (217). The most well characterized lncRNA in SMC, however, is MYOSLID (<u>MYO</u>cardin-induced <u>S</u>mooth muscle <u>L</u>ncRNA, <u>I</u>nducer of <u>D</u>ifferentiation). MYOSLID was identified in a screen for lncRNAs that were significantly upregulated by myocardin overexpression in human coronary SMC. MYOSLID contains 3 CArG boxes in its promoter. In addition to myocardin, MYOSLID is also regulated by TGFβ/SMAD signaling. Importantly, MYOSLID is localized to the cytoplasm, and thus does not directly affect SMC-specific gene transcription. Instead, MYOSLID is required for actin polymerization as well as SMAD2 phosphorylation, which regulate downstream SRF- and TGFβ-dependent smooth muscle genes, respectively. As partial evidence of this, knockdown of MYOSLID significantly reduces expression of SMA, CNN, and SM22 in human coronary SMC (218).

ENCODE Consortium, UCSC Genome Browser, and GTEx Database

Our lab collaborated with several members of the ENCODE Consortium (Terry Furey, Gregory Crawford, and Jason Lieb) to identify DHS in human aortic SMC. Data from these efforts as well as SRF ChIP-seq were uploaded to the UCSC Genome Browser (https://genome.ucsc.edu) for use in experiments by our lab. The UCSC

Browser contains extremely useful bioinformatic datasets of transcriptionally interesting

features deposited by different labs. One advantage of this tool is that information from

multiple cell types is available, which is useful for making determinations regarding cell-

type specificity of respective gene regions. Briefly, selected features that can be used to

make predictions about active promoter/enhancer regions include H3K27Ac, H3K4me1,

and DHS identified in various cell types. Furthermore, the UCSC Broswer integrates

data from predictive biobases, such as miRNA binding sites from TargetScan as well as

tissue specific gene expression from GTEx. All of these features allow the user to

analyze the multitude of transcription mechanisms that potentially regulate expression

of a gene of interest.

Another useful web-based tool, the Genotype Tissue Expression (GTEx)

database (www.gtexportal.org), catalogues RNA-seq data from 53 different tissues as

well as the genotype associated with each sample so eQTLs can be calculated for given

genes. Users can view the top genes expressed in a specific tissue, search for eQTLs

based on a gene or SNP ID, as well as view gene expression across all tissue types.

One recent feature is the "histology image viewer," where the user can view various

tissue samples, each with an attached pathology note.

Genetic and molecular basis for blood pressure regulation[1]

RhoA signaling and hypertension

While monogenic diseases affecting renal salt-handling contribute to

hypertension, the fundamental cause of high blood pressure is increased peripheral

vascular resistance. Increased vascular resistance is a direct result of increased SMC

---

[1] The remaining sections of Chapter 1 are from a review published in The World Journal of Hypertension. The original citation is: Bai X, Dee R, Mangum KD, Mack CP, Taylor JM. RhoA signaling and blood pressure: The consequence of failing to "Tone it Down". *World J Hypertens*.

contractility, which is regulated by myosin light chain (MLC) phosphorylation. Activation

of G-protein coupled receptors (GPCRs) by vasoconstrictors (angiotensin II, endothelin-

1, etc.) leads to RhoA activation and a rise in intracellular calcium. RhoA signals

through its effectors, ROCK and mDia1/2, to increase actin polymerization, which has a

direct effect on vessel tone. Calcium-calmodulin-dependent phosphorylation of MLC by

myosin light chain kinase (MLCK) is the predominant mechanism regulating SMC

contractility. ROCK inhibits myosin light chain phosphatase, thereby leading to

sustained MLC phosphorylation and SMC contractility (Figure 1.5). Given the

importance of RhoA in regulating SMC contractility, it is no surprise that perturbation in

upstream mediators or downstream effectors of RhoA in SMC affects blood pressure.

Deletion of the SMC-specific RhoGAP GRAF3 (ARHGAP42) results in significant

hypertension in mice due to increased RhoA activity and vascular resistance (219). In

mouse models of hypertension, the RhoGEF p115 mediates angiotensin II-dependent

RhoA activity and SMC contractility, while LARG is required for salt-induced

hypertension (104, 220). While it is clear that RhoA directly increases SMC contractility

and blood pressure, the degree to which RhoA-dependent upregulation of contractile

gene expression in SMC contributes to hypertension is not as apparent.

Public health relevance of hypertension

Hypertension is a devastating disease associated with significant morbidity and

mortality due to detrimental pressure-related effects on the kidneys, heart, lungs, brain,

and peripheral vasculature. Hypertension affects roughly 80 million people

(approximately 32.6% of adults) in the United States alone and was predicted to be

primarily responsible for 25% of deaths worldwide in 2010 (221). Despite the fact that

nearly 70 drugs (from 15 distinct classes of compounds) are approved for treatment of
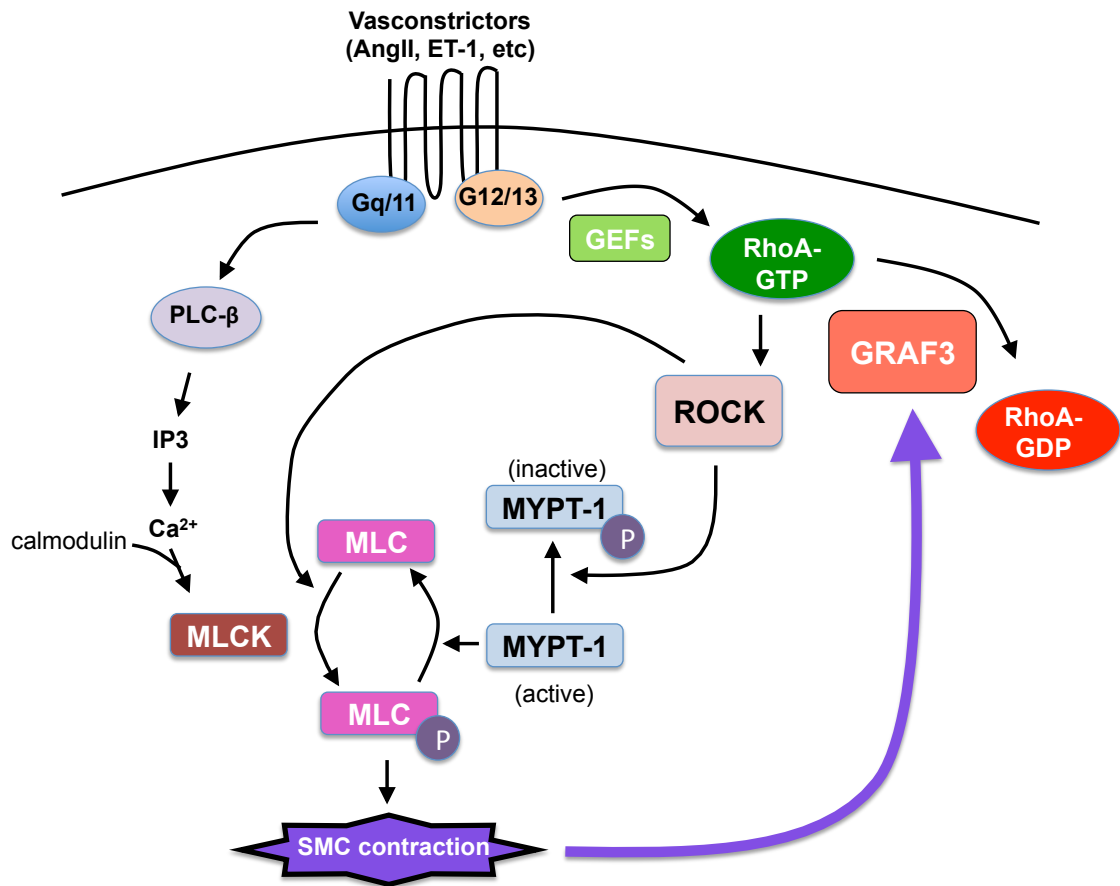
Figure 1.5. Signaling mechanisms regulating SMC contraction. Vasoconstrictors bind to GPCRs, leading to calcium/calmodulin-dependent activation of myosin light chain kinase (MLCK), which phosphorylates myosin light chain (MLC). MLC is also activated by Rho-coiled kinase (ROCK). Phosphorylated myosin light chain incrases SMC contraction. In reponse to GPCR stimulation, GEFs promote RhoA-GTP, which activates ROCK. ROCK inhibits myosin phosphatase (MYPT-1), thereby leading to sustained MLC phosphorylation. RhoA is inactivated by the RhoGAPs, GRAF3. GRAF3 expression is upregulated with sustained cell stretch to limit the amount of SMC contraction. P, phosphorylation.

hypertension in the United States, estimates project that reasonable BP control is achieved in only about half of hypertensive patients. This reality coupled with recent projections that the incidence of hypertension will increase to about 41% in the US by 2030, indicate the urgent need for better screening and treatment modalities (222). Improvements in the detection and management of hypertension will undoubtedly be accomplished through a better understanding of the complex etiology of this disease.

One way to better predict patient response to therapy is to gain a more comprehensive understanding of the genes and genetic variants that influence BP regulation. Recent projections indicate that up to 60% of BP variation can be explained by genetic factors, but that no single gene exerts a principal effect. Thus, BP is considered to have a complex non-Mendelian mode of inheritance. Indeed a combination of classic positional cloning strategies in families with numerous affected members combined with more recent population-based GWAS studies have led to the identification of 25 rare mutations and 53 SNPs that are predicted to contribute to BP control (223). The aim of this section of is to highlight variants that impinge on the expression or activity of members of the RhoA signaling axis.

RhoA-related forms of monogenic hypertension

Virtually all known cases of monogenic hypertension are associated with volume expansion resulting from mutations in genes involved in renal salt handling or hormones that affect mineralocorticoid activity. However, although hypertensive patients with Gordon's Syndrome (pseudohypoaldosteronism type IIE) present with salt handling abnormalities, the high BP in these patients is caused by an autosomal dominant mutation in the Cullin-3 gene (224). Interestingly, this E3 ligase helps target RhoA for proteosomal degradation and *in vitro* studies indicate that increased RhoA/ROCK

signaling in vascular SMC may also play a role in Gordon's Syndrome patients.

Exclusion of exon 9 abrogates the Cullin-3 dependent interactions between RhoBTB

and the E3 ligase and as RhoBTB serves as a chaperone to recruit RhoA to this

degradation complex, expression of exon 9-deficient Cullin-3 leads to aberrant RhoA

accumulation (225, 226).

SNPs/EQTLs in RhoA-signaling molecules

Because Rho kinases are major RhoA effector proteins and because both animal

and human studies have shown that treatment with Rho-kinase inhibiting compounds

lowers BP, a number of case-controlled studies were designed to determine if genetic

variants in these genes might influence the development of human hypertension (Figure

1.6). One group examined the effect of ROCK2 genetic variations on BP in 168 pairs of

mono- and dizygotic twins. In this study, four variants were identified in ROCK2, the

most notable of which was a nonsynonymous SNP in exon 10 that resulted in a

substitution of Thr with Asn at amino acid 431. Importantly, the Asn substitution was

associated with increased systemic vascular resistance and BP and was predicted to

account for 3-5% of the BP variance between these patients (227). Another study in

which 18 tag SNPs within the ROCK2 locus were genotyped in 586 normotensive

controls and 607 hypertensive Caucasian patients identified a haplotype defined by four

SNPs (rs965665, rs10178332, rs6755196, rs10929732) that was recessively associated

with a lower risk of hypertension (p=0.003). However, a subsequent study in a separate

population of 1344 Chinese patients with coronary artery disease and hypertension and

1267 ethnically and geographically matched controls did not find an association

between this haplotype and either BP or cardiovascular disease (228, 229). Thus, future

studies are necessary to determine the relevance of these SNPs with respect to BP
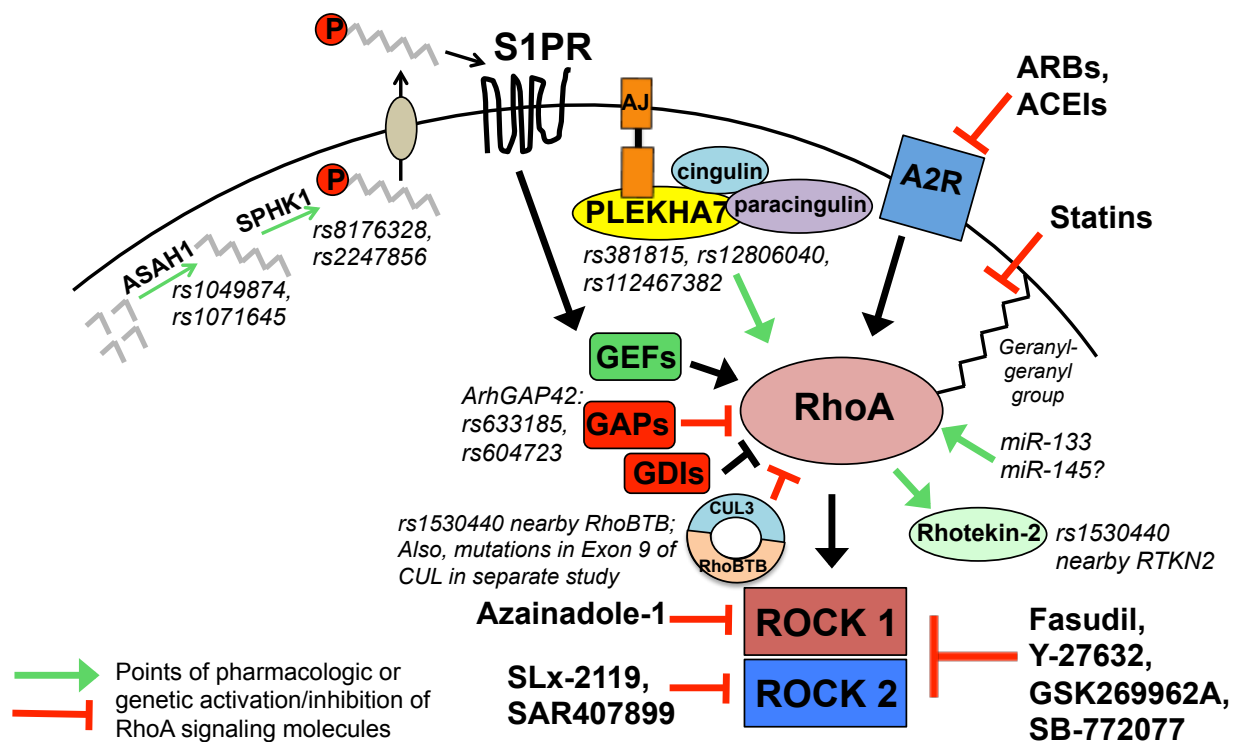
Figure 1.6. Pharmacologic and genetic regulation of the RhoA signaling axis.
Schematic ndicating the sites of action of pharmacological inhibitors (bold) of RhoA
signaling molecules. Polymorphisms (SNPs/eQTLs) that could influence RhoA signaling
are also shown. AJ: Adherens junction; A2R: Angiotensin type II receptor; ARBs:
Angiotensin receptor blockers; ACEIs: Angiotensin converting enzyme inhibitors;
ASAH1: Acid ceramidase; SPHK1: Sphingosine kinase 1.

control in the general population.

Recent studies have implicated artery stiffness in the pathology of HTN and this parameter has been shown to be a valuable predictor of end organ failure (230-234). Decreased vessel compliance elevates the mechanical load on the myocardium but also increases peripheral pulse-pressure in the microvasculature resulting in tissue damage in high flow organs such as the brain and kidneys. Until very recently, increased vascular stiffness during aging or the development of HTN was thought to result from changes in extracellular matrix content and composition (i.e. elastin degradation, collagen deposition, etc.). However, new studies suggest that the intrinsic mechanical properties of VSMC (including RhoA-dependent formation of force-generating actin filaments, and increased cell adhesion to the extracellular matrix) may also play a role (235, 236). Notably, Liao *et. al.* identified two SNPs in ROCK2 that were in complete linkage disequilibrium and associated with arterial stiffness in 1483 un-selected patients from a Chinese population in Taiwan. Subsequent *in vitro* studies revealed that both SNPs were functional. One SNP, rs978906, affected ROCK2 expression by interfering with microRNA(miR)-1183 binding to its 3'UTR, while the other, rs9808232, which was located in a protein-coding region, increased ROCK2 activity (237).

As noted above, S1P is a major upstream activator of RhoA in SMC and has vasoconstrictive effects *in vivo* (238). Interestingly, Fenger *et. al.* assessed the significance of 353 genetic variants contained within exons of genes in the metabolic sphingolipid network. Of these SNPs, 34 and 40 haplotypes were associated with changes in diastolic or systolic pressures, respectively, in their 2556 subjects. They found that while the BP effects could not be explained by any single gene, several 2-

gene interaction pairs were highly correlated with BP variations. S1P is generated from ceramide in a process that involves two critical enzymes ceramidase (ASAH1) and sphingosine 1- kinase (SPHK1) and the most significant of the 2-gene interactions identified were contained in these genes (239, 249), further supporting a role for RhoA signaling in the development of hypertension. It is likely that future gene interaction studies such as these will provide a powerful approach to both predict hypertension risk and possibly inform treatment options.

In the past decade, many GWAS studies have identified common genetic variations in coding and non-coding genomic regions that vary between individuals and are associated with changes in BP and several of these variants occur in genes linked to the Rho signaling cascade. Notably, one GWAS study that used hypertension as a dichotomous trait identified eight loci associated with BP, and two of these variants were located in RhoA-related genes. One of the target genes was the aforementioned RhoBTB1, which functions with the Cullin-3 complex to maintain low RhoA levels (224, 225). Another SNP was found at the rhotekin-2 (RHTKN) locus. Although rhotekin was one of the first identified RhoA effector molecules (it has high affinity to Rho-GTP and is widely used in pull down assays for activated RhoA, (241)), how Rhotekin functions at a cellular level is still unclear. Nonetheless this association is provocative and clearly indicates that future studies are warranted. Two separate GWAS for BP variation and hypertension have identified significant association signals in the RhoA-interacting protein, plekstrin homology domain containing family A member 7 (PLEKHA7) (242, 243). PLEKHA7 is highly expressed in the kidney and heart and localizes on the cytoplasmic surface of adherens junctions, where it interacts with junctional proteins cingulin and paracingulin to regulate the activity of Rho family GTPases, including RhoA

(244). While the functional SNP(s) have yet to be identified, the finding that PLEKHA7 is required for the development of salt-induced hypertension *in vivo*, highlights the functional importance of this RhoA-interacting protein in BP regulation (245).

Collectively, these studies will likely have important implications in the future diagnosis and treatment of hypertension. For example, patients predicted to exhibit aberrantly high levels of RhoA signaling may respond better to anti-hypertensive regimens directly targeting vessel tone, compared to those that target blood volume. Moreover, they reveal that the RhoA signaling axis may provide highly selective targets for the treatment of human hypertension and related cardiovascular sequelae.

Objectives of this dissertation research

It is clear that numerous transcription mechanisms regulate SMC differentiation and that many of the pathways required during vascular development also lead to phenotypic switching of the SMC during disease. The first major component of this research has been to determine the transcription mechanisms regulating expression of GRAF3, a smooth muscle-specific RhoGAP that negatively regulates blood pressure. To address this, this objective has been divided into four major aims. 1) To identify DNA variants in the GRAF3 gene that regulate its expression, 2) To determine the transcription mechanisms driving allele-specific expression of GRAF3, 3) To correlate SNPs with GRAF3 expression and blood pressure in humans, and 4) To identify additional, non-SRF dependent transcription mechanisms that regulate GRAF3 expression. A second major focus of this dissertation has been to discover novel mechanisms regulating MRTF-A function, which includes identification of MRTF-A binding partners and post-translational modifications and their effects on SMC differentiation.

CHAPTER 2: BLOOD PRESSURE-ASSOCIATED POLYMORPHISM

CONTROLS ARHGAP42 EXPRESSION VIA SERUM RESPONSE

FACTOR DNA BINDING[2]

Overview

Our recent demonstration that smooth muscle cell (SMC) selective expression of ARHGAP42 controls blood pressure by inhibiting RhoA-dependent contractility provided a novel mechanism for the blood pressure-associated locus within this gene. The goals of the current study were to identify polymorphisms that affect *ARHGAP42* expression and to better assess ARHGAP42's role in the development of hypertension. Using DNaseI hypersensitivity methods and ENCODE data, we identified a regulatory element encompassing SNP rs604723 that exhibited strong SMC-selective, allele-specific activity. Importantly, CrispR/Cas9-mediated deletion of this element in cultured human SMC significantly reduced endogenous *ARHGAP42* expression. DNA binding and transcription assays demonstrated that the minor T allele variation at rs604723 increased the activity of this fragment by promoting SRF's interaction with a cryptic SRF cis element. *ARHGAP42* expression was increased by cell stretch and sphingosine 1-phosphate in a RhoA-dependent manner, and *Arhgap42* deletion enhanced the progression of hypertension in mice treated with DOCA-salt. Our analysis of a well-characterized cohort of untreated borderline hypertensive patients suggested that *ARHGAP42* genotype has important implications in regard to hypertension risk. Taken

---

together, our data add significant insight into the genetic mechanisms that control blood pressure and provide a novel, perhaps individualized, target for antihypertensive therapies.

Introduction

Although hypertension is a major risk factor for stroke, myocardial infarction, and kidney failure (248), surprisingly little is known about the genetic mechanisms that contribute to its development. Genome wide association studies have begun to identify common genetic variants that contribute to variations in blood pressure (BP) (see (223, 249) for reviews). While some of these loci have been fairly well-characterized others are found within genes that have no known connection to the control of BP. One such locus was identified on chromosome 11 within the GTPase activating protein (GAP), *ARHGAP42* (250-252). The minor allele at this locus was associated with a decrease in BP of ~0.5 mm Hg per allele and had a minor allele frequency (MAF) of 0.27 in the European population in which it was identified (251).

ARHGAP42, also known as GRAF3, is a member of the GRAF (GAP for Rho Associated with Focal adhesion kinase) family of Rho-specific GAPs previously characterized by our group (253-256). Based upon our demonstration that ARHGAP42 was highly and selectively expressed in smooth muscle in mouse and human tissues (219) and the fact that RhoA signaling controls smooth muscle cell (SMC) contractility (257), we hypothesized that ARHGAP42's association with BP was mediated by its ability to modulate vascular resistance. Indeed, *Arhgap42*-deficient mice exhibited significant hypertension and increased pressor responses to AngII and endothelin-1, and these effects were prevented by treatment with the Rho-kinase (ROCK) inhibitor, Y-27632 (219). Further supporting this idea, we showed that large and small arteries from

Arhgap42-deficient mice exhibited increased contractility in vitro and in vivo, while kidney structure and function were unchanged.

According to the Haplo-reg v4 database from the Broad Institute, the BP-associated allele in the European population is currently defined by 4 single nucleotide polymorphisms (SNPs rs604723, rs633185, rs607562, and rs667575) in high linkage disequilibrium (LD) ($r^2 > 0.8$). Importantly, all of these SNPs are present within the non-coding 80Kb *ARHGAP42* first intron. Thus, we hypothesized that minor allele variations within the BP-associated locus increase *ARHGAP42* expression by enhancing the transcriptional activity of a yet to be identified regulatory element. The goals of the present study were to identify the transcription mechanisms that drive *ARHGAP42* expression in SMC, to test whether variations within the *ARHGAP42* BP-associated locus affect *ARHGAP42* transcription, and to further characterize the role of *ARHGAP42* expression in the regulation of BP and the development of human hypertension.

Materials and Methods

Cell culture

Human aortic, coronary, and bronchial smooth muscle cells were purchased from Lonza and maintained in smooth muscle growth medium-2 (SmGM-2) supplemented with growth factors and 5% FBS. Primary aortic SMC were isolated from 2 month old Wistar rats as previously described (63). In brief, thoracic aortae were stripped of endothelial and adventitial layers by microdissection and then SMC were dispersed by treatment with trypsin and collagenase. Cells were maintained in Dulbecco's modified eagle medium supplemented with F12 and 10% fetal bovine serum and used from passage 5–15. SMC preparations are routinely tested for smooth muscle-differentiation marker gene expression and only those that are deemed at least 85% pure by these

measurements are utilized for further experimentation. Primary mouse endothelial cells were immortalized by transformation with Large T-antigen and maintained in Dulbecco's Modified E Medium (Gibco).

Generation and characterization of ArhGAP42$^{gt/gt}$SM-MHC^{creERT2} mice

The *Arhgap42* gene trap mouse line was created as previously described (219). In brief, *Arhgap42* gene trap ES cells (SIGTR ES CE0477) were obtained from the Mutant Mouse Regional Resource Center (University of California, Davis). Chimeric mice were produced in-house by blastocyst injection of *Arhgap42*$^{+/gt}$ ES cells using standard procedures, and a *Arhgap42*$^{gt/gt}$ line on a C57/Bl6 background was generated by backcrossing for at least 8 generations. For ARHGAP42 rescue experiments, *Arhgap42*$^{gt/gt}$ mice were bred to a tamoxifen-inducible SM-MHC^{creERT2} line generously provided by Stefan Offermanns (University of Heidelberg, Germany) on a pure C57/Bl6 background. Cre activity in this model was controlled by treatment with tamoxifen (100 mg/kg) by IP injection for 5 consecutive days or oral gavage for 3 consecutive days. All experiments were performed in male mice 2-4 months old using age, sex, and littermate genetic controls. Genotyping was performed using DNA isolated from tail biopsies using either LacZ (5′-GCATCGAGCTGGGTAATAAGCGTTGGCAAT; 3′-GACACCAGACCAACTGGTAATGGTAGCGAC) or locus-specific primers (5′-TTCGTTGAGACAACTGCACACC; 3′-CCCTTCACACTTTGCTCTCTTAGC).

Blood pressure measurements

Conscious blood pressure measurements were made in mice aged 9–20 weeks by radio-telemetry using the PA-C10 telemeter (Data Sciences International) or tail cuff methods using the BP-100 probe (Iworx). For telemetry, after positioning the telemetry catheter tip in the thoracic aorta (fed through the left carotid), the transmitter was

inserted subcutaneously on the back/flank of mice. Mice were housed individually in a standard polypropylene cage placed on a radio receiver, maintained in a 12 h light/dark cycle, and allowed 7 days of recovery/equilibration before BP measurements were begun. All BP measurements were recorded and stored using the Ponemah v6.10 system (Data Sciences International). Five-minute recordings were collected every 30 min and data were analyzed using Excel software. Tail cuff measurements were performed as previously described (219). In brief, mice were fitted with the BP-100 probe and subjected to 20 BP measurements over 20 min every day (between 14:00 and 16:00) for 7 consecutive days.

DNase Hypersensitivity

Approximately 80 million fresh HuAoSMC were serum starved for 24 hours and then washed twice with cold 1X PBS. Cells were pooled and collected in cold RSB buffer (10 mM Tris-Cl, pH 7.4, 10 mM NaCl, 3 mM $MgCl_2$). Nuclei were isolated by lysing cells in RSB buffer + 0.1% NP-40 and centrifuging at 500xg for 10 min. at 4°C. Supernatant was removed from the pellet. Pelleted nuclei were suspended in cold 1X DNase incubation buffer (NEB) and mixed. The nuclei suspension was treated with 1 U DNaseI (Sigma, D5025) for 15 min at 37°C. After 15 min, 50 mM EDTA was added to stop the digestion reaction. DNase I-digested DNA was embedded in low-melt agarose plugs to minimize additional shearing, and then blunt-ended, extracted, and ligated to biotinylated linkers (Linker 1a: 5'-Bio-ACAGGTTCAGAGTTCTACAGTCCGAC-3'; Linker 1b: 5-GTCGGACTGTAGAACTCTGAAC-Amm-3'). Biotinylated fragments were digested with MmeI and incubated with streptavidin-coated Dynal beads to purify digested DNA fragments. A second linker was ligated to the MmeI-digested DNA-linker-bead complex, and purified DNA fragments were PCR-amplified, sequenced by Illumina/Solexa (Linker

2a: 5'-P-TCGTATGCCGTCTTCTGCTTG-3'; Linker 2b: 5'-

CAAGCAGAAGACGGCATACGANN-3'), and then aligned to the human genome using

Bowtie.

For targeted, allele-specific DNase Hypersensitivity assays, nuclei from

heterozygous HuAortic SMC were treated with increasing amounts of DNaseI from 0 to

1mg. Reactions were subjected to PCR using primers specific to the major-C or minor-T

alleles and PCR band intesities were expressed relative to untreated samples set to 1.

Generation of luciferase constructs, DNA transfection, and reporter assays

Regulatory regions of interest were PCR amplified from human aortic smooth

muscle genomic DNA and then cloned into the pGL3 basic vector (Promega). HuBrSMC

or EC were seeded in 24-well culture plates the day prior to transfections at a density of

approximately 2.5×10^4 cells/well. Cells were transfected with 50 ng DNA per well. In co-

expression experiments, cells were transfected with 25 ng of luciferase reporter DNA

and 25 ng of flag-tagged myocardin or empty expression construct per well. In all

experiments, cells were transfected in triplicate and a promoterless pGL3 basic vector

was transfected in parallel. After 48 hours of incubation at 37°C, luciferase assays were

performed using the Steady-Glo Luciferase Kit (Promega) following the manufacturer's

instructions. Raw luciferase values were normalized to the activity of the promoterless

pGL3 vector.

Electrophoretic mobility shift assays (EMSA)

HuAoSMC nuclear lysates were prepared using the Nuclear Isolation kit from

ThermoScientific. Lysates were dialyzed in Dignam Buffer D (20 mM HEPES, pH 7.9,

20% (v/v) glycerol, 0.1 M KCL, 0.2 mM EDTA, 0.5 mM PMSF, and 0.5 mM DTT). Flag-

tagged SRF was translated in vitro using the TnT kit (Promega). Major and minor allele

633185 and rs604723 gel shift probes were prepared by PCR amplifying a 100 bp fragment from the corresponding DHS1 or DHS2 luciferase reporter plasmids with the polymorphism at the center. Each binding reaction contained 10 ug lysate or 1 ul in vitro translated-SRF, 20,000 cpms of ^{32}P-labeled oligonucleotide probe, and 0.20 ug dIdC in binding buffer (10 mmol/L Tris, pH 7.5, 50 mmol/L NaCl, 100 mmol/L KCl, 1 mmol/L DDT, 1mmol/L EDTA, 5% glycerol).

Chromatin Immunoprecipitation (ChIP) experiments

ChIP assays were performed according to X-ChIP protocol (Abcam) with slight modifications. In brief, HuAo or coronary (HuCo) SMC were fixed for 5 minutes in 0.7% formaldehyde. The crosslinking reaction was stopped by incubating cells with 0.125 M glycine for 5 minutes. Cells were scraped in lysis buffer (5 mM PIPES, pH 8.0, 85 mM KCl, 0.5% NP40) and then nuclei isolated by centrifugation at 2,300xg for 5 minutes. Nuclei lysis buffer (50 mM Tris-Cl, pH 8.1, 10 mM EDTA, 0.13% SDS) was added to pelleted nuclei. Chromatin was sheared into 500 bp fragments by sonication and immunoprecipitated with 1 ug of anti-SRF antibody (Santa Cruz, cat# sc-335) or normal rabbit IgG antibody (Cell Signaling, cat# 2729) as a negative control for non-specific binding. An alpha-tubulin antibody was used for a loading control (Sigma, cat# T6074).

SRF affinity precipitations

Nuclear extracts from human aortic SMCs were prepared using NUPER nuclear extraction kit (Thermo Scientific) according to manufacturer protocol. For precipitations, 5' biotinylated 20 bp double stranded oligonucleotides (2.5 mM final concentration) were combined with 200 mg of nuclear extract in binding buffer (10mM Hepes pH7.4, 8% glycerol, 1mM MgCl2, 0.05% Triton x100, DTT 1.3 mM, protease and phosphatase inhibitors) at room temperature w/ rotation. After 10 min, streptavidin agarose beads

(CL-4B, SIGMA 8588) were added and reactions were incubated for another 30 min. After 2 washes (KCl 75mM, Hepes 5mM pH7.4, MgCl2 0.5mM, glycerol 4%, Tween 20 0.05%, DTT 1mM) precipitates were eluted in 2x sample buffer and run on a 10% SDS-PAGE for Western blotting with an SRF Ab (Santa Cruz).

SRF knockdown

The following short-interfering (si)RNAs were obtained from Invitrogen; nontargeted control siRNA (NTC) (to GFP) 5'-GGUGCGCUCCUGGACGUAGCC-3', SRF 5'-UAAUACUCAUGGCAAACAU[dT][dT]-3' (sense) and 5'-AUGUUUGCCAUGAGUAUUA[dT][dT]-3' (antisense). SRF siRNA was obtained as a sense/antisense mixture. Human bronchial SMC (HuBrSMC) were transfected with 50 nM SRF or NTC siRNA using Dharmafect siRNA transfection reagent (Dharmacon). For luciferase assays in SRF knockdown cells, siNTC or siSRF-treated HuBrSMC were split 48 hours after knockdown and then seeded into 24-well culture plates. The following day, NTC and SRF knockdown cells were transfected with pGL3-promoterless, -DHS2C, or -DHS2T constructs. Luciferase experiments were performed 48 hours following transfection of pGL3 reporters. For allele specific transcript measurements, HuAoSMC were harvested 72 hours after knockdown.

Quantitative PCR

RNA was isolated from cells or tissues using RNeasy mini kit (Qiagen). RNA was treated with DNAse (Qiagen) to eliminate contaminating genomic DNA. RNA underwent first strand cDNA synthesis using the iScript cDNA synthesis kit (BioRad). 20 ng cDNA was used in quantitative or semi-quantitative PCR assays. Semi-quantitative PCR primers; mouse *Arhgap42* exons 1–4, 5'-CTGCCCACTCTGGAGTTCAGCG, 3'-GCTGCACCGATCTGTTCTTTTCG; mouse *Arhgap42* exons 10-17, 5'-

GAACCGATTTACACGTTACCCG, 3′-GGTTGGACCAAATATGACACCG; GAPDH, 5′-ATGGGTGTGAACCACGAGAA, 3′-GGCATGGACTGTGGTCATGA. Real-time PCR primers; *ARHGAP42* exons 2-4, 5'-TTGGAGATGCAGAAACTGATGA, 3'-TTTGAATCAGTCTACGCCTTTCTTC; rat *Arhgap42*, 5'-TTCTGCATCTCCGATACAGTC, 3'-ATCAAAGAGCTGCTGAAGGATG; GAPDH, 5′-ATGGGTGTGAACCACGAGAA, 3′-GGCATGGACTGTGGTCATGA. allele-specific PCR primers for rs604723 variation, 5'-TGTTGTTCCAAGGGTTCTT-3' (T) and 5'-TGTTGTTCCAAGGGTTCTC -3' (C).

CrispR/Cas9-mediated gene editing

Guide RNAs that flanked the 100 bp conserved DHS2 region (see below for sequences) were designed using sgRNA CRISPR design tool from the Zhang lab (38) and cloned into the sgRNA expression cassette of the pSpCas9(BB)-2A-Puro (PX459) plasmid (Addgene Cat#62988). HuBrSMC were transfected with either 15 mg of PX459 plasmid or with 7.5 mg of PX459 plasmid containing each guide RNA. 48h after transfection, cells were treated with puromycin (2 mg/mL) for 48 h and then allowed to recover in normal growth media for an additional 24 h. Genomic DNA and mRNA were isolated using the AllPrep DNA/RNA Kit (Qiagen). Deletion efficacy was tested by PCR using primers that flanked the deleted region. ARHGAP42 message was measured using semi-quantitative PCR as described above. Guide RNAs used were as follows; gRNA1sense 5'-CACCGCTTGGAACAACATTAGACTG; gRNA1as 5'-AAACCAGTCTAATGTTGTTCC AAGC; gRNA2sense 5'-CACCGCAGCTGGACTGTGGGTCAGA; gRNA2as 5'-AAACTCTGACCCACAGTCCAGCTGC.

Cell and vessel stretch assays

The Flexercell FX-4000 Tension apparatus (Flexcell International Corp, NC, USA) utilizes regulated vacuum pressure to deform flexible-bottomed culture plates. Rat aortic SMCs were cultured on collagen I coated BioFlex culture plates and were loaded into the FX-4000T cyclic tension device and subjected to 0 or 20% equibiaxial elongation at 1Hz for 18 hours. Longitudinally cut rat portal vein strips were placed into ex vivo culture in DMEM/F-12 with 2% dialyzed FCS and 10 nM insulin as previously described (258, 259). Strips were stretched for 3 days by attaching a 600 mg stainless steel weight at one end of the vessel. Mouse portal vein rings were cultured as above and subjected to 300 mg of stretching force for 5 days. For LacZ staining, tissues were rinsed in phosphate-buffered saline (PBS) and fixed in 4% paraformaldehyde for 20 min at room temperature. After three 10-min washes in PBS, tissues were incubated overnight at RT in X-Gal staining solution (in PBS; 2mM MgCl, 5 mM ferrocyanide, 5 mM ferricyanide, 0.1% sodium deoxycholate, 0.2% NP-40, and 1 mg/ml of X-Gal). Tissues were processed for standard microscopy including H and E staining.

Hypertension models

For DOCA-salt experiments, mice were implanted subcutaneously with a 50mg 21-day slow-release DOCA pellet (Innovative Research of America) and fed 0.9% NaCl in drinking water for 3 weeks. Control mice were subjected to a sham operation and fed water. For L-NAME experiments, mice were treated with L-NAME in drinking water (450 mg/L) for 14 days. All groups were maintained on standard chow.

Human subjects

In brief, participants were enrolled via a combination of passive (signs) and active (e-mail) recruitment. Potentially eligible participants included adults 30 years or older,

with a recent office (clinic) BP measurement that was borderline high (120-149 mm Hg) systolic and/or 80-95 mm Hg diastolic with neither value greater than 149/95 mm Hg). Exclusion criteria included diabetes, pregnancy, dementia, any condition that would preclude wearing an ambulatory BP monitor, and persistent atrial fibrillation or other arrhythmia. Written informed consent took place during the first visit, during which time the patients were given ample opportunity to ask questions and to review the consent form in detail. In addition to carefully measured triplicate office BP measurements, participants underwent 24-hour ambulatory blood pressure monitoring (ABPM) using the Oscar 2 oscillometric monitor (Suntech Medical, Morrisville, NC). The monitors were programmed to measure BP at 30 minute intervals from 6am to 10pm and at 1 hour intervals from 10pm to 6am. The minimum number of readings we accepted as an adequate ABPM session was 14 for awake and 6 for sleep. ARHGAP42 genotype at rs604723 and rs2055450 were determined on patient blood samples as previously described (219).

Statistics

All data represent least three separate experiments presented as means ± SEM. Means were compared by two-tailed Student's *t*-test or analysis of variance (where indicated) and statistical significance was considered as a *p* value of <0.05. All gels shown are representative of at least three individual experiments and band intensities were quantified using ImageJ software.

Study Approval

The present studies in animals and/or humans were reviewed and approved by an appropriate institutional review board. All animal procedures were approved by the Institutional Animal Care and Use Committee (IACUC) of the University of North

Carolina (Chapel Hill, NC). All animals were housed in facilities accredited by the American Association for Accreditation of Laboratory Animal Care. All clinical investigations were conducted according to Declaration of Helsinki principles and have been approved by the Institutional Review Board (IRB) at the University of North Carolina, Chapel Hill, NC (IRB: UNC 10-0595). All human study procedures took place in a clinical research center and all subjects provided informed consent prior to their participation in the study.

Results

Allele-specific differences of *ARHGAP42* expression in SMC

To begin to test our hypothesis that BP-associated variations in the *ARHGAP42* gene have allele specific effects on *ARHGAP42* expression in SMC, we developed PCR primers that can distinguish between the major C and minor T alleles at the rs604723 SNP and used qPCR to measure *ARHGAP42* mRNA levels in human aortic SMC cultures that are heterozygous at the *ARHGAP42* BP-associated locus. One caveat to this approach is that it can only measure unprocessed transcripts that contain the first intron. As shown in Figure 2.1A, ARHGAP42 transcripts containing the minor allele were significantly higher than those containing the major allele, and control experiments +/- DNAse and +/- reverse transcriptase confirmed that these results were not influenced by contaminating genomic DNA. In strong support of these findings, the NIH-sponsored GTEx consortium identified an expression quantitative trait locus (eQTL) at rs604723 by correlating ARHGAP42 mRNA levels in human tibial artery samples with *ARHGAP42* genotype (260). As shown in Figure 2.1B, our more recent analysis of GTex data revealed that ARHGAP42 mRNA levels in aorta and coronary artery samples were approximately 3 fold higher from individuals homozygous for the
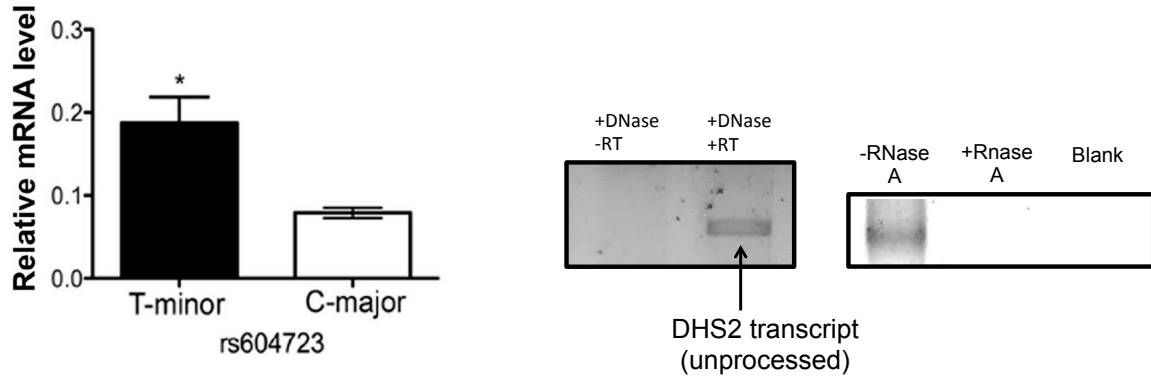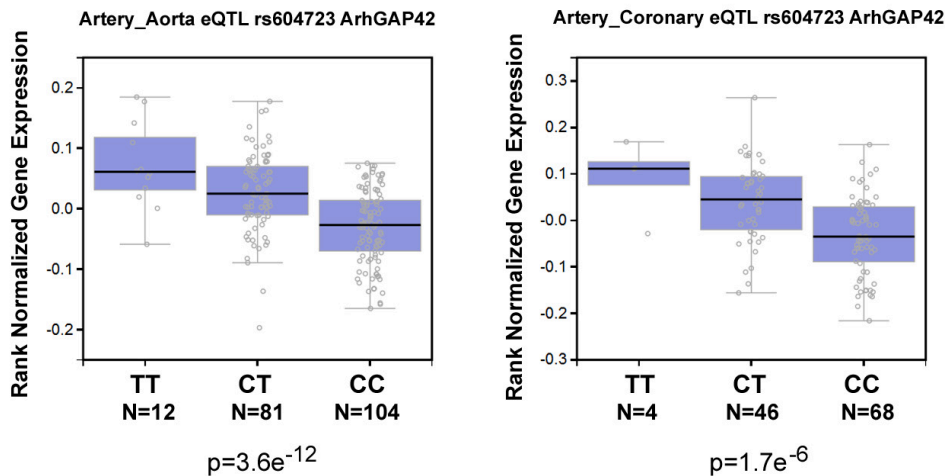
Figure 2.1. *ARHGAP42* expression in SMC is regulated by allele-specific mechanisms and controls blood pressure. A) Total RNA isolated from HuAoSMC heterozygous at the rs604723 SNP (C/T) was subjected to first strand cDNA synthesis using reverse transcriptase. Reaction products were then subjected to a TaqMan-based PCR assay using allele-specific primers to the ARHGAP42 rs604723 variation. Data represent mean ± SEM of n=4 experiments; *p<0.01 versus the major C allele; (student's t-test). **B)** ARHGAP42 mRNA levels were measured by the Genotype-Tissue Expression (GTEx) consortium. The minor T ARHGAP42 allele at the rs604723 polymorphism was significantly associated with increased *ARHGAP42* expression in aortic and coronary artery samples.

minor allele at rs604723 than in samples taken from individuals homozygous for the major allele. Aside from a relatively small difference in *ARHGAP42* expression in subcutaneous adipose (a highly vascularized tissue), *ARHGAP42* eQTLs were not detected in other organs strongly supporting the idea that the BP effects of this locus are mediated by changes in *ARHGAP42* expression in SMC.

ARHGAP42 expression in SMC controls blood pressure

To provide additional direct evidence that *ARHGAP42* expression in SMC is critical for BP regulation, we rescued its expression in our hypertensive global *Arhgap42*-deficient genetrap mice (*Arhgap42*$^{gt/gt}$) by crossing them to a SM-MHC^{creERT2} line that expresses a tamoxifen-inducible Cre under the control of the smooth muscle myosin heavy chain promoter (104). As shown in Figure 2.1C, the inhibitory *Arhgap42* gene-trap cassette is flanked by loxP sites, and treatment of *Arhgap42*$^{gt/gt}$SM-MHC^{creERT2} mice with tamoxifen permanently restored *ARHGAP42* expression in aortic SMCs, and completely reversed the hypertensive phenotype in this model by 2 weeks after tamoxifen treatment (Figure 2.1D). These data provide conclusive evidence that *ARHGAP42* levels in SMC control BP homeostasis and that the hypertensive phenotype in *Arhgap42*$^{gt/gt}$ mice was reversible and most likely due to an increase in SMC contractility.

ARHGAP42 genotype and human hypertension

To better assess ARHGAP42's role in the development of human hypertension, we genotyped a group of 346 borderline hypertensive patients who were part of a clinical study comparing the effectiveness of blood pressure monitoring protocols at the University of North Carolina (See (261, 262) and Suppl Table I). Importantly, blood pressures in this group were extremely well-characterized by repeated office

C
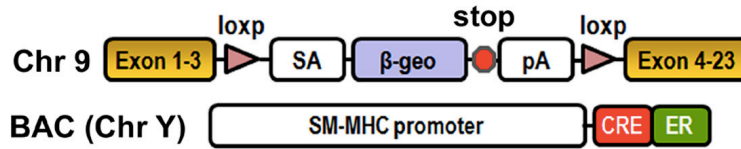
D
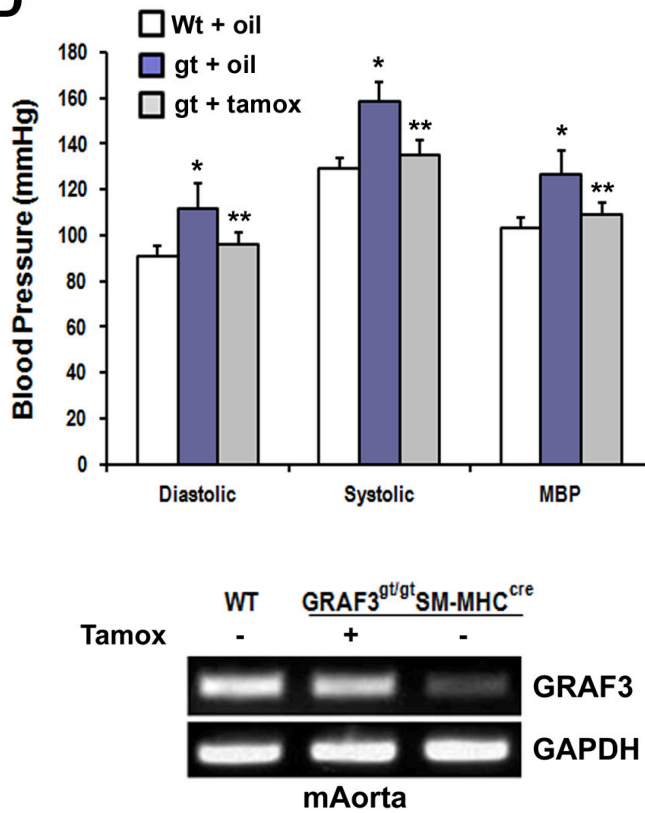
Figure 2.1 (continued). *ARHGAP42* **expression in SMC is regulated by allele-specific mechanisms and controls blood pressure. C)** Schematic of the *Arhgap42* gene trap and SMMHC-CreERT2 mice used for SMC-specific *ARHGAP42* rescue experiments. **D)** Wt and *Arhgap42*gt/gtSM-MHCcreERT2 mice were injected intraperitoneally with vehicle (corn oil) or tamoxifen (100 mg/kg) for 5 consecutive days as indicated. Two weeks after the last injection, BP was measured by tail cuff method and *ARHGAP42* mRNA levels in the aorta were measured by semi-quantitative RT-PCR analysis using primers to exons 1 and 4. Data are expressed as mean± SEM; n=6 for Wt and Arhgap42gt/gtSM-MHCcreERT2 mice with vehicle treatment, n=5 for Arhgap42gt/gtSM-MHCcreERT2 mice with tamoxifen treatment. *p<0.05 versus Wt, **p<0.05 vs. corn oil treated (ANOVA). Note that tamoxifen treatment restored *ARHGAP42* expression and reduced blood pressure to Wt levels (representative of 3 separate experiments).

measurements and none of these individuals were being treated with anti-hypertensive therapies. Several findings illustrated in Table 2.1 are worth noting. First, we observed an age-independent decrease in BP in subjects homozygous for the minor allele than in subjects homozygous for the major allele (76.9 mmHg vs 81.8 mmHg; p=0.028). The relative magnitude of this decrease (5mmHg vs 1mmHg measured in GWAS) suggested that *ARHGAP42*'s effects on BP may be greater than originally estimated. Second, the MAF (as defined by rs604723) trended lower in the group of patients that were categorized as hypertensive as defined by AHA guidelines (systolic BP > 140 mm Hg), and the percentage of subjects that exhibited hypertension trended lower in subjects who had copies of the minor allele (69%, 64%, and 60% for the C/C, C/T and T/T genotypes, respectively). Finally, the MAF of the protective T allele in this cohort was dramatically lower in African Americans than in Caucasians (6.5% vs. 26.6%; p<0.001), and sequencing of over 1,000 individuals from this and additional UNC cardiovascular cohorts (263-266) confirmed this result.

Identification of regulatory elements within the *ARHGAP42* gene.

It is clear that gene regulatory regions exhibit distinct chromatin signatures, and we and others have shown that SMC-specific gene expression is regulated by alterations in chromatin structure (194, 195, 63, 97). Thus, to prioritize our search for regulatory regions that drive ARHGAP42 expression, we performed DNase hypersensitivity measurements in human aortic SMC to identify regions of open chromatin. As shown in the *ARHGAP42* gene schematic in Figure 2.2A, we identified two approximately 600 bp DNAse hypersensitivity sites (DHS1 and DHS2) within the first intron and a larger DHS that covered about 2Kb of the transcription start site (TSS). Additional analyses of ENCODE data sets revealed that all three regions were marked by histone

rs604723 Genotype	C/C	C/T	T/T
Syst BP	130.3	130.2	126.3
Diast BP	81.8	81.1	^76.9

rs604723 Genotype	C/C	C/T	T/T	MAF
Caucasian	147	108	19	26.6%
African Amer.	54	8	0	*6.5%
Other	5	8	1	*35.7%

rs604723 Genotype	C/C	C/T	T/T	MAF
HTN (%)	141 (69)	78 (64)	12 (60)	22.1%
NON HTN (%)	63 (31)	44 (36)	8 (40)	26.1%

Table 2.1 Analysis of *ARHGAP42* genotype and blood pressure in human populations. A group of 346 borderline hypertensive patients were genotyped at the rs604723 variation using a Taqman-based allelic discrimination assay. The resulting genotypes were then correlated with repeated office blood pressure measurements or hypertension status (i.e. greater or less than 140 mmHg) or grouped by race. ^ $p<0.05$ vs diastolic BP measured in patients homozygous for the major allele (C/C); * $p<0.001$ vs MAF in Caucasians; Chi-squared test.

modifications known to be associated with transcriptionally active regions (i.e. H3K4 methylation and H3K27 acetylation) and contained stretches of highly conserved sequence. Of particular interest, the rs604723 SNP was in the middle of a highly conserved 100 bp region at the center of DHS2. All three regions were PCR amplified from human genomic DNA and cloned into the pGL3 luciferase vector. It is important to note that the DHS1 region was extended to include the nearby SNP, rs633185, so that the functional effects of this variation could be tested. Also, because the other two SNPs within the BP-associated LD block (rs607562 and rs667575) were not near open chromatin regions or conserved DNA sequences, we did not further examine their contributions to *ARHGAP42* expression.

As shown in Figure 2.2B, the DHS2 exhibited very strong transcriptional activity (38 fold over the promoterless pGL3 vector) that was significantly higher in SMC than in endothelial cells suggesting that this element is an important driver of SMC-selective ARHGAP42 expression. The TSS exhibited moderate activity in SMC and in EC consistent with idea that it functions as more of a basal promoter. We next used site-directed mutagenesis to generate allelic series for the rs633185 and rs604723 SNPs within the context of the DHS1 and DHS2 regulatory elements, respectively. As shown in Figure 2.2C, the DHS2 containing the minor T allele exhibited significantly higher activity than the DHS2 containing the major C allele while the variation at rs633185 had no effect on the relatively low SMC-selective activity of the DHS1 region. Interestingly, the rs604723 variation did not affect DHS2 activity in EC.

To test whether the DHS2 element was required for expression of the endogenous *ARHGAP42* gene, we used CrispR/Cas9-mediated gene editing to delete the 100 bp conserved element within the DHS2 in human bronchial SMC cultures (Figure 2.2D).
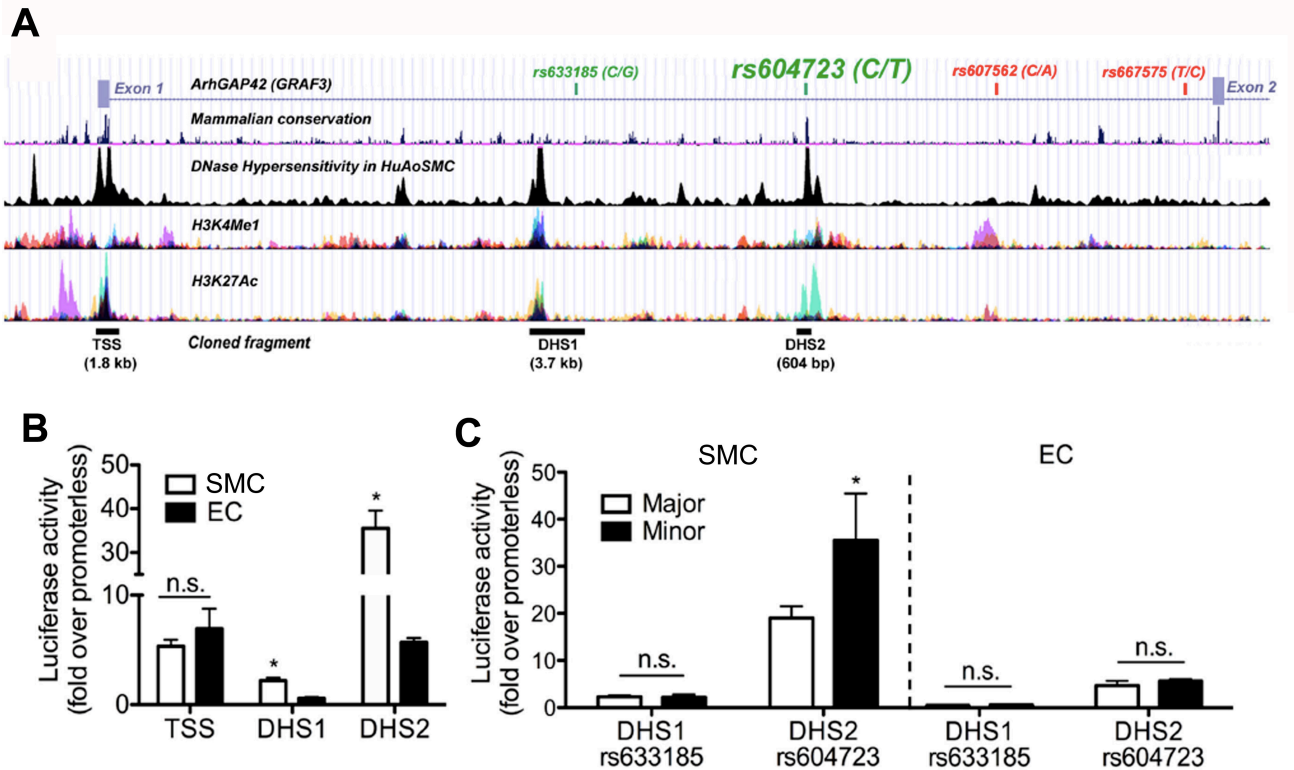
Figure 2.2. An enhancer within the *ARHGAP42* first intron displays strong SMC-specific and allele-specific activity and is required for endogenous *ARHGAP42* expression. A) Map of the chromatin determinations used to characterize potential regulatory elements near the *ARHGAP42* BP-associated locus. The SNPs that define the BP-associated allele ($r^2 > 0.8$) are shown at the top. **B)** The indicated DNase hypersensitive (DHS) regions were cloned into the pGL3 luciferase vector and transfected into primary human bronchial SMC and mouse ECs. Luciferase activity in cell lysates was measured two days later and is expressed as fold over the promoterless pGL3 vector. Data represent mean ± SEM of n=6 experiments; *p<0.001 versus in ECs (student's t-test) **C)** Site-directed mutagenesis was used to test the effects of the major/minor alleles on DHS1 and DHS2 enhancer activity. Data represent mean ± SEM of n=6 experiments; *p<0.01 versus the major allele (student's t-test).

Although we observed somewhat variable deletion efficacy (from 45-95% in 5 separate experiments), our deletion protocol resulted in a significant decrease in ARHGAP42 mRNA expression (Figure 2.2E). These results strongly support our conclusion that the DHS2 region regulates *ARHGAP42* expression and that rs604723 is the functional SNP in this BP-associated LD block.

The minor allele sequence at rs604723 binds SRF.

To begin to identify the mechanisms that mediate the transcriptional activity of the DHS2 fragment and the effects of the minor T allele variation, we used gel shift assays to compare protein binding to 100bp probes that encompassed the highly conserved region at the center of the DHS2. As shown in supplemental figure III, we observed two relatively weak T-allele specific binding complexes one of which had a mobility similar to that of SRF, a transcription factor known to be critical for SMC-specific gene expression (see (29) for a review). Interestingly, the presence of the minor T allele at rs604723 results in a DHS2 sequence that conforms to a consensus SRF-binding CArG element at 8 out of 10 residues while the presence of the major C allele within the A/T rich region would be predicted to inhibit SRF binding to this sequence (see Figure 2.3A). To test the involvement of SRF we performed additional gel shift assays using recombinant SRF protein. Our results clearly show that the minor T-allele sequence interacted with SRF while the major C allele sequence did not (Figure 2.3B). Similar results were obtained when biotin-labeled T and C allele oligonucleotides probes were conjugated to avidin coated beads and used to precipitate SRF from SMC lysates (Figure 2.33C). We next used ChIP assays to test whether SRF bound to the DHS2 in the context of the endogenous *ARHGAP42* gene. As shown in figure 3D, we observed significant SRF binding in our human aortic SMC that are heterozygous (C/T) at rs604723 but no

D

AGTAGGGTGAGCATAACTTCTTTTCCCATGACCCTCAG<u>TCTAATGTTGTTCCAAGG</u>

rs604723
     *
GTTCC<u>T</u>TACTTAGAAATGCCTTGATAACCGCATTCATTCCTGACATACCCCACCCCC

AACACACACAACTGCTGAGTGCCATCT<u>GACCCACAGTCCAGCTGCAGCTTTTAAAA</u>
                                sgRNA2
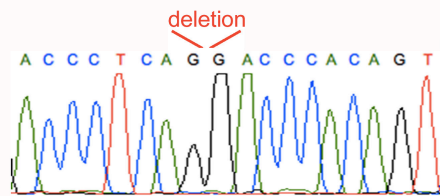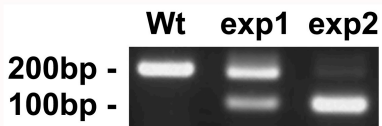
E
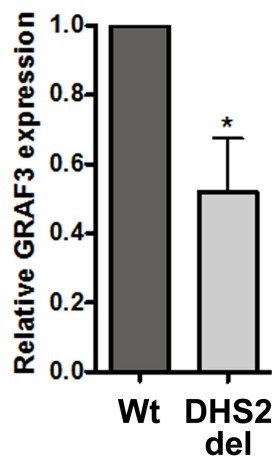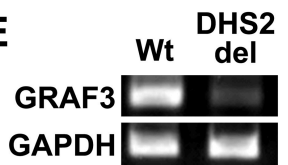
Figure 2.2 (continued). An enhancer within the *ARHGAP42* first intron displays strong SMC-specific and allele-specific activity and is required for endogenous *ARHGAP42* expression. D) Schematic of the 102 bp deletion (in red) generated by our CrispR/Cas9-mediated gene editing protocol. **E)** *ARHGAP42* message was measured by semi quantitative RT PCR in human bronchial SMC cultures transfected with expression plasmids encoding Cas9 and the guide RNAs shown in D (n=5). The reduction in *ARHGAP42* expression was normalized to the efficiency of DHS2 deletion which ranged from 45-95%. Data represent mean ± SEM of n=5 seperate experiments *p<0.05 versus cells transfected with empty guide RNA expression plasmid (student's t-test).
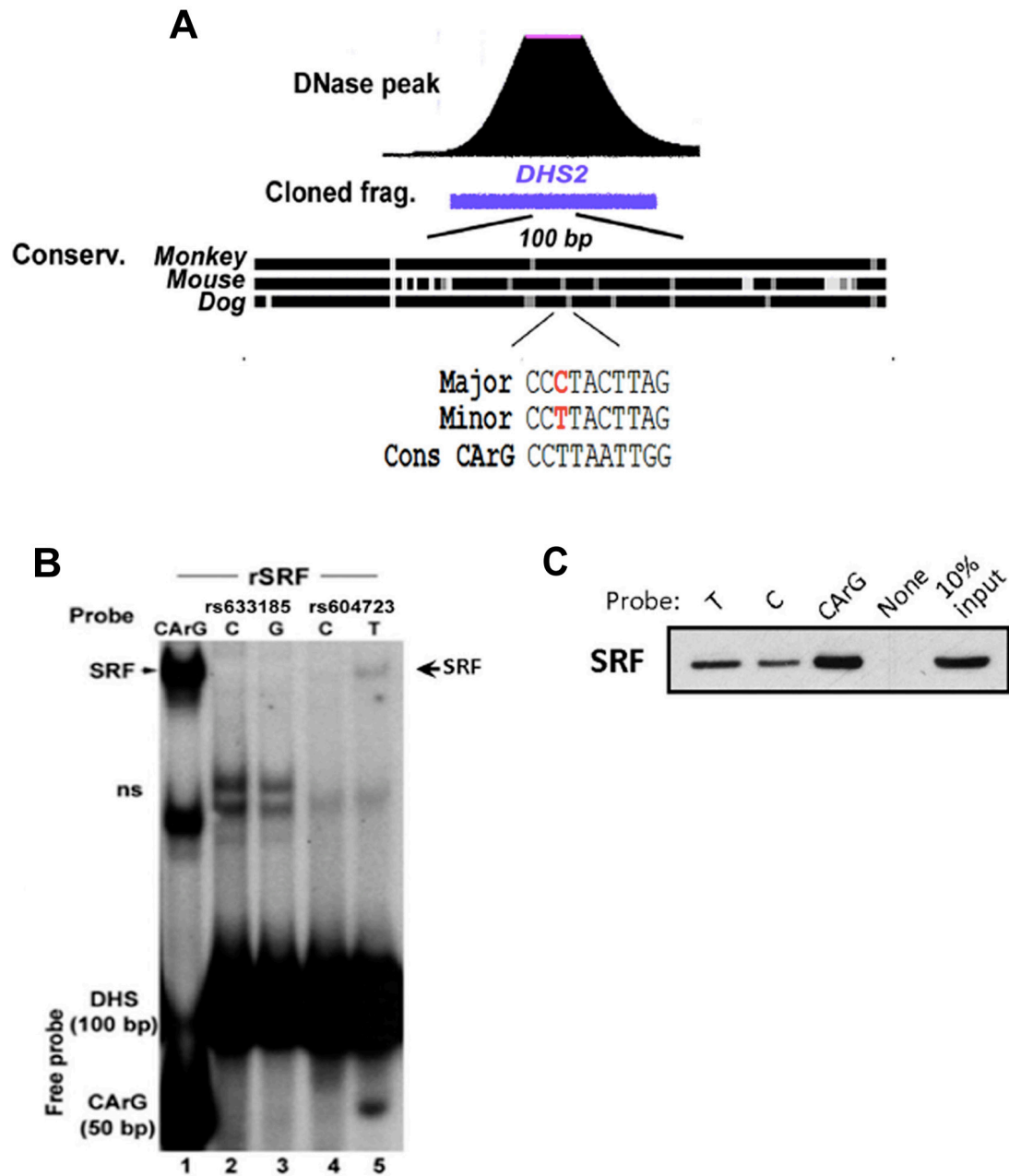
Figure 2.3. The minor T allele at rs604723 promotes SRF binding. A) Schematic of sequence conservation at the center of the DHS2 region and of CArG homology at the rs604723 SNP. **B)** Gel shift assays were performed by combining recombinant SRF with radiolabeled 100 bp oligonucleotide probes containing the major or minor alleles at rs633185 and rs604723. Representative image shown from n=2. **C)** Biotin-labeled 20 bp oligonucleotides containing the major C or minor T allele at rs604723 or a consensus CArG element were conjugated to streptavidin beads and incubated with HuAoSMC nuclear extracts. Washed immunoprecipitates were analyzed for the presence of SRF by Western blotting. Data are representative of two separate experiments.

binding when ChIP assays were performed in human coronary SMC that are homozygous major (C/C) at this sequence. Moreover, the increased presence of T allele-containing DNA in SRF immunoprecipitates (Figures 2.3E) strongly suggested that SRF interacts more readily with this sequence in the context of the endogenous gene, and targeted allele-specific DNAse hypersensitivity assays revealed that the DHS2 region containing the T-allele sequence was in a more active chromatin conformation (Figure 2.3F).

SRF is required for *ARHGAP42* expression and for the effects of the rs604723 variation

To test whether ARHGAP42, like most other SMC-specific markers, is regulated by SRF we used several gain/loss of function approaches. As shown in Figure 2.4A, over-expression of the SRF cofactor, myocardin, in HuBrSMC transactivated the DHS2-luciferase fragment containing the minor T allele by 12 fold, but had significantly less of an effect on the DHS2 fragment containing the major C allele. Moreover, knockdown of SRF in these cells by siRNA decreased the transcriptional activity of the DHS2 minor allele to a level that was similar to that of the major allele (Figure 2.4B). Importantly, SRF knockdown in our HuAoSMC line also decreased the level of endogenous ARHGAP42 message containing the minor allele as measured by our allele-specific RT PCR methods (Figure 2.4C).

***ARHGAP42* expression is upregulated by RhoA signaling**

We and others have shown that RhoA signaling enhances SMC-specific gene expression by promoting the nuclear localization of the myocardin-related transcription factors (MRTFs) (100, 106, 267). In support of this mechanism, *ARHGAP42* expression in primary rat aortic SMCs was up-regulated by sphingosine 1-phosphate (S1P), a
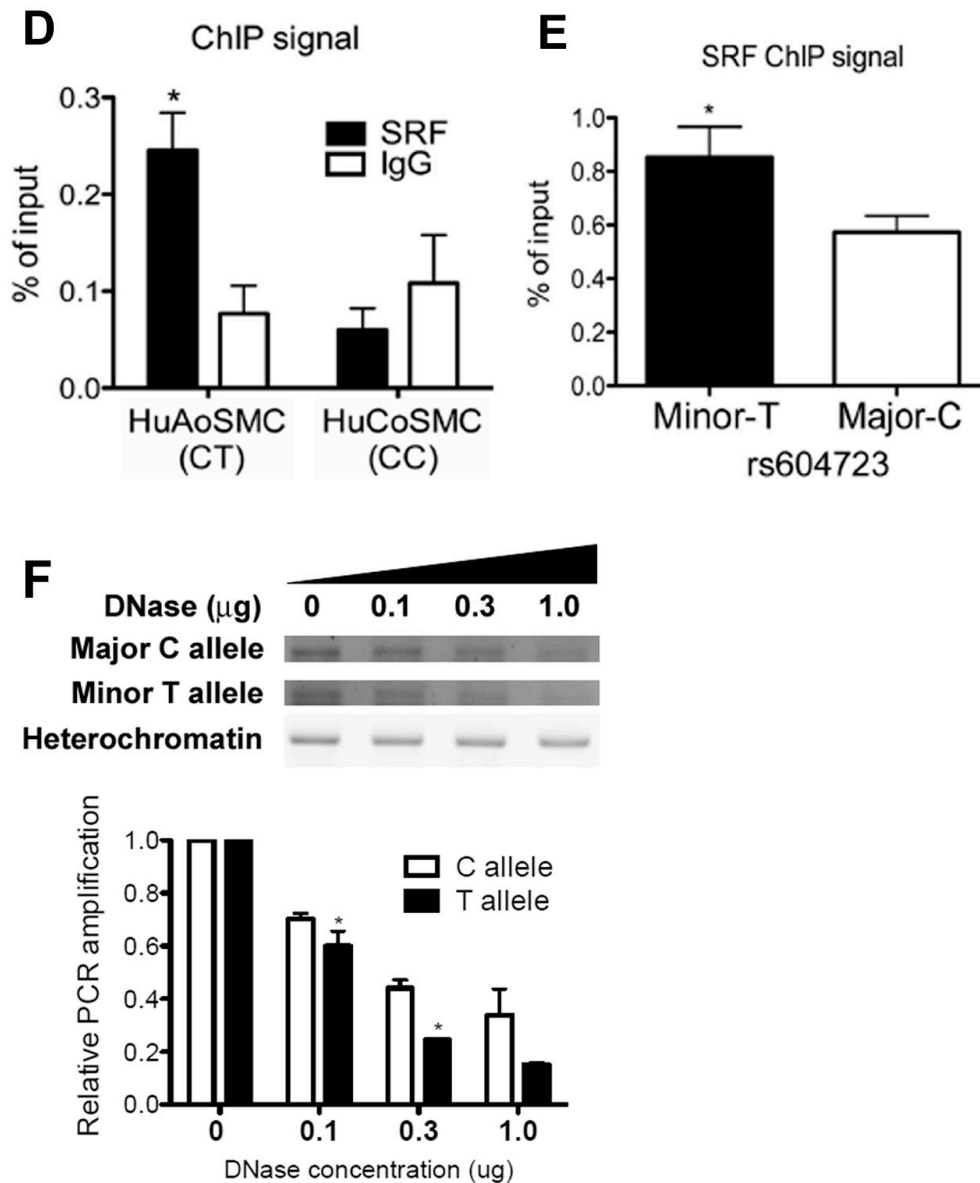
Figure 2.3 (continued). The minor T allele at rs604723 promotes SRF binding. D) ChIP assays were used to measure SRF binding to the DHS2 region in cultured HuAoSMC and HuCoSMC that are heterozygous (CT) and homozygous major (CC) at the rs604723 SNP, respectively. Data represent mean ± SEM of n=4 experiments; *p<0.05 vs IgG in HuAoSMC (student's t-test) **E)** SRF-ChIP immunoprecipitates from HuAoSMC were subjected to a TaqMan-based assay that discriminates between the major and minor alleles at the rs604723 SNP. Data represent mean ± SEM of n=4 experiments;*p<0.01 versus major allele (student's t-test). **F)** Increasing amounts of DNase I (0-1 μg) were added to permeabilized nuclei isolated from HuAoSMC. Following genomic DNA isolation, allele-specific primers were used to amplify a 300 bp region containing the rs604723 SNP. Data represent mean ± SEM of n=3 experiments;*p<0.05 (student's t-test).
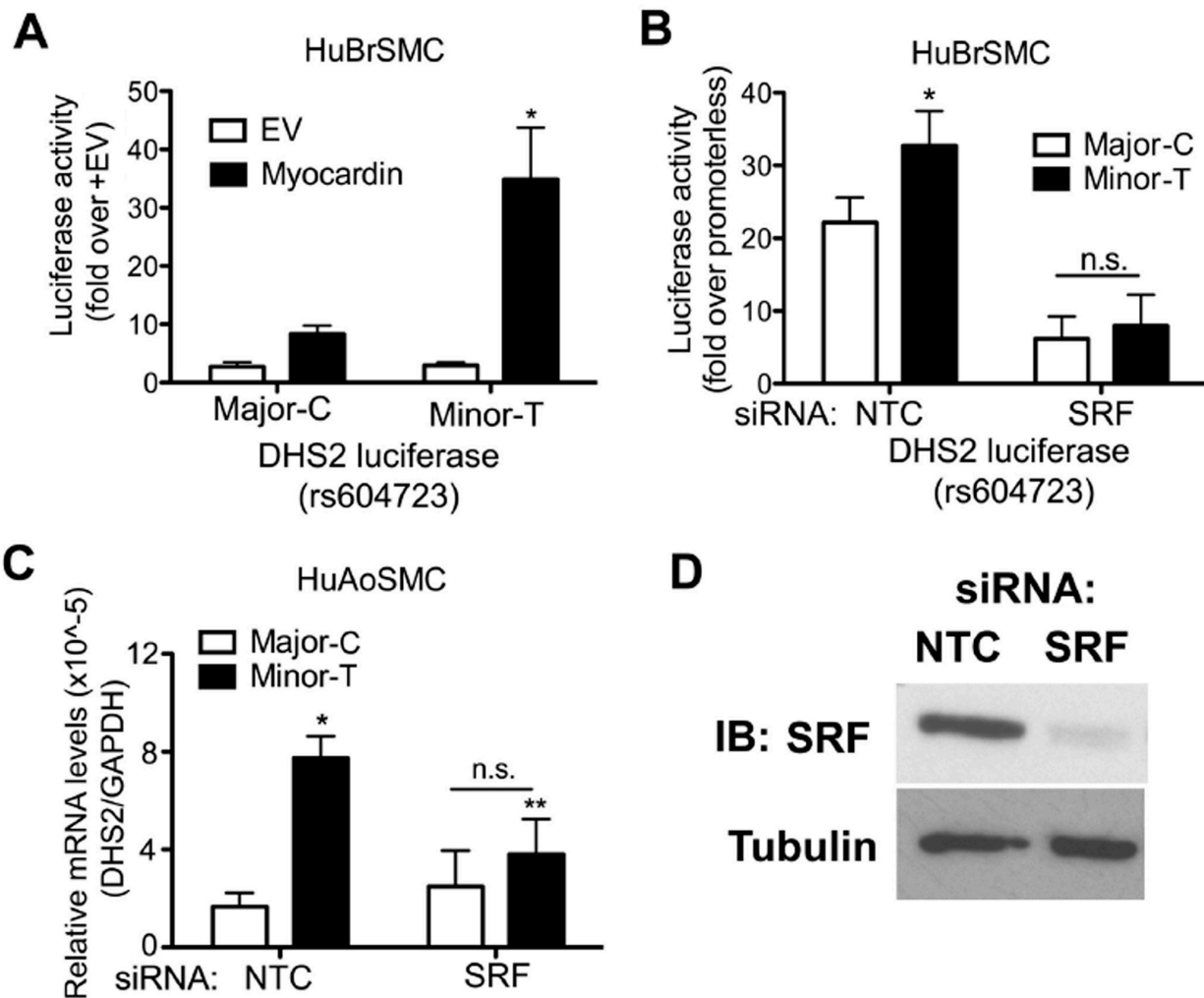
Figure 2.4. The allele-specific activity of the DHS2 enhancer is SRF-dependent. A) Major and minor DHS2 luciferase constructs were transfected into HuBrSMC along with myocardin or empty expression vector. Data represent mean ± SEM of n=5 experiments;*p<0.05 versus major allele plus Myocardin (student's t-test). **B)** DHS2-luciferase activity was measured in HuBrSMC treated with control (NTC) or SRF siRNA. Data represent mean ± SEM of n=6 experiments; *p<0.01 versus the minor allele (student's t-test). **C)** Allele-specific GRAF3 mRNA levels were measured by semi-quantitative RT PCR in control and SRF knockdown HuAoSMC. Data represent mean ± SEM of n=3 experiments; *p<0.05 versus the major C allele in control cells; **p<0.05 versus minor T allele in control cells (student's t-test). **D)** Confirmation of SRF knockdown in SMC treated with control or SRF siRNAs. Data are representative of 3 separate experiments.

strong activator of RhoA signaling in many cell-types including SMC (97), and this effect was abolished by pretreatment with the rho-kinase inhibitor, Y27632 (Figure 2.5A). Physical forces such as cell stretch and tension are also well known activators of RhoA signaling and are known to be increased in the vessel wall under hypertensive conditions (258). As shown in Figure 2.5B, ARHGAP42 mRNA levels were significantly upregulated in SMC cultures subjected to cyclic stretch using the FX-4000T Flexcell system™ and this effect was also rho-kinase-dependent. ARHGAP42 mRNA levels were also upregulated in isolated portal vein segments subjected to static stretch (Figure 2.5C). The fact that LacZ expression was upregulated by stretch in portal veins isolated from *Arhgap42* LacZ genetrap mice strongly indicated that this effect was mediated transcriptionally (Figure 2.5D).

Activation of *ARHGAP42* expression attenuates the development of hypertension

Since RhoA/MRTF/SRF-dependent up-regulation of ARHGAP42 would serve as as a transcriptionally mediated negative feedback loop for RhoA signaling in SMC, we postulated that this mechanism prevents excessive SMC constriction by hypertensive signals. In support of this idea, and in accordance with the results of our cell stretch experiments, arterial ARHGAP42 mRNA levels were significantly increased in mice made hypertensive by L-NAME or DOCA-salt regimens (Figures 2.6A and 2.6B). To test whether upregulation of *ARHGAP42* expression under these conditions counteracted the development of hypertension, we subjected Wt and *ARHGAP42* deficient mice (*Arhgap42*[gt/gt]SM-MHC[creERT2]) to a DOCA-salt regimen and monitored blood pressure by telemetry. Although the initial DOCA-salt mediated increase in BP was similar in both groups (Figure 2.6C), blood pressure in *Arhgap42*[gt/gt]SM-MHC[creERT2] continued to increase over the next week at a rate of 1.5 mmHg/d compared to 0.9 mmHg/d in Wt

mice (p<0.05). As previously observed, the BP pressure difference between these two groups was completely reversed by treatment of *Arhgap42*$^{gt/gt}$SM-MHC^{creERT2} with tamoxifen which also restored *ARHGAP42* expression (Supplemental Figure IV).
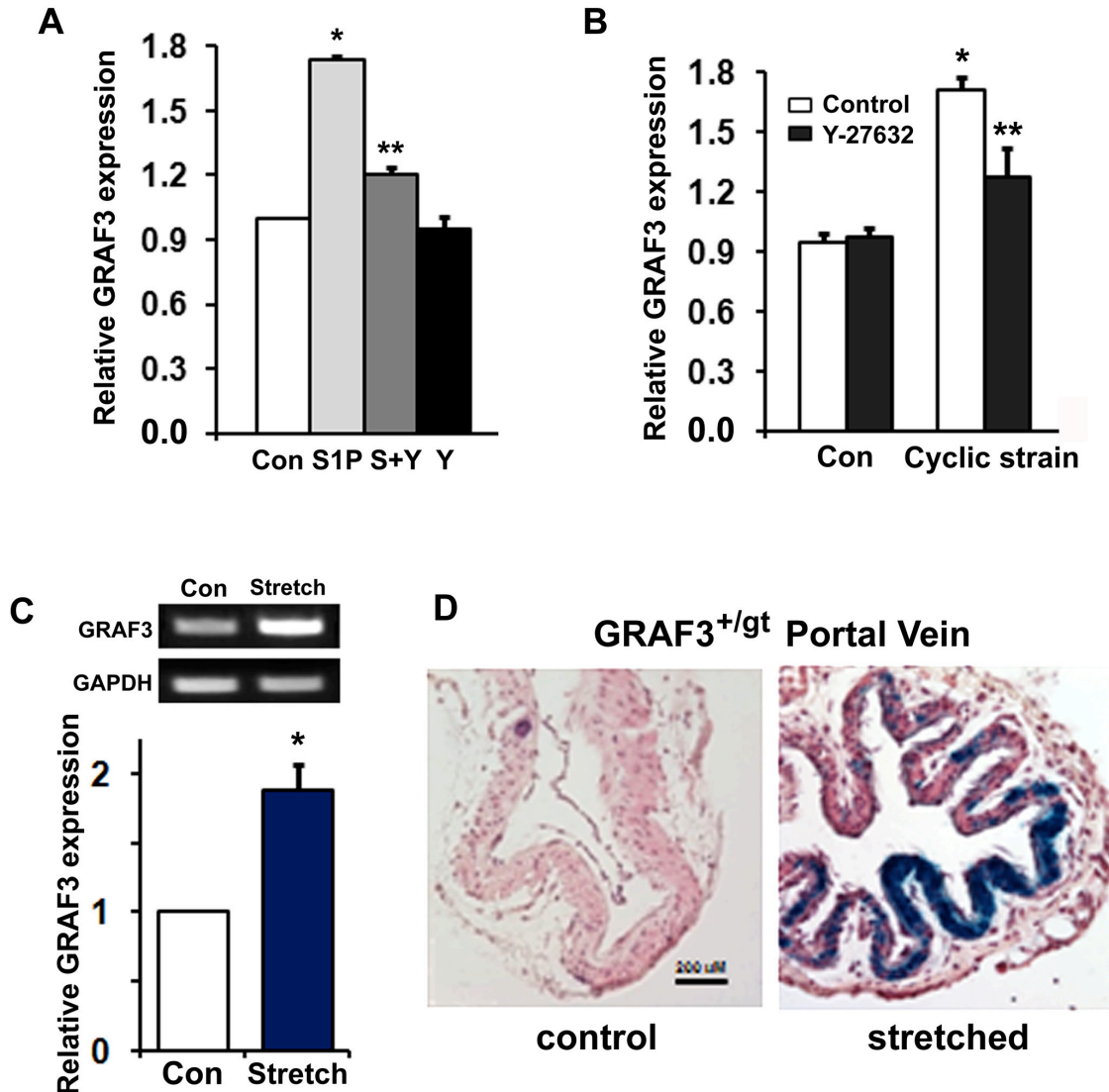
Figure 2.5. *ARHGAP42* **expression is activated by RhoA signaling and cell stretch**
A) Primary rat aortic SMCs were treated with 10 μM sphingosine 1-phosphate (S1P) ±
the rho-kinase inhibitor, Y-27632. *ARHGAP42* expression was measured after 72 h by
seimi-quantitative PCR. Data represent mean ± SEM of 4 experiments; *p< p<0.001
versus control; ** p<0.001 versus S1P-treated (ANOVA). n=4. **B)** Using the FX-4000T
Flexcell system™, primary rat aortic SMCs were subjected to 0 (Ctrl) or 20% equibiaxial
elongation at 1Hz (cyclic strain). *ARHGAP42* message was measured at 18 hours by
qPCR. Data represent mean ± SEM; n=3 from two independent experiments; * p<0.001
versus no cyclic strain, ** p<0.05 versus minus Y-27632 (ANOVA). **C)** Rat portal veins
placed in ex vivo culture were subjected to 0 or 600 mg of static stretching force. At 72 h
ARHGAP42 message was measured by semi-quantitative RT PCR. Graph shows
ImageJ-based quantification of 3 independent experiments. *p<0.05 (student's t-test)
D) Portal veins isolated from *Arhgap42*[+/gt] mice were cultured ex vivo and subjected to 0
or 300 mg of static stretching force for 5 days. After Lac Z staining, tissues were
processed for standard microscopy including hematoxylin and eosin staining. Scale bar
= 200 microns. Data are representative of three independent experiments.
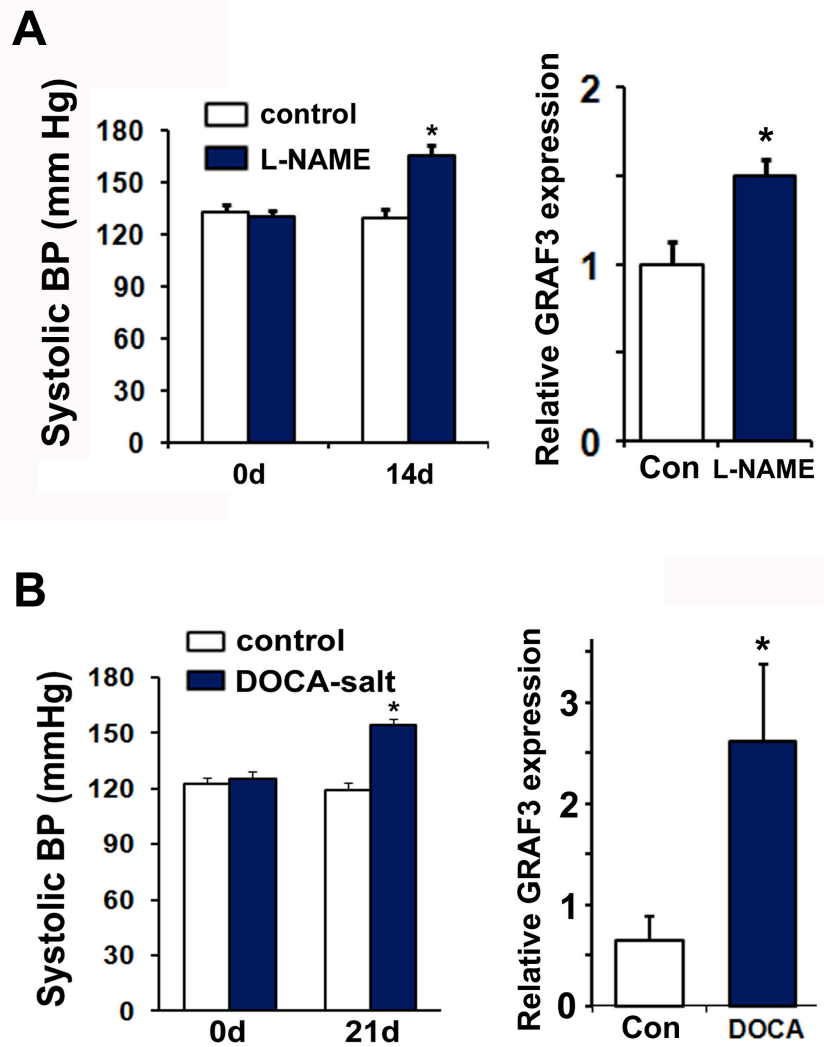
Figure 2.6. *ARHGAP42* expression limits the development of hypertension.   A) Wt mice were treated with L-NAME (450 mg/L in drinking water). After 14 days blood pressure was measured by tail cuff method, and *ARHGAP42* message in isolated mesenteric arteries was measured by quantitative PCR. Data represent mean ± SEM; n=4 per group; *p<0.05 versus untreated (student's t-test). **B)** Wt mice were implantated with a 50mg slow-release DOCA pellet and then fed 0.9% NaCl in drinking water. After 3 weeks blood pressure was measured by tail cuff method, and *ARHGAP42* message in aorta was measured by quantitative PCR. *p<0.05 versus untreated; n = 6 per group (student's t-test).

C
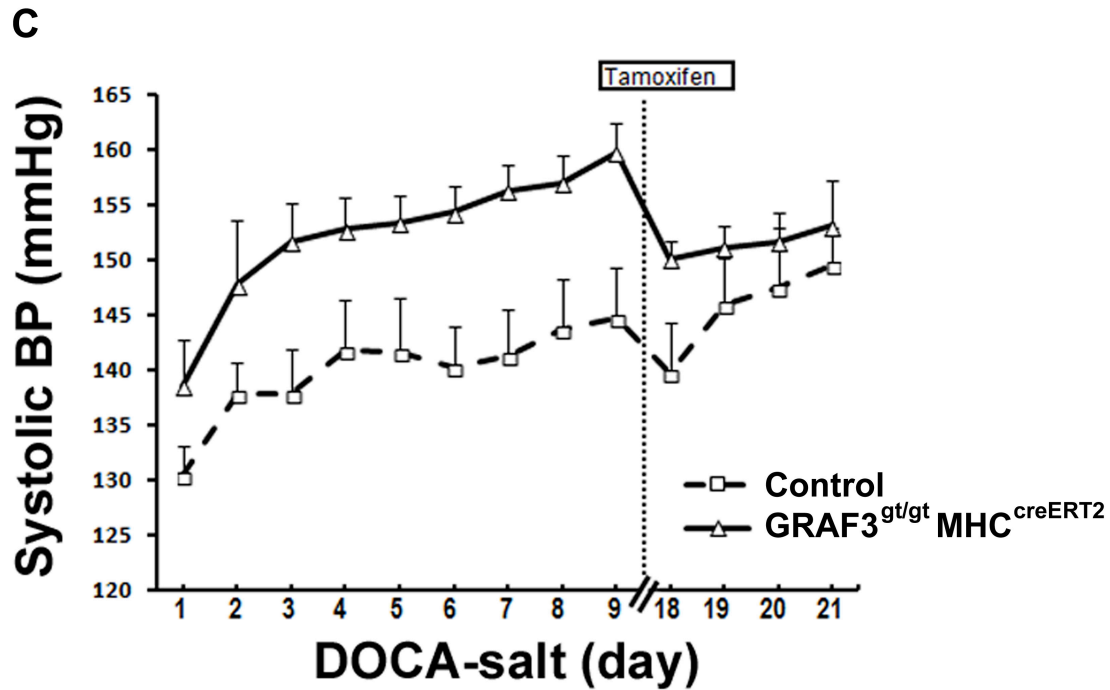
Figure 2.6 (continued). *ARHGAP42* **expression limits the development of hypertension. C)** Following radio-telemeter implantation and equilibration, 3 Wt and 5 *Arhgap42*^gt/gt^SM-MHC^creERT2^ mice were implantated with a 50mg slow-release DOCA pellet and then fed 0.9% NaCl in drinking water for 3 weeks. Ten days after the start of the DOCA-salt regimen, both groups were treated with tamoxifen (100 mg/kg) by oral gavage for 3 consecutive days. Graph represents average mean arterial blood pressure averaged over each 24h period. $p < 0.05$ (SlopesTest).
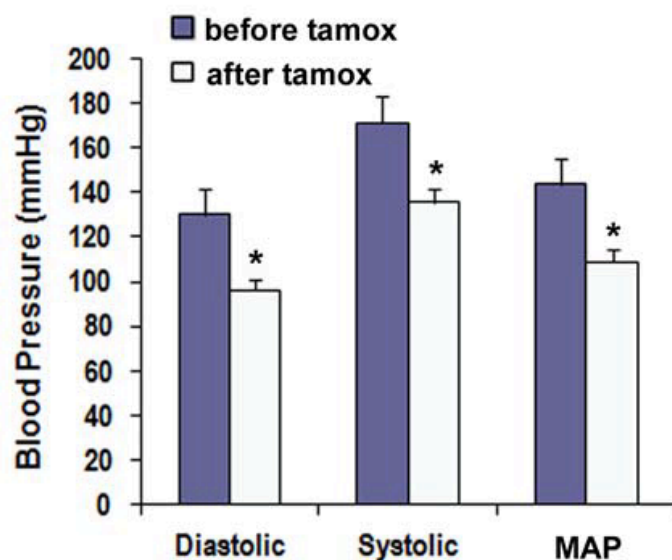
Supplemental Figure II. Tamoxifen treatment of *Arhgap42*[gt/gt]SM-MHC[creERT2] mice restored blood pressure homeostasis. Blood pressure was measured by tail cuff method before and two weeks after the start of tamoxifen treatment (100 mg/kg IP for 5 consecutive days). Data are expressed as mean ± SEM; n=5* p<0.05 vs before tamoxifen (student's t-test 2 tailed).

HuAoSMC Extracts

Probe	rs633185		rs604723	
Allele	C	G	C	T
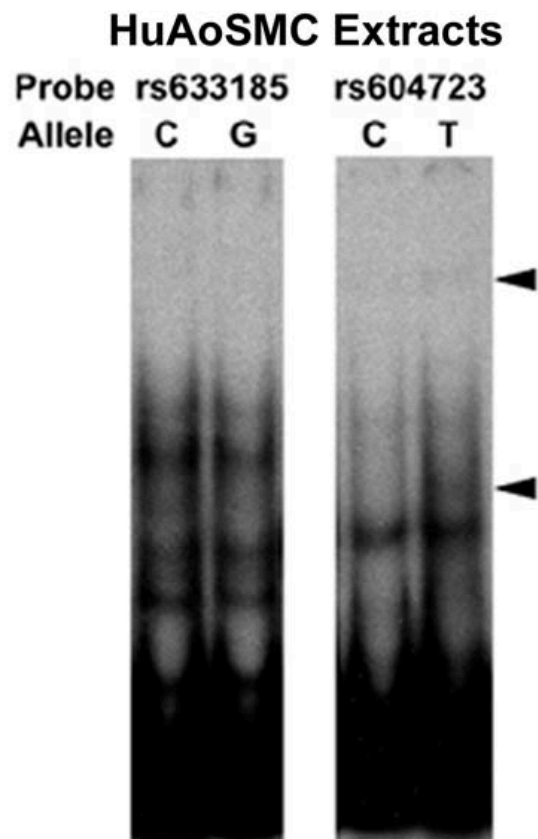
Supplemental Figure III. Gel shift assays were performed by combining nuclear lysates from HuAoSMC with radiolabeled 100 bp oligonucleotide probes containing the major or minor alleles at rs633185 and rs604723. Arrowheads mark allele-specific bands. Gel is representative of two individual experiments.
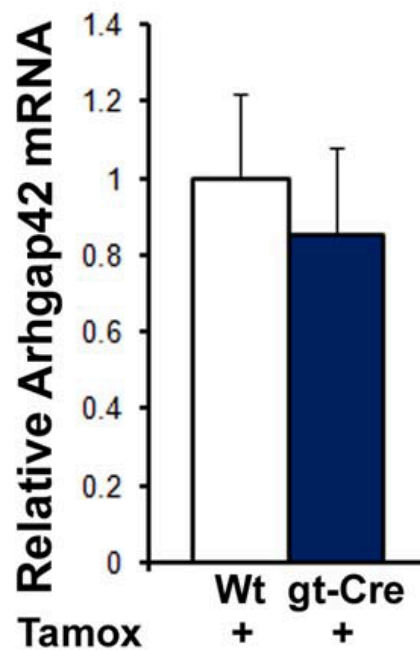
Supplemental Figure IV. Tamoxifen treatment of DOCA-salt-treated *Arhgap42*^{gt/gt}SMMHC^{creERT2} mice restored *ARHGAP42* expression in mesenteric arteries. Wt and *Arhgap42*^{gt/gt}SMMHC^{creERT2} mice were implantated with a 50mg slow-release DOCA pellet and then fed 0.9% NaCl in drinking water for 3 weeks. Ten days after the start of the DOCA-salt regimen, both groups were treated with tamoxifen by oral gavage of 1 mg for 3 consecutive days. Mice were sacrificed 12d after the start of tamoxifen treatment and Arhgap42 message was measured in isolated mesenteric arteries by qPCR. *ARHGAP42* expression was normalized to *GAPDH* and is expressed relative to Wt. Data are expressed as mean ± SEM; n=5 for Wt; n=7 for *Arhgap42*^{gt/gt}SMMHC^{creERT2} mice, p=0.6595 (student's t-test).

A

Exon 23 ARHGAP42 Exon 24 1,063 bp TMEM133 (hypothetical)

Gene structure
(chr11:100,858,086-100,864,815)

PCR primers 1 → ← 2 ← 3

RNA seq

B

ARHGAP42

TMEM133

□ CTRL
■ ARHGAP42 SiRNA
■ TMEM133 SiRNA

C

1.9Kb Prim 1+3
0.85Kb Prim 1+2
0.14Kb GAPDH
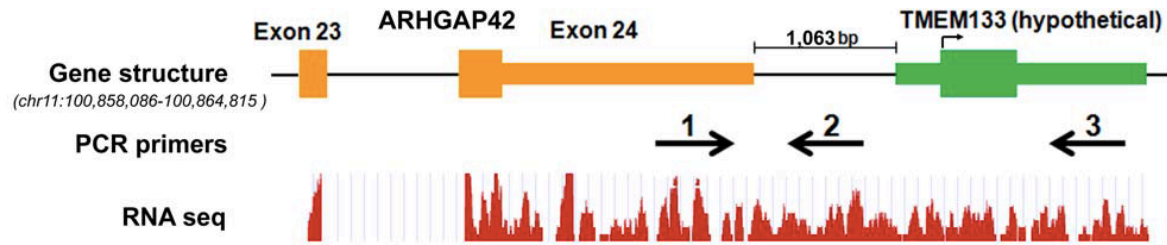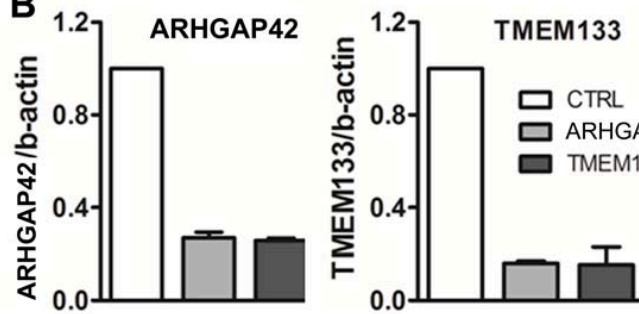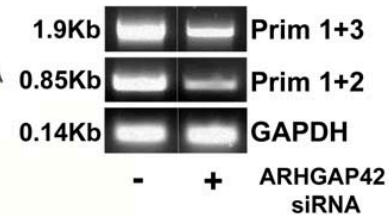
− + ARHGAP42 siRNA

Supplemental Figure V. *TMEM133* is an extension of the *ARHGAP42* 3'UTR. A) RNA seq data from HuAoSMC near the genomic region containing *TMEM133*. **B)** siRNA targeted against *ARHGAP42* or *TMEM133* had identical effects on *ARHGAP42* and *TMEM133* mRNA levels as measured by qPCR. Data are expressed as mean ± SEM of three independent experiments. **C)** mRNA was isolated from HuAoSMCs +/- siRNA to *ARHGAP42*. Following DNase treatment, RT PCR was performed using the primers shown in A. Data represent three independent experiments.

Characteristic	Mean ± SD or percent
Age, mean (yrs)	48 ± 12
Age category, %	
30-44 yrs	44
45-64 yrs	45
65+ yrs	11
% female	53
Race, %	
White	77
Black	19
Other	4
Body mass index, mean (kg/m^2)	29 ± 6
Body mass index category, %	
Normal	27
Overweight	36
Obese	38
Total cholesterol (mg/dl), mean	200 ± 38
Current smoker, %	7
Office systolic BP (mm Hg), mean	130 ± 13
Office diastolic BP (mm Hg), mean	81 ± 9
Clinic hypertension, %	29

SD, standard deviation

Supplemental Table I. Characteristics of clinical cohort

rs604723	C/C	C/T	T/T	MAF
African American	326	32	0	*4.5%
Caucasian	359	274	40	26.3%

rs2055450	A/A	A/T	T/T	MAF
African American	311	47	0	*6.6%
Caucasian	346	290	37	27.0%

rs604723 vs rs2055450	LD r^2	LD D'
African American	0.56	0.89
Caucasian	0.83	0.92

Supplemental Table II. Analysis of *ARHGAP42* genotype in human populations. 1,031 patients from several clinical cohorts were genotyped at the rs604723 and rs2055450 variations using Taqman-based allelic discrimination assays. Linkage disequilibrium for these variations was calculated using R. * p<0.001 vs MAF in Caucasians; Chi-squared test.

Discussion

We have previously shown that the Rho-specific GTPase activating protein, ARHGAP42, is highly and selectively expressed in SMC and that global gene-trap-mediated reduction in ARHGAP42 levels resulted in hypertension (219). By characterizing the transcription mechanisms that control human ARHGAP42 expression, we have now identified a novel mechanism for the BP-associated locus within the *ARHGAP42* first intron. Our data strongly indicate that rs604723 is the causative SNP at this locus and that the minor T allele variation increases *ARHGAP42* expression by promoting SRF binding to a SMC-selective intronic regulatory element. Our demonstration that the minor *ARHGAP42* allele is more highly expressed in HuAoSMCs, when coupled with similar data from human artery samples, strongly supports our hypothesis that this variation reduces blood pressure by inhibiting RhoA-dependent constriction of resistance vessels.

To our knowledge, this is the first demonstration of a genetic variant that alters SRF-binding and that directly connects SRF function to a GWAS locus. Although we have not yet identified the precise mechanisms that control *ARHGAP42* transcription, our data are in excellent agreement with the known role of SRF in the regulation of SMC-specific gene expression (29). DHS2 transcriptional activity was responsive to myocardin overexpression, and knockdown of SRF clearly decreased the activity of the DHS2 regulatory element and of endogenous ARHGAP42 mRNA containing the minor T-allele. Because most SMC marker genes are regulated by multiple SRF binding CArG elements (14, 32, 268), it will be important to determine whether additional CArGs are critical for endogenous ARHGAP42 expression. Interestingly, we saw little effect of SRF knockdown on ARHGAP42 mRNA containing the major C allele. Although this may be

explained by residual SRF expression in SRF knockdown cells, it may suggest that SRF is not absolutely required for expression of the major *ARHGAP42* allele or that enhanced *ARHGAP42* expression of the minor allele is more sensitive to SRF levels. The latter possibility would be consistent with the low binding affinity of this degenerate CArG element. The DHS2 fragment containing the major allele exhibits relatively high transcriptional activity suggesting that sequences outside of the SRF binding region are important and we are currently attempting to identify the transcriptional mechanisms involved. It is also interesting to note that the DHS2 element had significant transcriptional activity on its own and when cloned upstream of a heterologous minimal promoter (data not shown) suggesting that its contributions to *ARHGAP42* transcription are complex and that it does not function as an enhancer in the traditional sense.

We cannot rule out the possibility that other SNPs in the rs604723 LD block play a role in the control of ARHGAP42 expression and/or blood pressure regulation. During the completion of the current studies, Kato et.al. demonstrated that a minor allele variation 7.5 Kb upstream from the *ARHGAP42* transcription start site (rs2055450) was associated with decreased BP in European, East Asian, and South Asian populations as well as methylation of a DNA region within the *ARHGAP42* first intron (6). According to the 1000 genomes database and additional genotyping of our Caucasian and African American patient populations (Suppl Table II), rs2055450 is in relatively high LD with rs604723 significantly extending the functional significance of the minor *ARHGAP42* allele in the control of blood pressure in diverse human populations. However, like the other SNPs within the *ARHGAP42* blood pressure locus, rs2055450 is not located in a region that exhibits sequence conservation or open/active chromatin signatures. Thus, when coupled with our extensive data on the role of the DHS2 and rs604723, it is likely

that rs2055450 and the other variations in this LD block are "bystanders" in regard to the regulation of ARHGAP42 expression and blood pressure. In support of this conclusion, the rs633185 SNP (the variation nearest to a potential regulatory element) had no effect on the transcriptional activity of the DHS1 fragment or protein binding to a 100 bp probe containing this sequence (see Supplemental Figure III)

Interestingly, the GTEx data base indicates that minor *ARHGAP42* allele LD block was significantly associated with increased expression of TMEM33, a hypothetical, uncharacterized RNA just downstream of *ARHGAP42*. However, as shown in Supplemental Figure V, our RNA seq and targeted RT PCR data indicate that TMEM133 is not transcribed as a separate gene, but is actually an extension of the *ARHGAP42* 3' UTR. These data fully explain why variations that alter *ARHGAP42* expression also affect "TMEM133", and by default, eliminate changes in TMEM133 expression as an explanation for the blood pressure locus within *ARHGAP42*.

Our data add to a growing body of evidence that common non-coding variants alter cardiovascular risk by altering transcription factor binding and gene expression (268, 269), and support previous studies implicating RhoA signaling in the regulation of BP homeostasis in mice (14, 36, 37). Our human genetic data from well-characterized untreated patients confirmed that the minor *ARHGAP42* allele was associated with decreased blood pressure. Although the effect size may be relatively small, it has been observed in multiple diverse populations (250-252) indicating that *ARHGAP42* genotype plays an important role. Although our data support the possibility that *ARHGAP42* *genotype* contributes to the susceptibility of African Americans to the development of hypertension (248), the very low MAF in this population has also made it difficult to confirm this idea. Given the paucity of genetic mechanisms that explain this

susceptibility, we are expanding our genotyping and blood pressure analyses in this population. Our results also suggest that *ARHGAP42* genotyping could also prove useful for individualizing antihypertensive therapies. For example, we predict that hypertensive patients homozygous for the major allele would respond better to antihypertensive agents that target SMC contractility (an endpoint directly controlled by RhoA) and that hypertensive patients homozygous for the minor allele may respond better to agents that target cardiac or kidney function. Finally, the regulation of ARHGAP42 expression and/or activity provides a novel therapeutic target for the development of antihypertensive therapies.

CHAPTER 3: IDENTIFICATION OF TRANSCRIPTION MECHANISMS THAT REGULATE EXPRESSION OF THE SMOOTH MUSCLE-SPECIFIC, BLOOD PRESSURE-ASSOCIATED GENE, ARHGAP42

Overview

Our group recently demonstrated that the smooth muscle-specific RhoGAP, GRAF3, is required for adequate blood pressure control, as deletion of this RhoGAP resulted in significant hypertension in mice. Further, variations within the GRAF3 gene are associated with alterations in blood pressure in the human population, and we were the first to demonstrate that the rs604723 minor allele variant increased GRAF3 expression by promoting SRF binding to a novel regulatory DNaseI Hypersensitivity Site (DHS) in the first intron. Interestingly, the major allele-containing DHS still exhibited significant activity, suggesting that additional factors regulate the transcription activity of this region. Based on our finding that this DHS was required for GRAF3 expression, we sought to identify the transcription mechanisms regulating the full activity of this key regulatory region. Here, using sequence analysis, affinity purification, chromatin immunoprecipitation, and gain and loss of function experiments, we identify two transcription factors, RBPJ and TEAD1, that bind to a core DHS sequence to regulate GRAF3 expression. We also demonstrate regulation of GRAF3 expression by a long non-coding RNA (AK124326) at GRAF3's transcription start site and by the microRNA mir-505-3p that targets GRAF3's 3' UTR. This study is the first to identify a transcriptional unit composed of SRF, RBPJ, and TEAD1 that regulates expression of a

smooth muscle-specific, blood-pressure gene and provides a novel mechanism regulating GRAF3 expression by two non-coding RNAs.

Introduction

Hypertension contributes to significant morbidity and mortality due to its effects on the cardiovascular, nervous, and renal organ systems. Despite its prevalence and adverse effects on multiple organ systems, the exact genetic and epigenetic mechanisms leading to hypertension are not completely understood. Accordingly, the majority of individuals with high blood pressure have "essential" hypertension, which has no known cause. Indeed, very few Mendelian cases of hypertension exist, suggesting that hypertension is largely a disease of multiple genetic interactions. To begin to dissect these highly complex genetic pathways that contribute to hypertension, genome-wide association studies (GWAS) have identified candidate genes that may play a role in blood pressure regulation by locating single nucleotide polymorphisms (SNPs) in genes whose function was previously unknown (250-252). In support of the utility of this approach, many of these disease-associated SNPs are located within well-characterized genes known to be important for blood pressure regulation.

Separate GWAS identified SNPs within the first intron of the GRAF3 gene that were associated with changes in blood pressure in the human population. The minor allele (MAF = 0.27), defined by SNPs rs633185 and rs604723 that are in perfect linkage disequilibrium, was associated with a 0.5 mmHg reduction in blood pressure (250-252). In collaboration with the Taylor lab, we demonstrated that GRAF3 was a RhoGAP expressed selectively in smooth muscle that was essential for normal blood pressure, thus providing a potential mechanism for the GRAF3 blood pressure locus in the development of human hypertension (219). Recently, using DNase I hypersensitivity

81

and ENCODE data, we identified a regulatory element that contained rs604723 and exhibited strong allele-specific, SMC-selective activity. Deletion of the SNP-containing region using CRISPR/Cas9 led to a significant reduction in GRAF3 expression. The rs604723 minor T-allele variant increased SRF binding to this region, and SRF was required for the effect of the minor allele on GRAF3 transcription. GRAF3 expression was increased by cell stretch and sphingosine 1-phosphate in a RhoA-dependent manner, and deletion of GRAF3 increased the development of hypertension in mice treated with DOCA-salt. Furthermore, the minor allele correlated with lower blood pressures in a cohort of untreated patients with borderline hypertension (273).

Based on the fact that changes in GRAF3 expression play a major role in the development of hypertension in the human population, identifying the transcription mechanisms that control GRAF3 expression in SMCs will be important for further understanding of blood pressure regulation. We have already shown that GRAF3 expression is regulated in an SRF- and RhoA-dependent manner, similar to other SMC-specific genes, including SMA, SM22, calponin, and SM-MHC (14, 63, 66, 69, 273). It is well established that while SRF and the myocardin factors are potent drivers of smooth muscle-specific gene expression. In brief, SRF binds to CArG elements in promoter and enhancer regions of smooth muscle-specific genes. Myocardin and MRTF-A/B bind to SRF to transactivate SMC differentiation (71, 100). Although SRF and the myocardin transcription factors play a requisite role in SMC differentiation, it is clear that additional transcription factors are also responsible, since myocardin overexpression alone does not fully recapitulate the entire gene repertoire that defines a SMC (76). Furthermore, SMA and SM22 expression in the mouse precede myocardin expression, suggesting that unidentified transcription factors expressed early in development contribute to SMC

differentiation (14, 15).

SMC differentiation is also regulated by non-coding RNAs, including microRNAs (miRNAs) and long non-coding RNAs (lncRNAs). Generally, miRNAs bind directly to the 3' UTR of transcribed genes to decrease mRNA stability, thereby resulting in decreased target gene expression. The most well characterized miRNAs with respect to SMC differentiation are mir-143 and mir-145, which are significantly enriched in vascular SMCs and transcribed as a cluster from the same gene (209). Transcription of mir-143/145 is regulated by SRF and myocardin and is further transactivated by the Nkx factors. Mir-143/145 regulates the balance between contractile and synthetic smooth muscle gene programs. Specifically, mir-143/145 maintains differentiation by stabilizing myocardin, which further enhances transcription of the miRNA cluster in a positive feedback manner. Additionally, mir-143/145 represses expression of KLF4 and Elk-1, which both antagonize the myocardin-SRF interaction. Thus, by stabilizing myocardin and repressing KLF4 and Elk-1, mir-143/145 maintains SMC differentiation by upregulating contractile smooth muscle markers. One of the most well-known examples of lncRNAs that regulate SMC-specific differentiation is MYOSLID (MYOcardin-induced Smooth muscle LncRNA, Inducer of Differentiation), which was identified in a screen for lncRNAs that were significantly upregulated by myocardin overexpression in human coronary SMC (218). MYOSLID contains 3 CArG boxes in its promoter, which bind SRF, as determined by chromatin immunoprecipitation experiments. MYOSLID expression is also regulated by TGFβ/SMAD signaling. Importantly, MYOSLID is localized to the cytoplasm, and thus does not directly affect SMC-specific gene transcription. Rather, MYOSLID is required for actin stress fiber formation and SMAD2 phosphorylation and thus exerts significant regulation over downstream SRF- and

TGFβ-dependent smooth muscle genes, respectively.

The goals of the present study were to identify the transcription mechanisms that regulate expression of the smooth muscle-specific gene, GRAF3. To begin to do this, we first defined the minimal core region within the blood pressure-associated DHS that mediated GRAF3 transcription. Then, we used multiple biochemical and mutation approaches to identify transcription factors that bind to this core DHS region and regulate its activity. Next, to determine if one or more of these factors are required for GRAF3 expression, we utilized several loss-of-function approaches including siRNA-mediated gene knockdown as well as a smooth muscle-specific deletion mouse model. Finally, we describe additional miRNA and lncRNA-based mechanisms that regulate GRAF3 expression.

Materials and Methods

Cell culture

Human aortic and bronchial smooth muscle cells were purchased from Lonza and maintained in Clonetics Smooth Muscle Growth Medium-2 (SMGM-2) and supplemented with growth factors and 5% FBS (Lonza).

Plasmids

For the SRF-dCas9 fusion protein, SRF was subcloned into the pcDNA-dCas9-VP64 vector (Addgene, plasmid #47107) in which VP64 had been cut out. pcDNA-dCas9 (plasmid #47106) and pSPgRNA (plasmid #47108) were purchased from Addgene. pGL3-GRAF3 DHS reporter constructs were generated as previously described (273). RBPJ and TEAD1 site mutations were introduced in pGL3-DHS plasmids using the QuickChange site-directed mutagenesis protocol. All mutations were verified by Sanger sequencing. For 3' UTR stability experiments, the GRAF3 3' UTR

was amplified from HuAoSMC genomic DNA by PCR and then cloned into pGL3 basic vector using In Fusion cloning (Clontech).

Luciferase assays

HuBrSMC were seeded in 24-well plates the day prior to transfections at a density of approximately 2.5×10^4 cells/well. 10T1/2 cells were seeded in 48-well format plates at a density of 1.2×10^4 cells/well the day before transfecting. Cells were transfected with 50 ng DNA/well for 24-wells or 25 ng DNA/well for 48-wells and incubated at 37°C, and luciferase assays were performed 48 hours later. For Jagged-1 stimulation experiments, HuBrSMC were transfected with luciferase constructs and then trypsinized and plated on negative control or Jagged-coated dishes the following day. Values were measured 16 hours later. Luciferase assays were performed using the Steady-Glo Luciferase Kit (Promega) according to the manufacturer's instructions. Raw luciferase values were normalized to the activity of the promoterless pGL3 empty vector.

Jagged-1 coating

6-well plates were incubated with 3 ug of anti-human IgG (Fc-specific) (Sigma) diluted in PBS for 4 hours at room temperature. Following incubation, the antibody solution was completely removed. Wells were then coated with 3 ug rat Jagged-1, human Fc recombinant protein (R&D Systems) or 3 ug human Fc negative control recombinant protein (Millipore) diluted in PBS overnight at 4°C. The next day, the solution was aspirated and cells were seeded on coated plates for 16-24 hours after which cells were harvested for luciferase assays or RNA.

Mir-505-3p transfections

HuBrSMC were transfected in 6-wells with 80 nM mir-505-3p mimetic or negative

control mimetic (Invitrogen) for 48 hours.

Knockdowns

HuBrSMC were transfected with 20 nM siRNA targeted to TEAD1 or a GFP non-targeting negative control for 72 hours. RNAiMax (Invitrogen) was used as the transfection reagent. For knockdown of the AK124326 long non-coding RNA, HuBrSMc were transfected with 100 nM siRNA, using Dharmafect (Dharmacon) as the transfection reagent.

qRT-PCR

RNA was isolated from cells using the RNeasy mini kit (Qiagen) and treated with DNase (Qiagen) to eliminate contaminating genomic DNA. RNA was converted to cDNA using the iScript cDNA synthesis kit (Biorad). 12-50 ng cDNA was used in downstream quantitative real-time PCR.

Electrophoretic mobility shift assays

HuAoSMC nuclear lysates were prepared using the Nuclear Isolation kit from ThermoScientific. Lysates were dialyzed in Dignam Buffer D (20 mM HEPES, pH 7.9, 20% (v/v) glycerol, 0.1 M KCL, 0.2 mM EDTA, 0.5 mM PMSF, and 0.5 mM DTT). Each reaction contained 10 ug lysate or 1 ul in vitro translated-SRF, 20,000 cpms of 32P-labeled oligonucleotide probe, and 0.20 ug dIdC in binding buffer (10 mmol/L Tris, pH 7.5, 50 mmol/L NaCl, 100 mmol/L KCl, 1 mmol/L DDT, 1mmol/L EDTA, 5% glycerol).

Chromatin Immunoprecipitation (ChIP) experiments

ChIP assays were performed according to X-ChIP protocol (Abcam) with slight modifications. In brief, HuBrSMC were fixed for 5 minutes in 0.7% formaldehyde. The crosslinking reaction was stopped by incubating cells with 0.125 M glycine for 5 minutes. Cells were scraped in lysis buffer (5 mM PIPES, pH 8.0, 85 mM KCl, 0.5%

NP40) and then nuclei were isolated by centrifugation at 2,300xg for 5 minutes. Nuclei lysis buffer (50 mM Tris-Cl, pH 8.1, 10 mM EDTA, 0.13% SDS) was added to pelleted nuclei. Chromatin was sheared into 500 bp fragments by sonication and immunoprecipitated overnight at 4°C with 1 ug of anti-RBPJ antibody (Cell Signaling), anti-Notch3 antibody (Santa Cruz), anti-TEAD1 (Santa Cruz), or normal rabbit IgG antibody (Cell Signaling) or mouse IgG (Millipore) as a negative control for non-specific binding. For re-ChIP assays, chromatin was incubated with 1 ug of TEAD1 antibody. DNA was eluted with re-ChIP elution buffer and then diluted with 3x volume ChIP buffer. Eluted DNA was incubated with 1 ug RBPJ antibody or 1 ug normal rabbit IgG antibody.

SMC-specific RBPJ deletion

RBPJ floxed/floxed mice (RBPJ$^{f/f}$) were crossed with SM-MHC^{creERT2} mice, which were provided by Stefan Offermanns (University of Heidelberg, Germany). Experiments were performed in male mice 2-4 months old using age, sex, and littermate genetic controls. Genotyping was performed using DNA isolated from tail biopsies. Cre activity in this model was induced with tamoxifen (100 mg/kg) by IP injection for 5 consecutive days or oral gavage for 3 consecutive days. For controls, genotypically identical littermates were injected with corn oil. Approximately 1 week after the last tamoxifen administration, aorta and bronchi were harvested. Aortas were stripped of adventitia and bronchi were cleaned of surrounding non-SMC tissue. Tissues were frozen in liquid nitrogen, crushed, and protein was extracted in RIPA buffer. Protein expression was measured using standard Western blotting with an RBPJ antibody (Cell Signaling) and tubulin (Sigma) as a loading control.

Results

Engineering a novel dCas9-SRF fusion protein to target endogenous loci.

CRISPR-Cas9 has been used widely to modify specific genomic loci with minimal off targeting effects (70). Recently, a catalytically inactive "dead" Cas9 (dCas9) molecule has been generated by introducing D10A and H840A mutations that render the Cas9 nuclease inactive. In combination with sgRNAs, the dCas9 can used to target specific regulatory regions and disrupt gene expression by depositing dCas9 at these loci. In this manner, dCas9 provides a steric obstacle for critical transcription factors, which cannot bind to critical promoter/enhancer regions. As alluded to, this approach has been extremely useful for identifying functional regulatory regions in the endogenous gene context without using a gene editing CRISPR approach. More recently, transcriptional repressors (e.g., KRAB) and activators (e.g., VP64) have been fused to dCas9 to create synthetic transcription factors that strongly inhibit or enhance gene expression, respectively (271, 272). We took advantage of this novel approach by engineering an SRF-dCas9 molecule in which SRF was fused to the dCas9 molecule (Figure 3.1A). The SRF-dCas9 fusion protein was efficiently expressed in HuBrSMC (Figure 3.1B). Next, we designed sgRNAs that targeted the endogenous GRAF3 DHS locus (Figure 3.1C). Experiments with SRF-dCas9 were performed in parallel with dCas9. In order to control for non-specific effects of SRF on gene expression (rather than an effect due to targeting specific loci), SRF-dCas9/dCas9 was also transfected with sgRNA empty vector. As seen in Figure 3.1D, dCas9 targeted to the DHS reduced endogenous GRAF3 expression in HuBrSMC, suggesting that the dCas9 is a critical regulatory region. In line with our hypothesis, SRF-dCas9 targeted to DHS upregulated

GRAF3 expression; however, it was a small effect (Figure 3.1E). It is important to note that the effect of SRF at the DHS was most likely underestimated by this approach, since there were likely negative effects imparted by the steric hindrance of the dCas9-SRF molecule. Regardless, these data are in excellent agreement with our previous observations that SRF binding specifically to the DHS regulates GRAF3 expression.

Identification of the core regulatory region required for GRAF3 transcription.

We had previously determined that a 604 bp DHS within the GRAF3 first intron exhibited significant SMC-specific transcription activity. This DHS contained the SNP rs604723, however, apart from the minor T allele's positive effect on transcription activity of this region, the major C allele still exhibited 20-fold activity over empty vector (273). This suggested that transcription factors within the conserved DHS, in addition to SRF, mediated the full activity of this region. To begin to identify the transcription mechanisms that mediate non-SRF dependent regulation of the DHS fragment, we generated a deletion series comprised of 200 bp overlapping fragments that spanned the GRAF3 DHS. Each 200 bp fragment was cloned upstream of luciferase in a promoterless pGL3 vector, and the activity of each construct was measured in HuBrSMC. Two fragments that together spanned 200-500 bp showed the greatest luciferase activity (Figure 3.2). To narrow our search down to individual cis elements regulating activity of the entire 604 bp region, we generated another deletion series in which 100 bp fragments within the high activity 200-500 bp sequence were cloned into luciferase vectors and transfected into HuBrSMC as described. As shown in Figure 3.3A, a fragment from 300-400 bp nearly recapitulated the activity of the full length DHS (25-fold compared to 30-fold over empty pGL3 vector, respectively), suggesting that transcription factors binding to this core 100 bp region were required for GRAF3

transcription.

RBPJ and TEAD1 bind to a conserved sequence within the DHS.

To identify the transcription factors mediating the activity of the 300-400 bp region, we searched for consensus binding motifs throughout the 100 bp sequence (Figure 3.3B). We identified two GTGGG consensus sequences that bind the Notch transcription factor, RBPJ, in the smooth muscle myosin heavy chain promoter (120). One of these sites was well conserved in mammals. The Notch pathway is activated when a neighboring cell expressing Jagged-1 engages the notch receptor on the SMC, resulting in cleavage of the notch receptor intracellular domain (NICD) by gamma-secretase. NICD translocates into the nucleus to displace repressors that are bound to RBPJ (122). The NICD-RBPJ complex drives expression of downstream Notch target genes (123).

We also identified a conserved MCAT consensus cis element (CATTCCT), which binds the Hippo downstream transcription factor, TEAD1 (141). Of note, there was also a cryptic MCAT motif that varied from the consensus by one base pair embedded within the proximal part of the second MCAT site. Hippo activation leads to phosphorylation of the Mst1/2 serine/threonine kinases, which activate Lats1/2 serine/threonine kinases. Active Lats1/2 phosphorylate and inhibit Yap/Taz, which prevents their nuclear accumulation and subsequent activation of the TEAD transcription factors. Thus, Hippo activation represses TEAD-dependent gene expression, which is relieved by Hippo pathway inactivation when Yap/Taz translocate into the nucleus and bind the TEADs.

Our observations that RBPJ and/or TEAD1 bound to the GRAF3 DHS were based on in silico predictions using published consensus motifs. Thus, to directly test whether the 100 bp fragment harboring the predicted cis elements could bind their
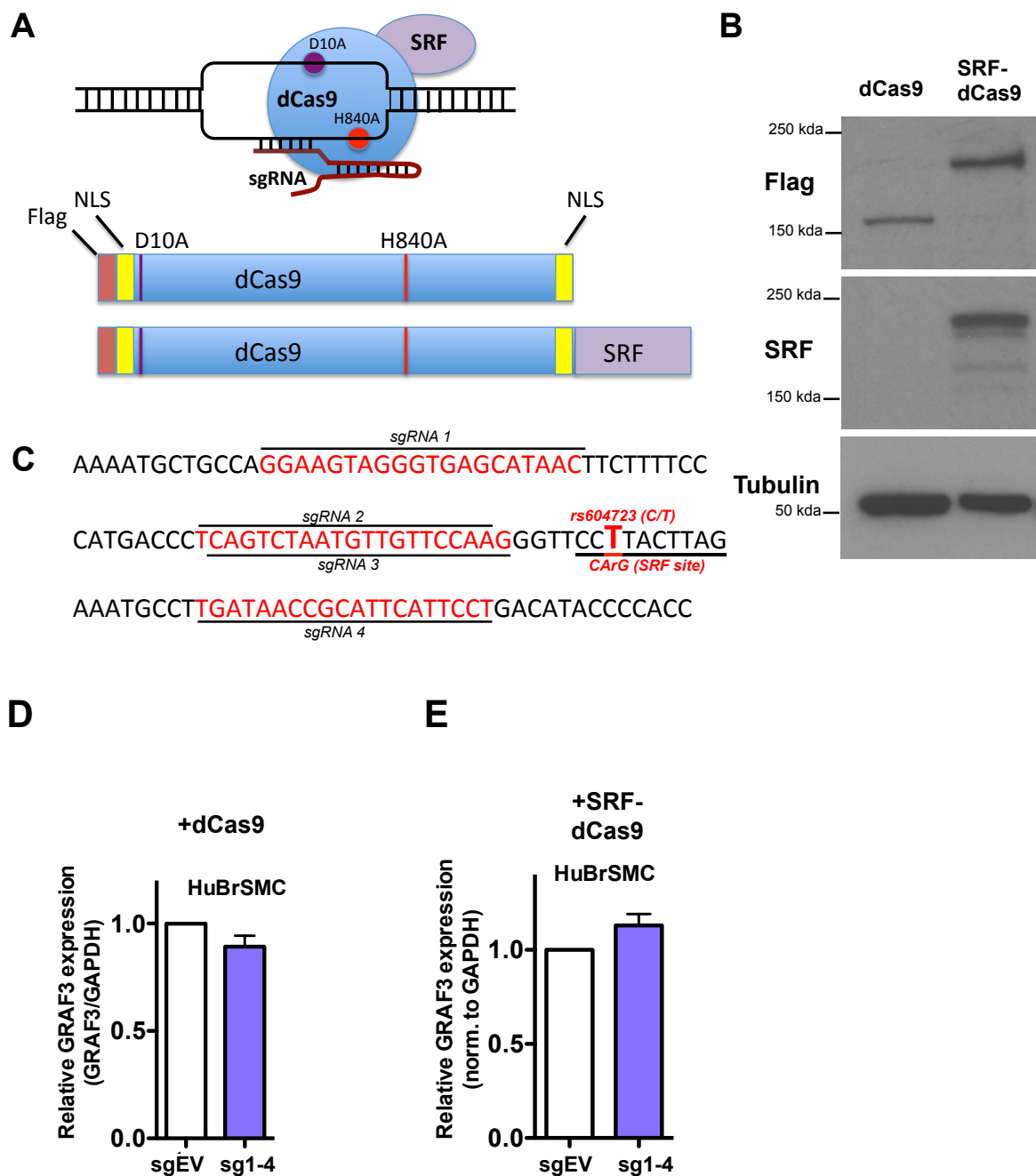
Figure 3.1. SRF targeted to the conserved DHS increases endogenous GRAF3 expression. A) Schematic of engineered SRF-dCas9 protein. **B)** Western blotting analysis of dCas9 and SRF-dCas9 expression in HuBrSMCs. **C)** Conserved 100 bp region within the GRAF3 DHS labeled with the sgRNAs used to target dCas9 and dCas9-SRF. **D)** HuBrSMC transfected with dCas9 or dCas9-SRF **(E)** and guide RNAs (sgRNAs) for 72 hours were collected for RNA isolation and downstream Taqman qRT-PCR for GRAF3 expression.
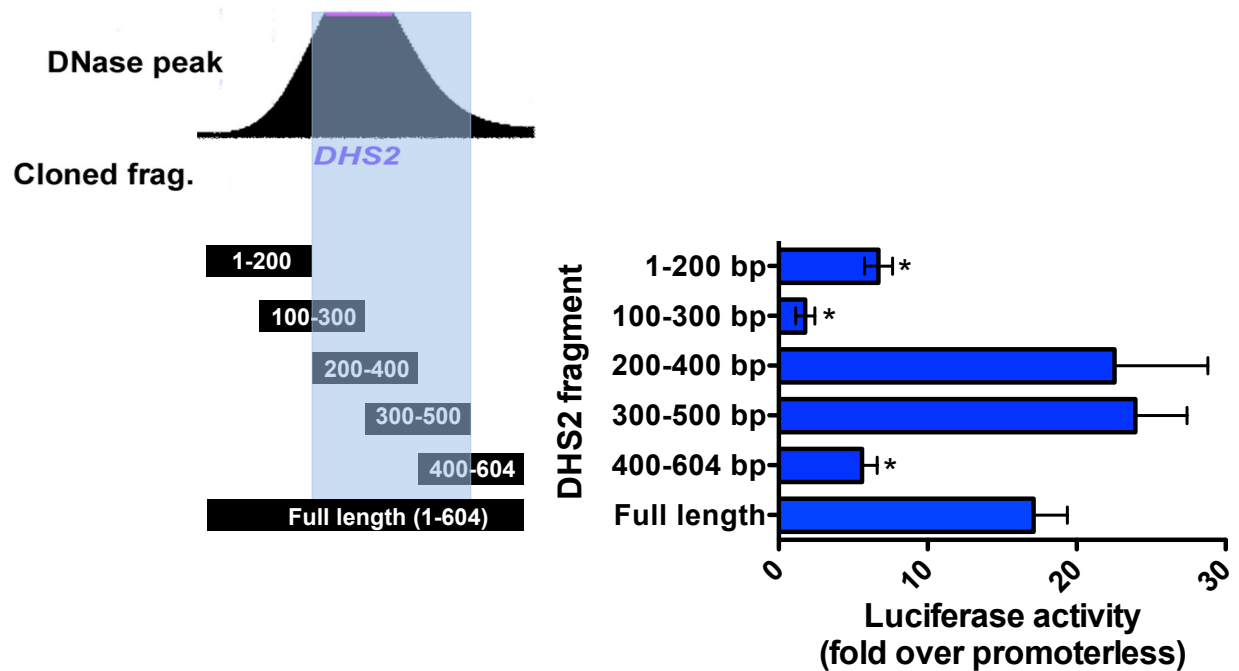
Figure 3.2. Preliminary mapping of the core regulatory region within the GRAF3 DHS. 200 bp overlapping regions spanning the full 604 bp DHS were cloned into the pGL3 vector and transfected into HuSMC. Luciferase assays were performed 48 hours later.
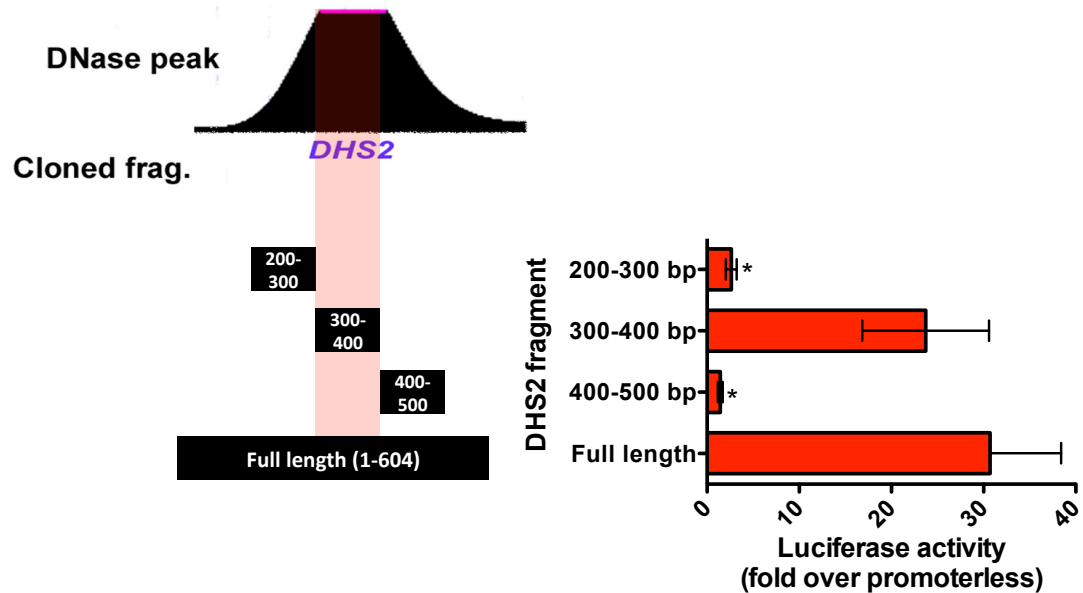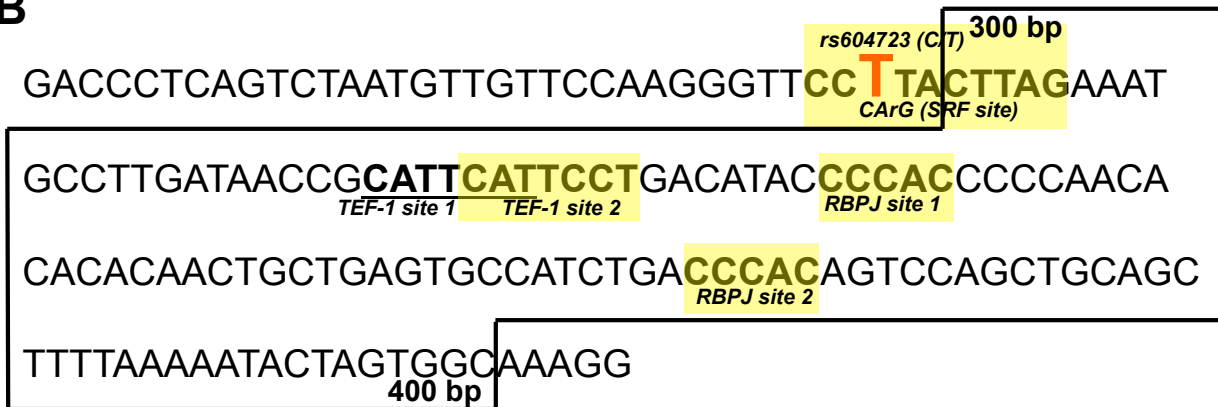
Figure 3.3. A core DNase I Hypersensitive regulatory region drives GRAF3 transcription. A) The 200-500 bp region exhibiting the highest transcription activity was divided into three 100 bp fragments and cloned separately into luciferase vectors (n=4). HuBrSMC were transfected for 48 hours and then luciferase assays were performed *p<0.05 (student's two-tailed t-test). B) 100 bp high transcription activity region is boxed and the predicted transcription factor binding sites are highlighted in yellow.

respective transcription factors, we synthesized 100 bp biotin-labeled oligonucleotide probes that contained the conserved RBPJ and MCAT cis elements. Probes were incubated with human SMC nuclear extracts to purify the protein complexes that bound to this region. As shown in Figure 3.4A, RBPJ, NICD, and TEAD1 were detected in the purified sample, and none of these were detected in the non-specific negative control sample. Additionally, RBPJ bound very strongly to this region in gel shift assays, as well as in supershift assays in which an RBPJ antibody was added to the probe-nuclear extract reaction (Figure 3.4B). In these experiments, we used gel shift probes that contained either the rs604723 C or T SNP, since SRF binding (T allele) could theoretically affect RBPJ binding to this region. There were no differences in RBPJ binding to C or T probes. Because in vitro transcription factor binding assays do not always reflect binding at the endogenous gene locus, we used chromatin immunoprecipitation (ChIP) to examine binding to the GRAF3 DHS in vivo. Chromatin from HuBrSMC was incubated with antibodies to RBPJ, TEAD1, or an IgG antibody to control for non-specific binding. ChIP'ed DNA was subjected to PCR using 100 bp primer sets that flanked the region containing RBPJ and TEAD1 binding sites. As observed in Figure 3.4C, both RBPJ and TEAD1 bound to the GRAF3 DHS in vivo.

Activity of the GRAF3 DHS is regulated by Notch/RBPJ and TEAD1.

To determine if RBPJ and TEAD1 binding were required for the transcription activity of the full-length DHS, we used site-directed mutagenesis to disrupt each transcription factor's predicted sequence within the pGL3-DHS construct. To assess the contribution of each binding site on DHS activity, we generated a variety of mutation constructs that contained mutation of a single binding site or combinations thereof. Each RBPJ site was mutated individually, and a construct was generated with both RBPJ

binding sites abolished. Because there were two overlapping MCAT motifs (one consensus and another proximal element that varied from the consensus by one base pair), our mutagenesis strategy abolished both MCAT sites. To determine if additional sequences in this region (other than the RBPJ and TEAD1 sites) were required for GRAF3 transcription, we also generated a reporter construct harboring mutations in both RBPJ sites and the TEAD1 site (Figure 3.5A). As seen in Figure 3.5B, mutation of both RBPJ binding sites led to an 80% reduction in DHS activity, while disruption of the TEAD1 site caused about a 50% decrease in activity. Mutation of all three binding sites did not decrease luciferase activity lower than that seen for the double RBPJ site mutant, indicating additional binding sites may exist or may reflex non-specific activity.

Given that mutation of both RBPJ binding sites led to an 80% decrease in luciferase activity, we hypothesized that Notch regulated GRAF3 transcription. To date, four notch receptors (1-4) have been identified; however, Notch3 is preferentially expressed in differentiated arterial SMC and cleaved to generate NICD3, which activates Notch target genes (126). Thus, to begin to test our hypothesis that Notch signaling upregulates GRAF3 transcription, we co-transfected a flag-NICD3 expression construct with the full-length DHS in 10T1/2 cells. NICD3 increased GRAF3 DHS activity by 6-fold, which was significantly diminished by mutation of both RPBJ binding sites (Figure 3.6A). Both endothelial and vascular SMC express the ligand Jagged-1, which binds to the Notch receptor (131). Thus, as another way to activate the Notch pathway, we seeded HuSMC transfected with pGL3-DHS luciferase constructs on recombinant Jagged-1 ligand. Activation of Notch by Jagged-1 increased DHS transcriptional activity by 2-fold (Figure 3.6B). Third, treatment with the gamma-secretase inhibitor, DAPT, which prevents NICD cleavage and thus inhibits Notch,
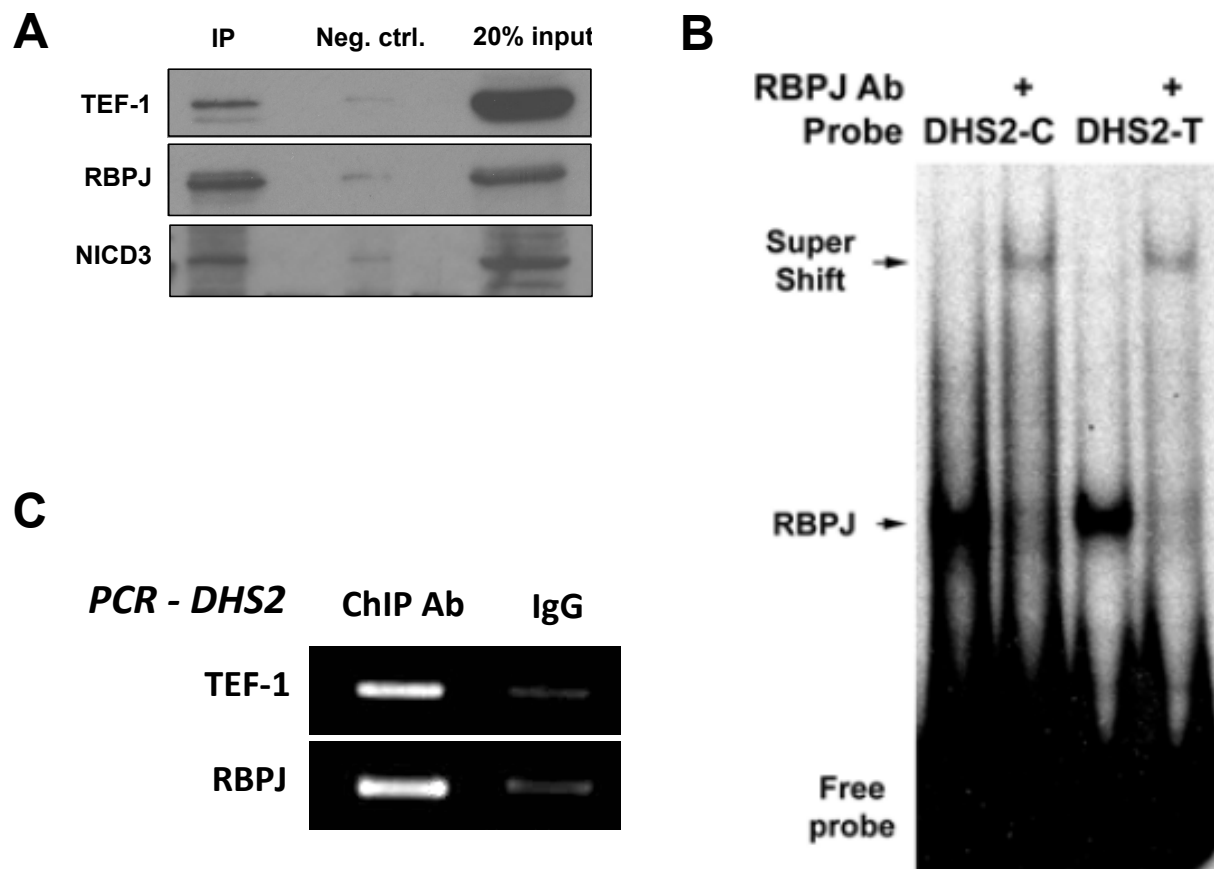
Figure 3.4. The core DHS regulatory region binds RBPJ and TEAD1. A) TEAD1, RBPJ, and NICD3 were affinity purified from HuSMC nuclear lysates with 100 bp biotin-tagged oligonucleotides linked to streptavidin beads. **B)** 20 bp probes containing the conserved RBPJ site were radiolabeled with P32 and incubated with HuSMC nuclear extracts. **C)** TEAD1 and RBPJ chromatin immunoprecipitation (ChIP) samples were subjected to targeted PCR using 300 bp primer sets spanning the GRAF3 DHS.
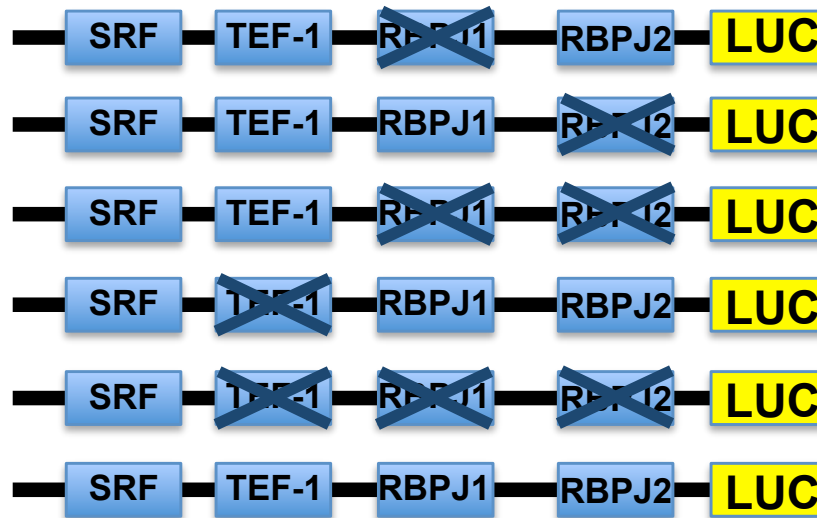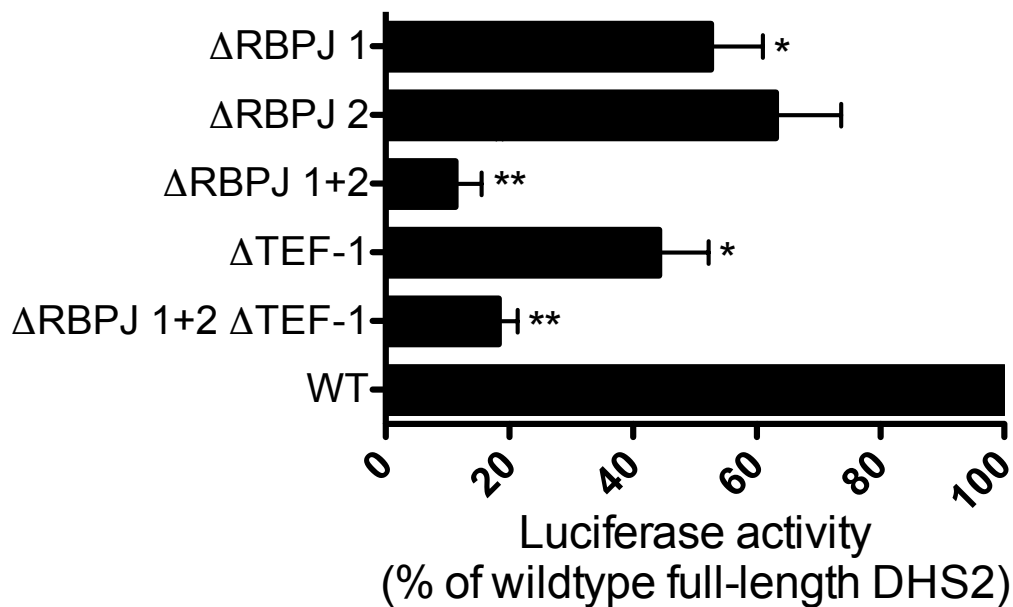
Figure 3.5. RBPJ and TEAD1 binding sites are required for GRAF3 transcription.
A) RBPJ and TEAD1 binding sites within the full-length DHS were mutated using site-directed mutagenesis. **B)** Constructs were transfected into HuBrSMC and luciferase assays were performed 48 hours later. Results are presented as % activity relative to the DHS2T-pGL3 construct. *p<0.05 compared to wild-type pGL3-DHS (student's two-tailed t-test).

significantly reduced DHS luciferase activity but not the activity of the minimal TK

negative control promoter that does not harbor RBPJ binding sites (Figure 3.6C).

Notably, there was no difference in response to Notch perturbation between C and T

alleles, which supports our gel shift experiments indicating that the presence of SRF

does not affect RBPJ binding, nor does Notch activate gene expression in an SRF-

dependent manner.

Endogenous GRAF3 expression in SMC is regulated by RBPJ and TEAD1.

Based on our observation that RBPJ binding was critical for DHS activity and that

the Notch pathway significantly upregulated GRAF3 transcription, we hypothesized that

Notch/RBPJ would also be required for endogenous GRAF3 expression. We first tested

this in vitro by plating human aortic SMC (HuAoSMC) on Jagged-1 ligand, as described

above. As demonstrated in Figure 3.7A, GRAF3 expression was upregulated by Notch

activation nearly 2-fold after 24 hours of stimulation with Jagged-1. To provide direct

evidence that RBPJ was essential for GRAF3 expression in vivo, we crossed mice

harboring an RBPJ floxed allele (RBPJ$^{f/f}$) to SM-MHC^{creERT2} mice that express a

tamoxifen-inducible Cre driven by the smooth muscle-myosin heavy chain (SM-MHC)

promoter (104). Upon injection with tamoxifen, Cre-recombinase translocates to the

nucleus where it excises the RBPJ allele, which is flanked by LoxP sites, only in cells

that express RBPJ and Cre. Because SM-MHC is a smooth muscle-specific promoter,

RBPJ is selectively deleted from Cre-expressing SMCs. As seen in Figure 3.7B,

tamoxifen injection reduced RBPJ expression by over half and completely abolished

GRAF3 expression compared to mice injected with corn oil. Our promoter data

suggested that TEAD1 regulated GRAF3 expression. Thus, to test if this was the case,

we used siRNA-mediated knockdown of TEAD1 in HuBrSMC. As shown in Figure 3.8A,
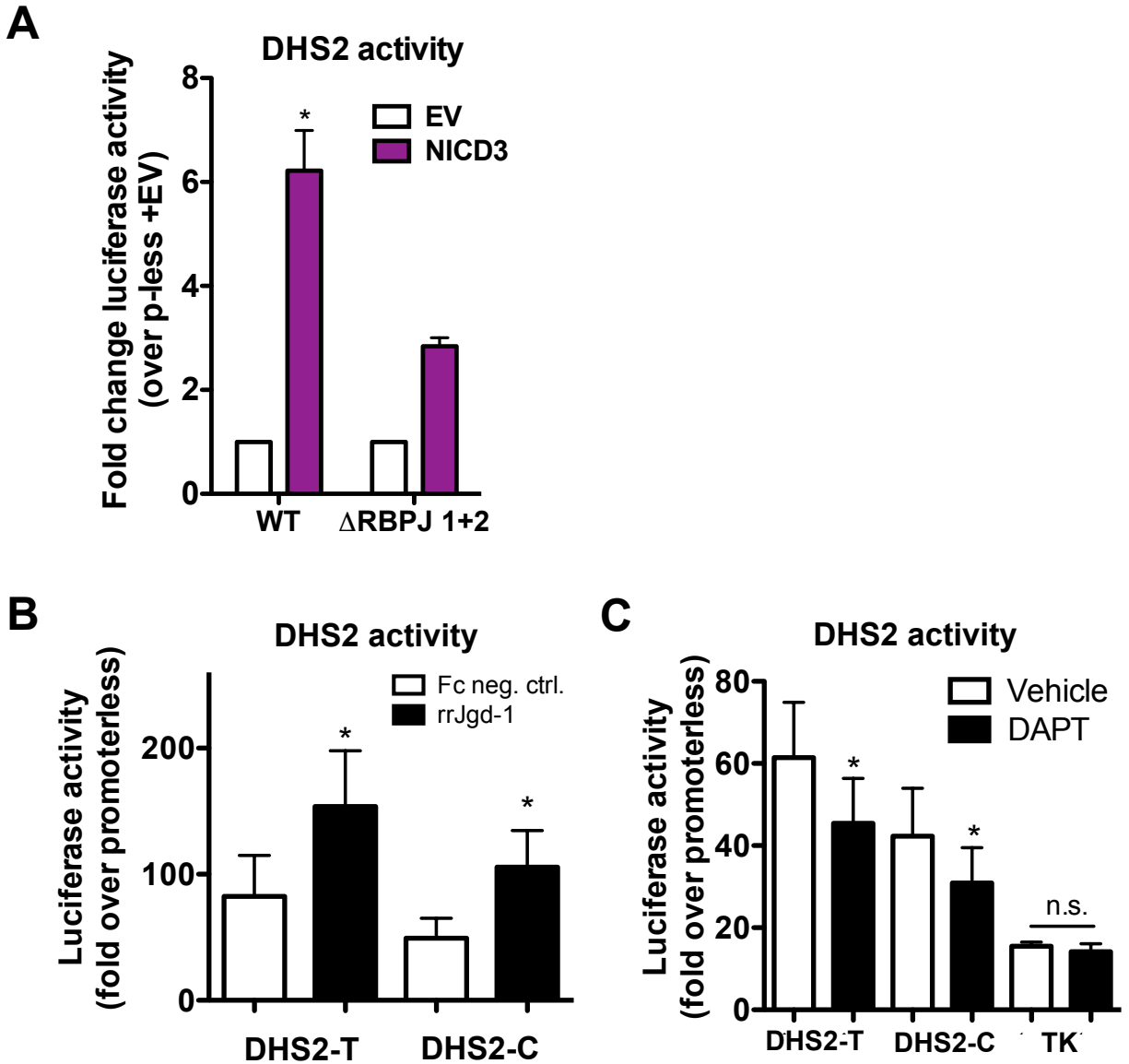
Figure 3.6. GRAF3 transcription is regulated by Notch signaling. A) Flag-NICD3 was co-expressed with pGL3-wildtype DHS or pGL3-DHS with mutated RBPJ sites. **B)** HuBrSMC were transfected with DHS-C or DHS-T luciferase constructs and then seeded onto recombinant negative control or jagged-1 protein. **C)** HuBrSMC were transfected with luciferase plasmids and then treated with DAPT for 16 hours. *p<0.05 compared to pGL3-RBPJ 1+2 mut and pGL3-TEAD1 mut (top); p<0.05 compared to negative control or vehicle (bottom).

knockdown of TEAD1 reduced GRAF3 expression by half.

Cooperativity between RBPJ and TEAD1.

It is accepted that transcription factor occupancy at promoters and enhancers can cooperatively regulate binding of other proteins (44). Given the proximity of the TEAD1 and RBPJ binding sites in the conserved DHS, we hypothesized that the two transcription factors may associate, and, perhaps, influence binding of each other. First, in order to determine if TEAD1 and RBPJ interacted, we carried out a co-immunoprecipitation in HuBrSMC nuclear extracts. Indeed, we were able to detect significant interaction between TEAD1 and RBPJ (Figure 3.8B). While this suggests physical interaction between the two transcription factors, it does not address if the two proteins are localized on the same DNA strand, as would be expected if the two were participating in a cooperative interaction. Thus, to directly test if the two proteins occupied the same DNA fragment, we performed Re-ChIP assays. ChIP using an RBPJ antibody incubated with TEAD1 ChIP'ed DNA revealed significant enrichment of RBPJ binding the same sequences to which TEAD1 was bound compared to an IgG negative control antibody (Figure 3.8C). We hypothesized that TEAD1 facilitated RBPJ, and, perhaps, Notch-dependent activation of GRAF3 transcription. To examine this possibility, we overexpressed flag-NICD3 with wildtype DHS- or with the DHS containing a mutant TEAD1 binding site-luciferase construct in 10T1/2 cells. Interestingly, TEAD1 binding was required for transactivation of DHS luciferase activity, strongly suggesting that TEAD1 enhances RBPJ binding to the GRAF3 DHS (Figure 3.8D).
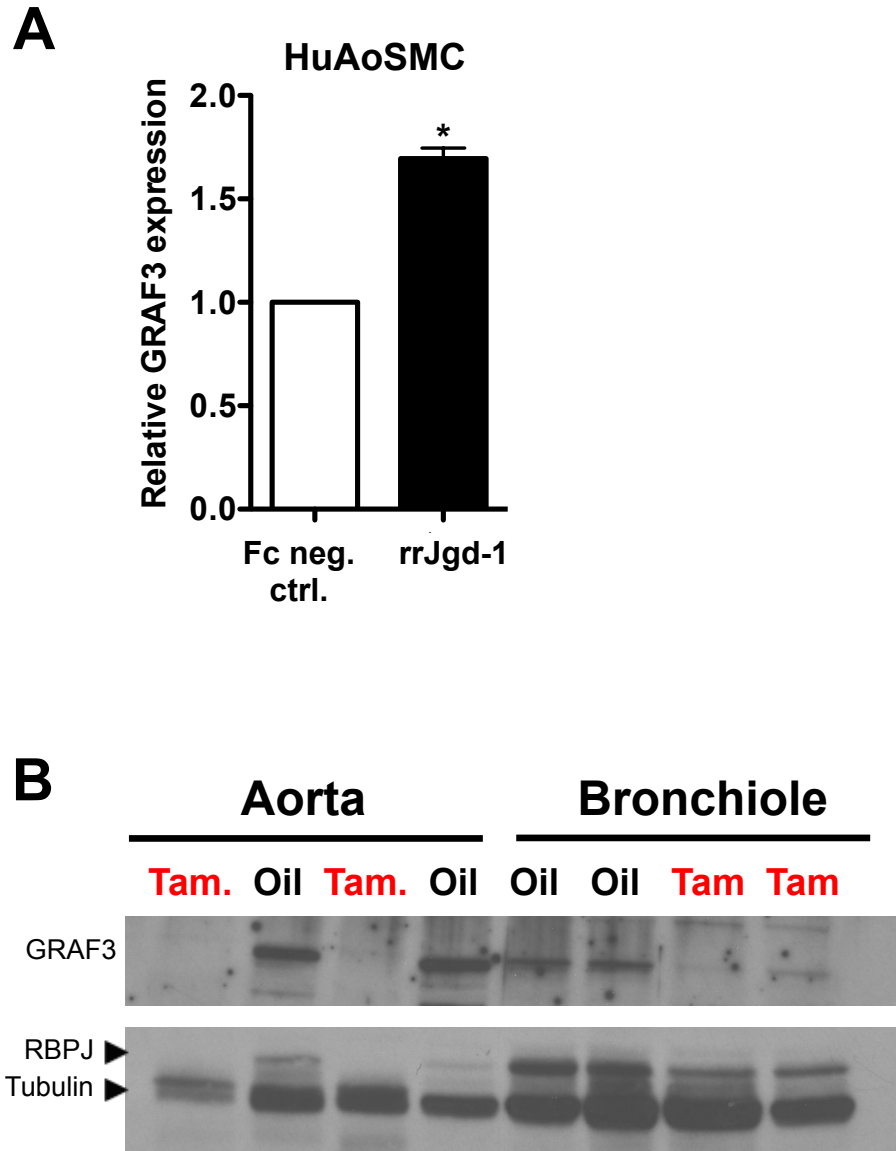
Figure 3.7. RBPJ/Notch is required for GRAF3 expression. A) HuSMC were plated on recombinant Jagged and GRAF3 expression was measured 24 hours later. **B)** SM-MHC Cre mice were crossed to RBPJ floxed/floxed mice to generate smooth muscle-specific deletion of RBPJ. GRAF3 was measured in aorta and bronchi protein lysates. *p<0.01 (student's two-tailed t-test).

The long non-coding RNA, AK124326, inhibits GRAF3 expression.

We sought to identify additional transcription mechanisms controlling GRAF3 expression. The long non-coding RNA, AK124326, is transcribed opposite to the GRAF3 gene and overlaps with the GRAF3 transcription start site (TSS) (Figure 3.9A). LncRNAs can affect transcription either in trans or in cis (213). Typically, in cis lncRNAs have some degree of overlap with their target gene, as is the case for AK124326. Thus, we hypothesized that AK124326 affected GRAF3 expression by competing with essential components of GRAF3's transcriptional machinery, such as RNA Pol II and specific transcription factors. To first determine if AK124326 was expressed in HuBrSMC, we designed primers that spanned the predicted first exon of this lncRNA. AK124326 expression was moderately low in SMC, but was increased upon serum starvation (data not shown). To test if AK124326 played a role in regulating GRAF3 expression, we designed a set of siRNAs to knockdown AK124326. As shown in Figure 3.9B, this siRNA set led to about a 60% reduction in AK124326 mRNA levels in HuBrSMC. We noticed variable knockdown efficiency of AK124326 and therefore used only SMC in which knockdown efficiency of mRNA was at least 50%. AK124326 knockdown resulted in about a 2-fold increase in GRAF3 expression, suggesting a repressive role for this lncRNA (Figure 3.9C). AK124326 overlaps with the first exon and TSS of GRAF3 and is transcribed opposite of the GRAF3 gene. Therefore, we examined the possibility that AK124326 functions in cis by inhibiting RNA polymerase II (RNA Pol II) and transcription factor binding to the GRAF3 promoter, thereby interfering with GRAF3 transcription. To address this question, we performed ChIP assays for RNA Pol II and H3K9Ac, which are features of active transcription, in siControl and siAK124326-treated HuBrSMC. We tested RNA Pol II and H3K9Ac enrichment at the
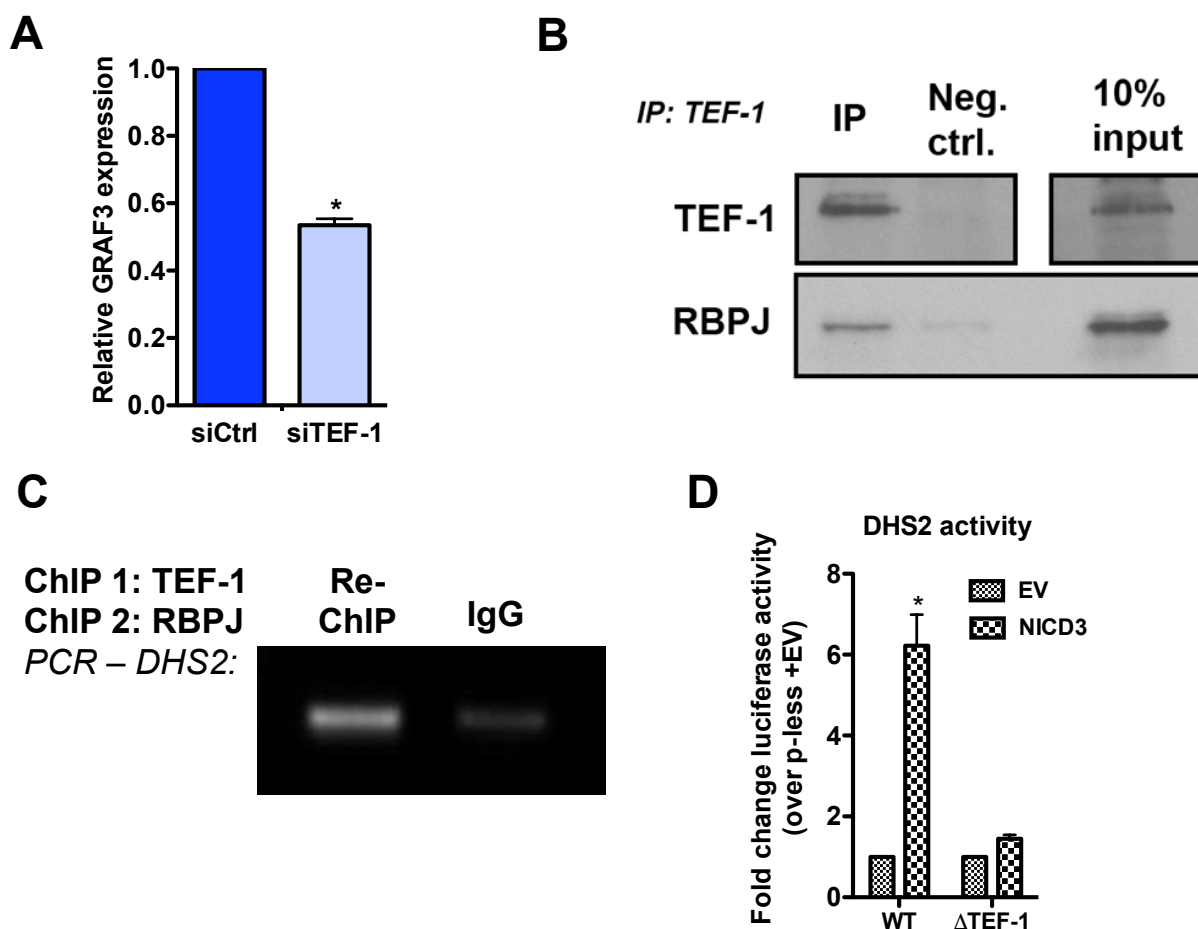
Figure 3.8. TEAD1 is required for GRAF3 expression. A) HuBrSMC were transfected with TEAD1 siRNA or control siRNA for 72 hours. GRAF3 expression was measured by TaqMan real-time PCR. B) Flag-NICD3 was co-expressed with pGL3-wildtype DHS or pGL3-DHS containing mutated TEAD1 site. C) TEAD1 was immunoprecipitated from HuBrSMC nuclear extracts and probed for RBPJ by SDS-PAGE Western blotting. D) TEAD1 ChIP samples were subjected to Re-ChIP for RBPJ, and Re-ChIP DNA was used in downstream targeted PCR with primers spanning the GRAF3 DHS. *p<0.01 (student's two-tailed t-test).

103

GRAF3 TSS and at a SMC-specific DHS in the GRAF3 4th intron, which exhibited

relatively high transcription activity in SMC (data not shown). As seen in Figure 3.9D,

AK124326 knockdown increased binding of RNA Pol II and H3K9Ac enrichment at the

TSS and SMC-specific DHS. This indicates that AK124326 is directly repressing

GRAF3 transcription.

mir-505-3p represses GRAF3 expression.

To continue our search for non-coding mechanisms that regulated GRAF3

expression, we used the Target Scan algorithm on the UCSC genome browser to

identify miRNAs predicted to target the 3' UTR of the GRAF3 gene. One conserved

miRNA, mir-505-3p, was predicted with high confidence to target the GRAF3 3' UTR

(Figure 3.10A, B). Accordingly, we hypothesized that mir-505-3p would inhibit GRAF3

expression. To test this, we transfected a mir-505-3p mimetic into HuBrSMC and

measured GRAF3 expression by TaqMan qRT-PCR. Interestingly, mir-505-3p reduced

endogenous GRAF3 message by approximately 25% compared to the negative control

mimetic (Figure 3.10C). Because the predominant mechanisms underlying gene

silencing by miRNAs is via 3' UTR targeting and mRNA destabilization, we first

examined whether the 3' UTR of GRAF3 could enhance the message stability. As such,

we cloned the 1.2 kb distal (3') most portion of the GRAF3 3' UTR downstream of

luciferase in the promoterless pGL3 vector and then transfected this construct into

HuBrSMC. As seen in Figure 3.10D, the GRAF3 3' UTR increased luciferase by

approximately 30-fold over empty vector, indicating that this region functions as a robust

stabilizer of the mature GRAF3 transcript. These data suggest that targeting of the

GRAF3 3'UTR by mir-505 post-transcriptionally represses relative levels of GRAF3

message in SMC.
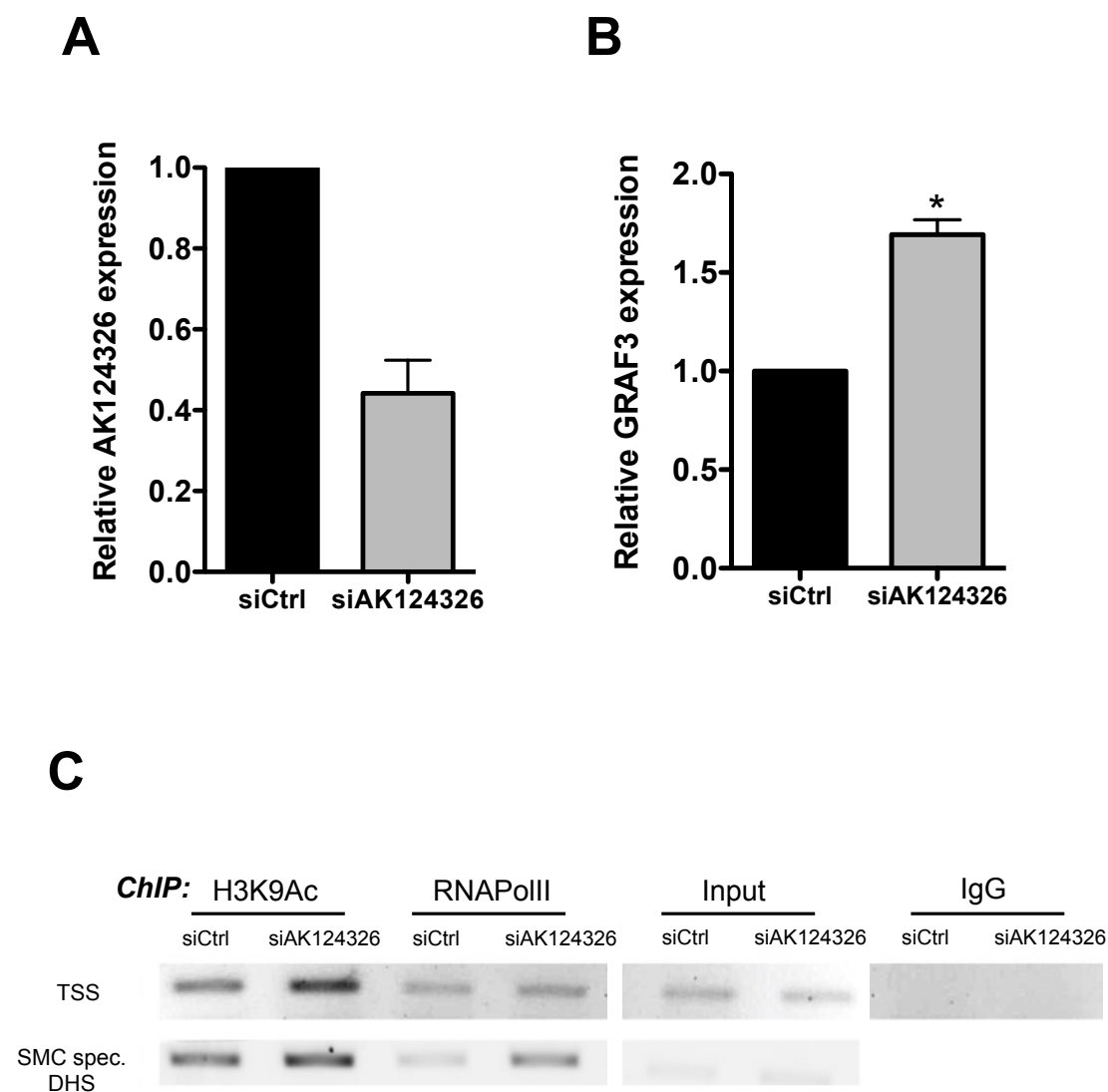
Figure 3.9. The LNC RNA AK124326 negatively regulates GRAF3 expression. A) HuBrSMC were transfected with control siRNA or siRNA targeting siAK124326 LNC RNA for 24 or 48 hrs. **B)** GRAF3 expression was measured by TaqMan qRT-PCR 48 hours after AK124326 knockdown. **C)** Control and AK124326 knockdown HuBrSMC were subjected to H3K9Ac and RNAPolII ChIP, and ChIP'ed DNA was subjected to downstsream PCR using primers to the GRAF3 transcription start site (TSS) or SMC specific DHS.

A

Gene structure
(chr11:100,858,086-100,864,815)

Exon 23   Exon 24   GRAF3 3' UTR

GRAF3

mir-505

RNA seq

B

GRAF3 3' UTR (TMEM133)

5' ...AAUCUUACAUAAGAAUGUUGACA...

              | | | | | | | |

3'   UCCUUUGGUCGUUCACAACUGC

mir-505-3p

C

Relative GRAF3 expression

*

Control   mir-505-3p

D

Luciferase

Fold change luciferase activity
(over p-less +EV)

■ pGL3 empty
□ pGL3-GRAF3 3' UTR
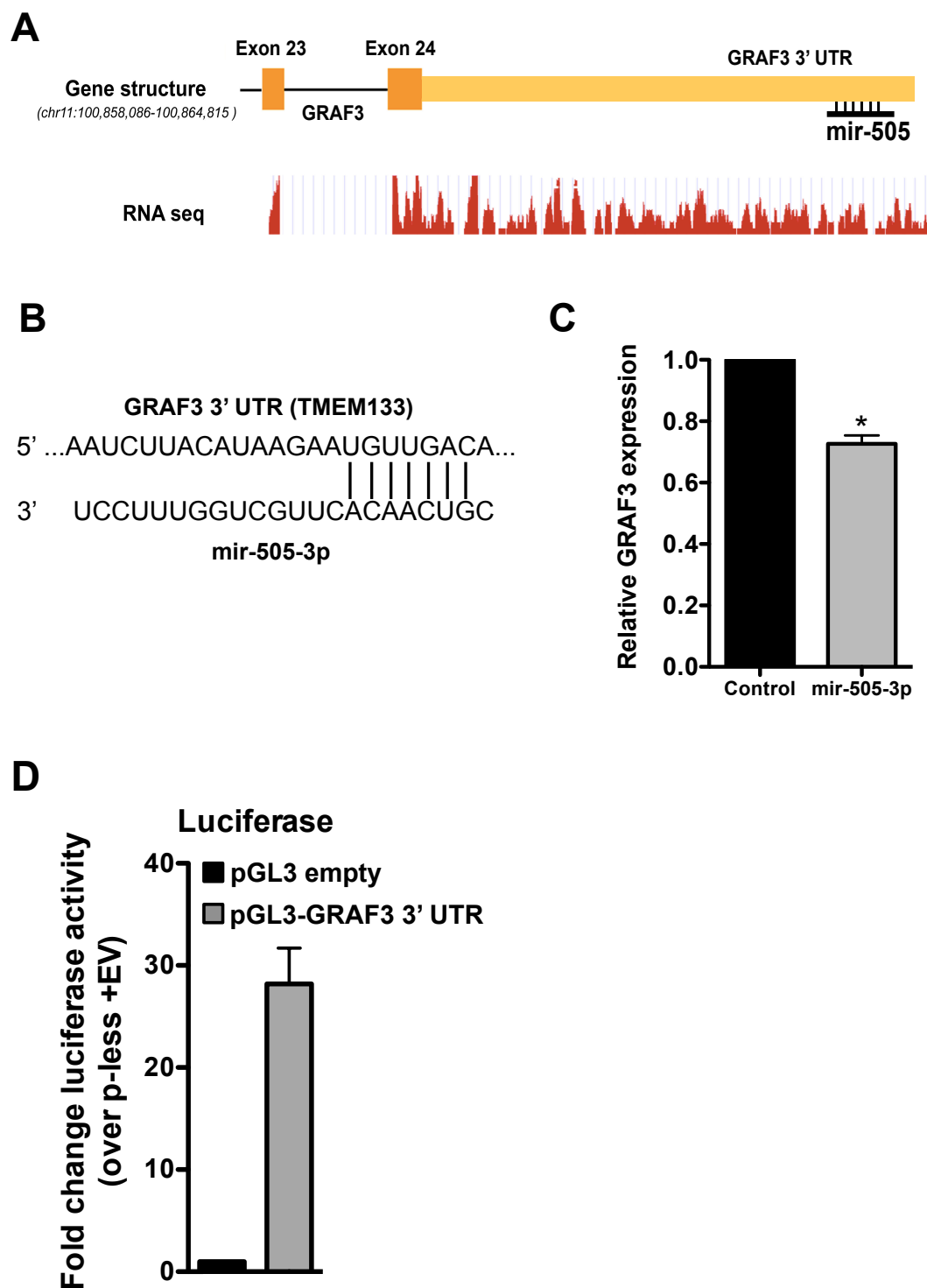
Figure 3.10. mir-505-3p suppresses GRAF3 expression. A, B) Diagram of mir-505-3p conservation and alignment with the GRAF3 (TMEM133) 3' UTR. **C)** mir-505-3p overexpression in HuBrSMC for 48 hrs. decreased GRAF3 expression relative to a negative control non-targeting mir. **D)** A 1.2Kb extension of the GRAF3 3' UTR was cloned into the pGL3 basic vector and transfected into HuBrSMC.

Discussion

We previously demonstrated that the smooth muscle-specific Rho-GAP GRAF3 was required for blood pressure regulation and that the rs604723 minor allele, located in the first intron of GRAF3, decreased hypertensive risk by increasing GRAF3 expression (219, 273). In the current study, we have continued to identify transcription mechanisms that regulate GRAF3 expression and provide strong evidence that RBPJ and TEAD1, in addition to SRF, converge at the blood pressure-associated regulatory region to control GRAF3 expression.

Our previous work showed that GRAF3 expression was regulated in an SRF-dependent manner. Accordingly, we propose that RBPJ, TEAD1, and SRF are essential transcriptional regulators of smooth muscle differentiation. This hypothesis has in part stemmed from our observation that CACCC and CArG elements cluster in DNase Hypersensitive Sites of smooth muscle-specific genes and previous studies that demonstrated interaction between SRF and TEAD1 (unpublished data, 144). The significance of this enrichment has yet to be determined, but it is likely that the co-occurrence of these three motifs mark key regulatory regions in smooth muscle-specific genes important for their transcription. It will be interesting to determine if expression of RBPJ, TEAD1, and SRF altogether mark a specific SMC lineage and/or if overexpression of these factors is sufficient to induce SMC differentiation from an undifferentiated precursor cell.

Our study indicates that TEAD1 and its binding MCAT sequence (CATTCCT) are required for GRAF3 expression in SMCs. These findings are in excellent agreement with previous data demonstrating that the MCAT element is necessary for endogenous expression of other smooth muscle-specific genes (142, 143). However, as these other

studies suggested, yet-to-be-identified transcription mechanisms cooperate with TEAD1 /MCAT to drive cell type-specific gene expression during different developmental windows. One such mechanism identified in the present study was the ability of the MCAT motif to regulate Notch-dependent GRAF3 transcription. It is highly likely that this effect was due to the inability of Notch to transactivate the MCAT mutant DHS, rather than a secondary effect of the mutation abolishing all promoter activity since there was still 50% remaining luciferase activity in the mutant compared to wild-type DHS in the absence of Notch. Importantly, Notch inhibition with DAPT did not affect upstream YAP localization or phosphorylation in SMCs, indicating that RBPJ and TEAD1 cooperativity occurs very locally at the GRAF3 DHS. Given the interaction between RBPJ and TEAD1 as well as the enrichment of RBPJ at TEAD1-bound DNA, an attractive hypothesis is that TEAD1 occupancy at an MCAT motif regulates RBPJ binding to its adjacent promoter-enhancer region. It will be critical to test this hypothesis in the context of other smooth muscle-specific gene promoters that are enriched for TEAD1 and RBPJ binding sites.

GRAF3 expression is regulated by a complex negative feedback mechanism, whereby RhoA activity increases the expression of GRAF3, which ultimately inhibits RhoA (273). In hypertension, SMCs are subjected to significant cell stretch, which increases RhoA activity. In response to this, MRTFs translocate into the nucleus to increase GRAF3 expression by binding to SRF, ultimately limiting RhoA activation (180-182). Interestingly, in response to endothelial cell stretch, the Hippo effectors YAP and TAZ translocate into the nucleus to activate gene expression, similar to the MRTFs (274). Thus, as is the case for MRTF/SRF-dependent transcription, increased RhoA signaling during hypertension may increase the association between YAP/TAZ with

TEAD1 to increase GRAF3 expression and consequently limit RhoA activity. Although the rs604723 SNP did not seem to influence RBPJ binding or Notch-dependent GRAF3 transcription, whether or not the presence of SRF bound to the minor T-allele affects TEAD1 DNA binding is still undetermined. This is an attractive hypothesis since previous studies indicate that SRF and TEAD1 physically interact (144). In this model, increased cell stretch may synergistically enhance GRAF3 expression via a RhoA-SRF-TEAD1-dependent mechanism. Future studies will examine this fascinating possibility.

Tight control of GRAF3 expression is a key mechanism regulating blood pressure (219). Thus, we hypothesized that higher order transcription mechanisms may fine tune GRAF3 expression. Transcriptional control of gene expression is highly complex and involves not only transcription factors, as described above, but also non-coding mechanisms of gene regulation. The long non-coding RNA, AK124326, functions in cis to decrease GRAF3 expression by preventing RNA Pol II from binding to the TSS. Interestingly, a similar effect was observed when we analyzed RNA Pol II enrichment at a downstream smooth muscle-specific DHS within the GRAF3 fourth intron, suggesting that AK124326 sponges RNA Pol II as well as other transcription factors from these regulatory regions. Another intriguing possibility is that this long non-coding RNA influences complex chromatin interactions between the GRAF3 TSS and downstream enhancer regions. Mir-505-3p also significantly decreased GRAF3 expression. Interestingly, mir-505-3p was detected at much higher levels in the plasma of hypertensive patients than in healthy controls, suggesting it plays a role in blood pressure regulation (275). The authors of this study argued that mir-505's effects on blood pressure were mediated by its ability to silence the FGF18 gene thereby affecting endothelial function. Although endothelial dysfunction has been reported in

hypertension, the authors disregard effects on other cell types, such as SMCs, which have a direct role in the pathogenesis of hypertension. We propose that mir-505-3p targets the GRAF3 3' UTR to reduce GRAF3 expression, thereby increasing RhoA activity, SMC contractility, vascular tone, and blood pressure.

CHAPTER 4: IDENTIFICATION OF MRTF-A POST-TRANSLATIONAL MODIFICATIONS AND BINDING PARTNERS

Overview

Tight control over myocardin-related transcription factor (MRTF-A/B) activity is essential for proper regulation of smooth muscle differentiation. The goal of the current study was to identify novel mechanisms regulating MRTF-A function. To accomplish this, we used a mass spectrometry-based approach to identify novel MRTF-A binding partners and post-translational modifications. We identified the smooth muscle-specific histone lysine methyltransferase PRDM6 as an MRTF-A interacting protein. MRTF-A physically interacted with PRDM6 in co-immunoprecipitation and far western assays. Importantly, knockdown of PRDM6 significantly reduced expression of smooth muscle-specific genes, including SMA, SM22, calponin, and SM-MHC ($p < 0.05$). Furthermore, MRTF-A was significantly methylated in vivo at its N-terminus. After testing several candidate protein lysine methyltransferases (PKMTs) in vitro, we determined that SET7/9 and SMDY2 methylated MRTF-A. Both PKMTs also methylated MRTF-A in vivo; however, only SMYD2 interacted with MRTF-A. Interestingly, SMYD2 methylated MRTF-A at K27, which is located within the nuclear localization sequence in MRTF's N-terminal RPEL domain, and overexpression of SMYD2 inhibited MRTF-A nuclear localization and MRTF-dependent SMC promoter activity. These studies present novel evidence that MRTF-A is controlled by SMYD2-mediated methylation. Furthermore, our identification of the MRTF-A interactome in SMC will be useful in identifying innovative mechanisms regulating SMC differentiation.

Introduction

Smooth muscle cell (SMC) differentiation is regulated by a host of mechanical, genetic, and epigenetic cues, all of which exert transcriptional control over SMC-specific genes (29). Differentiated SMCs must express various contractile markers in order to carry our important functions throughout development and in the healthy adult blood vessel. Intriguingly, SMCs are unlike other cells in that they do not terminally differentiate and can revert to immature gene programs. This so called phenotypic switching involves the downregulation of contractile genes and upregulation of proliferative genes in the SMC, and is a hallmark of different vascular diseases (19). SMC gene transcription is largely regulated by serum response factor (SRF) and the myocardin family of transcription factors (MRTF-A and MRTF-B) (63, 71, 79). SRF binds to CArG elements in the promoters of SMC-specific genes. While SRF is a strong activator of smooth muscle gene transcription, MRTF-A and MRTF-B are required for maximum transcriptional activation. Therefore, SMC differentiation is highly dependent on MRTF function and the processes that regulate it. Under basal conditions MRTF-A and -B are sequestered in the cytoplasm by monomeric G-actin. In response to various stimuli that activate the small GTPase RhoA, the MRTFs rapidly translocate into the nucleus to bind SRF and activate SRF/MRTF-dependent genes. Nuclear translocation of the MRTFs is tightly linked to actin dynamics. G-actin is bound to conserved RPEL domains in MRTF-A and -B. Interestingly, there are two basic nuclear localization sequences (NLS) embedded in the RPEL domains, which are both masked by G-actin (98, 99). RhoA activation mediates actin polymerization through its effectors, the formins (mDia1/2) and Rho kinase (ROCK) (106). Briefly, RhoA activation relieves the autoinhibited state of mDia1/2, thus allowing them to mediate F-actin capping, which is

required for actin filament assembly and polymerization. ROCK activates LIM kinase, which inhibits the actin destabilizer, cofilin. Thus, in response to RhoA-dependent actin polymerization, G-actin is freed from the MRTFs, thereby exposing the NLS and allowing MRTF nuclear translocation via an importin-based mechanism. Our lab was one of the first to show that nuclear translocation of the MRTFs was required for SMC differentiation (100). In agreement with these studies, the Mack lab provided strong evidence that sphingosine 1-phosphate (S1P), a strong activator RhoA, stimulates MRTF-A nuclear translocation (97). Furthermore, inhibition of RhoA signaling with the ROCK inhibitor Y-27632 prevents MRTF-A nuclear accumulation and expression of various SMC-specific genes, including smooth muscle alpha actin (SMA), transgelin (SM22), calponin (CNN), and smooth muscle-myosin heavy chain (SM-MHC) (100).

In addition to the N-terminal RPEL domains, the myocardin factors contain other conserved domains that are are important for their function. A highly basic region and glutamine-rich region are required for interaction of the myocardin factors with SRF. Myocardin, MRTF-A, and MRTF-B also share a SAP domain, which mediates chromatin and nuclear organization in other proteins (101). However, its function in the myocardin factors is less understood. All three members also contain a leucine zipper-like (LZ) domain and a transactivation domain (TAD). The LZ domain mediates homo- and heterodimerization between myocardin and the MRTFs. The TAD is required for transactivation of SRF-dependent genes. However, while there is almost complete sequence conservation between the TADs of MRTF-A and MRTF-B, there is only about 30% homology between the TADs of MRTFs and myocardin, suggesting disparate modes of regulation between the MRTFs versus myocardin.

Several studies have identified post-translational modifications (PTMs) that

directly affect activity of myocardin and the MRTFs. Acetylation of myocardin by p300 enhances its association with SRF, leading to upregulation of smooth muscle- and cardiac-specific genes (110). Myocardin is also phosphorylated by PKC, GSK3β, and ERK, all of which inhibit myocardin-dependent smooth muscle gene transcription (112, 113). Early studies identified a critical ERK phosphorylation site within MRTF-A (S454), which inhibited MRTFs nuclear localization by promoting its interaction with cytoplasmic G-actin (115). More recent reports indicate that MRTF-A is phosphorylated at multiple other residues, each of which has varied effects on its nuclear localization (116). Interestingly, sumoylation of MRTF-A represses its ability to transactivate smooth muscle promoters, while SUMO activates myocardin at cardiac genes (117, 118). Clearly, tight post-translational regulation of the myocardin family of transcription factors is an important mechanism controlling smooth muscle gene expression in response to different stimuli and contexts.

MRTF-A is expressed in multiple cell types, while myocardin is expressed mainly in smooth and cardiac muscle. Currently, it is unknown why cells, despite expressing relatively high levels of MRTF-A, still differentiate into non-SMC and, to some extent, non-mesenchmal lineages. Here, we investigate the hypothesis that PKMTs limit the activity of MRTF-A in non-SMCs, thereby inhibiting smooth muscle differentiation in these other cell types. Furthermore, it is possible that yet-to-be identified PTMs and/or binding partners control SMC phenotypic switching that occurs in disease. The work herein lays the groundwork for future studies that may examine some of these points of MRTF-A regulation in various developmental and disease-associated contexts.

Materials and Methods

Immunoprecipitations

For identification of binding partners, mouse SMCs were grown to 80% confluence and then scraped and lysed in RIPA buffer plus protease and phosphatase inhibitors. Approximately 2 mg of protein was incubated with protein G beads Dynabeads (Invitrogen) linked to anti-MRTF-A antibody (Santa Cruz) or rabbit IgG antibody to control for non-specific binding (Cell signaling) overnight at 4°C with rotation. The following day, immunoprecipitated reactions were washed extensively in RIPA buffer and then boiled in sample buffer. Eluted complexes were submitted directly for mass spectrometry analysis. For identification of MRTF-A post-translational modifications, COS-7 cells were transfected with Flag-MRTF-A or Flag-empty vector expression plasmids. After 48 hours, cells were scrapped and collected in RIPA buffer. Cleared cell lysates were incubated with Flag M2 magnetic beads (Sigma) overnight. Immunoprecipitated reactions were washed the following day, eluted from beads in sample buffer, and then run on an 8% SDS-PAGE gel, which was submitted to the mass spectrometry core at UNC.

LC/MS/MS analysis

For the endogenous MRTF-A IP experiment, samples underwent LC/MS/MS analysis on a nanoACQUITY-Orbitrap Velos. Samples were eluted over a 150 min. gradient from 1-40%, where mobile phase A was 0.1% formic acid and mobile phase B was acetonitrile with 0.1% formic acid. The top 8 most intense ions were chosen for HCD fragmentation. For Flag-tagged samples immunoprecipiated from COS-7 cells, gel bands were excised and the proteins were reduced, alkylated, and digested with trypsin. The peptides were extracted, lyophilized, and resuspended in 2% acetonitrile/98%

(0.1% formic acid). Samples were analyzed in duplicate using LC-MS/MS on a nanoACQUITY-Orbitrap Velos similar to above.

GST pulldowns

GST pulldowns were performed as described previously. In brief, cells were lysed in RIPA buffer and incubated with fusion protein immobilized on GST beads for 2 hours at 4C. Beads were washed with RIPA buffer and boiled in sample buffer for 5 mintues to elute pulled down complexes. Samples were loaded on SDS-PAGE gels and analyzed by standard Western blotting.

Far Western blotting

Flag-tagged proteins were immmunoprecipitated from COS-7 cells, then resolved by SDS-PAGE, transferred to nitrocellulose, and proteins were renatured according to previously established methods (276). Renatured proteins were incubated with GST-PRDM6 recombinant protein diluted in blocking buffer. GST interacting proteins were detected using a homemade GST antibody.

Cytochalasin D treatments

Cells were treated with 10 uM cytochalsin D for 30 minutes prior to immunoprecipitations. Once lysates were harvested, cytochalasin D was again added to the IP reaction at 1:1000 to prevent G-actin-MRTF binding.

siRNA knockdowns

Rat aortic SMCs were plated in 6-well dishes approximately 100K cells/well the day prior to knockdowns. SMCs were treated with 80 nM PRDM6 or GFP non-targeting siRNA. RNA was collected 72 hours after knockdown using the RNeasy kit (Qiagen). RNA underwent first strand cDNA synthesis (Biorad), and approximately 20 ng cDNA was used in downstream qRT-PCR using SYBR green chemistry.

Immunofluorescence

10T1/2s were seeded at 17K/well in 4-well chamber slides the day before transfections. Cells were co-transfected with Flag-EV or Flag-SMYD2 and GFP-MRTF-A plasmids. After 48 hours, cells were fixed in 4% paraformaldehyde, permeabilized in 0.4% triton x-100 in PBS, and blocked in 20% goat serum/3% BSA. Cells were incubated with an anti-flag antibody (Santa Cruz) and an anti-rabbit 488-conjugated alexafluor secondary antibody. Cells were counterstained with DAPI in all experiments. Cells in multiple fields were counted.

In vitro methyltransferase assays

In vitro methyltransferase assay were performed as previously described (192). In brief, recombinant proteins (Epicypher and abcam) were incubated with 2 uCi SAM-H3 for 1 hour at 37C. Reactions were boiled for 5 minutes and resolved by SDS-PAGE. Gels were fixed, stained in coomassie, and incubated in EN3HANCE reagent (Amersham). Gels were dried for 2 hours and then exposed to autoradiography. For modified in vitro methyltransferase assays, GST-MRTF-A beads were incubated with 2 uM cold SAM (NEB) for 2 hours with or without recombinant SMYD2 enyzme. Beads were washed in methylation buffer and incubated with cleared 10T1/2 cell lysate for 2 hours. Immunprecipitated samples were washed and analyzed by SDS-PAGE Western blotting.

In vivo methylation experiments

Endogenous MRTF-A or overexpressed flag-MRTF-A were immunoprecipitated from cells as described above and resolved by SDS-PAGE Western blotting using a mono-methyl-lysine antibody (Cell signaling).

Results

Identification of SMC-specific MRTF-A binding partners

To begin to uncover novel mechanisms regulating SMC differentiation, we employed a mass spectrometry-based approach to identify MRTF-A binding partners. In brief, endogenous MRTF-A was immunoprecipitated from mouse SMCs using a commercial antibody, and purified complexes were submitted to the UNC Michael Hooker Proteomics Core for LC/MS/MS analysis. Identified binding partners are listed in Table 4.1. The peptide coverage of immunoprecipitated MRTF-A was 26.8%. Gene Ontology (GO) analysis was performed on the MRTF-A binding partners to highlight specific pathways and cell functions the identified proteins were involved in. Not surprisingly some of the most enriched classifications were transcriptional regulation, chromatin, and differentiation. Several interesting proteins belonging to these categories include the histone acetyltransferase, p300, which is a known MRTF-A interacting protein; SMC hinge domain 1, which is associated with transcriptional repression at specific gene loci; importin 9, which MRTF-A utilizes to enter the nucleus; and the histone arginine methyltransferase, CARM1. Interestingly, a number of RhoA/actin-associated proteins were also identified, including the RhoA GEF, LARG. We were excited to identify the smooth muscle-specific histone methyltransferase, PRDM6. While little is known about this protein, studies indicate that PRDM6 inhibits SMC differentiation by associating with the H3K9-specific methyltransferase, G9a, and enhancing its repressive ability (278). Based on these reports as well as its highly selective expression in SMC, we chose to pursue PRDM6 further.

Validation of PRDM6 as an MRTF-A binding partner

The high sensitivity gained from using mass spectrometry to identify binding

Uniprot Accession	Name	Abbreviation
Q5SWU9	acetyl-Coenzyme A carboxylase alpha	Acaca
Q07417	acyl-Coenzyme A dehydrogenase, short chain	Acads
Q8K3H0	adaptor protein, phosphotyrosine interaction, PH domain and leucine zipper containing 1	Appl1
A2AE38	adhesion molecule with Ig like domain 1	Amigo1
O89020	afamin	Afm
P24549	aldehyde dehydrogenase family 1, subfamily A	Aldh1a1
A6ZI44	aldolase A, fructose-bisphosphate	Aldoa
D3YW52	alpha-2-macroglobulin	A2m
F8VPN4	amylo-1,6-glucosidase, 4-alpha-glucanotransferase	Agl
E9Q414	apolipoprotein B	Apob
P48999	arachidonate 5-lipoxygenase	Alox5
P61164	ARP1 actin-related protein 1A, centractin alpha	Actr1a
P41233	ATP-binding cassette, sub-family A (ABC1), member 1	Abca1
Q8K440	ATP-binding cassette, sub-family A (ABC1), member 8b	Abca8b
Q9JJ59	ATP-binding cassette, sub-family B (MDR/TAP), member 9	Abcb9
Q9WU60	attractin	Atrn
Q9JLV1	BCL2-associated athanogene 3	Bag3
P59017	BCL2-like 13 (apoptosis facilitator)	Bcl2l13
Q8CI94	brain glycogen phosphorylase	Pygb
Q6GQW0	BTB (POZ) domain containing 11	Btbd11
A0PJK7	cadherin-related family member 5	Cdhr5
Q923T9	calcium/calmodulin-dependent protein kinase II gamma	Camk2g
A0A0G2JGS4	calcium/calmodulin-dependent protein kinase II, delta	Camk2d
O88456	calpain, small subunit 1	Capns1
Q08093	calponin 2	Cnn2
P47936	cannabinoid receptor 2 (macrophage)	Cnr2
B2RS76	carboxypeptidase B1 (tissue)	Cpb1
Q60737	casein kinase 2, alpha 1 polypeptide	Csnk2a1
Q549Q4	CD2 antigen	Cd2
Q3TI84	CDC16 cell division cycle 16	Cdc16
E9PVY0	CDC42 binding protein kinase alpha	Cdc42bpa
Q7TT50	CDC42 binding protein kinase beta	Cdc42bpb
Q6NV72	cDNA sequence BC068281	BC068281
Q8CH18	cell division cycle and apoptosis regulator 1	Ccar1
Q6A065	centrosomal protein 170	Cep170
Q99LI7	cleavage stimulation factor, 3' pre-RNA, subunit 3	Cstf3
D3YUP1	coactivator-associated arginine methyltransferase 1	Carm1
Q02788	collagen, type VI, alpha 2	Col6a2
P01027	complement component 3	C3
P01029	complement component 4B (Chido blood group)	C4b
A2A432	cullin 4B	Cul4b
Q8CID0	cysteine and glycine-rich protein 2 binding protein	Csrp2bp
Q7TMB8	cytoplasmic FMR1 interacting protein 1	Cyfip1
K3W4R0	dynein, axonemal, heavy chain 17	Dnah17
L7N1Y0	dynein, axonemal, heavy chain 7B	Dnah7b
B2RWS6	E1A binding protein p300	Ep300
Q8BL66	early endosome antigen 1	Eea1
Q05BC3	echinoderm microtubule associated protein like 1	Eml1
F8WJ93	echinoderm microtubule associated protein like 4	Eml4
E9QAU4	enhancer trap locus 4	Et14
Q8BH95	enoyl Coenzyme A hydratase, short chain, 1, mitochondrial	Echs1
Q8BGS1	erythrocyte membrane protein band 4.1 like 5	Epb41l5
Q3ULL5	eukaryotic translation initiation factor 2, subunit 2 (beta)	Eif2s2
Q3UW53	family with sequence similarity 129, member A	Fam129a
Q3UW64	glucosamine (UDP-N-acetyl)-2-epimerase/N-acetylmannosamine kinase	Gne
Q9CQZ1	heat shock factor binding protein 1	Hsbp1
Q9JK92	heat shock protein 8	Hspb8
P01942	hemoglobin alpha, adult chain 1	Hba-a1
Q3UDW8	heparan-alpha-glucosaminide N-acetyltransferase	Hgsnat
Q20BD0	heterogeneous nuclear ribonucleoprotein A/B	Hnrnpab
Q8VDM6	heterogeneous nuclear ribonucleoprotein U-like 1	Hnrnpul1
Q9JIY5	HtrA serine peptidase 2	Htra2
O88703	hyperpolarization-activated, cyclic nucleotide-gated K+ 2	Hcn2
P01751	immunoglobulin heavy variable 1-72	Ighv1-72
A0A075B666	immunoglobulin kappa chain variable 13-85	Igkv13-85
Q91YE6	importin 9	Ipo9
D3Z627	integrin alpha L	Itgal
Q9QXH4	integrin alpha X	Itgax
E9QAD8	IQ motif and Sec7 domain 2	Iqsec2
E9Q9B7	kinase D-interacting substrate 220	Kidins220)
E9Q0J5	kinesin family member 21A	Kif21a
B7ZNG0	kinesin family member 7	Kif7
Q91W40	kinesin light chain 3	Klc3

Table 4.1. MRTF-A binding partners in mouse SMC. MRTF-A was immunoprecipitated from mouse SMCs, and binding partners were identified by LS/MS/MS analysis.

119

B2RWI2	lactamase, beta	Lactb
Q8R502	leucine rich repeat containing 8 family, member C	Lrrc8c
Q8CGK3	lon peptidase 1, mitochondrial	Lonp1
V9GX48	M-phase phosphoprotein 9	Mphosph9
Q9EQQ9	meningioma expressed antigen 5 (hyaluronidase)	Mgea5
P25206	minichromosome maintenance complex component 3	Mcm3
Q52KC3	minichromosome maintenance complex component 5	Mcm5
Q80X85	mitchondrial ribosomal protein S7	Mrps7
Q8K4J6	MKL (megakaryoblastic leukemia)/myocardin-like 1	Mkl1
Q3U2W2	MYB binding protein (P160) 1a	Mybbp1a
Q80TM9	nischarin	Nisch
Q99K48	non-POU-domain-containing, octamer binding protein	Nono
Q60632	nuclear receptor subfamily 2, group F, member 1	Nr2f1
Q9CQF3	nudix (nucleoside diphosphate linked moiety X)-type motif 21	Nudt21
Q8CGY8	O-linked N-acetylglucosamine (GlcNAc) transferase (UDP-N-acetylglucosamine:polypeptide-N-acetylglucosaminyl transferase)	Ogt
Q8VGB4	olfactory receptor 985	Olfr985
A2AEG2	oral-facial-digital syndrome 1 gene homolog (human)	Ofd1
B2RRE7	OTU domain containing 4	Otud4
A0A0G2JDJ3	paired immunoglobin-like type 2 receptor alpha	Pilra
Q9R0L6	pericentriolar material 1	Pcm1
Q8BVZ1	perilipin 5	Plin5
Q8BH04	phosphoenolpyruvate carboxykinase 2 (mitochondrial)	Pck2
Q64737	phosphoribosylglycinamide formyltransferase	Gart
Q8K1N2	pleckstrin homology like domain, family B, member 2	Phldb2
B2RXS4	plexin B2	Plxnb2
P59470	polymerase (RNA) III (DNA directed) polypeptide B	Polr3b
Q3UZD5	PR domain containing 6	Prdm6
Q3V0P3	predicted gene 1527	Gm1527
Q58EV5	predicted gene, 21596	Gm21596
P70268	protein kinase N1	Pkn1
B2RXQ2	protein tyrosine phosphatase, receptor type, f polypeptide (PTPRF), interacting protein (liprin), alpha 1	Ppfia1
Q3TMZ1	pyrroline-5-carboxylate reductase family, member 2	Pycr2
Q9DCC4	pyrroline-5-carboxylate reductase-like	Pycrl
O35551	rabaptin, RAB GTPase binding effector protein 1	Rabep1
Q3UYI5	ral guanine nucleotide dissociation stimulator-like 3	Rgl3
E9PW37	RAS protein activator like 2	Rasal2
Q5SWN2	replication protein A1	Rpa1
Q99P72	reticulon 4	Rtn4
Q9EP71	retinoic acid induced 14	Rai14
E9PUF7	Rho guanine nucleotide exchange factor (GEF) 1	Arhgef1
Q8C033	Rho guanine nucleotide exchange factor (GEF) 10	Arhgef10
F8VQN6	Rho guanine nucleotide exchange factor (GEF) 12	Arhgef12
Q91VI7	ribonuclease/angiogenin inhibitor 1	Rnh1
P62918	ribosomal protein L8	Rpl8
P62855	ribosomal protein S26	Rps26
A0A087WRF9	RIKEN cDNA 1700088E04 gene	1700088E04Rik
E9QM90	RIKEN cDNA 2310035C23 gene	2310035C23Rik
G3X8V5	ring finger protein 219	Rnf219
F8WJE0	SAM domain and HD domain, 1	Samhd1
Q9EQC5	SCY1-like 1 (S. cerevisiae)	Scyl1
A2AIX1	SEC16 homolog A, endoplasmic reticulum export factor	Sec16a
M9MMK0	sema domain, immunoglobulin domain (Ig), short basic domain, secreted, (semaphorin) 3B	Sema3b
Q543J5	serine (or cysteine) peptidase inhibitor, clade C (antithrombin), member 1	Serpinc1
Q9JI11	serine/threonine kinase 4	Stk4
Q6ZPE2	SET binding factor 1	Sbf1
Q3TRJ7	SH3-domain GRB2-like 1	Sh3gl1
P56873	Sjogren's syndrome/scleroderma autoantigen 1 homolog (human)	Sssca1
F8VPQ4	SLIT-ROBO Rho GTPase activating protein 3	Srgap3
Q6P5D8	SMC hinge domain containing 1	Smchd1
Q80UJ1	solute carrier family 22 (organic anion transporter), member 20	Slc22a20
Q58A65	sperm associated antigen 9	Spag9
Q8VIJ6	splicing factor proline/glutamine rich (polypyrimidine tract binding protein associated)	Sfpq
O54988	STE20-like kinase	Slk
P58871	tankyrase 1 binding protein 1	Tnks1bp1
Q9D2E2	target of EGR1, member 1 (nuclear)	Toe1
Q3URV1	TBC1 domain family, member 32	Tbc1d32
Q05895	thrombospondin 3	Thbs3
A2ASS6	titin	Ttn
Q52L67	trans-2,3-enoyl-CoA reductase	Tecr
Q62351	transferrin receptor	Tfrc
P37804	transgelin	Tagln
Q3UBX0	transmembrane protein 109	Tmem109
Q80WC3	trinucleotide repeat containing 18	Tnrc18
Q9Z1A1	Trk-fused gene	Tfg
Q6F4J0	tubulin, gamma 2	Tubg2
Q9ES34	ubiquitin protein ligase E3B	Ube3b
F6WJB7	ubiquitin specific peptidase 34	Usp34
F8VPU6	ubiquitin specific peptidase 9, Y chromosome	Usp9y
Q9CR26	vesicle (multivesicular body) trafficking 1	Vta1
E9Q743	WD repeat domain 66	Wdr66
Q6NXJ0	WW, C2 and coiled-coil domain containing 2	Wwc2
Q9JKB3	Y box protein 3	Ybx3

Table 4.1 (continued). MRTF-A binding partners in mouse SMC. MRTF-A was immunoprecipitated from mouse SMCs, and binding partners were identified by LS/MS/MS analysis.

120

partners can lead to false positives and/or interactions that are not significantly meaningful. Thus, in order to validate PRDM6 as a bona fide binding partner of MRTF-A, we used several approaches. First, we performed co-immunoprecipitation experiments in 10T1/2 cells overexpressing myc-PRDM6. In these experiments, myc-PRDM6 was immunoprecipitated from cell lysates, and precipitated samples were analyzed by SDS-PAGE Western blotting. As seen in Figure 4.1A, an interaction was detected between endogenous MRTF-A and myc-PRDM6. As another measure of binding, we incubated GST-PRDM6 beads with 10T1/2 cell lysates and analyzed the purified complexes by Western blotting. In these experiments, MRTF-A was purified with GST-PRDM6 (Figure 4.1B). To begin to map the MRTF-A domains that mediated the interaction with PRDM6, we used a standard deletion MRTF-A series previously generated by our lab. A total of three MRTF-A constructs were used. The first fragment, which contained the first N-terminal 108 amino acid residues of MRTF-A, contained the RPEL domains that mediate the interaction with G-actin. The second fragment spanned residues 109-475 and contained the B1 basic domain, the Q-rich domain, and the SAP domain. Finally, the third fragment, which corresponded to residues 480-930, encoded the LZ and TAD. In order to determine which of these regions within MRTF-A interacted with PRDM6, and thus begin to understand how PRDM6 might be regulating MRTF, we performed additional co-immunoprecipitation experiments in which we overexpressed myc-PRDM6 with each of the flag-tagged MRTF-A fragments. As observed in Figure 4.1C, PRDM6 interacted with the N-terminal 1-108 fragment and the central 109-475 fragment. In separate experiments, we determined that PRDM6 could bind actin. Thus, to exclude the possibility that actin mediated the PRDM6-MRTF interaction, we treated COS-7 cells that were co-transfected with flag-MRTF-A and myc-PRDM6 as well as the

121

immunoprecipitation reactions with cytochalasin D. Cytochalasin D inhibits G-actin-MRTF binding. Thus, abolishing this interaction would also be expected to prevent PRDM6 from co-precipitating with MRTF-A if G-actin was bridging the two proteins. As shown in Figure 4.2A, cytochalasin D reduced the levels of G-actin that bound to MRTF-A, but did not affect PRDM6 binding to full-length MRTF-A. To further test whether actin binding to the RPEL domain mediated the interaction with PRDM6 with this fragment, we performed co-immunoprecipitation with myc-PRDM6 and the flag-MRTF-A 1-108 fragment. Immunprecipitation reactions were treated with cytochalasin D. As seen in Figure 4.2B, cytochalsin D completely inhibited the interaction between PRDM6 and the RPEL domain, indicating that PRDM6 was not directly binding to this region. In agreement with these experiments, PRDM6 was still able to interact with a flag-MRTF-A construct lacking the RPEL domain (Figure 4.2C). These experiments indicated that actin was not required for interaction between the two proteins, suggesting that PRDM6 was directly binding to MRTF-A at the 109-475 region. To test this hypothesis, we analyzed the PRDM6-MRTF interaction by Far Western. In these experiments, purified bait proteins are resolved by standard SDS-PAGE and transferred to a membrane. Denatured proteins are renatured, blocked, incubated with a recombinant protein probe, and then analyzed by standard Western blotting. In our particular experiment, we subjected immunoprecipitated full-length MRTF-A as well as the different MRTF-A fragments to Far Western using a GST-PRDM6 probe. As observed in Figure 4.3, using an anti-GST antibody, we detected direct binding of the GST-PRDM6 probe to only full-length MRTF-A as well as the 109-475 fragment, which contains the SRF binding and SAP domains.
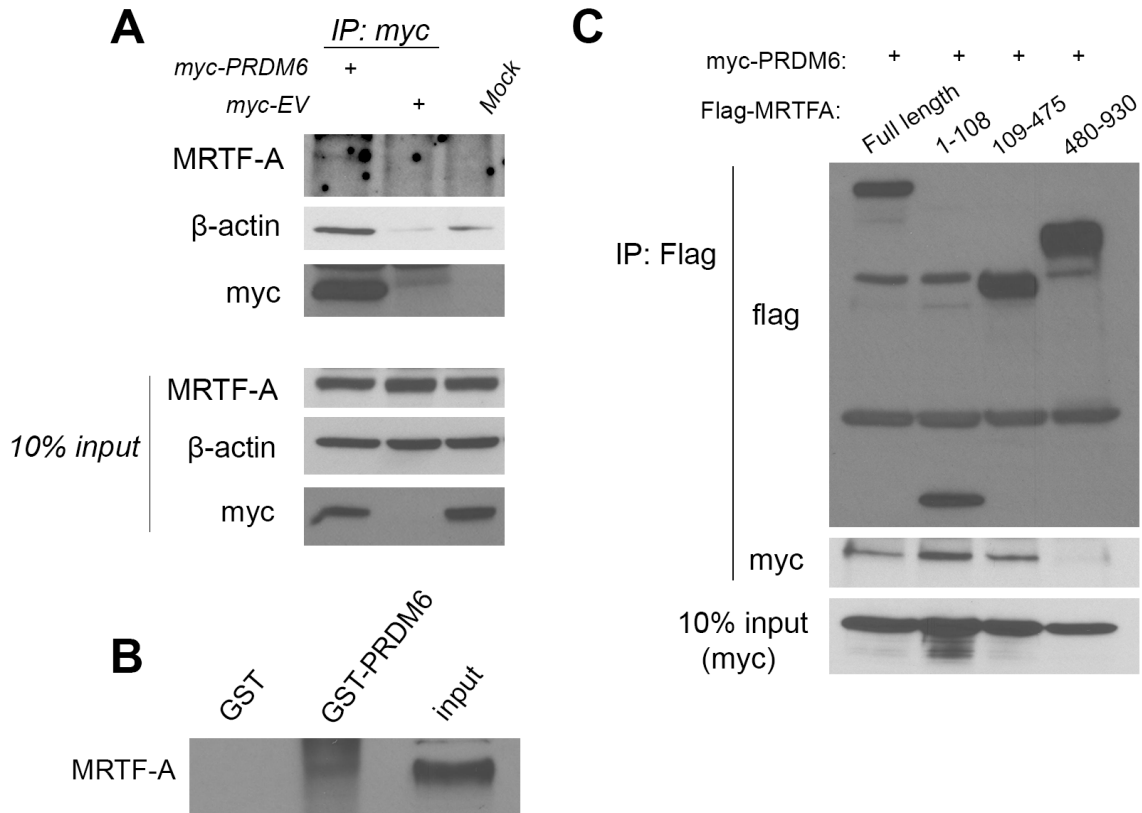
Figure 4.1. The N-terminal RPEL domains and basic/Q-rich/SAP region of MRTF-A mediate its interaction with PRDM6. **A)** 10T1/2s were transfected with myc-PRDM6 or myc-EV. Lysates were collected and underwent immunoprecipitation with a myc antibody. Immunoprecipitates were run on SDS-PAGE gel and probed for MRTF-A by Western blotting **B)** Mouse SMC lysates were incubated with GST-PRDM6 or GST fusion proteins linked to beads. GST pulldown samples were resolved by SDS-PAGE and probed for MRTF-A. **C)** Lysates from COS cells transfected with myc-PRDM6 and different flag-MRTFA fragments were incubated with Flag M2 beads. IP samples were analyzed by Western blotting for myc.
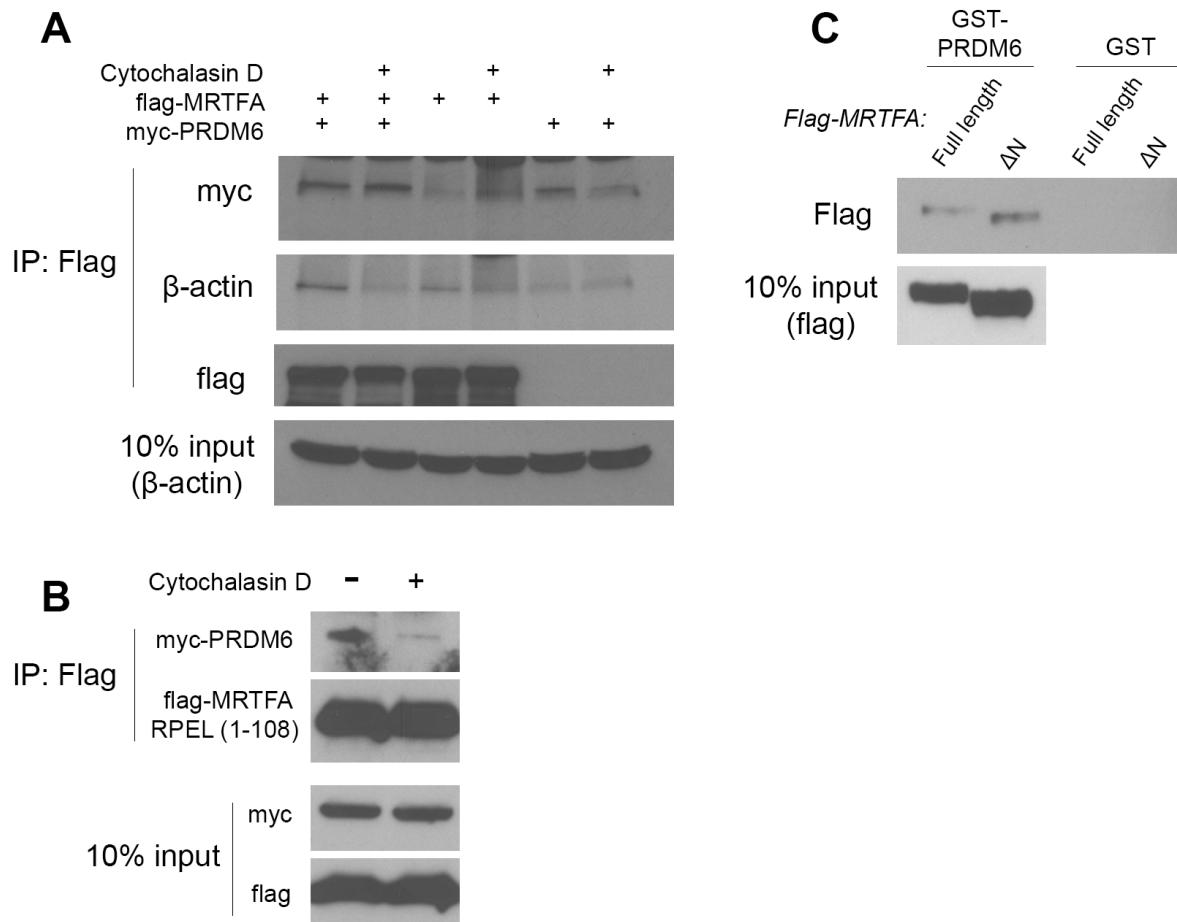
Figure 4.2. Actin bridges MRTF-A and PRDM6 through MRTF's N-terminal RPEL domains. **A)** COS cells transfected with flag-MRTFA and myc-PRDM6 were treated with Cytochalasin D, and lysates were incubated with Flag M2 beads. Samples were subjected to Western blotting for myc and β-actin. **B)** Same as in A) except flag-RPEL domain of MRTF-A was transfected with myc-PRDM6 instead of full length MRTF-A. **C)** GST-PRDM6 or GST fusion protein on beads were incubated with lysates from COS cells expressing either full length flag-MRTFA or flag-MRTFA lacking the N-terminal RPEL domains.

PRDM6 is required for SMC differentiation

One previous study indicated that PRDM6 repressed SMC differentiation (278). To determine if this was the case, we designed siRNAs to knockdown PRDM6 in rat aortic SMC and then measured expression of smooth muscle markers in this cell type. As seen in Figure 4.4, PRDM6 knockdown significantly reduced the relative expression levels of SMA, SM22, calponin, and SM-MHC by approximately 50%. These data are very different from reports by Davis et al., showing that PRDM6 knockdown increased expression of smooth muscle markers. Of note, this particular study did not assess expression levels of SMA, SM22, or calponin, but instead measured other markers.

Identification of post-translational modifications on MRTF-A

It is clear that post-translational modifications play a major role in regulating protein function (109). Thus, we set out to identify novel PTMs on MRTF-A, hypothesizing that one or more of these would affect MRTF function and downstream smooth muscle gene expression. In the mass spectrometry experiment to identify novel MRTF-A binding partners in SMC, we found that MRTF-A was phosphorylated at Threonine 488 (T488). These data are in agreement with studies that also identified phosphorylation at T488 (115, 116). One limitation of PTM discovery by mass spectrometry is the low level of stoichiometry of modified to unmodified endogenous protein. To overcome this, we used an overexpression approach in mouse SMC and in COS-7 cells, which are routinely used for these types of experiments because they are readily transfectable and they express recombinant protein at very high levels, making them highly suitable for detecting PTMs by mass spectrometry. In each experiment, we transfected flag-MRTF-A or a flag-empty vector (to serve as a control for non-specific binding) and immunoprecipitated the flag-tagged protein 48 hours later. In the case of
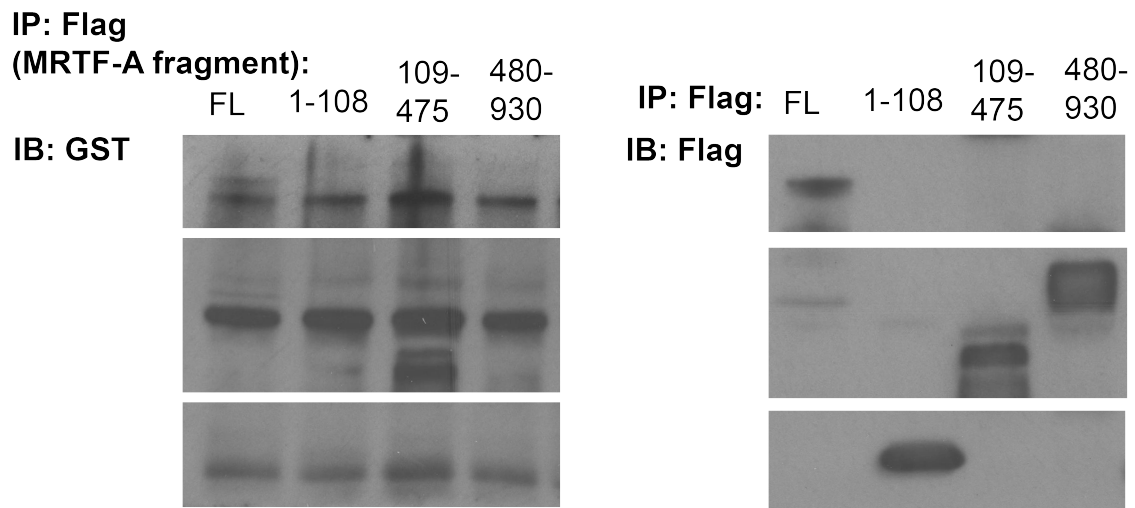
Figure 4.3. PRDM6 interacts directly with the SRF-binding reigon of MRTF-A. Flag-MRTF-A fragments were purified from cos cells and subjected to Far Western blotting using an anti-GST antibody.
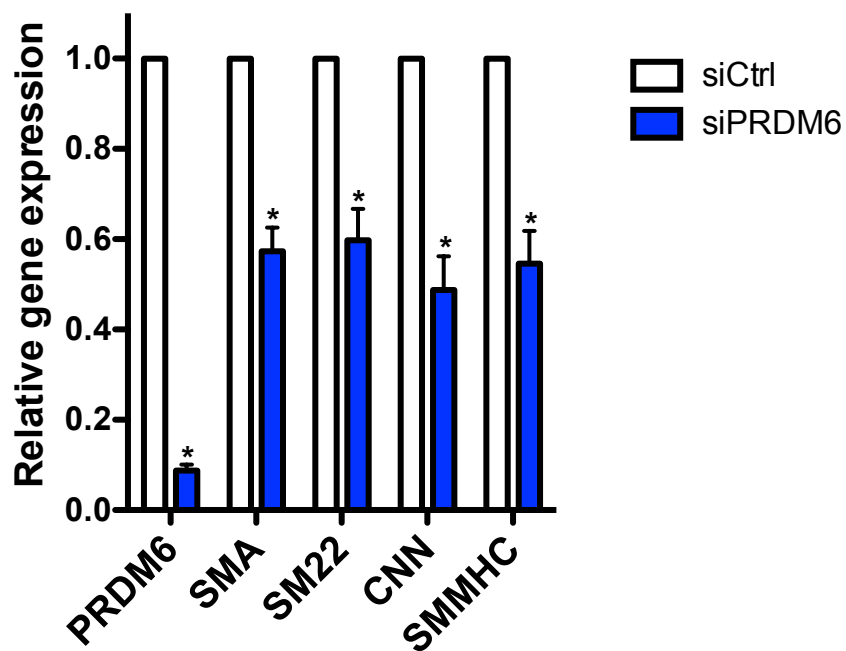
Figure 4.4. PRDM6 is required for SMC differentiation. Rat aortic SMCs were treated with siRNAs targeted to PRDM6 or a control non-targeting siRNA for 72 hours. Smooth muscle marker gene expression was analyzed by qRT-PCR and normalized to GAPDH, *p<0.05.

the overexpression experiment in mouse SMCs, the entire immunoprecipitated mixture was submitted to the UNC Proteomics Core for LC/MS/MS analysis. However, immunoprecipitated samples from COS-7 cells were resolved by SDS-PAGE, and the flag-MRTF-A bands were excised and submitted for mass spectrometry analysis. Several findings from this experiment are worth noting. First, MRTF-A immunoprecipitated from mouse SMCs was phosphorylated at Serine 492 (S492), which was one of the phosphorylation sites confirmed in previous reports (115). Second, phosphorylation was detected with high confidence on a peptide containing Serine 810, Tyrosine 817, and Threonine 822, indicating that one of these residues was phosphorylated. Finally, COS-7 overexpressed MRTF-A was significantly phosphorylated and methylated. Many of the phosphorylation sites identified in this experiment were corroborated by recent data from the Treisman Lab showing that phosphorylation of over 25 different serine and threonine residues differentially controlled MRTF-A localization (116). Given this already published data, we chose not to assess the contribution of phosphorylation on MRTF-A activity any further. We were surprised to find that MRTF-A was substantially methylated at multiple lysines and arginines. Because PTMs, including methylation, can result from byproducts of the mass spectrometry analysis procedure, we first tested whether endogenous MRTF-A was methylated in vivo. From previous experiments, we had already established a protocol for efficiently immunoprecipitating endogenous MRTF-A from SMCs, thereby allowing us to examine the methylation status of MRTF-A in vivo. Immunoprecipitated MRTF-A was subjected to SDS-PAGE Western using a specific antibody to mono-methyllysine. As seen in Figure 4.5A, MRTF-A was methylated in SMCs. Our mass spectrometry determinations indicated that lysine methylation occurred throughout

128

MRTF-A. To narrow our search for functional methyllysines, we used our in vivo

methylation IP protocol to detect regions of MRTF-A that were methylated in cells. Flag-

MRTF-A fragments were immunoprecipitated from COS-7 cells and subjected to

Western blotting with the anti-methyllsyine antibody. As shown in Figure 4.5B,

methylation was detected on fragments 1-108 and fragments 109-475.

Identification of lysine methyltransferases that methylate MRTF-A

Numerous studies have demonstrated that lysine methylation of non-histone

proteins regulates their activity, stability, and interaction with other proteins (179-181,

192). Interestingly, many common SET-containing protein lysine methyltransferases

(PKMTs) that were once thought to methylate only histones have been implicated in

methylating non-histone proteins. Importantly, several PKMTs have known consensus

sites in the targets they recognize. Thus, we scanned the N-terminal and central regions

of MRTF-A for known consensus sites recognized by PKMTs. Of note, we identified

several SMYD2 sites, one G9a site, and two SET7/9 sites (Figure 4.6). We also

hypothesized that PRDM6, which was identified as an MRTF-A binding partners in

SMCs, may methylate MRTF-A. We next screened each of these predicted PKMTs in

an in vitro methyltransferase assay with GST-N-terminal MRTF-A (1-260). As seen in

Figure 4.7A, SMYD2 and SET7/9 methylated MRTF-A in vitro. In support of these data,

SMDY2 increased methylation of MRTF-A in vivo as did SET7/9 (Figure 4.7B, C). Of

note, basal MRTF-A methylation was reduced by a catalytically inactive SET7/9 H297A

mutant construct, implying this mutant functioned as a dominant negative in this

experiment. Given that our rationale for analyzing SMYD2 and SET7/9 was based on

our identification of their conserved target sites within MRTF-A, we expected mutation of

lysine (K) to arginine (R) at each of the predicted sites to abolish SMYD2- and SET7/9-
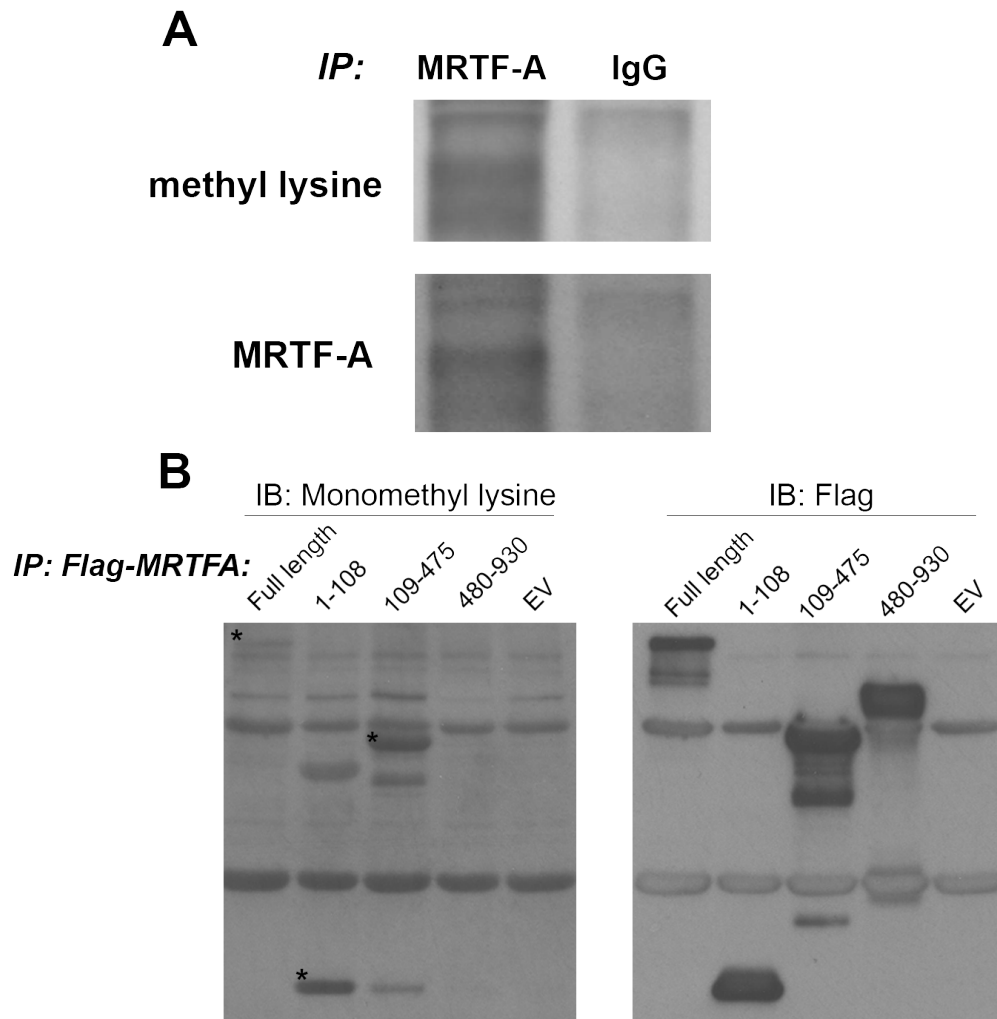
Figure 4.5. MRTF-A is methylated in vivo. A) MRTF-A was immunoprecipitated in various SMC lines and probed for monomethyl lysine (MMK) to detect methylation on MRTF-A in vivo. **B)** Flag-MRTFA fragments were transfected into COS cells and then IP'd. Purified fragmented underwent Western blotting for MMK.

dependent methylation. To date, we have only performed mutational analysis for the

SMYD2 target lysines. As shown in Figure 4.8A, out of four lysines that were in

predicted SMYD2 target sites (282), K27 was the only site required for SMYD2-

dependent methylation of MRTF-A. In order to increase our sensitivity of MRTF-A

methylation by SMYD2, we performed an in vitro methyltransferase assay with cold

SAM and GST-N-terminal MRTF-A either with or without SMYD2 and then submitted

the reactions for quantitative mass spectrometry analysis. These results were highly

consistent with our data that K27 is the predominant SMYD2 methylation site, which

was methylated nearly 12-fold over the unmethylated peptide obtained from the in vitro

reaction without SMYD2 (Figure 4.8B). Also consistent with our initial in vitro

experiments, K60 was not methylated by SMYD2. Moreover, K237 was methylated by

approximately 5-fold over the unmethylated peptide, indicating that our previous

analysis of the K237R mutant may have underestimated the degree of methylation of

this lysine. Further, SMYD2 overexpression increased MRTF-A methylation in vivo,

which was prevented by the K27R mutant in vivo (not shown). The observation that

mutating K27 noticeably abolished methylation of MRTF-A by SMYD2 in vivo suggests

that methyl-K27 is in high stoichiometry relative to unmethylated lysine 27.

K27 is required for nuclear import of MRTF-A

K27 is located within the B2 region of MRTF-A's RPEL domain, and previous

studies using scanning alanine mutagenesis indicate that this location is essential for

MRTF nuclear localization (99). To determine if K27 is required for nuclear import, we

introduced a lysine to alanine mutation at K27 and transfected 10T1/2 cells with

wildtype or K27A flag-MRTF-A. As shown in Figure 4.9A and B, the K27A MRTF-A

mutant was constitutively cytoplasmic in nearly 80% of the cells, whereas wildtype flag-

Figure 4.6. Additional predicted methylation sites within MRTF-A. Multiple methyltransferase targets were present in the N-terminus of MRTF-A. These included SMYD2, G9a, and SSET7/9 sites (substrate lysines in red).

132
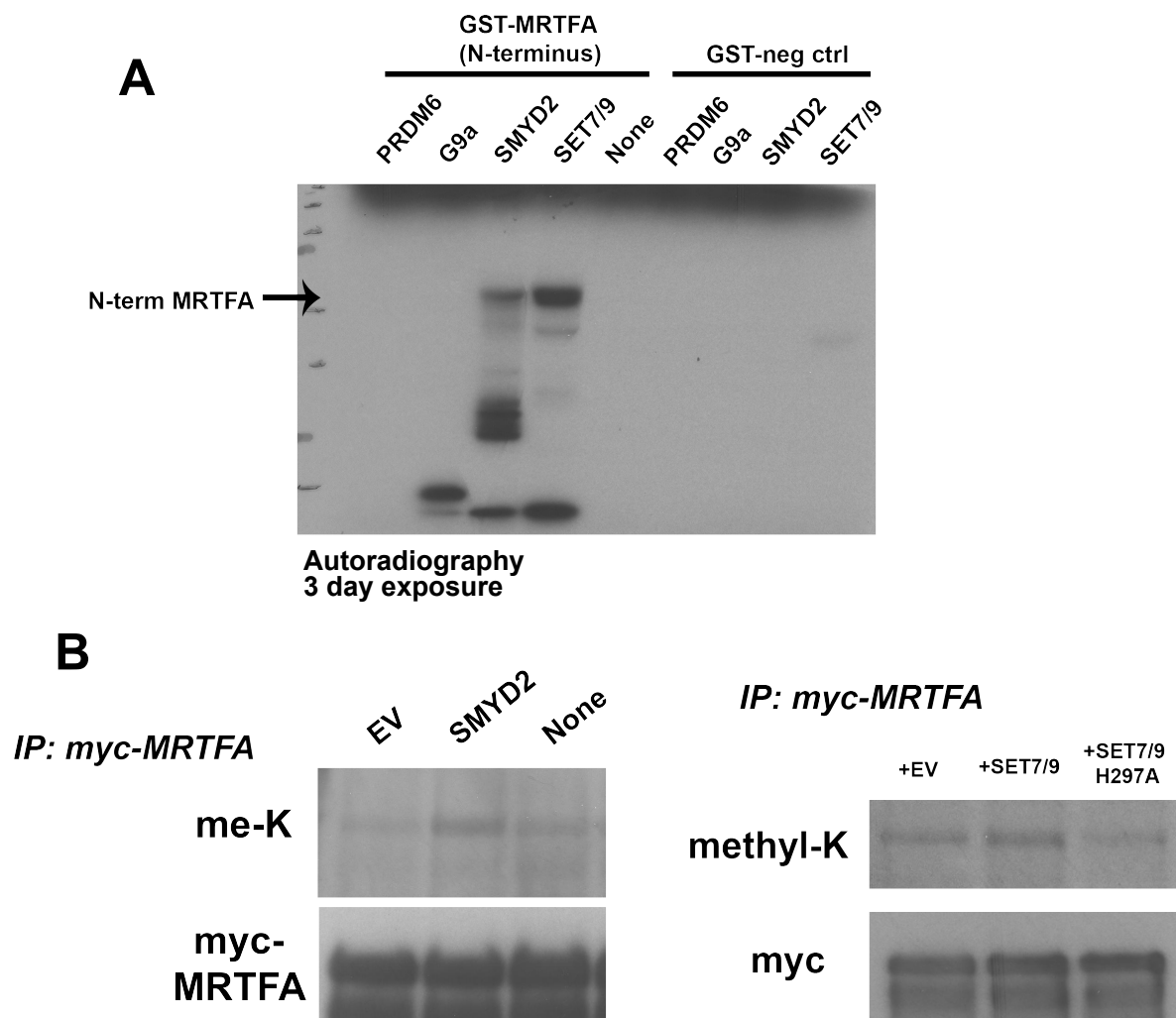
Figure 4.7. SMYD2 and SET7/9 methylate MRTF-A in vitro and in vivo. A) In vitro methyltransferase assay was performed with 2 ug of each methyltransferase, 2 ug of GST-N.-term. MRTF-A, and 2 uCi of SAM-3H. Reactions were allowed to incubate at 37 degrees C for 1 hour after which reaction were run on an SDS-PAGE. The gel was dried and exposed to autoradiography. **B)** Myc-MRTF-A was co-expressed with SMYD2 or SET7/9 **(C)** in COS-7 cells. Myc-MRTF-A was immunoprecipitated and analyzed by Western blotting using a mono-methyl-lysine antibody.

133
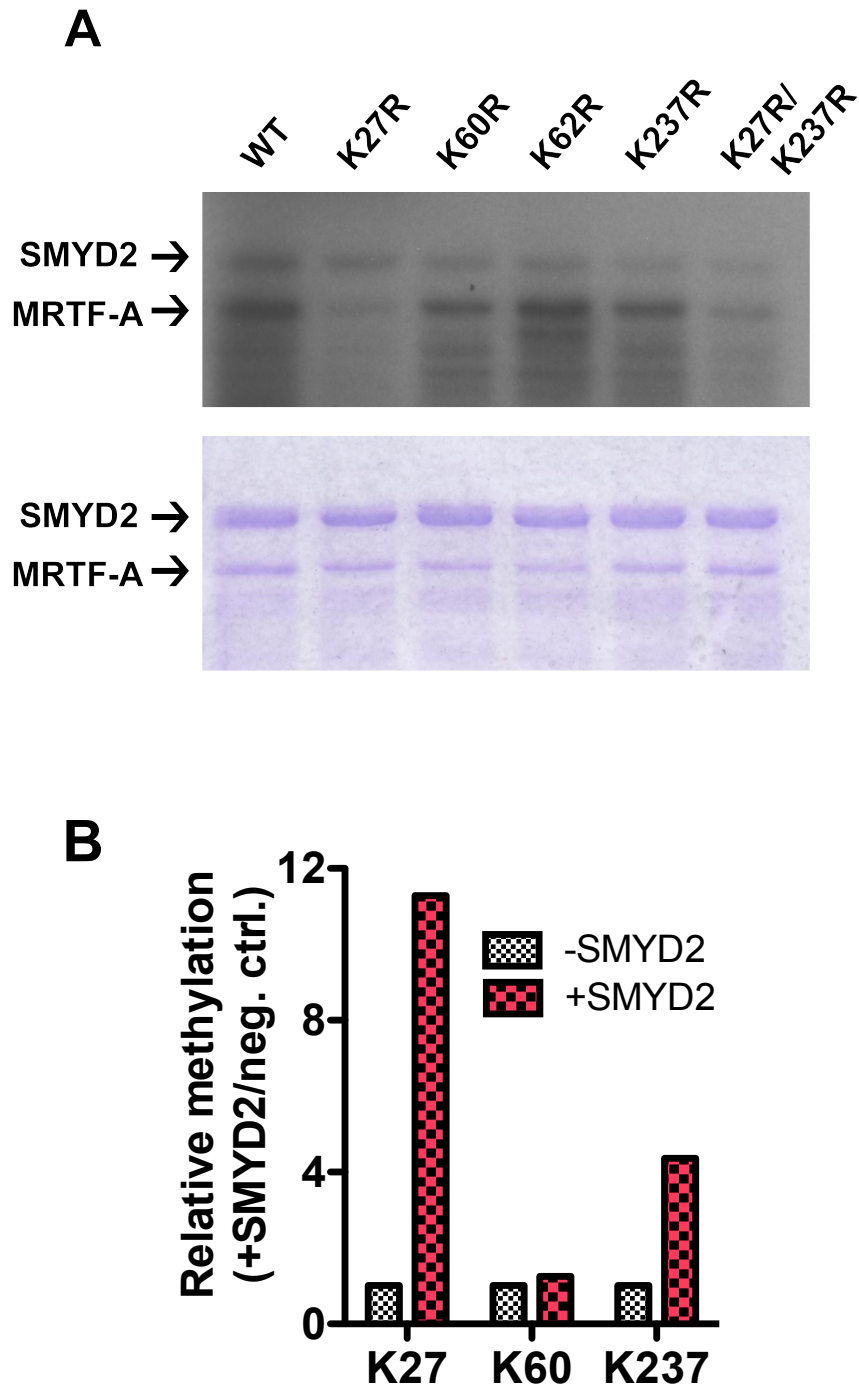
Figure 4.8. SMYD2 methylates MRTF-A at K27. A) In vitro methyltransferase assays were performed with SMYD2 and K>R mutants for eadh of the predicted SMYD2-target sites. **B)** In vitro methyltransferase assay performed with SMYD2, GST-N.term MRTFA, and cold SAM. Reactions were submitted to mass spectrometry for quantitiatve identification of methylated lysines.

MRTF-A was purely cytoplasmic in only 10% of the 10T1/2s. These data provide compelling evidence that K27 is absolutely required for MRTF-A nuclear localization and support our hypothesis that methylation of K27 regulates MRTF-A localization.

SMYD2 interacts with MRTF-A

Because histone modifiers can form stable complexes with transcription factors, as is the case for the H3K9-specific demethylase Jmj1a and the myocardin factors, we pursued the idea that SMYD2 and MRTF-A might interact. Flag-SMYD2 and myc-MRTF-A were co-expressed in COS-7 cells, and MRTF-A was immunoprecipitated using an anti-myc antibody. Because our data suggested that SET7/9 strongly methylates MRTF-A, we also performed co-immunoprecipitation experiments with Flag-SET7/9 and myc-MRTF-A. As seen in Figure 4.10, SMYD2 and MRTF-A interacted strongly, further supporting the hypothesis that SMYD2 regulates MRTF-A function. Of note, SET7/9 did not interact with MRTF-A. This later observation does not diminish our finding that SET7/9 methylates MRTF-A, since methylation is a transient event that does not require a stable interaction between the PKMT and substrate.

SMYD2 inhibits MRTF-A nuclear localization

Several lines of evidence indicated that SMYD2 might affect MRTF-A nuclear import. First, SMYD2 is located almost exclusively in the cytoplasm. Second, SMYD2 methylates MRTF-A at K27, which is located within a highly conserved NLS. Third, the K27A MRTF-A mutant was constitutively cytoplasmic. To begin to examine the interesting possibility that SMYD2 regulates MRTF-A nuclear entry, we overexpressed GFP-MRTF-A with flag-empty vector or with flag-SMYD2 in 10T1/2s for 24 hours, which was followed by 16 hours of overnight serum starvation. In some experiments, after serum starvation 10T1/2s were stimulated with 10% serum for one hour to induce

A
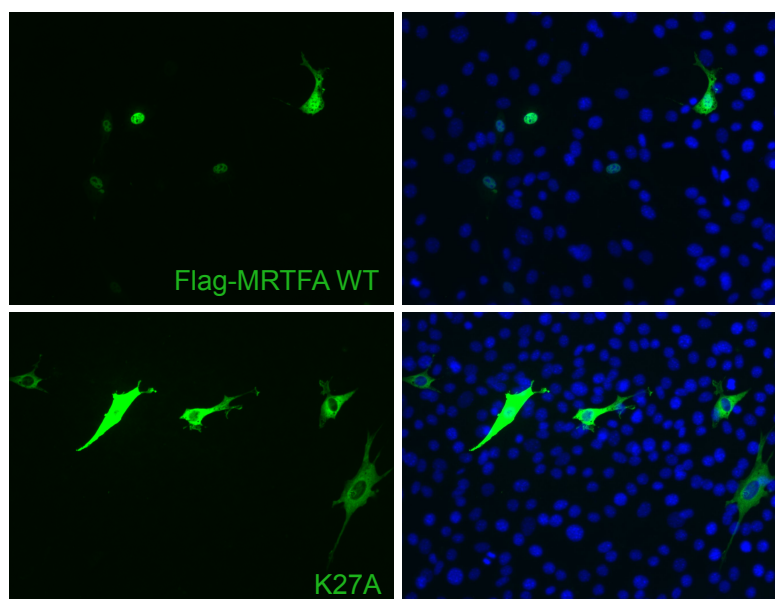
B
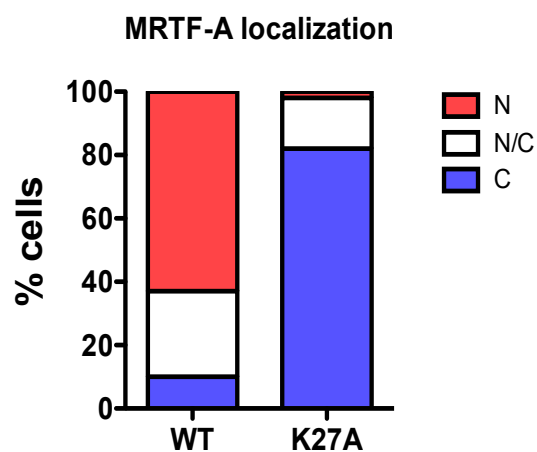
Figure 4.9. K27 is essential for MRTF-A nuclear import. A) flag-MRTFA wild-type and K27A were transfecged into 10T1/2s, incubated, with flag antibody, and counterstained with DAPI. B) Quantitation of panel A results. Four different fields were counted in 4-well chamber slides.
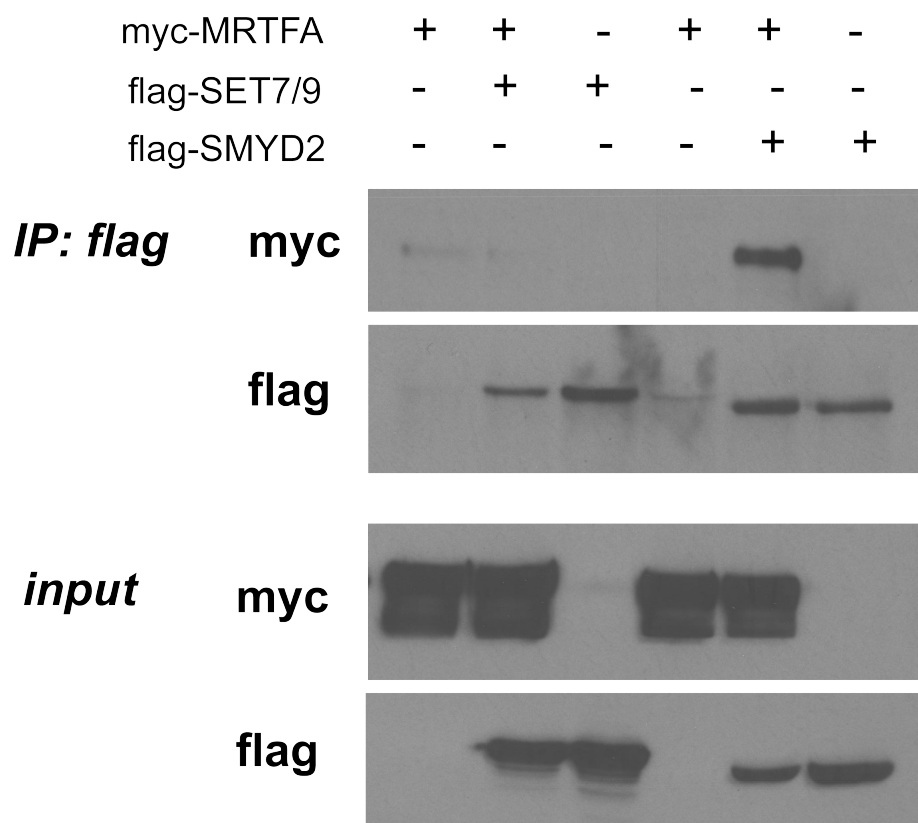
Figure 4.10. SMYD2 interacts with MRTF-A. Co-immunoprecipiation in COS-7 cell lysates transfected with myc-MRTF-A and flag-SET7/9 or flag-SMYD2 plasmids. IP's were perfomed with a flag antibody (Sigma) and purified complexes were analyzed via standard Western blotting using a myc antibody to detect binding.

nuclear localization of GFP-MRTF-A. As shown in Figure 4.11A, in the serum starved 10T1/2s, GFP-MRTF-A was nuclear in 15% of cells co-transfected with the empty vector control. However, GFP-MRTF-A was nuclear in only 7% of cells co-transfected with flag-SMYD2. In the 10% serum stimulated condition, the results were even more striking. GFP-MRTF-A was nuclear in 72% of control cells but only 40% in cells expressing flag-SMYD2. MRTF-A enters the nucleus via an importin-dependent mechanism. Very briefly, the B1 and B2 regions within MRTF's RPEL domain bind the importin-α/β heterodimer (99). Therefore, we hypothesized methyl-K27 would have a lower affinity for importin compared to unmethylated-MRTF-A. To investigate whether this was the case, we developed an assay to differentially test methylated versus unmethylated MRTF-A binding. In short, equal amounts of beads containing GST-N-term MRTF-A, which includes the RPEL, B1, and B2 domains, was subjected to the cold in vitro methyltransferase assay with and without recombinant SMYD2. After 2 hours of in vitro methylation, beads were used to purify importin-β from 10T1/2 cell lysates. As indicated in Figure 4.11B, methylated (+SMYD2) MRTF-A bound significantly less importin-β, which was consistent with our data that SMYD2-mediated methylation inhibits MRTF-A nuclear localization.

SMYD2 inhibits MRTF-A dependent smooth muscle transcription

Nuclear localization of the MRTFs strongly upregulates smooth muscle-specific gene transcription (100). Indeed, inhibiting MRTF-A nuclear entry with pharmacologic agents such as leptomycin B, which prevents G-actin dissociation from the MRTFs, dramatically reduces expression of SMC markers. Based on these well-supported pieces of data in conjunction with our striking evidence that SMYD2-mediated methylation of MRTF-A at K27 inhibits its localization, we hypothesized that SMYD2

would negatively regulate MRTF-dependent smooth muscle transcription. Indeed, in luciferase assays SMYD2 inhibited relative MRTF-A transactivation of the smooth muscle alpha-actin promoter by nearly half (Figure 4.12).

Actin dynamics regulate MRTF-A band shifts

Prior Western blot data from our lab indicated that MRTF-A was present in two fractions: lower and higher molecular weight species. Interestingly, the higher molecular weight MRTF-A fraction was induced with serum stimulation. Each fraction was separated from the other by approximately 10 kD. Studies by Prywes et al. demonstrated similar size differences for MRTF-A, which were attributed to phosphorylation at three residues. Interestingly, these same phospho-residues were identified in our mass spectrometry experiments. We hypothesized that this band shift also resulted from additional PTMs. In separate experiments, we noticed that treatment of SMCs with cytochalasin D, which frees MRTF-A from G-actin, also induced a higher molecular weight fraction (Figure 4.13). While outside the scope of this dissertation, this data led us to pursue the idea that actin dynamics are intricately linked to MRTF-A modifications, especially methylation. This is a highly likely scenario given that K27 is located within the actin-binding RPEL domain. In support of this, we noticed that the K27R mutant led to a lower molecular weight species compared to wildtype MRTF-A, suggesting that methylation at K27 itself contributes to increased molecular weight and/or that methylation at this residue controls PTMs at other sites (data not shown).
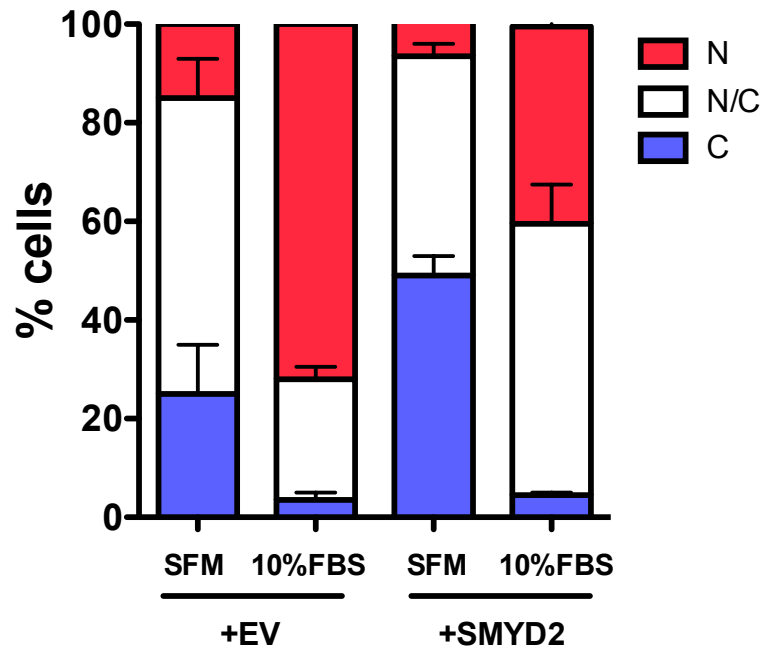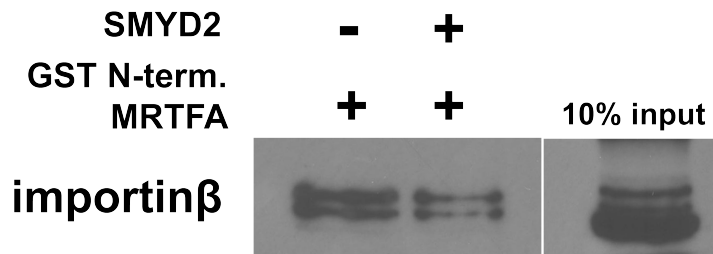
Figure 4.11. SMYD2 inhibits MRTF-A nuclear localization. A) GFP-MRTFA was co-expressed with flag-EV or flag-SMYD2 in 10T1/2s seeded in 4-well chamber slides. Cells were serum starved the day after transfections for approximately 16 hours and then left in SFM or stimulated with 10% serum. Separate fields were counted in all experiments (n=2). **B)** GST-MRTFA beads underwent methylation by SMYD2 (or without SMDY2 as an unmethylated negative control) and were then used to purify importin from 10T1/2 cell lysates.
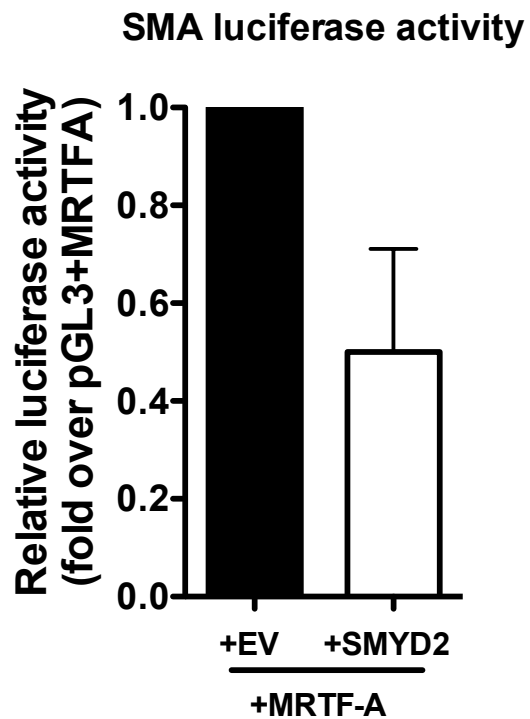
Figure 4.12. SMYD2 inhibits MRTF-A-dependent promoter activity. 10T1/2s were co-transfected with a pGL3-SMA promoter construct, MRTF-A, and either EV or SMYD2. Luciferase assays were performed 48 hours later. Values are presented as fold-change over pGL3 EV plus MRTF-A (n=2).

Cytochalasin D

- +
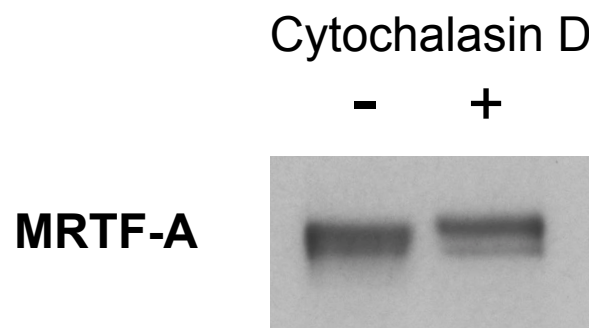
MRTF-A

Figure 4.13. Cytochalasin D treatment induced formation of the higher mobility MRTF-A species. 10T1/2s were treated for 1 hour with Cytochalasin D to inhibit the MRTF-A-G-actin interaction. Lysates were collected and analyzed by Western blotting using a commercial MRTF-A antibody (Santa Cruz).

Discussion

Here, we present several novel pieces of data. First, MRTF-A interacts with the histone lysine methyltransferase, PRDM6, and PRDM6 knockdown resulted in a significant decrease in smooth muscle-specific gene expression. Previous studies demonstrated that PRDM6 repressed SMC differentiation and promoted the expression of proliferative gene in primary SMCs, while we show the opposite (278). Thus, it is highly likely that PRMD6 exerts context-specific control over SMC gene transcription, which is a well-characterized phenomenon for chromatin remodelers. Interestingly, one polymorphism, rs13359291, within the human PRDM6 gene is linked to blood pressure (252). Based on its highly SMC-selective expression pattern and requirement for smooth muscle gene expression, we hypothesize that the PRDM6 blood pressure locus (defined by 14 SNPs in high linkage disequilibrium that are located in the second intron of PRDM6) alters blood pressure by affecting PRDM6 expression. In strong support of our hypothesis, the GTEx database indicates that the rs13359291 minor allele is associated with decreased PRDM6 expression. Importantly, each copy of the minor allele is correlated with a 0.57 mmHg increase in blood pressure. With all of this in mind, we hypothesize that lower PRDM6 expression leads to higher blood pressures. Studies by our lab have already shown that PRDM6 knockdown does not affect MLC phosphorylation. Since PRDM6 knockdown reduced SMC marker expression, one possible mechanism is that minor allele carriers have reduced smooth muscle markers, leading to vasculature that is more sensitive to phenotypic modulation. Of course, this hypothesis still needs to be tested. We have also begun to identify the SNP(s) that affect PRDM6 expression. As mentioned above, there are a total of 14 SNPs, several of which cluster around DNase Hypersensitive sites and conserved regions.

An important remaining question is how PRDM6 affects SMC differentiation. Our initial hypothesis was that PRDM6 methylated MRTF-A; however, our data indicate that this is not the case. Rather, it is possible that PRDM6 is working with other methyltransferases such as G9a to methylate key histones at SMC-specific gene loci. Targeted H3K9me chromatin immunoprecipitation in control versus PRDM6 knockdown SMC will be critical for answering this question. Finally, coding mutations in PRDM6 cause patent ductus arteriosus (PDA) (284, 285). Although PDA is thought to be caused by a decrease in smooth muscle contraction and/or SM marker gene expression during development, how exactly PRDM6 contributes is undetermined.

Second, we present strong evidence that SMYD2 and SET7/9 methylate MRTF-A in vitro and in vivo. The SMYD family of lysine methyltransferases consists of five proteins (SMYD1-5) that contain highly conserved SET and MYND domains. The SMYDs are preferentially expressed in cardiac and skeletal muscle and have been shown to regulate myofiber assembly (283). While it is known that SMYD2 is highly expressed in cardiomyoctyes, to our knowledge, no other studies to date have examined SMYD2 expression in SMC. Importantly, SMYD2 methylates MRTF-A at K27, which is embedded within MRTF's NLS. Interestingly, SMYD2 inhibited MRTF-A nuclear localization and MRTF-dependent transactivation of SM promoter activity in luciferase assays. It is currently unknown why non-SMC that, despite expressing SRF, and in the cases of cardiomyocytes, also myocardin and the MRTFs, fail to differentiate into SMC. One hypothesis of ours is that cell type-specific mechanisms repress the smooth muscle gene program. For example, SMYD2 is highly expressed in left ventricle (GTEx). Therefore, SMYD2 may inhibit MRTF-A nuclear localization in cardiomyocytes to inhibit SMC differentiation. To more directly address this, experiments are needed to

144

probe for SM markers in SMYD2-knockdown cardiomyocytes. Re-expression of SM-specific genes after SMYD2 knockdown would support this interesting hypothesis.

One particularly observation is that while amino acid 27 is both evolutionarily conserved and conserved between MRTF-A and MRTF-B, amino acid 27 in myocardin is actually an arginine, which cannot be methylated. It is well-known that myocardin is nearly constitutively nuclear in SMC, while the MRTFs translocate in and out of the nucleus in response to various stimuli. Thus, the difference between K and R at this residue may explain in part why myocardin is more nuclear, especially coupled with the fact that myocardin's affinity for importin is much higher than MRTF-A's. Indeed, the K27R MRTF-A mutant exhibited increased affinity for importin. Additional experiments are needed to determine if the K27R mutant is more nuclear than wild-type MRTF-A as well as in the presence and absence of SMYD2. It is also important to note that in a mass spectrometry screen for SMYD2 methyl-substrates, K27 was identified in MRTF-B, thus lending even greater confidence to our results. Furthermore, when comparing the sequences of all the identified SMYD2 substrates, the consensus sequence of a SMYD2 methylatable site was "KR". Given that the KR motif is highly enriched in the NLS of other proteins, a very attractive hypothesis is that SMYD2-mediated methylation of lysines within NLS is a conserved mechanism to fine-tune nuclear localization in these other proteins. While this is a very broad-sweeping hypothesis that applies to lysine methylation of NLS contained within negative and positive regulators, additional investigation into this may yield fascinating results.

Post-translational modifications can affect other PTMs on nearby residues within the same molecule. For example, methylation of p53 by SET7/9 enhances its acetylation (286). Data from our studies and others indicates that MRTF-A is

145

phosphorylated at multiple serine and threonines (115, 116). Thus, it is possible that methylation of MRTF-A affects phosphorylation or vice versa. This is especially plausible given that the serum-inducible shift that represents MRTF-A phosphorylation seemed to be diminished in the K27R mutant.

Finally, while not fully explored in the current work work, SET7/9 strongly methylated MRTF-A. Our lab is currently making K to R mutations for the two SET7/9 target sites within MRTF-A, K224 and K227, to directly test if these are in fact the methylatable lysines. SET7/9 methylation of the transcription factor YY1 increases its binding to p53, RAD1, and ABL1 promoters (192). Thus, it is plausible that SET7/9 may affect the transcription activity of MRTF-A. Interestingly, both K224 and K227 are located within the B1 region that mediates SRF binding. Importantly, a recent report of SET7/9 knockdown in mouse embryonic stem cells showed that SET7/9 was required for induction of SMC-specific genes including SMA, SM22, CNN1, and others (191). Although the authors suggested that SET7/9 modified SRF, they did not present convincing data to show this. Rather, SET7/9-mediated methylation of MRTF-A may enhance binding to SRF at CArGs within smooth muscle-specific genes, thereby upregulating SMC differentiation in ES cells. This is a highly novel and exciting hypothesis that our lab will address.

CHAPTER 5: CONCLUSIONS, PERSPECTIVES, AND FUTURE DIRECTIONS

Pharmacological regulation of RhoA and Rho-dependent pathways

Current standard of care

Despite the importance of RhoA signaling in the development of hypertension, few treatments are currently available that target this signaling axis. However, some commonly used anti-hypertensives may interfere with RhoA signaling. For example, since RhoA-dependent regulation of vascular tone is a major contributor to AII-mediated increases in BP, the highly utilized class of anti-hypertensives that target AII (i.e. ACE inhibitors and AII receptor blockers) may exert some of their BP lowering effects by reducing RhoA activation (220, 246). Moreover, although used to treat high cholesterol, HMG-CoA reductase inhibitors such as simvastatin and atorvastatin also have anti-hypertensive properties (247) and their BP lowering effects have been attributed to their ability to block RhoA signaling. RhoA is known to be modified by covalent attachment of a geranylgeranyl isoprenyl to a C-terminal Cys, and this modification (which is blocked by simvastatin treatment) is required for membrane localization and activation of RhoA (286).

ROCK inhibitors

While not yet included in standard of care treatment for hypertension, several pharmacologic agents have been developed for inhibiting Rho kinases. In general, kinases make good drug targets due to the relative ease of targeting specific molecules to the ATP-binding pockets of these enzymes. To date, most of the Rho kinase

inhibitors utilized in animal studies and clinical trials target the ATP-binding pockets of both ROCK isoforms (288-290). Although not clinically used in the United States, studies abroad provide compelling evidence for the use of this therapeutic approach for BP control. One particularly effective ROCK inhibitor, fasudil, is currently used in Japan to treat cerebral vasospasm and clinical trials determined that fasudil was also effective in decreasing peripheral vascular resistance in hypertensive patients (291).

Despite the wide use of these pharmacologic agents in cells and animal disease models, neither fasudil nor Y-27632 exhibit suitable specificity for a therapeutic as they can inhibit the activity of several other kinases including PKC, PKA, and MLCK, at higher concentrations (292, 293). These compounds also suffer from having short half-lives, which is a highly undesirable attribute of a drug designed to treat a longstanding disease (294). Thus, there is great need for development of additional potent, yet specific, ROCK inhibitors that can be safely used in patients (295). While a few such compounds have been developed recently with such attributes (296-300), whether any these compounds exhibit the necessary selectivity and pharmacogenetic profiles required for BP management in patients requires further study. Moving forward, given the importance of RhoGEFs and RhoGAPs in the control of SM contractility and BP, we believe that it will be possible to engineer clinically-relevant small molecule regulators of these enzymes that could be used to develop new and effective anti-hypertensive therapies.

Future of anti-hypertensive therapy: Personalization of drug regimens

Current anti-hypertensive therapy is often empirically based and involves multiple drug regimens (301, 302) – an approach that is moderately effective at best as it frequently contributes to unwanted side effects and intolerance or non-adherence to

medication. Accordingly, more effective and specific anti-hypertensive agents that inhibit targets very selectively are necessary. Moreover, based on the fact that BP is a highly variable trait among individuals, a better understanding of the genetic mechanisms regulating this disease is critical for a more personalized treatment plan for patients. Given the numerous regulatory and counter-regulatory mechanisms modulating the RhoA axis, this central axis provides an excellent opportunity for identifying genetic biomarkers that correlate with different levels of hypertensive risk and drug responses.

Indeed, genetic variations in both upstream activators and downstream mediators of RhoA have been linked to BP regulation. Screening for such variants could potentially be used to tailor more effective individualized treatments. For example, one study showed that the BP lowering effects of the ACE inhibitors or the angiotensin receptor blockers were more pronounced in patients carying a GG genotype at the -391 RGS2 (Regulators of G-protein signaling 2) locus when compared to responses in GC or CC genotype carriers, while no differences were observed in the responses to calcium channel antagonists (303). Although RGS2 is known to couple to ATR1, the underlying mechanism by which these polymorphisms lead to altered sensitivity is currently unknown. Another example is seen with the association between polymporphisms in the G-protein coupled receptor kinase 4 gene and reduced BP-lowering effects of the b-blocker atenolol (304). Whether any of the aforementioned Rho-signaling SNPs influence specific responses to or bio-availability of anti-hypertensive treatments remains a critical unexplored question. The clinical utility of targeting the RhoA pathway should also be further explored.

GRAF3 rs604723 genotype as a predictor of response to anti-hypertensive therapy

Another component of the RhoA axis that has significant implications for

predicting patient response to anti-hypertensives is the RhoGAP, GRAF3. GRAF3 is required for blood pressure homeostasis, since GRAF3 deficient mice are significantly hypertensive (219). A major focus of this dissertation has been to identify polymorphisms in the GRAF3 gene that regulate its expression, since SNPs in this locus were linked to blood pressure in the human population (250, 251). As such, the current study has made great strides in identifying the basis for blood pressure regulation in the human population. Collectively, this research indicates that the rs604723 modifies hypertensive risk by affecting SRF binding at a novel intronic regulatory region (273). The minor allele at this blood pressure locus enhances SRF binding, thereby increasing GRAF3 expression, and decreasing RhoA-dependent SMC contractility. Furthermore, cell stretch increased GRAF3 expression. Because resistance vessels of hypertensive individuals are under significant strain, this presents a novel mechanism whereby vessel stretch, which leads to SMC phenotypic switching and vascular remodeling, increases GRAF3 expression to counteract the increased SMC contractility.

Patients harboring the rs604723 major allele have increased blood pressure and decreased GRAF3 expression. Therefore, based on the fact that decreased GRAF3 expression results in increased RhoA-dependent SMC contractility, we hypothesize that that patients with the major allele (i.e., increased SMC contractility) will be more responsive to anti-hypertensive regimens that target SMC contractility directly rather than diuretics. As already listed, some of these agents include ACE inhibitors, Ang II receptor blockers, and better yet, ROCK inhibitors. We also predict that patients will exhibit increased dose responsiveness to these drugs per copy of the major allele. In collaboration with the Taylor Lab, these analyses correlating GRAF3 genotype with drug

responsiveness are underway.

Regulation of MRTF-A-dependent transcription as a way to direct SMC differentiation

In atherosclerosis and restenosis, SMCs undergo extensive phenotypic modulation characterized by downregulation of contractile gene expression and upregulation of growth-related genes that promote proliferation and matrix production (21). These transcriptional changes contribute to a SMC phenotype that is detrimental to the health of the blood vessel, ultimately leading to atherosclerotic plaque rupture and/or intimal hyperplasia. Both of these processes lead to vessel occlusion and decreased downstream tissue perfusion, which can result in stroke and/or myocardial infarction. For these reasons, atherosclerosis and restenosis contribute to significant morbidity and mortality in the United States. Given that many of the disease features are initiated by transcriptional changes in the SMC, identification of novel SMC-selective inhibitors of this process are crucial. This dissertation research has identified roles for select epigenetic modifiers in regulating SMC differentiation. Furthermore, given their cell type-specific expression patterns, they could perhaps represent novel targets for directing SMC differentiation during phenotypic switching.

One interesting possibility is that SMDY2 prevents MRTF-A nuclear translocation during phenotypic switching, thereby contributing to reduced SMC gene transcription. This is certainly the case for Erk-mediated phosphorylation, which enhances MRTF's binding to G-actin and cytoplasmic sequestration (115). Testing the following hypotheses will likely address this: Does SMYD2 expression increase in vascular SMCs during diseases like atherosclerosis and restenosis? If so, will inhibiting SMYD2 rescue some of the reduction in SMC-specific transcription that occurs during phenotypic

151

switching? Interestingly, LLY-507, a SMYD2 selective pharmacologic inhibitor, is

commercially available and may be useful for answering some of these important

questions (305).

REFERENCES

1. Majesky MW, Dong XR, Hoglund V, Mahoney WM,Jr, Daum G. The adventitia: A dynamic interface containing resident progenitor cells. *Arterioscler Thromb Vasc Biol.* 2011 Jul; 31(7): 1530-1539. PMCID: PMC3382115.

2. Majesky MW, Horita H, Ostriker A, Lu S, Regan JN, Bagchi A, Dong XR, Poczobutt J, Nemenoff RA, Weiser-Evans MC. Differentiated smooth muscle cells generate a subpopulation of resident vascular progenitor cells in the adventitia regulated by Klf4. *Circ Res.* 2017 Jan 20; 120(2): 296-311. PMCID: PMC5250562.

3. Bautch VL. VEGF-directed blood vessel patterning: From cells to organism. *Cold Spring Harb Perspect Med.* 2012 Sep 1; 2(9): a006452. PMCID: PMC3426816.

4. Paik JH, Skoura A, Chae SS, Cowan AE, Han DK, Proia RL, Hla T. Sphingosine 1-phosphate receptor regulation of N-cadherin mediates vascular stabilization. *Genes Dev.* 2004 Oct 1; 18(19): 2392-2403. PMCID: PMC522989.

5. Liu Y, Wada R, Yamashita T, Mi Y, Deng CX, Hobson JP, Rosenfeldt HM, Nava VE, Chae SS, Lee MJ, Liu CH, Hla T, Spiegel S, Proia RL. Edg-1, the G protein-coupled receptor for sphingosine-1-phosphate, is essential for vascular maturation. *J Clin Invest.* 2000 Oct; 106(8): 951-961. PMCID: PMC314347.

6. Gaengel K, Niaudet C, Hagikura K, Lavina B, Muhl L, Hofmann JJ, Ebarasi L, Nystrom S, Rymo S, Chen LL, Pang MF, Jin Y, Raschperger E, Roswall P, Schulte D, Benedito R, Larsson J, Hellstrom M, Fuxe J, Uhlen P, Adams R, Jakobsson L, Majumdar A, Vestweber D, Uv A, Betsholtz C. The sphingosine-1-phosphate receptor S1PR1 restricts sprouting angiogenesis by regulating the interplay between VE-cadherin and VEGFR2. *Dev Cell.* 2012 Sep 11; 23(3): 587-599.

7. Hellstrom M, Kalen M, Lindahl P, Abramsson A, Betsholtz C. Role of PDGF-B and PDGFR-beta in recruitment of vascular smooth muscle cells and pericytes during embryonic blood vessel formation in the mouse. *Development.* 1999 Jun; 126(14): 3047-3055.

8. Stratman AN, Schwindt AE, Malotte KM, Davis GE. Endothelial-derived PDGF-BB and HB-EGF coordinately regulate pericyte recruitment during vasculogenic tube assembly and stabilization. *Blood.* 2010 Nov 25; 116(22): 4720-4730. PMCID: PMC2996127.

9. Gaengel K, Genove G, Armulik A, Betsholtz C. Endothelial-mural cell signaling in vascular development and angiogenesis. *Arterioscler Thromb Vasc Biol.* 2009 May; 29(5): 630-638.

10. Armulik A, Abramsson A, Betsholtz C. Endothelial/pericyte interactions. *Circ Res.* 2005 Sep 16; 97(6): 512-523.

11. Stratman AN, Malotte KM, Mahan RD, Davis MJ, Davis GE. Pericyte recruitment during vasculogenic tube assembly stimulates endothelial basement membrane matrix formation. *Blood.* 2009 Dec 3; 114(24): 5091-5101. PMCID: PMC2788982.

12. Lindahl P, Johansson BR, Leveen P, Betsholtz C. Pericyte loss and microaneurysm formation in PDGF-B-deficient mice. *Science.* 1997 Jul 11; 277(5323): 242-245.

13. Liu H, Zhang W, Kennard S, Caldwell RB, Lilly B. Notch3 is critical for proper angiogenesis and mural cell investment. *Circ Res.* 2010 Oct 1; 107(7): 860-870. PMCID: PMC2948576.

14. Mack CP, Owens GK. Regulation of smooth muscle alpha-actin expression in vivo is dependent on CArG elements within the 5' and first intron promoter regions. *Circ Res.* 1999 Apr 16; 84(7): 852-861.

15. Li L, Miano JM, Cserjesi P, Olson EN. SM22 alpha, a marker of adult smooth muscle, is expressed in multiple myogenic lineages during embryogenesis. *Circ Res.* 1996 Feb; 78(2): 188-195.

16. Miano JM, Cserjesi P, Ligon KL, Periasamy M, Olson EN. Smooth muscle myosin heavy chain exclusively marks the smooth muscle lineage during mouse embryogenesis. *Circ Res.* 1994 Nov; 75(5): 803-812.

17. Miano JM, Olson EN. Expression of the smooth muscle cell calponin gene marks the early cardiac and smooth muscle cell lineages during mouse embryogenesis. *J Biol Chem.* 1996 Mar 22; 271(12): 7095-7103.

18. Majesky MW. Developmental basis of vascular smooth muscle diversity. *Arterioscler Thromb Vasc Biol.* 2007 Jun; 27(6): 1248-1258.

19. Owens GK. Molecular control of vascular smooth muscle cell differentiation and phenotypic plasticity. *Novartis Found Symp.* 2007; 283: 174-91; discussion 191-3, 238-41.

20. Gomez D, Swiatlowska P, Owens GK. Epigenetic control of smooth muscle cell identity and lineage memory. *Arterioscler Thromb Vasc Biol.* 2015 Dec; 35(12): 2508-2516. PMCID: PMC4662608.

21. Alexander MR, Owens GK. Epigenetic control of smooth muscle cell differentiation and phenotypic switching in vascular development and disease. *Annu Rev Physiol.* 2012; 74: 13-40.

22. Bennett MR, Sinha S, Owens GK. Vascular smooth muscle cells in atherosclerosis. *Circ Res.* 2016 Feb 19; 118(4): 692-702. PMCID: PMC4762053.

23. Gomez D, Owens GK. Smooth muscle cell phenotypic switching in atherosclerosis. *Cardiovasc Res.* 2012 Jul 15; 95(2): 156-164. PMCID: PMC3388816.

24. NHLBI Factbook, Chapter 4, Disease Statistics. 2012. Accessed Feb 10, 2017.

25. Tabas I, Garcia-Cardena G, Owens GK. Recent insights into the cellular biology of atherosclerosis. *J Cell Biol.* 2015 Apr 13; 209(1): 13-22. PMCID: PMC4395483.

26. Tabas I, Bornfeldt KE. Macrophage phenotype and function in different stages of atherosclerosis. *Circ Res.* 2016 Feb 19; 118(4): 653-667. PMCID: PMC4762068.

27. Zimmer S, Grebe A, Latz E. Danger signaling in atherosclerosis. *Circ Res.* 2015 Jan 16; 116(2): 323-340.

28. Bentzon JF, Otsuka F, Virmani R, Falk E. Mechanisms of plaque formation and rupture. *Circ Res.* 2014 Jun 6; 114(12): 1852-1866.

29. Mack CP. Signaling mechanisms that regulate smooth muscle cell differentiation. *Arterioscler Thromb Vasc Biol.* 2011 Jul; 31(7): 1495-1505. PMCID: PMC3141215.

30. Kawai-Kowase K, Owens GK. Multiple repressor pathways contribute to phenotypic switching of vascular smooth muscle cells. *Am J Physiol Cell Physiol.* 2007 Jan; 292(1): C59-69.

31. Janknecht R, Ernst WH, Pingoud V, Nordheim A. Activation of ternary complex factor elk-1 by MAP kinases. *EMBO J.* 1993 Dec 15; 12(13): 5097-5104. PMCID: PMC413771.

32. Marais R, Wynne J, Treisman R. The SRF accessory protein elk-1 contains a growth factor-regulated transcriptional activation domain. *Cell.* 1993 Apr 23; 73(2): 381-393.

33. Shore P, Sharrocks AD. The transcription factors elk-1 and serum response factor interact by direct protein-protein contacts mediated by a short region of elk-1. *Mol Cell Biol.* 1994 May; 14(5): 3283-3291. PMCID: PMC358695.

34. Wang Z, Wang DZ, Hockemeyer D, McAnally J, Nordheim A, Olson EN. Myocardin and ternary complex factors compete for SRF to control smooth muscle gene expression. *Nature.* 2004 Mar 11; 428(6979): 185-189.

35. Yoshida T, Gan Q, Shang Y, Owens GK. Platelet-derived growth factor-BB represses smooth muscle cell marker genes via changes in binding of MKL factors and histone deacetylases to their promoters. *Am J Physiol Cell Physiol.* 2007 Feb; 292(2): C886-95.

36. Kozaki K, Kaminski WE, Tang J, Hollenbach S, Lindahl P, Sullivan C, Yu JC, Abe K, Martin PJ, Ross R, Betsholtz C, Giese NA, Raines EW. Blockade of platelet-derived growth factor or its receptors transiently delays but does not prevent fibrous cap formation in ApoE null mice. *Am J Pathol.* 2002 Oct; 161(4): 1395-1407. PMCID: PMC1867295.

37. He C, Medley SC, Hu T, Hinsdale ME, Lupu F, Virmani R, Olson LE. PDGFRbeta signalling regulates local inflammation and synergizes with hypercholesterolaemia to promote atherosclerosis. *Nat Commun.* 2015 Jul 17; 6: 7770. PMCID: PMC4507293.

38. Madsen CS, Regan CP, Hungerford JE, White SL, Manabe I, Owens GK. Smooth muscle-specific expression of the smooth muscle myosin heavy chain gene in transgenic mice requires 5'-flanking and first intronic DNA sequence. *Circ Res.* 1998 May 4; 82(8): 908-917.

39. Manabe I, Owens GK. The smooth muscle myosin heavy chain gene exhibits smooth muscle subtype-selective modular regulation in vivo. *J Biol Chem.* 2001 Oct 19; 276(42): 39076-39087.

40. Wamhoff BR, Hoofnagle MH, Burns A, Sinha S, McDonald OG, Owens GK. A G/C element mediates repression of the SM22alpha promoter within phenotypically modulated smooth muscle cells in experimental atherosclerosis. *Circ Res.* 2004 Nov 12; 95(10): 981-988.

41. Miano JM. Serum response factor: Toggling between disparate programs of gene expression. *J Mol Cell Cardiol.* 2003 Jun; 35(6): 577-593.

42. Deaton RA, Gan Q, Owens GK. Sp1-dependent activation of KLF4 is required for PDGF-BB-induced phenotypic modulation of smooth muscle. *Am J Physiol Heart Circ Physiol.* 2009 Apr; 296(4): H1027-37. PMCID: PMC2670704.

43. Liu Y, Sinha S, McDonald OG, Shang Y, Hoofnagle MH, Owens GK. Kruppel-like factor 4 abrogates myocardin-induced activation of smooth muscle gene expression. *J Biol Chem.* 2005 Mar 11; 280(10): 9719-9727.

44. Salmon M, Gomez D, Greene E, Shankman L, Owens GK. Cooperative binding of KLF4, pELK-1, and HDAC2 to a G/C repressor element in the SM22alpha promoter mediates transcriptional silencing during SMC phenotypic switching in vivo. *Circ Res.* 2012 Aug 31; 111(6): 685-696. PMCID: PMC3517884.

45. Turner EC, Huang CL, Govindarajan K, Caplice NM. Identification of a Klf4-dependent upstream repressor region mediating transcriptional regulation of the myocardin gene in human smooth muscle cells. *Biochim Biophys Acta.* 2013 Nov; 1829(11): 1191-1201.

46. Buccheri D, Piraino D, Andolina G, Cortese B. Understanding and managing in-

stent restenosis: A review of clinical data, from pathogenesis to treatment. *J Thorac Dis.* 2016 Oct; 8(10): E1150-E1162.

47. De Jaegere PP, De Feyter PJ, Van der Giessen WJ, Serruys PW. Intracoronary stents: A review of the experience with five different devices in clinical use. *J Interv Cardiol.* 1994 Apr; 7(2): 117-128.

48. Serruys PW, Keane D. Randomized trials of coronary stenting. *J Interv Cardiol.* 1994 Aug; 7(4): 331.

49. Fischman DL, Leon MB, Baim DS, Schatz RA, Savage MP, Penn I, Detre K, Veltri L, Ricci D, Nobuyoshi M. A randomized comparison of coronary-stent placement and balloon angioplasty in the treatment of coronary artery disease. stent restenosis study investigators. *N Engl J Med.* 1994 Aug 25; 331(8): 496-501.

50. Davies MG, Owens EL, Mason DP, Lea H, Tran PK, Vergel S, Hawkins SA, Hart CE, Clowes AW. Effect of platelet-derived growth factor receptor-alpha and -beta blockade on flow-induced neointimal formation in endothelialized baboon vascular grafts. *Circ Res.* 2000 Apr 14; 86(7): 779-786.

51. Fingerle J, Johnson R, Clowes AW, Majesky MW, Reidy MA. Role of platelets in smooth muscle cell proliferation and migration after vascular injury in rat carotid artery. *Proc Natl Acad Sci U S A.* 1989 Nov; 86(21): 8412-8416. PMCID: PMC298292.

52. Sirois MG, Simons M, Edelman ER. Antisense oligonucleotide inhibition of PDGFR-beta receptor subunit expression directs suppression of intimal thickening. *Circulation.* 1997 Feb 4; 95(3): 669-676.

53. Narita N, Heikinheimo M, Bielinska M, White RA, Wilson DB. The gene for transcription factor GATA-6 resides on mouse chromosome 18 and is expressed in myocardium and vascular smooth muscle. *Genomics.* 1996 Sep 1; 36(2): 345-348.

54. Mano T, Luo Z, Malendowicz SL, Evans T, Walsh K. Reversal of GATA-6 downregulation promotes smooth muscle differentiation and inhibits intimal hyperplasia in balloon-injured rat carotid artery. Circ Res. 1999 Apr 2;84(6):647-54. PubMed PMID: 10189352.

55. Paige SL, Plonowska K, Xu A, Wu SM. Molecular regulation of cardiomyocyte differentiation. *Circ Res.* 2015 Jan 16; 116(2): 341-353. PMCID: PMC4299877.

56. Bharathy N, Ling BM, Taneja R. Epigenetic regulation of skeletal muscle development and differentiation. *Subcell Biochem.* 2013; 61: 139-150.

57. Braun T, Gautel M. Transcriptional mechanisms regulating skeletal muscle differentiation, growth and homeostasis. *Nat Rev Mol Cell Biol.* 2011 Jun; 12(6):

349-361.

58. Norman C, Runswick M, Pollock R, Treisman R. Isolation and properties of cDNA clones encoding SRF, a transcription factor that binds to the c-fos serum response element. *Cell.* 1988 Dec 23; 55(6): 989-1003.

59. Shore P, Sharrocks AD. The MADS-box family of transcription factors. *Eur J Biochem.* 1995 Apr 1; 229(1): 1-13.

60. Nurrish SJ, Treisman R. DNA binding specificity determinants in MADS-box transcription factors. *Mol Cell Biol.* 1995 Aug; 15(8): 4076-4085. PMCID: PMC230646.

61. Molkentin JD, Olson EN. Combinatorial control of muscle development by basic helix-loop-helix and MADS-box transcription factors. *Proc Natl Acad Sci U S A.* 1996 Sep 3; 93(18): 9366-9373. PMCID: PMC38433.

62. Arsenian S, Weinhold B, Oelgeschlager M, Ruther U, Nordheim A. Serum response factor is essential for mesoderm formation during mouse embryogenesis. *EMBO J.* 1998 Nov 2; 17(21): 6289-6299. PMCID: PMC1170954.

63. McDonald OG, Wamhoff BR, Hoofnagle MH, Owens GK. Control of SRF binding to CArG box chromatin regulates smooth muscle gene expression in vivo. *J Clin Invest.* 2006 Jan; 116(1): 36-48. PMCID: PMC1323266.

64. Chen CH, Wu ML, Lee YC, Layne MD, Yet SF. Intronic CArG box regulates cysteine-rich protein 2 expression in the adult but not in developing vasculature. *Arterioscler Thromb Vasc Biol.* 2010 Apr; 30(4): 835-842. PMCID: PMC2841712.

65. Chen M, Zhang W, Lu X, Hoggatt AM, Gunst SJ, Kassab GS, Tune JD, Herring BP. Regulation of 130-kDa smooth muscle myosin light chain kinase expression by an intronic CArG element. *J Biol Chem.* 2013 Nov 29; 288(48): 34647-34657. PMCID: PMC3843077.

66. Mack CP, Thompson MM, Lawrenz-Smith S, Owens GK. Smooth muscle alpha-actin CArG elements coordinate formation of a smooth muscle cell-selective, serum response factor-containing activation complex. *Circ Res.* 2000 Feb 4; 86(2): 221-232.

67. Strobeck M, Kim S, Zhang JC, Clendenin C, Du KL, Parmacek MS. Binding of serum response factor to CArG box sequences is necessary but not sufficient to restrict gene expression to arterial smooth muscle cells. *J Biol Chem.* 2001 May 11; 276(19): 16418-16424.

68. Tomasek JJ, McRae J, Owens GK, Haaksma CJ. Regulation of alpha-smooth muscle actin expression in granulation tissue myofibroblasts is dependent on the intronic CArG element and the transforming growth factor-beta1 control

element. *Am J Pathol.* 2005 May; 166(5): 1343-1351. PMCID: PMC1606390.

69. Miano JM, Carlson MJ, Spencer JA, Misra RP. Serum response factor-dependent regulation of the smooth muscle calponin gene. *J Biol Chem.* 2000 Mar 31; 275(13): 9814-9822.

70. Han Y, Slivano OJ, Christie CK, Cheng AW, Miano JM. CRISPR-Cas9 genome editing of a single regulatory element nearly abolishes target gene expression in mice--brief report. *Arterioscler Thromb Vasc Biol.* 2015 Feb; 35(2): 312-315. PMCID: PMC4304932.

71. Du KL, Ip HS, Li J, Chen M, Dandre F, Yu W, Lu MM, Owens GK, Parmacek MS. Myocardin is a critical serum response factor cofactor in the transcriptional program regulating smooth muscle cell differentiation. *Mol Cell Biol.* 2003 Apr; 23(7): 2425-2437. PMCID: PMC150745.

72. Yoshida T, Sinha S, Dandre F, Wamhoff BR, Hoofnagle MH, Kremer BE, Wang DZ, Olson EN, Owens GK. Myocardin is a key regulator of CArG-dependent transcription of multiple smooth muscle marker genes. *Circ Res.* 2003 May 2; 92(8): 856-864.

73. Zaromytidou AI, Miralles F, Treisman R. MAL and ternary complex factor use different mechanisms to contact a common surface on the serum response factor DNA-binding domain. *Mol Cell Biol.* 2006 Jun; 26(11): 4134-4148. PMCID: PMC1489092.

74. Long X, Creemers EE, Wang DZ, Olson EN, Miano JM. Myocardin is a bifunctional switch for smooth versus skeletal muscle differentiation. *Proc Natl Acad Sci U S A.* 2007 Oct 16; 104(42): 16570-16575. PMCID: PMC2034223.

75. Hoofnagle MH, Neppl RL, Berzin EL, Teg Pipes GC, Olson EN, Wamhoff BW, Somlyo AV, Owens GK. Myocardin is differentially required for the development of smooth muscle cells and cardiomyocytes. *Am J Physiol Heart Circ Physiol.* 2011 May; 300(5): H1707-21. PMCID: PMC3094091.

76. Yoshida T, Kawai-Kowase K, Owens GK. Forced expression of myocardin is not sufficient for induction of smooth muscle differentiation in multipotential embryonic cells. Arterioscler Thromb Vasc Biol. 2004 Sep;24(9):1596-601. PubMed PMID: 15231515.

77. Han Z, Li X, Wu J, Olson EN. A myocardin-related transcription factor regulates activity of serum response factor in drosophila. *Proc Natl Acad Sci U S A.* 2004 Aug 24; 101(34): 12567-12572. PMCID: PMC515097.

78. Cen B, Selvaraj A, Prywes R. Myocardin/MKL family of SRF coactivators: Key regulators of immediate early and muscle specific gene expression. *J Cell Biochem.* 2004 Sep 1; 93(1): 74-82.

79. Wang DZ, Olson EN. Control of smooth muscle development by the myocardin

family of transcriptional coactivators. *Curr Opin Genet Dev.* 2004 Oct; 14(5): 558-566.

80. Li S, Wang DZ, Wang Z, Richardson JA, Olson EN. The serum response factor coactivator myocardin is required for vascular smooth muscle development. *Proc Natl Acad Sci U S A.* 2003 Aug 5; 100(16): 9366-9370. PMCID: PMC170924.

81. Huang J, Wang T, Wright AC, Yang J, Zhou S, Li L, Yang J, Small A, Parmacek MS. Myocardin is required for maintenance of vascular and visceral smooth muscle homeostasis during postnatal development. *Proc Natl Acad Sci U S A.* 2015 Apr 7; 112(14): 4447-4452. PMCID: PMC4394251.

82.   Wei K, Che N, Chen F. Myocardin-related transcription factor B is required for normal mouse vascular development and smooth muscle gene expression. *Dev Dyn.* 2007 Feb; 236(2): 416-425.

83. Li S, Chang S, Qi X, Richardson JA, Olson EN. Requirement of a myocardin-related transcription factor for development of mammary myoepithelial cells. *Mol Cell Biol.* 2006 Aug; 26(15): 5797-5808. PMCID: PMC1592772.

84. Narumiya S. The small GTPase rho: Cellular functions and signal transduction. *J Biochem.* 1996 Aug; 120(2): 215-228.

85. Zuo Y, Oh W, Frost JA. Controlling the switches: Rho GTPase regulation during animal cell mitosis. *Cell Signal.* 2014 Dec; 26(12): 2998-3006. PMCID: PMC4293258.

86. Ridley AJ. Rho GTPase signalling in cell migration. *Curr Opin Cell Biol.* 2015 Oct; 36: 103-112. PMCID: PMC4728192.

87. Burridge K, Wennerberg K. Rho and rac take center stage. *Cell.* 2004 Jan 23; 116(2): 167-179.

88. Sadok A, Marshall CJ. Rho GTPases: Masters of cell migration. *Small GTPases.* 2014; 5: e29710. PMCID: PMC4107589.

89. Fritz RD, Pertz O. The dynamics of spatio-temporal rho GTPase signaling: Formation of signaling patterns. *F1000Res.* 2016 Apr 26; 5: 10.12688/f1000research.7370.1. eCollection 2016. PMCID: PMC4847568.

90. Garcia-Mata R, Boulter E, Burridge K. The 'invisible hand': Regulation of RHO GTPases by RHOGDIs. *Nat Rev Mol Cell Biol.* 2011 Jul 22; 12(8): 493-504. PMCID: PMC3260518.

91. Cook DR, Rossman KL, Der CJ. Rho guanine nucleotide exchange factors: Regulators of rho GTPase activity in development and disease. *Oncogene.* 2014 Jul 31; 33(31): 4021-4035. PMCID: PMC4875565.

92. Donnelly SK, Bravo-Cordero JJ, Hodgson L. Rho GTPase isoforms in cell motility: Don't fret, we have FRET. *Cell Adh Migr.* 2014; 8(6): 526-534. PMCID: PMC4594258.

93. Goicoechea SM, Awadia S, Garcia-Mata R. I'm coming to GEF you: Regulation of RhoGEFs during cell migration. *Cell Adh Migr.* 2014; 8(6): 535-549. PMCID: PMC4594598.

94. Etienne-Manneville S, Hall A. Rho GTPases in cell biology. *Nature.* 2002 Dec 12; 420(6916): 629-635.

95. Mack CP, Somlyo AV, Hautmann M, Somlyo AP, Owens GK. Smooth muscle differentiation marker gene expression is regulated by RhoA-mediated actin polymerization. *J Biol Chem.* 2001 Jan 5; 276(1): 341-347.

96. Esnault C, Stewart A, Gualdrini F, East P, Horswell S, Matthews N, Treisman R. Rho-actin signaling to the MRTF coactivators dominates the immediate transcriptional response to serum in fibroblasts. *Genes Dev.* 2014 May 1; 28(9): 943-958. PMCID: PMC4018493.

97. Lockman K, Hinson JS, Medlin MD, Morris D, Taylor JM, Mack CP. Sphingosine 1-phosphate stimulates smooth muscle cell differentiation and proliferation by activating separate serum response factor co-factors. *J Biol Chem.* 2004 Oct 8; 279(41): 42422-42430.

98. Mouilleron S, Langer CA, Guettler S, McDonald NQ, Treisman R. Structure of a pentavalent G-actin*MRTF-A complex reveals how G-actin controls nucleocytoplasmic shuttling of a transcriptional coactivator. *Sci Signal.* 2011 Jun 14; 4(177): ra40.

99. Pawlowski R, Rajakyla EK, Vartiainen MK, Treisman R. An actin-regulated importin alpha/beta-dependent extended bipartite NLS directs nuclear import of MRTF-A. *EMBO J.* 2010 Oct 20; 29(20): 3448-3458. PMCID: PMC2964165.

100. Hinson JS, Medlin MD, Lockman K, Taylor JM, Mack CP. Smooth muscle cell-specific transcription is regulated by nuclear localization of the myocardin-related transcription factors. *Am J Physiol Heart Circ Physiol.* 2007 Feb; 292(2): H1170-80.

101. Verbakel W, Carmeliet G, Engelborghs Y. SAP-like domain in nucleolar spindle associated protein mediates mitotic chromosome loading as well as interphase chromatin interaction. *Biochem Biophys Res Commun.* 2011 Aug 12; 411(4): 732-737.

102. Wang DZ, Li S, Hockemeyer D, Sutherland L, Wang Z, Schratt G, Richardson JA, Nordheim A, Olson EN. Potentiation of serum response factor activity by a family of myocardin-related transcription factors. *Proc Natl Acad Sci U S A.*

2002 Nov 12; 99(23): 14855-14860. PMCID: PMC137508.

103. Medlin MD, Staus DP, Dubash AD, Taylor JM, Mack CP. Sphingosine 1-phosphate receptor 2 signals through leukemia-associated RhoGEF (LARG), to promote smooth muscle cell differentiation. *Arterioscler Thromb Vasc Biol.* 2010 Sep; 30(9): 1779-1786. PMCID: PMC2930832.

104. Wirth A, Benyo Z, Lukasova M, Leutgeb B, Wettschureck N, Gorbey S, Orsy P, Horvath B, Maser-Gluth C, Greiner E, Lemmer B, Schutz G, Gutkind JS, Offermanns S. G12-G13-LARG-mediated signaling in vascular smooth muscle is required for salt-induced hypertension. *Nat Med.* 2008 Jan; 14(1): 64-68.

105. Mikelis CM, Palmby TR, Simaan M, Li W, Szabo R, Lyons R, Martin D, Yagi H, Fukuhara S, Chikumi H, Galisteo R, Mukouyama YS, Bugge TH, Gutkind JS. PDZ-RhoGEF and LARG are essential for embryonic development and provide a link between thrombin and LPA receptors and rho activation. *J Biol Chem.* 2013 Apr 26; 288(17): 12232-12243. PMCID: PMC3636907.

106. Staus DP, Blaker AL, Taylor JM, Mack CP. Diaphanous 1 and 2 regulate smooth muscle cell differentiation by activating the myocardin-related transcription factors. *Arterioscler Thromb Vasc Biol.* 2007 Mar; 27(3): 478-486.

107. Weise-Cross L, Taylor JM, Mack CP. Inhibition of diaphanous formin signaling in vivo impairs cardiovascular development and alters smooth muscle cell phenotype. *Arterioscler Thromb Vasc Biol.* 2015 Nov; 35(11): 2374-2383.

108. Staus DP, Weise-Cross L, Mangum KD, Medlin MD, Mangiante L, Taylor JM, Mack CP. Nuclear RhoA signaling regulates MRTF-dependent SMC-specific transcription. *Am J Physiol Heart Circ Physiol.* 2014 Aug 1; 307(3): H379-90. PMCID: PMC4121646.

109. Sims RJ,3rd, Reinberg D. Is there a code embedded in proteins that is based on post-translational modifications? *Nat Rev Mol Cell Biol.* 2008 Oct; 9(10): 815-820.

110. Cao D, Wang C, Tang R, Chen H, Zhang Z, Tatsuguchi M, Wang DZ. Acetylation of myocardin is required for the activation of cardiac and smooth muscle genes. *J Biol Chem.* 2012 Nov 9; 287(46): 38495-38504. PMCID: PMC3493894.

111. Cao D, Wang Z, Zhang CL, Oh J, Xing W, Li S, Richardson JA, Wang DZ, Olson EN. Modulation of smooth muscle gene expression by association of histone acetyltransferases and deacetylases with myocardin. *Mol Cell Biol.* 2005 Jan; 25(1): 364-376. PMCID: PMC538763.

112. Taurin S, Sandbo N, Yau DM, Sethakorn N, Kach J, Dulin NO. Phosphorylation of myocardin by extracellular signal-regulated kinase. *J Biol Chem.* 2009 Dec 4; 284(49): 33789-33794. PMCID: PMC2797148.

113. Li W, Wang N, Li M, Gong H, Liao X, Yang X, Zhang T. Protein kinase calpha inhibits myocardin-induced cardiomyocyte hypertrophy through the promotion of myocardin phosphorylation. *Acta Biochim Biophys Sin (Shanghai).* 2015 Sep; 47(9): 687-695.

114. Blaker AL, Taylor JM, Mack CP. PKA-dependent phosphorylation of serum response factor inhibits smooth muscle-specific gene expression. *Arterioscler Thromb Vasc Biol.* 2009 Dec; 29(12): 2153-2160. PMCID: PMC2783385.

115. Muehlich S, Wang R, Lee SM, Lewis TC, Dai C, Prywes R. Serum-induced phosphorylation of the serum response factor coactivator MKL1 by the extracellular signal-regulated kinase 1/2 pathway inhibits its nuclear localization. *Mol Cell Biol.* 2008 Oct; 28(20): 6302-6313. . PMCID: PMC2577419.

116. Panayiotou R, Miralles F, Pawlowski R, Diring J, Flynn HR, Skehel M, Treisman R. Phosphorylation acts positively and negatively to regulate MRTF-A subcellular localisation and activity. *Elife.* 2016 Jun 15; 5: 10.7554/eLife.15460. PMCID: PMC4963197.

117. Nakagawa K, Kuzumaki N. Transcriptional activity of megakaryoblastic leukemia 1 (MKL1) is repressed by SUMO modification. *Genes Cells.* 2005 Aug; 10(8): 835-850.

118. Wang J, Li A, Wang Z, Feng X, Olson EN, Schwartz RJ. Myocardin sumoylation transactivates cardiogenic genes in pluripotent 10T1/2 fibroblasts. *Mol Cell Biol.* 2007 Jan; 27(2): 622-632. PMCID: PMC1800801.

119. Castel D, Mourikis P, Bartels SJ, Brinkman AB, Tajbakhsh S, Stunnenberg HG. Dynamic binding of RBPJ is determined by notch signaling status. *Genes Dev.* 2013 May 1; 27(9): 1059-1071. PMCID: PMC3656323.

120. Rozenberg JM, Tesfu DB, Musunuri S, Taylor JM, Mack CP. DNA methylation of a GC repressor element in the smooth muscle myosin heavy chain promoter facilitates binding of the notch-associated transcription factor, RBPJ/CSL1. *Arterioscler Thromb Vasc Biol.* 2014 Dec; 34(12): 2624-2631. PMCID: PMC4239181.

121. Noseda M, Fu Y, Niessen K, Wong F, Chang L, McLean G, Karsan A. Smooth muscle alpha-actin is a direct target of Notch/CSL. *Circ Res.* 2006 Jun 23; 98(12): 1468-1470.

122. Gridley T. Notch signaling in vascular development and physiology. *Development.* 2007 Aug; 134(15): 2709-2718.

123. Krebs LT, Norton CR, Gridley T. Notch signal reception is required in vascular smooth muscle cells for ductus arteriosus closure. *Genesis.* 2016 Feb; 54(2):

86-90.

124. Lawson ND, Scheer N, Pham VN, Kim CH, Chitnis AB, Campos-Ortega JA, Weinstein BM. Notch signaling is required for arterial-venous differentiation during embryonic vascular development. *Development.* 2001 Oct; 128(19): 3675-3683.

125. Quillien A, Moore JC, Shin M, Siekmann AF, Smith T, Pan L, Moens CB, Parsons MJ, Lawson ND. Distinct notch signaling outputs pattern the developing arterial system. *Development.* 2014 Apr; 141(7): 1544-1552. PMCID: PMC4074308.

126. Wang T, Baron M, Trump D. An overview of Notch3 function in vascular smooth muscle cells. *Prog Biophys Mol Biol.* 2008 Jan-Apr; 96(1-3): 499-509.

127. Henshall TL, Keller A, He L, Johansson BR, Wallgard E, Raschperger E, Mae MA, Jin S, Betsholtz C, Lendahl U. Notch3 is necessary for blood vessel integrity in the central nervous system. *Arterioscler Thromb Vasc Biol.* 2015 Feb; 35(2): 409-420.

128. Buczek J, Blazejewska-Hyzorek B, Cudna A, Lusawa M, Lewandowska E, Kurkowska-Jastrzebska I, Czlonkowska A. Novel mutation of the NOTCH3 gene in a polish family with CADASIL. *Neurol Neurochir Pol.* 2016 Jul-Aug; 50(4): 262-264.

129. Morrow D, Guha S, Sweeney C, Birney Y, Walshe T, O'Brien C, Walls D, Redmond EM, Cahill PA. Notch and vascular smooth muscle cell phenotype. *Circ Res.* 2008 Dec 5; 103(12): 1370-1382.

130. Fouillade C, Monet-Lepretre M, Baron-Menguy C, Joutel A. Notch signalling in smooth muscle cells during development and disease. *Cardiovasc Res.* 2012 Jul 15; 95(2): 138-146.

131. Doi H, Iso T, Sato H, Yamazaki M, Matsui H, Tanaka T, Manabe I, Arai M, Nagai R, Kurabayashi M. Jagged1-selective notch signaling induces smooth muscle differentiation via a RBP-Jkappa-dependent pathway. J Biol Chem. 2006 Sep 29;281(39):28555-64. PubMed PMID: 16867989.

132. Doi H, Iso T, Yamazaki M, Akiyama H, Kanai H, Sato H, Kawai-Kowase K, Tanaka T, Maeno T, Okamoto E, Arai M, Kedes L, Kurabayashi M. HERP1 inhibits myocardin-induced vascular smooth muscle cell differentiation by interfering with SRF binding to CArG box. *Arterioscler Thromb Vasc Biol.* 2005 Nov; 25(11): 2328-2334.

133. Iso T, Chung G, Hamamori Y, Kedes L. HERP1 is a cell type-specific primary target of notch. *J Biol Chem.* 2002 Feb 22; 277(8): 6598-6607.

134. Meng Z, Moroishi T, Guan KL. Mechanisms of hippo pathway regulation.

Genes Dev. 2016 Jan 1; 30(1): 1-17. PMCID: PMC4701972.

135. Wackerhage H, Del Re DP, Judson RN, Sudol M, Sadoshima J. The hippo signal transduction network in skeletal and cardiac muscle. *Sci Signal.* 2014 Aug 5; 7(337): re4.

136. Zhao B, Lei QY, Guan KL. The hippo-YAP pathway: New connections between regulation of organ size and cancer. *Curr Opin Cell Biol.* 2008 Dec; 20(6): 638-646. PMCID: PMC3296452.

137. Zhou Y, Huang T, Cheng AS, Yu J, Kang W, To KF. The TEAD family and its oncogenic role in promoting tumorigenesis. *Int J Mol Sci.* 2016 Jan 21; 17(1): 10.3390/ijms17010138. PMCID: PMC4730377.

138. Jin Y, Messmer-Blust AF, Li J. The role of transcription enhancer factors in cardiovascular biology. *Trends Cardiovasc Med.* 2011 Jan; 21(1): 1-5. PMCID: PMC3326381.

139. Liu F, Wang X, Hu G, Wang Y, Zhou J. The transcription factor TEAD1 represses smooth muscle-specific gene expression by abolishing myocardin function. *J Biol Chem.* 2014 Feb 7; 289(6): 3308-3316. PMCID: PMC3916534.

140. Pasquet S, Naye F, Faucheux C, Bronchain O, Chesneau A, Thiebaud P, Theze N. Transcription enhancer factor-1-dependent expression of the alpha-tropomyosin gene in the three muscle cell types. *J Biol Chem.* 2006 Nov 10; 281(45): 34406-34420.

141. Farrance IK, Mar JH, Ordahl CP. M-CAT binding factor is related to the SV40 enhancer binding factor, TEAD1. *J Biol Chem.* 1992 Aug 25; 267(24): 17234-17240.

142. Swartz EA, Johnson AD, Owens GK. Two MCAT elements of the SM alpha-actin promoter function differentially in SM vs. non-SM cells. *Am J Physiol.* 1998 Aug; 275(2 Pt 1): C608-18.

143. Gan Q, Yoshida T, Li J, Owens GK. Smooth muscle cells and myofibroblasts use distinct transcriptional mechanisms for smooth muscle alpha-actin expression. Circ Res. 2007 Oct 26;101(9):883-92. PubMed PMID: 17823374.

144. Gupta M, Kogut P, Davis FJ, Belaguli NS, Schwartz RJ, Gupta MP. Physical interaction between the MADS box of serum response factor and the TEA/ATTS DNA-binding domain of transcription enhancer factor-1. *J Biol Chem.* 2001 Mar 30; 276(13): 10413-10422.

145. Maeda T, Gupta MP, Stewart AF. TEAD1 and MEF2 transcription factors interact to regulate muscle-specific promoters. *Biochem Biophys Res Commun.* 2002 Jun 21; 294(4): 791-797.

146. Karasseva N, Tsika G, Ji J, Zhang A, Mao X, Tsika R. Transcription enhancer factor 1 binds multiple muscle MEF2 and A/T-rich elements during fast-to-slow skeletal muscle fiber type transitions. Mol Cell Biol. 2003 Aug;23(15):5143-64. PubMed PMID: 12861002; PubMed Central PMCID: PMC165722.

147. Nishida W, Nakamura M, Mori S, Takahashi M, Ohkawa Y, Tadokoro S, Yoshida K, Hiwada K, Hayashi K, Sobue K. A triad of serum response factor and the GATA and NK families governs the transcription of smooth and cardiac muscle genes. *J Biol Chem.* 2002 Mar 1; 277(9): 7308-7317.

148. Lepore JJ, Cappola TP, Mericko PA, Morrisey EE, Parmacek MS. GATA-6 regulates genes promoting synthetic functions in vascular smooth muscle cells. *Arterioscler Thromb Vasc Biol.* 2005 Feb; 25(2): 309-314.

149. Yin F, Herring BP. GATA-6 can act as a positive or negative regulator of smooth muscle-specific gene expression. *J Biol Chem.* 2005 Feb 11; 280(6): 4745-4752.

150. Jiang Y, Drysdale TA, Evans T. A role for GATA-4/5/6 in the regulation of Nkx2.5 expression with implications for patterning of the precardiac field. Dev Biol. 1999 Dec 1;216(1):57-71. PubMed PMID: 10588863.

151. Lien SC, Usami S, Chien S, Chiu JJ. Phosphatidylinositol 3-kinase/Akt pathway is involved in transforming growth factor-beta1-induced phenotypic modulation of 10T1/2 cells to smooth muscle cells. *Cell Signal.* 2006 Aug; 18(8): 1270-1278.

152. Molin DG, Poelmann RE, DeRuiter MC, Azhar M, Doetschman T, Gittenberger-de Groot AC. Transforming growth factor beta-SMAD2 signaling regulates aortic arch innervation and development. *Circ Res.* 2004 Nov 26; 95(11): 1109-1117.

153. Carvalho RL, Itoh F, Goumans MJ, Lebrin F, Kato M, Takahashi S, Ema M, Itoh S, van Rooijen M, Bertolino P, Ten Dijke P, Mummery CL. Compensatory signalling induced in the yolk sac vasculature by deletion of TGFbeta receptors in mice. *J Cell Sci.* 2007 Dec 15; 120(Pt 24): 4269-4277.

154. Gillis E, Van Laer L, Loeys BL. Genetics of thoracic aortic aneurysm: At the crossroad of transforming growth factor-beta signaling and vascular smooth muscle cell contractility. *Circ Res.* 2013 Jul 19; 113(3): 327-340.

155. Hu JH, Wei H, Jaffe M, Airhart N, Du L, Angelov SN, Yan J, Allen JK, Kang I, Wight TN, Fox K, Smith A, Enstrom R, Dichek DA. Postnatal deletion of the type II transforming growth factor-beta receptor in smooth muscle cells causes severe aortopathy in mice. *Arterioscler Thromb Vasc Biol.* 2015 Dec; 35(12): 2647-2656. PMCID: PMC4743752.

156. Jones JA, Spinale FG, Ikonomidis JS. Transforming growth factor-beta

signaling in thoracic aortic aneurysm development: A paradox in pathogenesis. *J Vasc Res.* 2009; 46(2): 119-137. PMCID: PMC2645475.

157. Pezzini A, Del Zotto E, Giossi A, Volonghi I, Costa P, Padovani A. Transforming growth factor beta signaling perturbation in the loeys-dietz syndrome. *Curr Med Chem.* 2012; 19(3): 454-460.

158. Wang Y, Krishna S, Walker PJ, Norman P, Golledge J. Transforming growth factor-beta and abdominal aortic aneurysms. *Cardiovasc Pathol.* 2013 Mar-Apr; 22(2): 126-132.

159. Loeys BL, Dietz HC. Loeys-dietz syndrome. In: Pagon RA, Adam MP, Ardinger HH, Wallace SE, Amemiya A, Bean LJH, Bird TD, Ledbetter N, Mefford HC, Smith RJH, Stephens K, editors. GeneReviews(R). Seattle (WA): University of Washington, Seattle. GeneReviews is a registered trademark of the University of Washington, Seattle. All rights reserved; 1993.

160. Ailawadi G, Moehle CW, Pei H, Walton SP, Yang Z, Kron IL, Lau CL, Owens GK. Smooth muscle phenotypic modulation is an early event in aortic aneurysms. *J Thorac Cardiovasc Surg.* 2009 Dec; 138(6): 1392-1399. PMCID: PMC2956879.

161. Nishimura G, Manabe I, Tsushima K, Fujiu K, Oishi Y, Imai Y, Maemura K, Miyagishi M, Higashi Y, Kondoh H, Nagai R. DeltaEF1 mediates TGF-beta signaling in vascular smooth muscle cell differentiation. *Dev Cell.* 2006 Jul; 11(1): 93-104.

162. Sinha S, Hoofnagle MH, Kingston PA, McCanna ME, Owens GK. Transforming growth factor-beta1 signaling contributes to development of smooth muscle cells from embryonic stem cells. *Am J Physiol Cell Physiol.* 2004 Dec; 287(6): C1560-8.

163. Hautmann MB, Madsen CS, Owens GK. A transforming growth factor beta (TGFbeta) control element drives TGFbeta-induced stimulation of smooth muscle alpha-actin gene expression in concert with two CArG elements. *J Biol Chem.* 1997 Apr 18; 272(16): 10948-10956.

164. Hirschi KK, Lai L, Belaguli NS, Dean DA, Schwartz RJ, Zimmer WE. Transforming growth factor-beta induction of smooth muscle cell phenotpye requires transcriptional and post-transcriptional control of serum response factor. *J Biol Chem.* 2002 Feb 22; 277(8): 6287-6295. PMCID: PMC4421896.

165. Liu Y, Sinha S, Owens G. A transforming growth factor-beta control element required for SM alpha-actin expression in vivo also partially mediates GKLF-dependent transcriptional repression. *J Biol Chem.* 2003 Nov 28; 278(48): 48004-48011.

166. Lee J, Moon HJ, Lee JM, Joo CK. Smad3 regulates rho signaling via NET1 in

the transforming growth factor-β-induced epithelial-mesenchymal transition of human retinal pigment epithelial cells*. *J Biol Chem.* 2010 Aug 20; 285(34): 26618-26627. PMCID: PMC2924101.

167. Tsapara A, Luthert P, Greenwood J, Hill CS, Matter K, Balda MS. The RhoA activator GEF-H1/Lfc is a transforming growth factor-beta target gene and effector that regulates alpha-smooth muscle actin expression and cell migration. *Mol Biol Cell.* 2010 Mar 15; 21(6): 860-870. PMCID: PMC2836967.

168. Morla AO, Mogford JE. Control of smooth muscle cell proliferation and phenotype by integrin signaling through focal adhesion kinase. *Biochem Biophys Res Commun.* 2000 May 27; 272(1): 298-302.

169. Roy J, Tran PK, Religa P, Kazi M, Henderson B, Lundmark K, Hedin U. Fibronectin promotes cell cycle entry in smooth muscle cells in primary culture. *Exp Cell Res.* 2002 Feb 15; 273(2): 169-177.

170. Turner CJ, Badu-Nkansah K, Crowley D, van der Flier A, Hynes RO. Alpha5 and alphav integrins cooperate to regulate vascular smooth muscle and neural crest functions in vivo. *Development.* 2015 Feb 15; 142(4): 797-808.

171. Wu Y, Huang Y, Herring BP, Gunst SJ. Integrin-linked kinase regulates smooth muscle differentiation marker gene expression in airway tissue. *Am J Physiol Lung Cell Mol Physiol.* 2008 Dec; 295(6): L988-97. PMCID: PMC2604790.

172. Thyberg J, Hultgardh-Nilsson A. Fibronectin and the basement membrane components laminin and collagen type IV influence the phenotypic properties of subcultured rat aortic smooth muscle cells differently. *Cell Tissue Res.* 1994 May; 276(2): 263-271.

173. Thyberg J. Phenotypic modulation of smooth muscle cells during formation of neointimal thickenings following vascular injury. *Histol Histopathol.* 1998 Jul; 13(3): 871-891.

174. Thyberg J, Blomgren K, Roy J, Tran PK, Hedin U. Phenotypic modulation of smooth muscle cells after arterial injury is associated with changes in the distribution of laminin and fibronectin. *J Histochem Cytochem.* 1997 Jun; 45(6): 837-846.

175. Taylor JM, Mack CP, Nolan K, Regan CP, Owens GK, Parsons JT. Selective expression of an endogenous inhibitor of FAK regulates proliferation and migration of vascular smooth muscle cells. *Mol Cell Biol.* 2001 Mar; 21(5): 1565-1572. PMCID: PMC86702.

176. Orr AW, Lee MY, Lemmon JA, Yurdagul A Jr, Gomez MF, Bortz PD, Wamhoff BR. Molecular mechanisms of collagen isotype-specific modulation of smooth muscle cell phenotype. Arterioscler Thromb Vasc Biol. 2009 Feb;29(2):225-31. doi: 10.1161/ATVBAHA.108.178749. Epub 2008 Nov 20. PubMed PMID:

19023090; PubMed Central PMCID: PMC2692987.

177. Tamura K, Chen YE, Lopez-Ilasaca M, Daviet L, Tamura N, Ishigami T, Akishita M, Takasaki I, Tokita Y, Pratt RE, Horiuchi M, Dzau VJ, Umemura S. Molecular mechanism of fibronectin gene activation by cyclic stretch in vascular smooth muscle cells. *J Biol Chem.* 2000 Nov 3; 275(44): 34619-34627.

178. Haga JH, Li YS, Chien S. Molecular basis of the effects of mechanical stretch on vascular smooth muscle cells. *J Biomech.* 2007; 40(5): 947-960.

179. Lemarie CA, Tharaux PL, Lehoux S. Extracellular matrix alterations in hypertensive vascular remodeling. *J Mol Cell Cardiol.* 2010 Mar; 48(3): 433-439.

180. Zeidan A, Nordstrom I, Albinsson S, Malmqvist U, Sward K, Hellstrand P. Stretch-induced contractile differentiation of vascular smooth muscle: Sensitivity to actin polymerization inhibitors. *Am J Physiol Cell Physiol.* 2003 Jun; 284(6): C1387-96.

181. Albinsson S, Hellstrand P. Integration of signal pathways for stretch-dependent growth and differentiation in vascular smooth muscle. *Am J Physiol Cell Physiol.* 2007 Aug; 293(2): C772-82.

182. Xu B, Song G, Ju Y, Li X, Song Y, Watanabe S. RhoA/ROCK, cytoskeletal dynamics, and focal adhesion kinase are required for mechanical stretch-induced tenogenic differentiation of human mesenchymal stem cells. *J Cell Physiol.* 2012 Jun; 227(6): 2722-2729.

183. Berger SL. The complex language of chromatin regulation during transcription. *Nature.* 2007 May 24; 447(7143): 407-412.

184. Alam H, Gu B, Lee MG. Histone methylation modifiers in cellular signaling pathways. *Cell Mol Life Sci.* 2015 Dec; 72(23): 4577-4592. PMCID: PMC4628846.

185. Spin JM, Maegdefessel L, Tsao PS. Vascular smooth muscle cell phenotypic plasticity: Focus on chromatin remodelling. *Cardiovasc Res.* 2012 Jul 15; 95(2): 147-155. PMCID: PMC3388815.

186. Binda O. On your histone mark, SET, methylate! *Epigenetics.* 2013 May 01; 8(5): 457-463. PMCID: PMC3741215.

187. Xu S, Zhong C, Zhang T, Ding J. Structure of human lysine methyltransferase Smyd2 reveals insights into the substrate divergence in smyd proteins. *J Mol Cell Biol.* 2011 Oct; 3(5): 293-300.

188. Lockman K, Taylor JM, Mack CP. The histone demethylase, Jmjd1a, interacts with the myocardin factors to regulate SMC differentiation marker gene

expression. *Circ Res.* 2007 Dec 7; 101(12): e115-23.

189. Sasaki K, Doi S, Nakashima A, Irifuku T, Yamada K, Kokoroishi K, Ueno T, Doi T, Hida E, Arihiro K, Kohno N, Masaki T. Inhibition of SET domain-containing lysine methyltransferase 7/9 ameliorates renal fibrosis. *J Am Soc Nephrol.* 2016 Jan; 27(1): 203-215. PMCID: PMC4696564.

190. Irifuku T, Doi S, Sasaki K, Doi T, Nakashima A, Ueno T, Yamada K, Arihiro K, Kohno N, Masaki T. Inhibition of H3K9 histone methyltransferase G9a attenuates renal fibrosis and retains klotho expression. *Kidney Int.* 2016 Jan; 89(1): 147-157.

191. Tuano NK, Okabe J, Ziemann M, Cooper ME, El-Osta A. Set7 mediated interactions regulate transcriptional networks in embryonic stem cells. *Nucleic Acids Res.* 2016 Nov 2; 44(19): 9206-9217. PMCID: PMC5100561.

192. Zhang W, Wu X, Shi T, Xu H, Yi J, Shen H, Huang M, Shu X, Wang F, Peng B, Xiao R, Gao W, Ding J, Liu W. Regulation of transcription factor yin yang 1 by SET7/9-mediated lysine methylation. *Sci Rep.* 2016 Feb 23; 6: 10.1038/srep21718. PMCID: PMC4763200.

193. Zhang M, Fang H, Zhou J, Herring BP. A novel role of Brg1 in the regulation of SRF/MRTFA-dependent smooth muscle-specific gene expression. *J Biol Chem.* 2007 Aug 31; 282(35): 25708-25716.

194. Zhou J, Zhang M, Fang H, El-Mounayri O, Rodenberg JM, Imbalzano AN, Herring BP. The SWI/SNF chromatin remodeling complex regulates myocardin-induced smooth muscle-specific gene expression. *Arterioscler Thromb Vasc Biol.* 2009 Jun; 29(6): 921-928. PMCID: PMC2730881.

195. Liu R, Leslie KL, Martin KA. Epigenetic regulation of smooth muscle cell plasticity. *Biochim Biophys Acta.* 2015 Apr; 1849(4): 448-453. PMCID: PMC4552189.

196. Li Y, Yu XY. Letter by li and yu regarding article, "ten-eleven translocation-2 (TET2) is a master regulator of smooth muscle cell plasticity". *Circulation.* 2014 Aug 19; 130(8): e71.

197. Liu R, Jin Y, Tang WH, Qin L, Zhang X, Tellides G, Hwa J, Yu J, Martin KA. Ten-eleven translocation-2 (TET2) is a master regulator of smooth muscle cell plasticity. *Circulation.* 2013 Oct 29; 128(18): 2047-2057. PMCID: PMC3899790.

198. Thurman RE, Rynes E, Humbert R, Vierstra J, Maurano MT, Haugen E, Sheffield NC, Stergachis AB, Wang H, Vernot B, Garg K, John S, Sandstrom R, Bates D, Boatman L, Canfield TK, Diegel M, Dunn D, Ebersol AK, Frum T, Giste E, Johnson AK, Johnson EM, Kutyavin T, Lajoie B, Lee BK, Lee K, London D, Lotakis D, Neph S, Neri F, Nguyen ED, Qu H, Reynolds AP, Roach V, Safi A, Sanchez ME, Sanyal A, Shafer A, Simon JM, Song L, Vong S,

Weaver M, Yan Y, Zhang Z, Zhang Z, Lenhard B, Tewari M, Dorschner MO, Hansen RS, Navas PA, Stamatoyannopoulos G, Iyer VR, Lieb JD, Sunyaev SR, Akey JM, Sabo PJ, Kaul R, Furey TS, Dekker J, Crawford GE, Stamatoyannopoulos JA. The accessible chromatin landscape of the human genome. *Nature.* 2012 Sep 6; 489(7414): 75-82. PMCID: PMC3721348.

199. Winter DR, Song L, Mukherjee S, Furey TS, Crawford GE. DNase-seq predicts regions of rotational nucleosome stability across diverse human cell types. *Genome Res.* 2013 Jul; 23(7): 1118-1129. PMCID: PMC3698505.

200. Furey TS. ChIP-seq and beyond: New and improved methodologies to detect and characterize protein-DNA interactions. *Nat Rev Genet.* 2012 Dec; 13(12): 840-852. PMCID: PMC3591838.

201. Pennisi E. Human genome is much more than just genes. Science Mag. News Article. 2012 Sep; http://www.sciencemag.org/news/2012/09/human-genome-much-more-just-genes. Accessed Feb 10, 2017.

202. Derrien T, Johnson R, Bussotti G, Tanzer A, Djebali S, Tilgner H, Guernec G, Martin D, Merkel A, Knowles DG, Lagarde J, Veeravalli L, Ruan X, Ruan Y, Lassmann T, Carninci P, Brown JB, Lipovich L, Gonzalez JM, Thomas M, Davis CA, Shiekhattar R, Gingeras TR, Hubbard TJ, Notredame C, Harrow J, Guigo R. The GENCODE v7 catalog of human long noncoding RNAs: Analysis of their gene structure, evolution, and expression. *Genome Res.* 2012 Sep; 22(9): 1775-1789. PMCID: PMC3431493.

203. Guttman M, Donaghey J, Carey BW, Garber M, Grenier JK, Munson G, Young G, Lucas AB, Ach R, Bruhn L, Yang X, Amit I, Meissner A, Regev A, Rinn JL, Root DE, Lander ES. lincRNAs act in the circuitry controlling pluripotency and differentiation. *Nature.* 2011 Aug 28; 477(7364): 295-300. PMCID: PMC3175327.

204. Li J, Tian H, Yang J, Gong Z. Long noncoding RNAs regulate cell growth, proliferation, and apoptosis. *DNA Cell Biol.* 2016 Sep; 35(9): 459-470.

205. Neppl RL, Wang DZ. Smooth(ing) muscle differentiation by microRNAs. *Cell Stem Cell.* 2009 Aug 7; 5(2): 130-132. PMCID: PMC4285345.

206. Davis BN, Hilyard AC, Nguyen PH, Lagna G, Hata A. Induction of microRNA-221 by platelet-derived growth factor signaling is critical for modulation of vascular smooth muscle phenotype. *J Biol Chem.* 2009 Feb 6; 284(6): 3728-3738. PMCID: PMC2635044.

207. Bazan HA, Hatfield SA, O'Malley CB, Brooks AJ, Lightell D,Jr, Woods TC. Acute loss of miR-221 and miR-222 in the atherosclerotic plaque shoulder accompanies plaque rupture. *Stroke.* 2015 Nov; 46(11): 3285-3287. PMCID: PMC4624519.

208. Liu X, Cheng Y, Zhang S, Lin Y, Yang J, Zhang C. A necessary role of miR-221 and miR-222 in vascular smooth muscle cell proliferation and neointimal hyperplasia. *Circ Res.* 2009 Feb 27; 104(4): 476-487. PMCID: PMC2728290.

209. Rangrez AY, Massy ZA, Metzinger-Le Meuth V, Metzinger L. miR-143 and miR-145: Molecular keys to switch the phenotype of vascular smooth muscle cells. *Circ Cardiovasc Genet.* 2011 Apr; 4(2): 197-205.

210. Boettger T, Beetz N, Kostin S, Schneider J, Kruger M, Hein L, Braun T. Acquisition of the contractile phenotype by murine arterial smooth muscle cells depends on the Mir143/145 gene cluster. *J Clin Invest.* 2009 Sep; 119(9): 2634-2647. PMCID: PMC2735940.

211. Xin M, Small EM, Sutherland LB, Qi X, McAnally J, Plato CF, Richardson JA, Bassel-Duby R, Olson EN. MicroRNAs miR-143 and miR-145 modulate cytoskeletal dynamics and responsiveness of smooth muscle cells to injury. *Genes Dev.* 2009 Sep 15; 23(18): 2166-2178. PMCID: PMC2751981.

212. Alajbegovic A, Turczynska KM, Hien TT, Cidad P, Sward K, Hellstrand P, Della Corte A, Forte A, Albinsson S. Regulation of microRNA expression in vascular smooth muscle by MRTF-A and actin polymerization. *Biochim Biophys Acta.* 2016 Dec 8.

213. Uchida S, Dimmeler S. Long noncoding RNAs in cardiovascular diseases. *Circ Res.* 2015 Feb 13; 116(4): 737-750.

214. Khalil AM, Guttman M, Huarte M, Garber M, Raj A, Rivea Morales D, Thomas K, Presser A, Bernstein BE, van Oudenaarden A, Regev A, Lander ES, Rinn JL. Many human large intergenic noncoding RNAs associate with chromatin-modifying complexes and affect gene expression. *Proc Natl Acad Sci U S A.* 2009 Jul 14; 106(28): 11667-11672. PMCID: PMC2704857.

215. Jarinova O, Stewart AF, Roberts R, Wells G, Lau P, Naing T, Buerki C, McLean BW, Cook RC, Parker JS, McPherson R. Functional analysis of the chromosome 9p21.3 coronary artery disease risk locus. *Arterioscler Thromb Vasc Biol.* 2009 Oct; 29(10): 1671-1677.

216. Motterle A, Pu X, Wood H, Xiao Q, Gor S, Ng FL, Chan K, Cross F, Shohreh B, Poston RN, Tucker AT, Caulfield MJ, Ye S. Functional analyses of coronary artery disease associated variation on chromosome 9p21 in vascular smooth muscle cells. *Hum Mol Genet.* 2012 Sep 15; 21(18): 4021-4029. PMCID: PMC3428153.

217. Congrains A, Kamide K, Oguro R, Yasuda O, Miyata K, Yamamoto E, Kawai T, Kusunoki H, Yamamoto H, Takeya Y, Yamamoto K, Onishi M, Sugimoto K, Katsuya T, Awata N, Ikebe K, Gondo Y, Oike Y, Ohishi M, Rakugi H. Genetic variants at the 9p21 locus contribute to atherosclerosis through modulation of ANRIL and CDKN2A/B. *Atherosclerosis.* 2012 Feb; 220(2): 449-455.

218. 220. Zhao J, Zhang W, Lin M, Wu W, Jiang P, Tou E, Xue M, Richards A, Jourd'heuil D, Asif A, Zheng D, Singer HA, Miano JM, Long X. MYOSLID is a novel serum response factor-dependent long noncoding RNA that amplifies the vascular smooth muscle differentiation program. *Arterioscler Thromb Vasc Biol.* 2016 Oct; 36(10): 2088-2099. PMCID: PMC5033703.

219. Bai X, Lenhart KC, Bird KE, Suen AA, Rojas M, Kakoki M, Li F, Smithies O, Mack CP, Taylor JM. The smooth muscle-selective RhoGAP GRAF3 is a critical regulator of vascular tone and hypertension. Nat Commun. 2013;4:2910. doi: 10.1038/ncomms3910. PubMed PMID: 24335996; PubMed Central PMCID: PMC4237314.

220. Guilluy C, Brégeon J, Toumaniantz G, Rolli-Derkinderen M, Retailleau K, Loufrani L, Henrion D, Scalbert E, Bril A, Torres RM, Offermanns S, Pacaud P, Loirand G. The Rho exchange factor Arhgef1 mediates the effects of angiotensin II on vascular tone and blood pressure. Nat Med. 2010 Feb;16(2):183-90. doi: 10.1038/nm.2079. PubMed PMID: 20098430.

221. Carretero OA, Oparil S. Essential hypertension. Part I: definition and etiology. *Circulation*. 2000;101:329-335.

222. Mozaffarian D, Benjamin EJ, Go AS, Arnett DK, Blaha MJ, Cushman M, de Ferranti S, Després JP, Fullerton HJ, Howard VJ. Heart disease and stroke statistics--2015 update: a report from the American Heart Association. *Circulation*. 2015;131:e29-322.

223. Padmanabhan S, Caulfield M, Dominiczak AF. Genetic and molecular aspects of hypertension. *Circ Res*. 2015;116:937-959.

224. Pelham CJ, Ketsawatsomkron P, Groh S, Grobe JL, de Lange WJ, Ibeawuchi SR, Keen HL, Weatherford ET, Faraci FM, Sigmund CD. Cullin-3 regulates vascular smooth muscle function and arterial blood pressure via PPARγ and RhoA/Rho-kinase. *Cell Metab*. 2012;16:462-472.

225. Boyden LM, Choi M, Choate KA, Nelson-Williams CJ, FarhiA, Toka Tikhonova IR, Bjornson R, Mane SM, Colussi G, Lebel M, Gordon RD, Semmekrot BA, Poujol A, Välimäki MJ, DeFerrari ME, Sanjad SA, Gutkin M, Karet FE, Tucci JR, Stockigt JR, Keppler-Noreuil KM, Porter CC, Anand SK, Whiteford ML, Davis ID, Dewar SB, Bettinelli A, Fadrowski JJ, Belsha CW, Hunley TE, Nelson RD, Trachtman H, Cole TR, Pinsk M, Bockenhauer D, Shenoy M, Vaidyanathan P, Foreman JW, Rasoulpour M, Thameem F, Al-Shahrouri HZ, Radhakrishnan J, Gharavi AG, Goilav B, Lifton RP. Mutations in kelch-like 3 and cullin 3 cause hypertension and electrolyte abnormalities. Nature 2012; 482: 98-102 [PMID: 22266938 DOI: 10.1038/nature10814]

226. Ibeawuchi SR, Agbor LN, Quelle FW, Sigmund CD. Hypertension causing Mutations in Cullin3 Protein Impair RhoA Protein Ubiquitination and Augment

the Association with SubstrateAdaptors. J Biol Chem 2015; 290: 19208-19217.

227. Seasholtz TM, Wessel J, Rao F, Rana BK, Khandrika S, Kennedy BP, Lillie EO, Ziegler MG, Smith DW, Schork NJ. Rho kinase polymorphism influences blood pressure and systemic vascular resistance in human twins: role of heredity. *Hypertension*. 2006;47:937-947.

228. Rankinen T, Church T, Rice T, Markward N, Blair SN, Bouchard C. A major haplotype block at the rho-associated kinase 2 locus is associated with a lower risk of hypertension in a recessive manner: the HYPGENE study. *Hypertens Res*. 2008;31:1651-1657.

229. Liu L, Cao Y, Cui G, Li Z, Sun J, Zhang L, Chen C, Wang Y, Wang P, Ding H. Association analysis of polymorphisms in ROCK2 with cardiovascular disease in a Chinese population. *PLoS One*. 2013;8:e53905.

230. Hashimoto J, Ito S. Some mechanical aspects of arterial aging: physiological overview based on pulse wave analysis. *Ther Adv Cardiovasc Dis*. 2009;3:367-378.

231. Williams B. Evaluating interventions to reduce central aortic pressure, arterial stiffness and morbidity--mortality. *J Hypertens*. 2012;30 Suppl:S13-S18.

232. Luft FC. Molecular mechanisms of arterial stiffness: new insights. *J Am Soc Hypertens*. 2012;6:436-438.

233. Moody WE, Edwards NC, Chue CD, Ferro CJ, Townend JN. Arterial disease in chronic kidney disease. *Heart*. 2013;99:365-372.

234. Safar ME, Nilsson PM. Pulsatile hemodynamics and cardiovascular risk factors in very old patients: background, sex aspects and implications. *J Hypertens*. 2013;31:848-857.

235. Galmiche G, Labat C, Mericskay M, Aissa KA, Blanc J, Retailleau K, Bourhim M, Coletti D, Loufrani L, Gao-Li J. Inactivation of serum response factor contributes to decrease vascular muscular tone and arterial stiffness in mice. *Circ Res*. 2013;112:1035-1045.

236. Qiu H, Zhu Y, Sun Z, Trzeciakowski JP, Gansner M, Depre C, Resuello RR, Natividad FF, Hunter WC, Genin GM. Short communication: vascular smooth muscle cell stiffness as a mechanism for increased aortic stiffness with aging. *Circ Res*. 2010;107:615-619.

237. Liao YC, Liu PY, Lin HF, Lin WY, Liao JK, Juo SH. Two functional polymorphisms of ROCK2 enhance arterial stiffening through inhibiting its activity and expression. *J Mol Cell Cardiol*. 2015;79:180-186.

238. Mendelson K, Evans T, Hla T. Sphingosine 1-phosphate signalling.

Development. 2014;141:5-9.

239. Fenger M, Linneberg A, Jeppesen J. Network-based analysis of the sphingolipid metabolism in hypertension. *Front Genet*. 2015;6:84.

240. Fenger M, Linneberg A, Jørgensen T, Madsbad S, Søbye K, Eugen-Olsen J, Jeppesen J. Genetics of the ceramide/sphingosine-1-phosphate rheostat in blood pressure regulation and hypertension. *BMC Genet*. 2011;12:44.

241. Ren XD, Kiosses WB, Schwartz MA. Regulation of the small GTP-binding protein Rho by cell adhesion and the cytoskeleton. *EMBO J*. 1999;18:578-585.

242. Levy D, Ehret GB, Rice K, Verwoert GC, Launer LJ, Dehghan A, Glazer NL, Morrison AC, Johnson AD, Aspelund T. Genome-wide association study of blood pressure and hypertension. *Nat Genet*. 2009;41:677-687.

243. Lin Y, Lai X, Chen B, Xu Y, Huang B, Chen Z, Zhu S, Yao J, Jiang Q, Huang H. Genetic variations in CYP17A1, CACNB2 and PLEKHA7 are associated with blood pressure and/or hypertension in She ethnic minority of China. *Atherosclerosis*. 2011;219:709-714.

244. Citi S, Pulimeno P, Paschoud S. Cingulin, paracingulin, and PLEKHA7: signaling and cytoskeletal adaptors at the apical junctional complex. *Ann N Y Acad Sci*. 2012;1257:125-132.

245. Endres BT, Priestley JR, Palygin O, Flister MJ, Hoffman MJ, Weinberg BD, Grzybowski M, Lombard JH, Staruschenko A, Moreno C. Mutation of Plekha7 attenuates salt-sensitive hypertension in the rat. *Proc Natl Acad Sci USA*. 2014;111:12817-12822.

246. Carbone ML, Brégeon J, Devos N, Chadeuf G, Blanchard A, Azizi M, Pacaud P, Jeunemaître X, Loirand G. Angiotensin II activates the RhoA exchange factor Arhgef1 in humans. *Hypertension*. 2015;65:1273-1278.

247. Kanaki AI, Sarafidis PA, Georgianos PI, Kanavos K, Tziolas IM, Zebekakis PE, Lasaridis AN. Effects of low-dose atorvastatin on arterial stiffness and central aortic pressure augmentation in patients with hypertension and hypercholesterolemia. *Am J Hypertens*. 2013;26:608-616.

248. Mozaffarian, D., et al. 2016. Executive Summary: Heart Disease and Stroke Statistics-2016 Update: A Report From the American Heart Association. *Circulation* 133:447-454.

249. Franceschini, N., Chasman, D.I., Cooper-DeHoff, R.M., and Arnett, D.K. 2014. Genetics, ancestry, and hypertension: implications for targeted antihypertensive therapies. *Curr Hypertens Rep* 16:461.

250. Wain, L.V., et al. 2011. Genome-wide association study identifies six new loci influencing pulse pressure and mean arterial pressure. *Nat Genet* 43:1005-1011.

251. Ehret, G.B., et al. 2011. Genetic variants in novel pathways influence blood pressure and cardiovascular disease risk. *Nature* 478:103-109.

252. Kato, N., et al. 2015. Trans-ancestry genome-wide association study identifies 12 genetic loci influencing blood pressure and implicates a role for DNA methylation. *Nat Genet* 47:1282-1293.

253. Taylor, J.M., Hildebrand, J.D., Mack, C.P., Cox, M.E., and Parsons, J.T. 1998. Characterization of graf, the GTPase-activating protein for rho associated with focal adhesion kinase. Phosphorylation and possible regulation by mitogen-activated protein kinase. *J Biol Chem* 273:8063-8070.

254. Doherty, J.T., Lenhart, K.C., Cameron, M.V., Mack, C.P., Conlon, F.L., and Taylor, J.M. 2011. Skeletal muscle differentiation and fusion are regulated by the BAR-containing Rho-GTPase-activating protein (Rho-GAP), GRAF1. *J Biol Chem* 286:25903-25921.

255. Taylor, J.M., Macklem, M.M., and Parsons, J.T. 1999. Cytoskeletal changes induced by GRAF, the GTPase regulator associated with focal adhesion kinase, are mediated by Rho. *J Cell Sci* 112 (Pt 2):231-242.

256. Hildebrand, J.D., Taylor, J.M., and Parsons, J.T. 1996. An SH3 domain-containing GTPase-activating protein for Rho and Cdc42 associates with focal adhesion kinase. *Mol Cell Biol* 16:3169-3178.

257. Somlyo, A.P., and Somlyo, A.V. 2004. Signal transduction through the RhoA/Rho-kinase pathway in smooth muscle. *J Muscle Res Cell Motil* 25:613-615.

258. Albinsson, S., Nordstrom, I., and Hellstrand, P. 2004. Stretch of the vascular wall induces smooth muscle differentiation by promoting actin polymerization. *J Biol Chem* 279:34849-34855.

259. Zeidan, A., Nordstrom, I., Dreja, K., Malmqvist, U., and Hellstrand, P. 2000. Stretch-dependent modulation of contractility and growth in smooth muscle of rat portal vein. *Circ Res* 87:228-234.

260. Consortium, G. 2015. Human genomics. The Genotype-Tissue Expression (GTEx) pilot analysis: multitissue gene regulation in humans. *Science* 348:648-660.

261. Viera, A.J., Lin, F.C., Tuttle, L.A., Shimbo, D., Diaz, K.M., Olsson, E., Stankevitz, K., and Hinderliter, A.L. 2015. Levels of office blood pressure and their operating characteristics for detecting masked hypertension based on

ambulatory blood pressure monitoring. *Am J Hypertens* 28:42-49.

262. Viera, A.J., Hinderliter, A.L., Kshirsagar, A.V., Fine, J., and Dominik, R. 2010. Reproducibility of masked hypertension in adults with untreated borderline office blood pressure: comparison of ambulatory and home monitoring. *Am J Hypertens* 23:1190-1197.

263. Schisler, J.C., et al. 2009. Stable patterns of gene expression regulating carbohydrate metabolism determined by geographic ancestry. *PLoS One* 4:e8183.

264. Theken, K.N., et al. 2012. Evaluation of cytochrome P450-derived eicosanoids in humans with stable atherosclerotic cardiovascular disease. *Atherosclerosis* 222:530-536.

265. Oni-Orisan, A., et al. 2016. Cytochrome P450-derived epoxyeicosatrienoic acids and coronary artery disease in humans: a targeted metabolomics study. *J Lipid Res* 57:109-119.

266. Halladay, J.R., Donahue, K.E., Hinderliter, A.L., Cummings, D.M., Cene, C.W., Miller, C.L., Garcia, B.A., Tillman, J., and DeWalt, D. 2013. The Heart Healthy Lenoir project--an intervention to reduce disparities in hypertension control: study protocol. *BMC Health Serv Res* 13:441.

267. Lagna, G., Ku, M.M., Nguyen, P.H., Neuman, N.A., Davis, B.N., and Hata, A. 2007. Control of phenotypic plasticity of smooth muscle cells by bone morphogenetic protein signaling through the myocardin-related transcription factors. *J Biol Chem* 282:37244-37255.

268. Li, L., Liu, Z., Mercer, B., Overbeek, P., and Olson, E.N. 1997. Evidence for serum response factor-mediated regulatory networks governing SM22alpha transcription in smooth, skeletal, and cardiac muscle cells. *Dev Biol* 187:311-321.

269. Musunuru, K., et al. 2010. From noncoding variant to phenotype via SORT1 at the 1p13 cholesterol locus. *Nature* 466:714-719.

270. Almontashiri, N.A., Antoine, D., Zhou, X., Vilmundarson, R.O., Zhang, S.X., Hao, K.N., Chen, H.H., and Stewart, A.F. 2015. 9p21.3 Coronary Artery Disease Risk Variants Disrupt TEAD Transcription Factor-Dependent Transforming Growth Factor beta Regulation of p16 Expression in Human Aortic Smooth Muscle Cells. *Circulation* 132:1969-1978.

271. Thakore PI, D'Ippolito AM, Song L, Safi A, Shivakumar NK, Kabadi AM, Reddy TE, Crawford GE, Gersbach CA. Highly specific epigenome editing by CRISPR-Cas9 repressors for silencing of distal regulatory elements. Nat Methods. 2015 Dec;12(12):1143-9. doi: 10.1038/nmeth.3630. PubMed PMID: 26501517; PubMed Central PMCID: PMC4666778.

272. Perez-Pinera P, Kocak DD, Vockley CM, Adler AF, Kabadi AM, Polstein LR, Thakore PI, Glass KA, Ousterout DG, Leong KW, Guilak F, Crawford GE, Reddy TE, Gersbach CA. RNA-guided gene activation by CRISPR-Cas9-based transcription factors. Nat Methods. 2013 Oct;10(10):973-6. doi: 10.1038/nmeth.2600. PubMed PMID: 23892895; PubMed Central PMCID: PMC3911785.

273. Bai X, Mangum KD, Dee RA, Stouffer GA, Lee CR, Oni-Orisan A, Patterson C, Schisler JC, Viera AJ, Taylor JM, Mack CP. Blood pressure-associated polymorphism controls ARHGAP42 expression via serum response factor DNA binding. J Clin Invest. 2017 Feb 1;127(2):670-680. doi: 10.1172/JCI88899. PubMed PMID: 28112683; PubMed Central PMCID: PMC5272192.

274. Aragona M, Panciera T, Manfrin A, Giulitti S, Michielin F, Elvassore N, Dupont S, Piccolo S. A mechanical checkpoint controls multicellular growth through YAP/TAZ regulation by actin-processing factors. Cell. 2013 Aug 29;154(5):1047-59. doi: 10.1016/j.cell.2013.07.042. PubMed PMID: 23954413.

275. Yang Q, Jia C, Wang P, Xiong M, Cui J, Li L, Wang W, Wu Q, Chen Y, Zhang T. MicroRNA-505 identified from patients with essential hypertension impairs endothelial cell migration and tube formation. Int J Cardiol. 2014 Dec 20;177(3):925-34. doi: 10.1016/j.ijcard.2014.09.204. PubMed PMID: 25449503.

276. Badorff C, Seeger FH, Zeiher AM, Dimmeler S. Glycogen synthase kinase 3beta inhibits myocardin-dependent transcription and hypertrophy induction through site-specific phosphorylation. Circ Res. 2005 Sep 30;97(7):645-54. PubMed PMID:16141410.

277. Sundberg-Smith LJ, Doherty JT, Mack CP, Taylor JM. Adhesion stimulates direct PAK1/ERK2 association and leads to ERK-dependent PAK1 Thr212 phosphorylation. J Biol Chem. 2005 Jan 21;280(3):2055-64. PubMed PMID: 15542607.

278. Davis CA, Haberland M, Arnold MA, Sutherland LB, McDonald OG, Richardson JA, Childs G, Harris S, Owens GK, Olson EN. PRISM/PRDM6, a transcriptional repressor that promotes the proliferative gene program in smooth muscle cells. Mol Cell Biol. 2006 Apr;26(7):2626-36. PubMed PMID: 16537907; PubMed Central PMCID: PMC1430312.

279. Zhang X, Peng D, Xi Y, Yuan C, Sagum CA, Klein BJ, Tanaka K, Wen H, Kutateladze TG, Li W, Bedford MT, Shi X. G9a-mediated methylation of ERα links the PHF20/MOF histone acetyltransferase complex to hormonal gene expression. Nat Commun. 2016 Mar 10;7:10810. doi: 10.1038/ncomms10810. PubMed PMID: 26960573; PubMed Central PMCID: PMC4792926.

280. Dhami GK, Liu H, Galka M, Voss C, Wei R, Muranko K, Kaneko T, Cregan SP, Li L, Li SS. Dynamic methylation of Numb by Set8 regulates its binding to p53

and apoptosis. Mol Cell. 2013 May 23;50(4):565-76. doi: 10.1016/j.molcel.2013.04.028. PubMed PMID: 23706821.

281. West LE, Gozani O. Regulation of p53 function by lysine methylation. Epigenomics. 2011 Jun;3(3):361-9. doi: 10.2217/EPI.11.21. PubMed PMID: 21826189; PubMed Central PMCID: PMC3151012.

282. Olsen JB, Cao XJ, Han B, Chen LH, Horvath A, Richardson TI, Campbell RM,Garcia BA, Nguyen H. Quantitative Profiling of the Activity of Protein Lysine Methyltransferase SMYD2 Using SILAC-Based Proteomics. Mol Cell Proteomics. 2016 Mar;15(3):892-905. doi: 10.1074/mcp.M115.053280. PubMed PMID: 26750096; PubMed Central PMCID: PMC4813708.

283. Du SJ, Tan X, Zhang J. SMYD proteins: key regulators in skeletal and cardiac muscle development and function. Anat Rec (Hoboken). 2014 Sep;297(9):1650-62. doi: 10.1002/ar.22972. Review. PubMed PMID: 25125178.

284. Li N, Subrahmanyan L, Smith E, Yu X, Zaidi S, Choi M, Mane S, Nelson-Williams C, Bahjati M, Kazemi M, Hashemi M, Fathzadeh M, Narayanan A, Tian L, Montazeri F, Mani M, Begleiter ML, Coon BG, Lynch HT, Olson EN, Zhao H, Ruland J, Lifton RP, Mani A. Mutations in the Histone Modifier PRDM6 Are Associated with Isolated Nonsyndromic Patent Ductus Arteriosus. Am J Hum Genet. 2016 Jun 2;98(6):1082-91. doi: 10.1016/j.ajhg.2016.03.022. PubMed PMID: 27181681; PubMed Central PMCID: PMC4908195.

285. Li N, Subrahmanyan L, Smith E, Yu X, Zaidi S, Choi M, Mane S, Nelson-Williams C, Behjati M, Kazemi M, Hashemi M, Fathzadeh M, Narayanan A, Tian L, Montazeri F, Mani M, Begleiter ML, Coon BG, Lynch HT, Olson EN, Zhao H, Ruland J, Lifton RP, Mani A. Mutations in the Histone Modifier PRDM6 Are Associated with Isolated Nonsyndromic Patent Ductus Arteriosus. Am J Hum Genet. 2016 Oct 6;99(4):1000. doi: 10.1016/j.ajhg.2016.09.003. PubMed PMID: 27716515; PubMed Central PMCID: PMC5065682.

286. Ivanov GS, Ivanova T, Kurash J, Ivanov A, Chuikov S, Gizatullin F, Herrera-Medina EM, Rauscher F 3rd, Reinberg D, Barlev NA. Methylation-acetylation interplay activates p53 in response to DNA damage. Mol Cell Biol. 2007 Oct;27(19):6756-69. PubMed PMID: 17646389; PubMed Central PMCID: PMC2099237.

287. Brandes RP. Statin-mediated inhibition of Rho: only to get more NO? *Circ Res*. 2005;96:927-929.

288. Olson MF. Applications for ROCK kinase inhibition. *Curr Opin Cell Biol*. 2008;20:242-248.

289. Davies SP, Reddy H, Caivano M, Cohen P. Specificity and mechanism of action of some commonly used protein kinase inhibitors. *Biochem*

J. 2000;351:95-105.

290. Liao JK, Seto M, Noma K. Rho kinase (ROCK) inhibitors. *J Cardiovasc Pharmacol*. 2007;50:17-24.

291. Masumoto A, Hirooka Y, Shimokawa H, Hironaga K, Setoguchi S, Takeshita A. Possible involvement of Rho-kinase in the pathogenesis of hypertension in humans. Hypertension 2001; 38:1307-1310 [PMID: 11751708 DOI: 10.1161/hy1201.096541].

292. Asano M, Nomura Y. Comparison of inhibitory effects of Y-27632, a Rho kinase inhibitor, in strips of small and large mesenteric arteries from spontaneously hypertensive and normotensive Wistar-Kyoto rats. *Hypertens Res*. 2003;26:97-106.

293. Uehata M, Ishizaki T, Satoh H, Ono T, Kawahara T, Morishita T, Tamakawa H, Yamagami K, Inui J, Maekawa M. Calcium sensitization of smooth muscle mediated by a Rho-associated protein kinase in hypertension. *Nature*. 1997;389:990-994.

294. Surma M, Wei L, Shi J. Rho kinase as a therapeutic target in cardiovascular disease. *Future Cardiol*. 2011;7:657-671.

295. Satoh K, Fukumoto Y, Shimokawa H. Rho-kinase: important new therapeutic target in cardiovascular diseases. *Am J Physiol Heart Circ Physiol*. 2011;301:H287-H296.

296. Dhaliwal JS, Badejo AM, Casey DB, Murthy SN, Kadowitz PJ. Analysis of pulmonary vasodilator responses to SB-772077-B [4-(7-((3-amino-1-pyrrolidinyl)carbonyl)-1-ethyl-1H-imidazo(4,5-c)pyridin-2-yl)-1,2,5-oxadiazol-3-amine], a novel aminofurazan-based Rho kinase inhibitor. *J Pharmacol Exp Ther*. 2009;330:334-341.

297. Doe C, Bentley R, Behm DJ, Lafferty R, Stavenger R, Jung D, Bamford M, Panchal T, Grygielko E, Wright LL. Novel Rho kinase inhibitors with anti-inflammatory and vasodilatory activities. *J Pharmacol Exp Ther*. 2007;320:89-98.

298. Boerma M, Fu Q, Wang J, Loose DS, Bartolozzi A, Ellis JL, McGonigle S, Paradise E, Sweetnam P, Fink LM. Comparative gene expression profiling in three primary human cell lines after treatment with a novel inhibitor of Rho kinase or atorvastatin. *Blood Coagul Fibrinolysis*. 2008;19:709-718.

299. Löhn M, Plettenburg O, Kannt A, Kohlmann M, Hofmeister A, Kadereit D, Monecke P, Schiffer A, Schulte A, Ruetten H. End-organ protection in hypertension by the novel and selective Rho-kinase inhibitor, SAR407899. *World J Cardiol*. 2015;7:31-42.

300. Löhn M, Plettenburg O, Ivashchenko Y, Kannt A, Hofmeister A, Kadereit D, Schaefer M, Linz W, Kohlmann M, Herbert JM. Pharmacological characterization of SAR407899, a novel rho-kinase inhibitor. *Hypertension*. 2009;54:676-683.

301. Carretero OA, Oparil S. Essential hypertension : part II: treatment. *Circulation*. 2000;101:446-453.

302. Epstein M, Bakris G. Newer approaches to antihypertensive therapy. Use of fixed-dose combination therapy. *Arch Intern Med*. 1996;156:1969-1978.

303. He F, Luo J, Zhang Z, Luo Z, Fan L, He Y, Wen J, Zhu D, Gao J, Wang Y. The RGS2 (-391, C& gt; G) genetic variation correlates to antihypertensive drug responses in Chinese patients with essential hypertension. *PLoS One*. 2015;10:e0121483.

304. Vandell AG, Lobmeyer MT, Gawronski BE, Langaee TY, Gong Y, Gums JG, Beitelshees AL, Turner ST, Chapman AB, Cooper-DeHoff RM. G protein receptor kinase 4 polymorphisms: β-blocker pharmacogenetics and treatment-related outcomes in hypertension. *Hypertension*. 2012;60:957-964.

305. Nguyen H, Allali-Hassani A, Antonysamy S, Chang S, Chen LH, Curtis C, Emtage S, Fan L, Gheyi T, Li F, Liu S, Martin JR, Mendel D, Olsen JB, Pelletier L, Shatseva T, Wu S, Zhang FF, Arrowsmith CH, Brown PJ, Campbell RM, Garcia BA, Barsyte-Lovejoy D, Mader M, Vedadi M. LLY-507, a Cell-active, Potent, and Selective Inhibitor of Protein-lysine Methyltransferase SMYD2. J Biol Chem. 2015 May 29;290(22):13641-53. doi: 10.1074/jbc.M114.626861. PubMed PMID: 25825497; PubMed Central PMCID: PMC4447944.